



**STUDIES TO IDENTIFY AND CHARACTERISE  
IGF-BINDING DETERMINANTS OF IGFBP-2**

**By**

**Graham D. Hobba, B.Sc (Hons)**

**A thesis submitted to the University of Adelaide, South Australia  
in fulfillment of the requirements for the degree of  
Doctor of Philosophy**

**January, 1999**

**Department of Biochemistry**

**University of Adelaide**

**South Australia.**

*what secrets hide  
in small vessels  
their colourless solutions?*

*This thesis is dedicated to Walter and Winifred Hobba*

## TABLE OF CONTENTS

ABSTRACT.....	4
STATEMENT OF ORIGINALITY.....	5
ACKNOWLEDGEMENTS.....	6
LIST OF FIGURES .....	7
LIST OF TABLES .....	8
ABBREVIATIONS .....	9
LIST OF ORIGINAL PUBLICATIONS .....	11
INTRODUCTION.....	13
<b>CHAPTER 1 - THE IGFbps: THEIR BIOLOGICAL ROLES AND MOLECULAR INTERACTIONS</b> .....	<b>15</b>
1.1 THE INSULIN-LIKE GROWTH FACTOR SYSTEM - AN OVERVIEW .....	16
1.1.1 <i>Biological Roles</i> .....	16
1.1.2 <i>IGF System Components And Their Distribution</i> .....	16
1.1.3 <i>IGF Receptors</i> .....	18
1.1.4 <i>IGFBPs</i> .....	18
1.1.5 <i>IGF System - Summary</i> .....	20
1.2 IGF STRUCTURE AND FUNCTION .....	20
1.2.1 <i>IGF Structure</i> .....	21
1.2.2 <i>IGF Function</i> .....	23
1.2.2.1 <i>Insulin And Insulin-Receptor Interactions</i> .....	24
1.2.2.2 <i>IGF And Type-1 IGF-Receptor Interactions</i> .....	24
1.2.2.3 <i>IGF And IGFBP Interactions</i> .....	25
1.2.3 <i>IGF Structure And Function – Summary</i> .....	26
1.3 IGFBP STRUCTURE.....	27
1.3.1 <i>IGFBP Primary Structure</i> .....	27
1.3.2 <i>The IGFBPs Have A Common Pattern Of Disulfide Bonds</i> .....	28
1.3.3 <i>IGFBP Secondary Structure Prediction</i> .....	32
1.4 IGFBP FUNCTION.....	33
1.4.1 <i>Localisation Determinants Of IGFBPs</i> .....	34
1.4.1.1 <i>Integrin Interactions</i> .....	34
1.4.1.2 <i>Glycosylation</i> .....	34
1.4.1.3 <i>Glycosaminoglycan Interactions</i> .....	35
1.4.2 <i>IGF-Release Mechanisms Of IGFBPs</i> .....	36
1.4.2.1 <i>Proteolysis Of IGFBPs</i> .....	37
1.4.2.2 <i>Phosphorylation</i> .....	37
1.4.2.3 <i>Integration of IGF Release With Cellular And Physiological Signals</i> .....	38
1.4.3 <i>IGFBP Structure And Function – Summary</i> .....	39
1.5 STUDIES TO IDENTIFY THE IGF BINDING SITE OF IGFBPS .....	39
1.5.1 <i>Naturally Occurring IGFBP Fragments</i> .....	40
1.5.2 <i>Deletion Studies</i> .....	40
1.5.3 <i>Random Mutagenesis</i> .....	41
1.5.4 <i>Knowledge Of The IGFBP Binding Site Of IGFs</i> .....	42
1.5.5 <i>Studies To Identify The IGF Binding Site Of IGFBPs - Summary</i> .....	42
1.6 AIMS AND EXPERIMENTAL STRATEGY.....	43
<b>CHAPTER 2 - RECOMBINANT EXPRESSION OF IGFBP-2 IN MAMMALIAN CELL CULTURE</b> .....	<b>45</b>
2.2 MATERIALS .....	47
2.2.1 <i>Bacterial Cell Culture</i> .....	47
2.2.2 <i>Mammalian Cell Culture</i> .....	48
2.2.3 <i>Chromatography and Electrophoresis</i> .....	49

2.3	METHODS.....	50
2.3.1	<i>Large-Scale Plasmid Production</i> .....	50
2.3.2	<i>Spectrophotometric Analysis of Plasmid DNA</i> .....	51
2.3.3	<i>Transfection of COS-1 Cells</i> .....	51
2.3.4	<i>Purification of bIGFBP-2 from Conditioned Medium</i> .....	52
2.3.4.1	<i>IGF-II Affinity Chromatography</i> .....	52
2.3.4.2	<i>Resource-S Cation Exchange Chromatography</i> .....	53
2.3.4.3	<i>Reverse-phase High Performance Liquid Chromatography (HPLC)</i> .....	53
2.3.4.4	<i>Quantitation of bIGFBP-2</i> .....	53
2.3.5	<i>SDS Polyacrylamide Gel Electrophoresis (SDS-PAGE)</i> .....	54
2.3.5.1	<i>Coomassie Blue Staining of SDS Polyacrylamide Gels</i> .....	54
2.3.5.2	<i>Silver Staining of SDS Polyacrylamide Gels</i> .....	55
2.3.5.3	<i><sup>125</sup>I-IGF-II Ligand Blot</i> .....	55
2.3.5.4	<i>Western Immunoblot for bIGFBP-2</i> .....	56
2.3.6	<i>N-terminal Sequence Analysis</i> .....	56
2.3.7	<i>Mass Spectrometry</i> .....	56
2.3.8	<i>Charcoal Binding Assay</i> .....	56
2.3.8.1	<i><sup>125</sup>I-IGF Titration</i> .....	56
2.3.8.2	<i>Competition Assays</i> .....	57
2.4	RESULTS.....	58
2.4.1	<i>Plasmid Purification</i> .....	58
2.4.2	<i>Transfection of COS-1 Cells</i> .....	58
2.4.3	<i>Purification of bIGFBP-2 From Conditioned Medium</i> .....	59
2.4.4	<i>Titration IGF Binding Assay</i> .....	63
2.4.5	<i>Competition IGF Binding Assay</i> .....	63
2.5	DISCUSSION.....	64
<b>CHAPTER 3 - CHEMICAL IODINATION OF IGFBP-2 AS A FUNCTIONAL AND STRUCTURAL PROBE.....</b>		<b>68</b>
3.1	INTRODUCTION.....	69
3.1.1	<i>Background</i> .....	69
3.1.2	<i>Iodination and Studies of the Insulin and IGF Systems</i> .....	69
3.1.3	<i>The Iodination Reaction</i> .....	70
3.1.4	<i>Overview of the Experimental Strategy</i> .....	71
3.2	MATERIALS.....	71
3.3	METHODS.....	72
3.3.1	<i>Titration of Reactive bIGFBP-2 Tyrosine Residues</i> .....	72
3.3.2	<i>HPLC Gel-Filtration at Acid pH</i> .....	73
3.3.3	<i>Iodinations of bIGFBP-2 for IGF Binding Assays</i> .....	73
3.3.4	<i>Iodinations of bIGFBP-2 for Peptide Mapping</i> .....	73
3.3.5	<i>Tryptic Mapping of bIGFBP-2</i> .....	74
3.4	RESULTS.....	75
3.4.1	<i>Titration of Reactive bIGFBP-2 Tyrosine Residues</i> .....	76
3.4.2	<i>Determination of the Biological Activity of Iodinated Forms of bIGFBP-2</i> .....	80
3.4.3	<i>Identification of IGF/IGFBP Binding Site</i> .....	82
3.5	DISCUSSION.....	88
<b>CHAPTER 4 - ALANINE SCREENING MUTAGENESIS ESTABLISHES TYR-60 OF IGFBP-2 AS A DETERMINANT OF IGF BINDING.....</b>		<b>95</b>
4.1	INTRODUCTION.....	96
4.2	MATERIALS.....	97
4.2.1	<i>General Chemicals and Materials</i> .....	97
4.2.2	<i>Molecular Biology Reagents</i> .....	98
4.2.3	<i>Bacterial Strains</i> .....	98
4.2.4	<i>Bacterial Culture Media and Solutions</i> .....	98
4.2.5	<i>Cell Culture Media</i> .....	99
4.2.6	<i>Chromatography and Electrophoresis</i> .....	99
4.3	METHODS.....	99
4.3.1	<i>Mutagenesis of the Tyr-60 Region of bIGFBP-2 – Overview</i> .....	99
4.3.2	<i>Construction of the Mutagenic Plasmid pGDH-1</i> .....	100
4.3.2.1	<i>Preparation of Vector and Insert DNA</i> .....	100
4.3.2.2	<i>Ligation of DNA</i> .....	101
4.3.2.3	<i>Transformation of E. coli</i> .....	102

4.3.2.4	Small-Scale Preparation of Plasmid DNA by the Alkaline Lysis Method .....	102
4.3.3	<i>Synthesis of Single-Stranded Template DNA</i> .....	103
4.3.4	<i>The In Vitro Mutagenesis Reaction</i> .....	103
4.3.5	<i>DNA Sequencing</i> .....	104
4.3.5.1	PCR DNA Sequencing With End-Labelled Primers .....	104
4.3.5.2	Dye Terminator DNA Sequencing .....	105
4.3.6	<i>Production of bIGFBP-2 Analogs</i> .....	106
4.3.7	<i>Analysis of the Mutant bIGFBP-2 Analogs</i> .....	106
4.3.7.1	SDS-PAGE and Western-Ligand Blot .....	106
4.3.7.2	Mass Spectrometry .....	106
4.3.7.3	Amino Acid Analysis .....	106
4.3.7.4	Circular Dichroism.....	107
4.3.7.5	Isoelectric Focussing.....	107
4.3.7.6	Soluble IGFBP Assay .....	107
4.3.7.7	BIAcore.....	107
4.4	<b>RESULTS</b> .....	108
4.4.1	<i>In Vitro Mutagenesis</i> .....	108
4.4.2	<i>Expression and Purification of bIGFBP-2 Analogs</i> .....	111
4.4.3	<i>Protein Characterisation</i> .....	112
4.4.4	<i>Circular Dichroism</i> .....	114
4.4.5	<i>Isoelectric Focussing Electrophoresis</i> .....	114
4.4.6	<i>Western Ligand Blots</i> .....	116
4.4.7	<i>Solution IGF Binding Assay</i> .....	116
4.4.8	<i>BIAcore Analysis</i> .....	118
4.5	<b>DISCUSSION</b> .....	123
<b>CHAPTER 5 – GENERAL DISCUSSION AND CONCLUDING REMARKS</b> .....		<b>127</b>
5.1	<b>SUMMARY OF FINDINGS</b> .....	128
5.2	<b>POSSIBLE IGF BINDING ROLES FOR TYR-60 AND VAL-59</b> .....	129
5.3	<b>IMPLICATIONS OF FINDINGS</b> .....	133
5.4	<b>FUTURE DIRECTIONS</b> .....	136

## ABSTRACT

The lack of information regarding the IGF binding mechanism of IGFbps constitutes a considerable gap in the understanding of IGFbp function. Therefore, this work sought to identify and characterise specific residues of bIGFBP-2 that comprise the IGF binding site. Initially, the bIGFBP/IGF complex was probed by chemical iodination followed by tryptic mapping. Iodination of bIGFBP-2 whilst in a complex with IGF resulted in a 5-fold protection of Tyr-60 in comparison to bIGFBP-2 iodinated alone. Furthermore, an 8-fold reduction in apparent affinity for IGF-I and a 4-fold reduction in apparent affinity accompanied iodination at Tyr-60 of bIGFBP-2. It was therefore concluded that Tyr-60 or flanking residues may directly participate in the bIGFBP-2/IGF interaction.

Alignment of the known amino acid sequences of the IGFbp family shows that there is a high degree of homology in the vicinity of Tyr-60 which is consistent with conserved protein function. To investigate this region, six analogs of bIGFBP-2 were constructed (Tyr-60→Phe and an alanine-scan across residues 59-63 inclusive). Western ligand blots showed that Val-59→Ala, Tyr-60→Ala and Tyr-60→Phe bIGFBP-2 were compromised in their ability to bind <sup>125</sup>I-IGF-II. However, only Tyr-60→Ala and Tyr-60→Phe bIGFBP-2 exhibited reduced equilibrium affinity for <sup>125</sup>I-IGF-I and <sup>125</sup>I-IGF-II in solution IGF-binding assays. Kinetic analyses in the BIAcore revealed that Val-59→Ala bIGFBP-2 associated with and dissociated from the IGF-I surface 5-fold more and 9.4-fold more rapidly than bIGFBP-2 to yield little overall change in the equilibrium affinity constant. Tyr-60→Phe bIGFBP-2 associated with and dissociated from the IGF-I surface 3.0-fold more slowly and 2.6-fold more rapidly than bIGFBP-2, with a net 8.4-fold drop in equilibrium affinity. In contrast, Tyr-60→Ala bIGFBP-2 associated with the IGF-I surface 5.0-fold more rapidly than bIGFBP-2, but exhibited an 18.4-fold more rapid release from this surface compared to bIGFBP-2 and thus sustained a 4.0-fold drop in equilibrium affinity. These results indicate that both the aromatic nature and the hydrogen bonding potential of the tyrosyl side-chain of Tyr-60 are important structural determinants of the IGF binding site of bIGFBP-2. In addition, the shape and hydrophobic nature of Val-59 may play a role in maintaining native contacts between IGFs and bIGFBP-2.

In conclusion, a two tiered approach has been used to firstly locate a novel IGF-binding region of bIGFBP-2 and subsequently characterise the specific IGF-binding

role of each residue in this region. For the first time, Val-59 and Tyr-60 of bIGFBP-2 have been shown to be determinants for IGF interactions.

## **STATEMENT OF ORIGINALITY**

This thesis contains no material which has been accepted for the award of any other degree or diploma in any University. To the best of my knowledge and belief it contains no material that has previously been published by any other person except where due reference is made. The author consents to the thesis being made available for photocopy and loan.

Graham D. Hobba

## ACKNOWLEDGEMENTS

It is with warm gratitude that I thank my supervisors Dr. John Wallace and Geoffrey Francis for their enthusiasm, critical thinking and continued support throughout this project. I also thank Dr. Briony Forbes for her excellent technical advice, encouragement and many great discussions. Thank-you to all of my fellow laboratory members and to members of the Biochemistry Department for all of their assistance and the many wonderful friendships. In particular I would like to thank Steven Polyak for helping design the mutant screen, Melinda Lucic, Chris Mavrangelos, Dr. Vicky Avery, Yui Jitrapakdee and Samantha Lien for helping bridge the gap between protein chemistry and molecular biology, Joe Wrin for tissue culture advice, Dr. Terry Mulhern for assistance with the Silicon Graphics workstation.

This research was generously funded by the Cooperative Research Centre for Tissue Growth and Repair. I would like to thank Katrina Downer and Jim Antoniou for organising the many short courses and activities that have broadened my Ph.D. studies at the CRC. I would also like to thank the organisers of the Lorne Protein Conference for their generous student travel grants over the past 4 years.

Some analyses of the bIGFBP-2 analogs were conducted at Pharmacia & Upjohn AB, Stockholm, Sweden. I would like to thank Professor Björn Nilsson and Dr. Göran Forsberg for their efforts in organising this research attachment. The overseas travel was funded by an Australian Society for Biochemistry and Molecular Biology Fellowship and a University of Adelaide travel Award, both of which are gratefully acknowledged. I thank Dr. Erland Holmberg and Agneta Löthgren for revealing secrets of the spectropolarimeter and the BIAcore instruments, respectively.

Special thanks to my parents Ian and Margaret Hobba for their fantastic support and interest over what seems to be an eternity of study. I would also like to thank both my new and extended families for their encouragement and for not mentioning the “T” word too often over the past 6 months.

Most importantly, I wish to thank my best supporter Jen Clarke for her love and encouragement.



## LIST OF FIGURES

- Fig. 1.1 Summary of IGF system interactions.
- Fig. 1.2 Sequence alignment and domain arrangement of IGFs and insulin.
- Fig. 1.3 Representations of insulin, IGF-I and IGF-II.
- Fig. 1.4 IGF-I Binding epitopes for the type-1 IGF-receptor and IGFBPs.
- Fig. 1.5 Sequence alignment of IGFBP sequences including a summary of IGFBP post-translational modifications.
- Fig. 1.6 Predicted partial disulfide bonding pattern for the IGFBP family.
- 
- Fig. 2.1 Vector map for pGF8.
- Fig. 2.2 Affinity purification of IGFBPs secreted into culture medium.
- Fig. 2.3 Cation exchange chromatography of affinity purified IGFBPs.
- Fig. 2.4 Reverse-phase HPLC of peak I from the cation exchange step.
- Fig. 2.5 Solution IGF binding assays with recombinant bIGFBP-2.
- 
- Fig. 3.1 The differential iodination strategy used to locate an IGF-binding region of bIGFBP-2.
- Fig. 3.2 Analysis of iodinated bIGFBP-2 species by HPLC gel-filtration chromatography.
- Fig. 3.3 The molar incorporation of iodine into bIGFBP-2 and resultant loss of tyrosine-fluorescence.
- Fig. 3.4 The IGF-binding assays of iodinated and non-iodinated bIGFBP-2 species.
- Fig. 3.5 Tryptic peptides of bIGFBP-2.
- Fig. 3.6 The tyrosine-fluorescence of resolved tryptic bIGFBP-2 peptides and trypsin.
- Fig. 3.7 Identification of iodinated tyrosyl peptides of bIGFBP-2.
- Fig. 3.8 Comparison of the iodination pattern of bIGFBP-2 iodinated in the presence of IGF-I and IGF-II.
- 
- Fig. 4.1 Sequence homology of the IGFBP family across the "Tyr-60 region".
- Fig. 4.2 A summary of the mutagenic oligonucleotides used to produce the bIGFBP-2 mutant analogs.

- Fig. 4.3 Agarose gel electrophoretic analysis of the products of *in vitro* mutagenesis reactions.
- Fig. 4.4 Diagnostic *RsaI* digestions of bIGFBP-2 mutant constructs in the expression vector pGF8.
- Fig. 4.5 SDS-PAGE and Western antibody blot analysis of bIGFBP-2 and bIGFBP-2 mutant analogs in conditioned medium.
- Fig. 4.6 Far-UV CD spectra of bIGFBP-2 and bIGFBP-2 mutants from 190 nm to 250 nm.
- Fig. 4.7 Isoelectric focussing of bIGFBP-2 and bIGFBP-2 mutant analogs.
- Fig. 4.8 SDS-PAGE analysis of purified bIGFBP-2 and bIGFBP-2 mutant analogs.
- Fig. 4.9 Solution-phase IGF binding assays of bIGFBP-2 and IGFBP-2 mutant analogs
- Fig. 4.10 BIAcore analysis of bIGFBP-2 and bIGFBP2 mutant analogs.
- Fig. 5.1 Summary of modifications to bIGFBP-2 and the resultant changes in affinity for IGF-I.
- Fig. 5.2 Sequence alignment of mini-IGFBP-5 and the homologous region of bIGFBP-2.
- Fig. 5.3 The location of “Tyr-60 region” residues of bIGFBP-2 in the molecular structure of mini-IGFBP-5.

## LIST OF TABLES

- Table 3.1 A summary of the molar fluorescence and molar iodine incorporation of iodo-bIGFBP-2 species.
- Table 3.2 A summary of bIGFBP-2 tryptic peptides identified by tyrosine-specific fluorescence.
- Table 3.3 A summary of bIGFBP-2 tryptic peptides identified by <sup>125</sup>I-radioactivity.
- Table 4.1 A summary of IGF binding parameters derived from solution binding assays,
- Table 4.2 A summary of kinetic parameters derived from the interaction of bIGFBP-2 species on IGF-coupled biosensor surfaces.

## ABBREVIATIONS

<sup>125</sup> I-IGF	radio-iodinated IGF-I tracer
ALS	acid labile subunit
BSA	bovine serum albumin
BCIP	5-bromo-4-chloro-3-indolyl phosphate
BCIG, X-GAL	5-bromo-4-chloro-3-indolyl-β-D-galactopyranoside
bIGFBP-2	bovine IGFBP-2
β-ME	2-mercaptoethanol
CD	circular dichroism
cDNA	complementary deoxyribonucleic acid
CIP	calf intestinal alkaline phosphatase
CPM	counts per minute
CRC	Co-operative Research Centre
DTE	dithioerythritol
DTT	dithiothreitol
DMEM	Dulbeccos Modified Eagle's Medium
<i>E. coli</i>	<i>Escherichia coli</i>
ECM	extracellular matrix
EDC	N-ethyl-N'-[(dimethylamino)propyl]carbodiimide
EDTA	ethylenediaminetetraacetic acid
ES-MS	electrospray mass spectrometry
FPLC	fast performance liquid chromatography
FCS	fetal calf serum
GAG	glycosaminoglycan
GH	growth hormone
Hepes	4-(2-hydroxyethyl)1-piperazine- ethanesulphonic acid
HOI	hypoiodous acid
HPLC	high performance liquid chromatography
IAA	iodoacetic acid
IGF-I and IGF-II	insulin-like growth factors I and II
IGFBP-1 to IGFBP-6	insulin-like growth factor binding proteins 1 to 6
IPTG	isopropyl β-D-thiogalactopyranoside
ITSS	Insulin-transferrin sodium selenite media supplement

LB	Luria-Bertani
NBT	nitroblue tetrazolium
NHS	N-hydroxysuccinimide
NMR	nuclear magnetic resonance
PAGE	polyacrylamide gel electrophoresis
PCR	polymerase chain reaction
PDB	Protein Data Bank, Brookhaven.
PEG	polyethyleneglycol
p.f.u	plaque forming units
RU	resonance units
SDS	sodium dodecyl sulphate
TFA	trifluoroacetic acid
Tris	2-amino-2-hydroxymethylpropane-1,3-diol
UV	ultra-violet

## LIST OF ORIGINAL PUBLICATIONS

This thesis is based on the following publications:

Hobba G.D., Forbes B.E., Parkinson E.J., Francis G.L., Wallace J.C. (1996) The insulin-like growth factor (IGF) binding site of bovine insulin-like growth factor binding protein-2 (bIGFBP-2) probed by iodination. *J. Biol. Chem.* **271**: 30529-36.

Hobba G.D., Lothgren A., Holmberg E., Forbes B.E., Francis G.L., Wallace J.C. (1998) Alanine screening mutagenesis establishes tyrosine 60 of bovine insulin-like growth factor binding protein-2 as a determinant of insulin-like growth factor binding. *J. Biol. Chem.* **273**: 19691-19698.

and conference proceedings:

Hobba G.D., Forbes B.E., Parkinson E.J., Francis G.L., Wallace J.C. (1995), The tryptic map of bovine insulin-like growth factor binding protein-2 (bIGFBP-2) - A step toward identifying the insulin-like growth factor binding site. Proceedings of the 20th Lorne Protein Conference, (Lorne, Vic., Australia). Poster.

Hobba G.D., Forbes B.E., Francis G.L., Wallace J.C. (1996) The binding site of insulin-like growth factors (IGFs) on insulin-like growth factor binding protein-2 (IGFBP-2) - IGF mediated protection against iodination. Proceedings of the 21st Lorne Protein Conference, (Lorne, Vic., Australia). Poster.

Hobba G.D., Forbes B.E., Francis G.L., Wallace J.C. (1996) Localisation of the IGF binding site on IGFBP-2. Proceedings of the 10th Symposium of The Protein Society (San Jose, CA, U.S.A.). Poster.

Hobba G.D., Forbes B.E., Francis G.L., Wallace J.C. (1996) Localisation of the IGF binding site on IGFBP-2. Proceedings of the 6th Biennial IGF Symposium (Sydney, NSW, Australia). Oral.

\*Hobba G.D., Forbes B.E., Francis G.L., Wallace J.C. (1997) Probing the IGF binding site of IGFBP-2 by mutagenesis. Proceedings of the 22nd Lorne Protein Conference, (Lorne, Vic., Australia). Poster.

Hobba G.D., Forbes B.E., Francis G.L., Wallace J.C. (1997) "The binding site of IGFBP-2 probed by mutagenesis. Proceedings of the 2nd European Symposium of The Protein Society (Cambridge, U.K.). Poster.

Hobba G.D., Forbes B.E., Francis G.L., Wallace J.C. (1997), "Probing the binding site for insulin-like growth factor (IGF) on IGF binding protein-2 by protein engineering. Proceedings of the Melbourne 1997 ASBMB conference, (Melbourne, Vic., Australia). Oral.

\*Hobba G.D., Forbes B.E., Francis G.L., Wallace J.C. (1998), "BIAcore Analysis of IGF binding to mutants of IGFBP-2. Proceedings of the 23rd Lorne Protein Conference, (Lorne, Vic., Australia). Poster.

\* indicates posters that were awarded prizes.

## INTRODUCTION

**“A common theme of growth factor biology is the existence of a substantial extracellular storage capacity in which sequestered factors are functionally inert. Growth factors are accessed and bio-activated via a further tier of closely regulated, target tissue-specific mechanisms” (Logan & Hill, 1992).**

Growth factors are soluble messenger molecules that stimulate cellular growth, differentiation and proliferation through specific receptor interactions on responsive cells. Essentially all cell types secrete a range of growth factors and in addition, display a variety of growth factor receptors. As responsive cells can be stimulated by both endocrine and locally produced growth factors, growth factor activity must be strictly regulated to prevent uncontrolled growth at inappropriate sites. The regulation of growth factor bio-availability is one key strategy that has evolved to coordinate cellular activation by growth factors (Logan & Hill, 1992).

The insulin-like growth factors (IGF-I and IGF-II) are excellent examples of growth factors whose bio-availability is strictly regulated after synthesis. The IGFs are ubiquitous, being the most abundant growth factor present in the circulation and are produced by most tissues of the body (reviewed by Humbel 1990; LeRoith 1996). Yet free IGFs are virtually undetectable in tissues or in serum. Instead, IGFs are almost exclusively found in protein complexes with members of a family of six structurally related high-affinity IGF binding proteins (IGFBP-1 to 6) (reviewed by Rechler, 1993; Baxter, 1994; Jones & Clemmons, 1995; Rajaram *et al.*, 1997). Therefore, after synthesis, the primary controls of IGF bio-availability and thus activity are firstly, the specific IGFBP to which the IGF is bound, secondly, the affinity of the IGF/IGFBP interaction and finally, the physical location of the IGF/IGFBP complex in the body.

The IGFs possess broad activities. They act systemically in an “insulin-like” fashion to influence serum glucose levels. At the cellular level they stimulate DNA, protein and carbohydrate synthesis. In addition, the IGFs exhibit potent anti-apoptotic effects and have been shown to stimulate terminal differentiation in some cell types. Given the diverse biological effects of IGFs and the central role of IGFBPs in the regulation of IGF activity, the molecular interactions between the IGFs and IGFBPs are of particular interest. High resolution NMR structures of both IGF-I and IGF-II have been published (Cooke *et al.*, 1991; Sato *et al.*, 1993; Torres *et al.*, 1995). Furthermore, some of the features of the IGF

structure that mediate receptor and IGFBP interactions have been identified by chemical modification (Maly & Lüthi, 1988; Moss *et al.*, 1990) and mutagenic strategies (Bach *et al.*, 1993; Bagley *et al.*, 1989; Cascieri *et al.*, 1988; Cascieri *et al.*, 1989a; Cascieri *et al.*, 1989b; Clemmons *et al.*, 1992; Francis *et al.*, 1993; Oh *et al.*, 1993). By contrast, the tertiary IGFBP fold is unknown and the amino acid residues that comprise the IGF binding site of the IGFbps are yet to be identified. Therefore, the main objective of the research presented in this thesis was to identify residues of the IGFBP-2 molecule that confer IGF affinity. The identification of such residues provides new insight into the IGF/IGFBP binding mechanism at the molecular level and will facilitate the design of novel IGFbps with modified activities.

This review will (1) briefly introduce the IGF system to provide an overview of its components and biological roles. Themes that are examined in more detail are: (2) the structure of IGFs and regions of the IGF structure that interact with the IGF-I receptor and IGFbps (3) the primary structure of IGFbps (4) features of IGFbps that influence IGF affinity and localisation and (5) indirect evidence of the IGF binding site on IGFbps and finally, (6) the aims and strategy of the research presented in this thesis.



**CHAPTER 1 - THE IGFBP<sub>s</sub>: THEIR BIOLOGICAL ROLES AND  
MOLECULAR INTERACTIONS**



## **1.1 The insulin-like growth factor system - an overview**

**“It remains a challenge to investigators to unravel the interplay among the IGFs, the IGF receptors and the IGFbps and their variants in the regulation of growth and development” (Firth, 1998)**

### **1.1.1 Biological Roles**

All recent reviews of IGF biology have reached similar conclusions: the IGF system plays a major role in the growth and differentiated function of essentially all tissues of the body (Florini *et al.*, 1996; Jones & Clemmons, 1995; LeRoith, 1996; Wood, 1995). Transgenic studies (reviewed by Jones & Clemmons, 1995; Wood, 1995) have conclusively shown that IGFs are essential for foetal growth and development. To a large extent IGF-I mediates the pituitary growth hormone (GH) stimulation of bone and skeletal muscle development which ultimately leads to longitudinal growth (reviewed by Florini *et al.*, 1996; Ohlsson *et al.*, 1998). Furthermore, IGFs are involved in regulating the function of mature organs such as the kidney (recently reviewed by Feld & Hirschberg, 1996). Finally, the IGF system has been proposed to acutely regulate the insulin sensitivity or resistance of the individual, according to their nutritional status (Froesch *et al.*, 1998).

The growth promoting and metabolic effects of IGFs *in vivo* can also be demonstrated *in vitro* with a diverse range of cell types in culture. The addition of IGFs to cell culture medium produces both short term stimulatory effects on protein and carbohydrate synthesis as well as longer term stimulatory effects on DNA synthesis, cell replication and differentiation (Jones & Clemmons, 1995). Thus, IGFs are considered to act as cell cycle progression factors, to act as potent mitogens, to specifically inhibit apoptosis, to specifically induce terminal differentiation and to regulate a variety of cell-specific functions such as chemotaxis and hormone secretion (Jones & Clemmons, 1995)

### **1.1.2 IGF System Components And Their Distribution**

The IGF system comprises a complicated network of specific protein-protein interactions that occur both in the circulation as well as in peripheral tissues, as summarised in Fig. 1.1. The components of this system include the IGF ligands (IGF-I and IGF-II), the IGF receptors (type-1 IGF receptor and type-2 IGF-receptor which is also known as the IGF-II/cation independent mannose-6-phosphate receptor), the IGF binding proteins (IGFBP-1 to 6) and finally, the molecules and enzymes that specifically bind to or modify

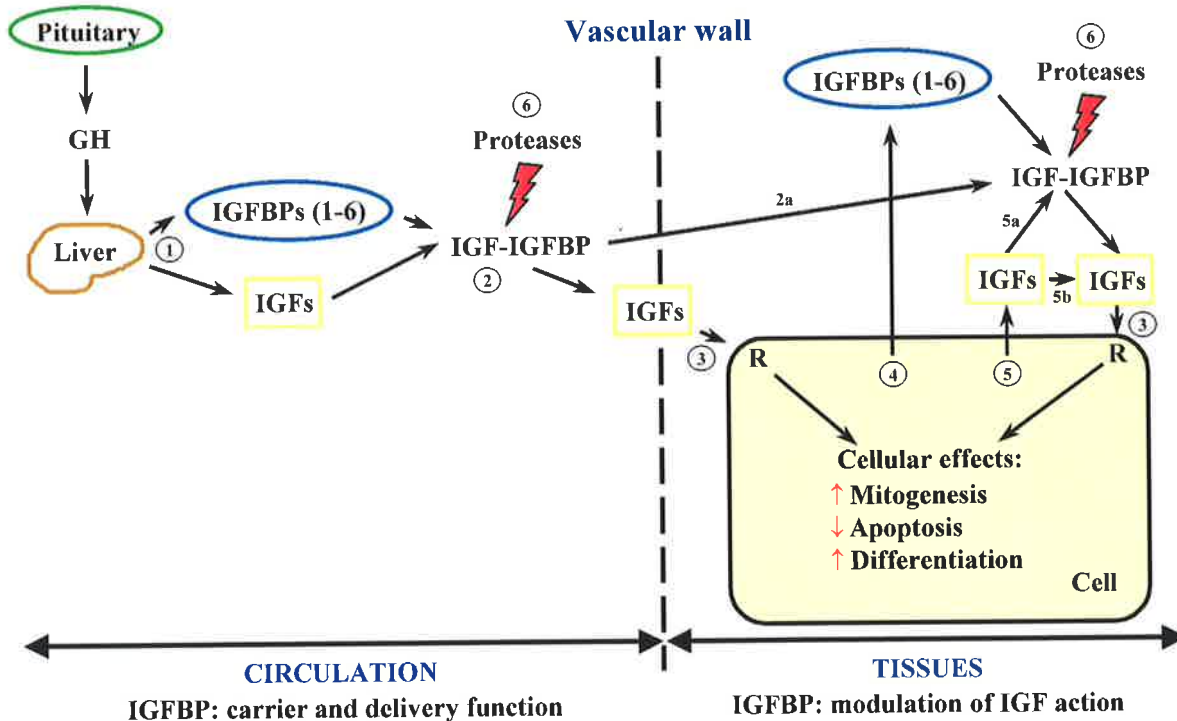


Fig. 1. **Summary of the IGF system interactions.** IGFs and IGFBPs that are produced by the liver and other organs are secreted into the circulation (1). Greater than 95 % of IGFs circulate in complexes with IGFBPs(1-6) and up to 70 % of IGFs circulate with ALS and IGFBP-3 in a ternary complex (reviewed, Rajaram *et al.*, 1997) (2). At 150 kDa, the ternary complex is too large to traverse the vascular wall, however binary complexes between specific IGFBPs and IGFs lead to tissue specific IGF delivery (2a). The cellular effects of IGFs are mediated by the type-1 IGF-receptor (R) which is found on the surface of responsive cells (3). IGFBPs (4) and IGFs (5) are also locally produced and IGFs can either bind IGFBPs, which will result in their latent storage (5a) or act in an autocrine-paracrine fashion (5b). Finally, proteases in circulation and in tissues (6) can increase the bioavailability of IGFs for type-1 IGF-receptor interactions by cleaving IGFBPs. Adapted from Cianfarini & Rossi, 1997.

IGFBPs to alter their affinity for IGFs, for example IGFBP specific proteases. The high levels of IGFs and IGFBPs in circulation suggests an endocrine role for the IGF system. Furthermore, IGF infusion produces systemic effects which include the suppression of glucose and circulating pituitary growth hormone (GH) levels (reviewed by Zapf, 1995) and enhanced glomerular filtration in the kidney (Feld & Hirschberg, 1996). However each tissue environment contains IGF ligand and a number of the IGFBPs. Moreover, essentially all cells possess IGF receptors, and therefore the IGF system must also act at an autocrine/paracrine level.

The liver is the major source of the IGFs in the circulation (reviewed by Humbel, 1990). With normal concentrations in the range of 25 nM to 40 nM (IGF-I) and 65 nM to 105 nM (IGF-II) the IGFs are the most abundant growth factor present in the serum of healthy human subjects (Humbel, 1990). By comparison, insulin levels in the circulation peak at between 0.3 nM and 0.5 nM after food is ingested (Karam, 1987). Pituitary growth hormone is the best known stimulator of IGF-I synthesis, however, the mechanisms that

regulate hepatic synthesis of IGF-II are less clear (Humbel, 1990). In the circulation, IGFs are found predominantly with IGFBP-3 and the acid labile subunit (ALS) in a 150 kDa ternary complex which is too large to traverse the vascular epithelium (Baxter, 1994). Whilst the ternary 150 kDa complex is the major circulating depot of IGFs, lower molecular weight binary complexes between IGFs and IGFBP-1, IGFBP-2, IGFBP-3 and IGFBP-6 which are free to leave the vascular compartment are also present (reviewed by Baxter, 1994 and more recently, Rajaram *et al.*, 1997). These binary complexes have been proposed to acutely modulate IGF metabolic activity and direct the transport of IGFs to specific tissues.

### **1.1.3 IGF Receptors**

IGF receptors mediate IGF activity at the cellular level and control the turnover and bio-availability of IGF-II. Mammals possess two distinct IGF receptors, the type-1 IGF-receptor and the type-2 IGF-receptor (reviewed by Humbel, 1990; Nissley & Lopaczynski, 1991). The type-1 IGF-receptor is a member of the insulin receptor super-family of tyrosine kinases (Nissley & Lopaczynski, 1991) which binds IGF-I with an affinity that is marginally higher than for IGF-II. Insulin also binds the type-1 IGF-receptor but with an affinity approximately 1000-fold less than IGF-I. Transgenic studies with type-1 IGF-receptor, IGF-I, IGF-II and type-2 IGF-receptor knockout mice show conclusively that the mitogenic and metabolic effects of IGFs are mediated by the type-1 IGF-receptor (Baker *et al.*, 1993). In contrast, the type-2 IGF-receptor, which only binds IGF-II with high affinity, has been shown to be primarily involved in endosomal trafficking. By sequestering IGF-II, the type-2 IGF-receptor may directly control the bio-availability of IGF-II for type-1 IGF-receptor interactions. It is likely that the type-2 IGF-receptor also plays a role in the removal and degradation of IGF-II (Sohar *et al.*, 1998).

### **1.1.4 IGFBPs**

Essentially all of the IGFs, whether in circulation or in the extracellular space, are associated with one of six IGFBPs (IGFBP-1 to 6). Each IGFBP displays multiple functions, some of which are common to all family members (such as IGF binding) and some that are unique (such as extracellular matrix binding, cell surface binding or specific protease sensitivity). Furthermore, each tissue and biological fluid exhibits a distinct pattern of the six IGFBPs due to cell specific IGFBP expression as well as unique localisation determinants that are characteristic of the different IGFBPs (reviewed by Rechler, 1993). Cell and tissue specific IGFBP expression patterns change during

Modifications to IGFbps that lead to a reduction in IGF-affinity, such as limited proteolysis and the interaction of IGFbps with other molecules such as glycosaminoglycans can lead to the release of IGFs and the full recovery IGF activity.

development and in response to pathological conditions (Zapf, 1995). It has therefore been predicted that each IGFBP plays a specific role in the tissue- and context-specific coordination of IGF activity (see reviews by Jones & Clemmons; 1995; Rechler, 1993).

The IGFBPs have been proposed to coordinate IGF activity in four major ways: by transporting IGFs in plasma, by controlling IGF half-life and clearance, by allowing tissue specific transport from the vasculature and finally, by directly modulating IGF access to the type-1 IGF-receptor (reviewed by Baxter, 1994; Jones & Clemmons, 1995; Rechler, 1993). IGFBPs directly modulate IGF biological activity by either inhibiting or potentiating IGF action. All of the IGFBPs, when added to cultured cells, inhibit the biological effects of IGFs in a dose dependent manner (reviewed by Jones & Clemmons; 1995; Rechler, 1993). The inhibitory activity of the IGFBPs arises from their ability to sequester IGFs in a latent complex that cannot activate the type-1 IGF-receptor. However, the inhibition of IGF activity by IGFBPs is reversible. Indeed, all of the IGFBPs (with the exception of IGFBP-4) can also potentiate IGF activity when pre-incubated with some cell types (Jones & Clemmons, 1995). The association of IGFBPs with cell surface and extracellular matrix glycosaminoglycans is a prerequisite for the potentiation of IGF activity (Conover *et al.*, 1990; Jones *et al.*, 1993c). Moreover, the association of some IGFBPs with cell surfaces or the extracellular matrix is known to reduce their affinity for IGF-ligand (reviewed by Jones & Clemmons, 1995). The IGFBPs may therefore potentiate IGF activity by co-localising IGFs to specific cell surfaces or extracellular matrix sites, where IGFs can then be slowly released at a rate that avoids down-regulation of the type-1 IGF receptor (Rechler, 1993).

Intensive study of the tissue distribution, expression patterns and gene regulation of IGFBP family members has led to some insight into specific roles for some IGFBPs (see detailed reviews by Jones & Clemmons, 1995; Rechler, 1993; Zapf, 1995). For example, the multi-hormonal control of IGFBP-1 expression, which resembles that of the gluconeogenic enzyme phosphoenolpyruvate carboxykinase (PEPCK), has suggested that IGFBP-1 plays a role in glucose counter regulation by inhibiting the hypoglycaemic effects of IGFs between meals (Lee *et al.*, 1993; Lewitt & Baxter, 1991; Powell *et al.*, 1993). Similarly, the ability of IGFBP-3 to form the abundant and long-lived 150 kDa ternary complex in circulation implicates IGFBP-3 as the major storage protein for the IGFs in blood (Baxter, 1994). However, much less is known regarding the specific physiological roles for IGFBP-2, IGFBP-4, IGFBP-5 and IGFBP-6 (Zapf, 1995).

IGFBP-2, the subject of this thesis, is widely expressed in the foetus where its expression pattern closely follows that of IGF-II (Wood *et al.*, 1992; Carr *et al.*, 1995). At

birth, however, IGFBP-2 expression is dramatically down-regulated and restricted to specific tissues (Wood *et al.*, 1992; Carr *et al.*, 1995). This has led to the prediction that IGFBP-2 may coordinate IGF actions during embryogenesis. It is therefore interesting that IGFBP-2 knock-out mice do not display any gigantism or tissue disorganisation but are morphologically normal with the exception of a 50 % reduced spleen mass and elevated circulating levels of IGFBP-1, IGFBP-3 and IGFBP-4 (Pintar *et al.*, 1995). In addition to a possible role in foetal development, IGFBP-2 may also participate in tumorigenesis. This prediction follows the observation that IGFBP-2 is secreted by a wide range of human tumor cell-lines in culture, including breast carcinomas, Wilms' tumour, neuroblastoma, retinoblastoma, colon carcinoma, liver adenocarcinoma and non-small-cell lung carcinoma (Reeve *et al.*, 1992). Furthermore, serum IGFBP-2 levels were found to be elevated in patients with epithelial ovarian cancer (Flyvbjerg *et al.*, 1997)

Clearly, it is difficult to determine specific roles for each IGFBP through the characterisation of tissue distribution, expression pattern or gene knock-out alone. Indeed, many basic questions regarding the IGFBP family as a whole remain. Why have so many IGFbps evolved? Can the concerted action of multiple IGFbps account for the broad range of IGF activities? What are the specific roles of each IGFBP? At the molecular level, is there a common IGF binding mechanism in the IGFBP family?

### **1.1.5 IGF System - Summary**

In summary, the IGFs exhibit a broad range of activities and play a key role in foetal development, normal growth and the maintenance of function in tissues and organs. Specific protein-protein interactions form the basis of the IGF system. In particular, IGF-IGFBP interactions are central to the post-translational control of IGF activity. Thus, a detailed understanding of the molecular basis for IGF and IGFBP interactions is necessary to unravel the complexity of IGF action. The next section of this review will describe the structures of IGF-I and IGF-II and summarise the elements of the IGF structures that are important for type-1 IGF receptor and IGFBP interactions.

## **1.2 IGF Structure and function**

**“In 1953, Frederick Sanger determined the amino acid sequence of the protein hormone insulin. This work was a landmark in biochemistry because it showed for the first time that a protein has a precisely defined amino acid sequence” (Stryer, 1988)**

### 1.2.1 IGF Structure

Rinderknecht and Humbel's discovery in 1978 that IGF-I and IGF-II not only possessed insulin-like activity, but also shared a high degree of sequence homology with pro-insulin (Rinderknecht & Humbel, 1978a; Rinderknecht & Humbel, 1978b) initiated the study of IGF structure and function. By 1978, the insulin molecule had been thoroughly characterised in terms of its biological activity, its mechanism of action via the insulin receptor and its structure (reviewed by Gammeltoft, 1984). The insulin structure provided the basis for the first IGF molecular models to be built (Blundell *et al.*, 1978). More recently, NMR structures of IGF-I (Cooke *et al.*, 1991; Sato *et al.*, 1993) and IGF-II (Terasawa *et al.*, 1994; Torres *et al.*, 1995) have enabled the detailed correlation of IGF structure-function relationships to be made.

A simple nomenclature for the description of IGF structures has been devised according to the pro-insulin structure (Blundell & Humbel, 1980). Thus, the A, B and C-domains of the single-chain IGF molecules correspond to the A, B and C chains of pro-insulin respectively. However, the IGFs differ from pro-insulin in their C-domains, which are much smaller and are not removed during processing and in the possession of an additional D-domain. In IGF-I, the amino acid residues Gly-1 to Thr-29, Gly-30 to Thr-41, Gly-42 to Cys-62 and Ala-63 to Ala-70 correspond to domains B, C, A and D respectively. Similarly, in IGF-II, the amino acid residues Ala-1 to Phe-28, Ser-29 to Arg-40, Gly-41 to Ala-61 and Thr-62 to Glu-67 correspond to domains B, C, A and D respectively. The homologous domain structures of IGF-I, IGF-II and insulin are illustrated by amino-acid alignment in Fig. 1.2.

The IGFs are extremely stable molecules that exhibit compact globular structures with hydrophobic cores. The IGF secondary structural framework is helical and this framework is stabilised by three disulfide bonds whose integrity are critical for full IGF-activity (Hober *et al.*, 1992; Milner *et al.*, 1995). In contrast, the N-terminus, the C-domain and the D-domain are three regions of high mobility in the IGF structure. The general topology of the IGF structure (illustrated in Fig. 1.3) is as follows; the N-terminus begins with a short flexible stretch of residues that leads directly into a large  $\alpha$ -helical structure (the B-helix). Directly following the B-helix is a  $\beta$ -turn and a short extended loop of 4 residues that terminates the B-domain. From the end of the B-domain, the polypeptide chain continues through the C-domain, a large flexible peptide of approximately 13 residues joining the B-domain to the A-domain. The A-domain begins with a short  $\alpha$ -helix



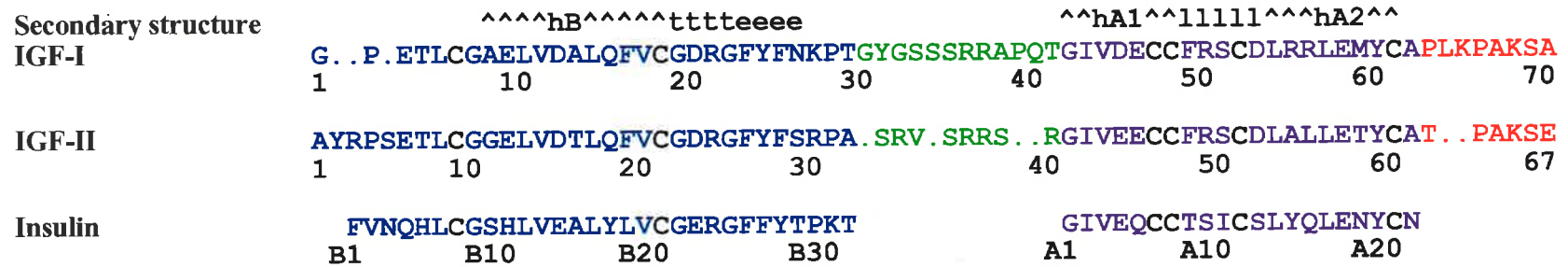


Fig. 1.2 - Sequence Alignment and Domain Arrangement of IGFs and insulin. The B, C, A and D domains of IGFs are coloured blue, green, magenta and red respectively. The conserved cysteine residues are shown in black. Secondary structure has been summarised and the symbols ^, t, e and l correspond to residues involved in helices, b-turns, extended structures and loops respectively. The numbering system of each protein is under the respective sequences.

structure (the A1-helix) which is linked to a second short  $\alpha$ -helical structure (the A2-helix) by a loop. The D-domain extends beyond the A2-helix as a flexible stretch of residues leading to the C-terminus. The A1 and A2 helices are held anti-parallel to one another by a disulfide bridge between the A1 helix and the loop between helices A1 and A2 (Cys-47:Cys-52 in IGF-I and Cys-46:Cys-51 in IGF-II). The A1 and A2 helices are stabilised in a planar orientation over the B helix by two disulfide bonds that link the beginning of the B-helix to the end of the A1-helix (Cys-6:Cys-48 in IGF-I and Cys-9:Cys-47 in IGF-II) and the end of the B-helix to the end of the A2-helix (Cys-18:Cys-61 in IGF-I and Cys-21:Cys-60 in IGF-II).

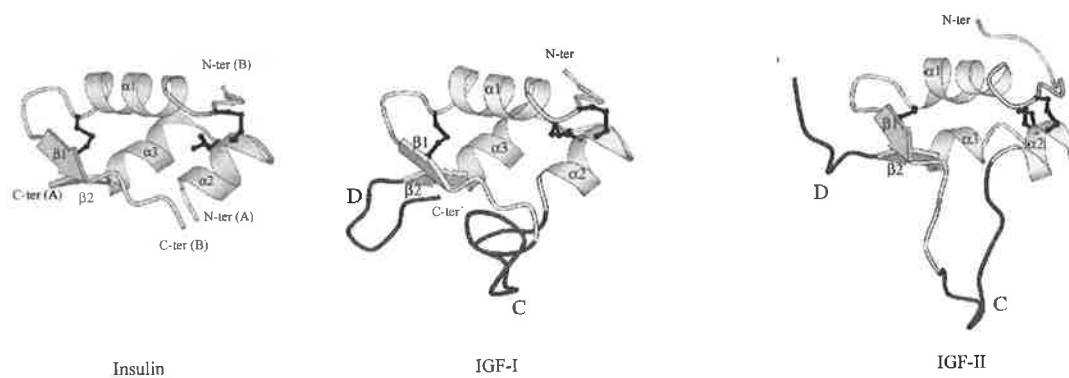


Fig. 1.3 - **Representations of insulin, IGF-I and IGF-II.** The N- and C-termini,  $\alpha$ -helical and  $\beta$ -strand regions of the molecules are labelled. The disulfide bonds are shown in black as ball and stick representations. The C- and D- domains of the IGFs are labelled. These regions of the molecule are highly flexible and their conformations shown here are for illustrative purposes only.

## 1.2.2 IGF Function

Three critical observations have been central to the definition of IGF structure-function relationships. Firstly, the insulin and IGF structures were shown to be homologous. Secondly, the moderate degree of cross-reactivity between insulin and the type-1 IGF-receptor suggested that the well characterised receptor binding region of insulin would provide direct insight into the receptor binding region of IGFs. Finally, as IGFBPs do not bind insulin, the IGFBP-binding region of IGFs could be identified in principle through the systematic generation of IGF/insulin chimeras.

### **1.2.2.1 Insulin And Insulin-Receptor Interactions**

The binding region of insulin for the insulin-receptor was shown to include several residues at the end of the A2-helix (Tyr-A19 and Asn-A21) and the aromatic residues of the extended structure following the B-helix (Phe-B24, Phe-B25 and Tyr-B26) by correlating the biological potency of a variety of chemically and sequence modified insulin analogs (reviewed by Gammeltoft, 1984). Heterogeneous  $^{125}\text{I}$ -labelled insulin exhibited reduced potency in insulin-receptor binding assays (Izzo *et al.*, 1964). Further investigation revealed that mono-iodination at Tyr-A19 led to a 50 % reduction in insulin affinity for the insulin receptor and a 50 % reduction biological potency (Gliemann *et al.*, 1979). Indeed, the mutagenic replacement of leucine for Tyr-A19 led to an insulin molecule with less than 0.1 % activity of the native molecule (Kitagawa *et al.*, 1984). The importance of the B-domain extended structure for receptor binding was shown by truncation studies. The C-terminal truncation of the insulin B-chain by 3 residues (Pro-B28, Lys-B29 and Ala-B30) had no effect on insulin potency (Katsoyannis *et al.*, 1971). However the further removal of 4 residues (Gly-B23, Phe-B24, Phe-B25 and Tyr-B26) led to an insulin molecule that was practically devoid of activity (Kikuchi *et al.*, 1980). Furthermore, the importance of Phe-B25 in insulin-receptor binding was confirmed by the chemical synthesis of Phe-B25→Leu insulin. This insulin analog, originally discovered in a diabetic patient in Chicago, possessed only 1-2 % of the activity of insulin (Kobayashi *et al.*, 1982).

### **1.2.2.2 IGF And Type-1 IGF-Receptor Interactions**

As predicted by ligand-receptor cross reactivity in the IGF and insulin pathways, elements of the insulin structure that were shown to be important in insulin-receptor binding (as described above) were also shown to be important in the IGF/type-1 IGF-receptor interaction. All of the tyrosine residues of IGF-I were protected from iodination when a complex between IGF-I and the type-1 IGF-receptor was iodinated (Maly and Lüthi, 1988). In terms of the A2-helix, mono-iodination at Tyr-60 of IGF-I (corresponding to Tyr-A19 of insulin) resulted in a 36 % reduction in type-1 IGF- receptor binding (Schäffer *et al.*, 1993) and Tyr-60→Leu IGF-I retained only 5 % of the wild-type type-1 IGF-receptor binding (Bayne *et al.*, 1990). The aromatic residues of the extended structure that follows the B-helix of insulin (Phe-B24, Phe-B25 and Tyr-B26) have counterparts in IGF-I (Phe-23, Tyr-24 and Phe-25) and IGF-II (Phe-26, Tyr-27 and Phe-28) as shown in Fig. 1.2. The generation of IGF analogs that corresponded to Phe-B25→Leu insulin confirmed that insulin and the IGFs share a common receptor binding surface. Accordingly,

the mutagenic substitution of leucine for Tyr-24 of IGF-I (Cascieri *et al.*, 1988) and Tyr-27 of IGF-II (Sakano *et al.*, 1991) resulted in IGF peptides that possessed only 1-5 % of their original type-1 IGF-receptor binding affinity.

### **1.2.2.3 IGF And IGFBP Interactions**

The IGF regions that interact with the IGFBPs were initially identified by the generation of insulin-IGF chimeras, an approach that is also known as homologue-scanning mutagenesis. This was possible because the insulin and IGF structures are homologous yet insulin has no measurable affinity for IGFBPs. Thus, the replacement of four IGF-I B-domain residues with their insulin counterparts (Glu-3→Gln, Thr-4→Ala, Gln-15→Tyr and Phe-16→Leu) resulted in an IGF-I analog that bound serum IGFBPs with less than 0.2 % of the affinity of IGF-I (Bayne *et al.*, 1988; Oh *et al.*, 1993). Des(1-3) IGF-I, a naturally occurring IGF-I analog with 0.2 % of wild-type IGFBP binding affinity for certain IGFBPs provided complementary evidence to suggest that Glu-3 of IGF-I was an important site of interaction with IGFBPs (Ballard *et al.*, 1987; Francis *et al.*, 1992). This was confirmed when it was shown that Glu-3→Arg IGF-I was even further compromised in its ability to bind serum IGFBPs (King *et al.*, 1992). Significantly, the corresponding IGF-II analogs des(1-6) IGF-II and Glu-6→Arg IGF-II (Francis *et al.*, 1993) also showed a dramatic reduction in IGFBP affinity with 0.3 % and 0.8 % of the affinity of IGF-II for serum IGFBPs. Therefore, a glutamic acid residue in the flexible N-terminal region leading to the B-helix can be considered as a requirement for the interaction between IGFs and IGFBPs.

Determinants for IGFBP binding have also been found in IGF A-domains by the homologue-scanning mutagenesis approach. In particular, residues of the intervening loop between helices A1 and A2 have been shown to be important in IGFBP interactions. Replacement of Phe-49, Arg-50 and Ser-51 of IGF-I (Cascieri *et al.*, 1989a,b) and Phe-48, Arg-49 and Ser-50 of IGF-II (Bach *et al.*, 1993) with the homologous residues in insulin (Thr-A8, Ser-A9 and Ile-A10) by mutagenesis led to a significant reduction in IGFBP binding. The residual IGFBP affinity of Phe-49→Thr, Arg-50→Ser, Ser-51→Ile IGF-I relative to IGF-I ranged between 2 % and 0.1 % depending on the IGFBP tested. Similarly, the residual IGFBP affinity of Phe-48→Thr, Arg-49→Ser, Ser-50→Ile IGF-II ranged between 15 % and 1 % relative to IGF-II depending on the IGFBP tested.

There is good evidence to suggest that the type-1 IGF-receptor and the IGFBP binding regions of the IGFs overlap. Whereas complex formation with the type-1 IGF-

receptor protected Tyr-24, Tyr-31 and Tyr-60 of IGF-I from iodination (Maly & Lüthi, 1988), complex formation between IGFs and IGFBP-2 also protected Tyr-60 of IGF-I and Tyr-59 of IGF-II from iodination (Moss *et al.*, 1991). In addition, an epitope mapping study of IGF-I identified seven unique monoclonal antibody groups that interfered with IGFBP binding and three of these groups also interfered with type-1 IGF-receptor interactions (Manes *et al.*, 1997). Therefore, although the key residues involved in type-1 IGF-receptor and IGFBP binding are on different faces of the IGF molecule as shown in Fig. 1.4, the IGF binding surfaces for IGFBPs and the type-1 IGF-receptor must extend beyond these critical residues. Furthermore, there has been no evidence to date that a ternary complex between an IGF, IGFBP and type-1 IGF-receptor can form.

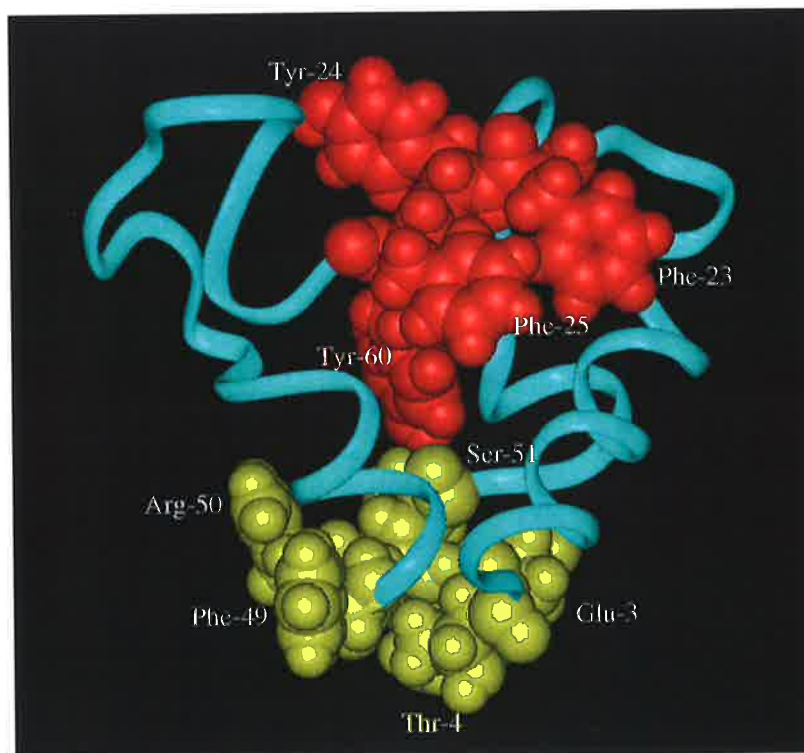


Fig. 1.4 – IGF-I Binding epitopes for the type-1 IGF-receptor and IGFBPs. Illustrated in red are residues of IGF-I that have previously been shown to play a role in type-1 receptor interactions as summarised above. In contrast, residues highlighted in yellow have been shown to comprise the IGFBP binding epitope of IGF-I. Interestingly, Tyr-60 of IGF-I (located at the centre of the diagramme) was protected from iodination by both the type-1 IGF-receptor (Maly & Lüthy, 1989) and bIGFBP-2 (Moss *et al.*, 1990). Therefore, it is likely that the IGF-I binding epitopes for the type-1 IGF-receptor and the IGFBPs overlap.

### 1.2.3 IGF Structure And Function – Summary

In summary, a wealth of information is available regarding the tertiary structures of IGF-I and IGF-II. Furthermore, many of the elements of the IGF structures that are

important for IGF-receptor and IGFBP interactions have been determined using a variety of approaches that include mutagenesis, epitope mapping and chemical modification. Armed with an understanding of IGF structure-function relationships, IGF analogs with novel activities have been engineered and produced. For example, mutagenic disruption of the IGFBP binding site has generated IGF analogues that are more potent growth stimulators than the parent IGF molecule (Cascieri *et al.*, 1989a,b; Francis *et al.*, 1992; Francis *et al.*, 1993).

In contrast to the IGFs, the archetypal IGFBP structure is unknown and furthermore, the residues of IGFBPs that comprise the IGF binding site remain to be identified. However, some aspects of IGFBP structure-function have undergone intensive study; binding sites for other molecules have been identified, as have a range of IGFBP post-translational modifications. The next section of this review will describe IGFBP primary structures and briefly summarise regions of the IGFBPs that are known to be post-translationally modified or to interact with other bio-molecules.

### **1.3 IGFBP STRUCTURE**

**“There is a considerable amount of structural information on some of the members of the IGF system, but not on the IGFBPs” (Spencer & Chan, 1995)**

The study of IGFBP structure is in its early stages. Although the primary structures of IGFBPs have been described, the lack of sequence homology between IGFBPs and proteins of known tertiary structure has prevented the generation of IGFBP molecular models. Also, until recently, the large-scale production of recombinant IGFBPs for structural studies has proven to be a major challenge. Furthermore, with molecular weights that range between 24 kDa and 45 kDa, the IGFBPs are somewhat too large for structure determination readily by NMR. Therefore, the structural characterisation of IGFBPs has relied heavily on sequence analysis.

#### **1.3.1 IGFBP Primary Structure**

IGFBP cDNAs and genes from a wide variety of species have been analysed to yield amino acid sequences for comparison. Conserved gene structures and distinct regions of amino acid sequence homology suggest that the IGFBPs possess three domains (Allander *et al.*, 1993; Baxter, 1994; Jones & Clemmons, 1995; Rechler, 1993). Multiple sequence alignments (Fig. 1.5) illustrate that two of these putative domains, the N- and C-

However, the IGFBP consensus motif is not found in IGFBP-6 sequences. Furthermore, the arrangement of the 3<sup>rd</sup>, 4<sup>th</sup> and 5<sup>th</sup> cysteine in IGFBP-6 (See Figure 1.5, panel *a*) bears subtle differences to the cysteine arrangement in all other IGFBPs. This suggests that in this region of the molecule, IGFBP-6 may possess a unique disulfide bonding pattern.

terminal cysteine-rich domains, are highly conserved, with regions of primary structure that approach 50 % sequence similarity (Landale *et al.*, 1995). It is therefore likely that the N- and C-terminal cysteine-rich domains contain the major structural components of the IGF binding site. In contrast, the middle domain of each IGFBP is unique, and often contains glycosylation, phosphorylation or protease sensitive sites that are IGFBP specific, as summarised in Fig. 1.5. Therefore, the connecting domains of the different IGFBPs may contain determinants that relate to the specific biological roles of each IGFBP.

Motif searching through IGFBP amino acid sequences initially suggested that the IGFBPs may possess sites of post-translational modification or sites of interaction with other proteins. Thus the Pro-Glu-Ser-Thr phosphorylation motif was found in the IGFBP-1 sequence, Asn-X-Ser/Thr N-glycosylation motifs existed in IGFBP-3 and IGFBP-4, numerous glycosaminoglycan-binding sequences were found in IGFBP family members and finally, the Arg-Gly-Asp integrin receptor binding motif was identified in IGFBP-1 and IGFBP-2, as reviewed by Shimasaki & Ling, 1991.

More recently, a range of post translationally modified IGFBP isoforms have been recombinantly produced by eukaryotic expression systems or purified from biological fluids. These modifications include glycosylation (Section 1.4.1.2), limited proteolysis (Section 1.4.2.1) and phosphorylation (Section 1.4.2.2). It has thus been confirmed that post-translational modification is one feature that distinguishes different IGFBPs from each other.

### **1.3.2 The IGFBPs Have A Common Pattern Of Disulfide Bonds**

A characteristic feature of all high-affinity IGFBP sequences is the conserved arrangement of 16 cysteine residues, 10 in the cysteine-rich N-terminal domain and 6 in the cysteine rich C-terminal domain. Indeed, the consensus motif for the identification of IGFBP family members in the Prosite Database of consensus sequences (Bairoch, 1991), Gly-Cys-Gly-Cys-Cys-(2X)-Cys-Ala-(6X)-Cys, includes 5 of the cysteine residues of the cysteine-rich N-terminal domain. All cysteine residues of the IGFBPs are believed to participate in disulfide bonds (Sommer *et al.*, 1991; Tressel *et al.*, 1991). Furthermore, disruption of the native disulfide bonds of IGFBPs by reducing agents (Sommer *et al.*, 1991; Tressel *et al.*, 1991) or by mutagenesis (Brinkman *et al.*, 1991a; Brinkman *et al.*, 1991b) was also observed to disrupt IGF binding.



Panel a

Alignment	1	15	16	30	31	45	46	60	61	75	76	90	91	105	106	120	125					
IBP1_B (1)	-----	APQWR	CAP	CSAERMAL	CPPV---	-----	PAS	-----	CPELTRS	AGCGCCPM	CALPLGAAC	GVATAR	CARGLSCRAL	PGEPR	PLHALTRGQGAC	MTS	F---CDEAT	-----	(90)			
IBP1_H (1)	-----	APWQC	CAP	CSAEKLAL	CPPV---	-----	SAS	-----	CSEVTRS	AGCGCCPM	CALPLGAAC	GVATAR	CARGLSCRAL	PGEQQ	PLHALTRGQGAC	VQE	S---DASAPHA	-----	(91)			
IBP1_M (1)	-----	APQWH	CAP	CTAERLELC	CPPV---	-----	PAS	-----	CPEISR	PAGCGCCPT	CALPLGAAC	GVATAR	CAQGLSCRAL	PGEPR	PLHALTRGQGAC	VLE	F---AAPATSSLSGS	Q----	(97)			
IBP2_B (1)	-----	EVLFR	CPP	CTPESLAACK	PPP---	PGAAAG	PAGDARVP	C-ELVRE	PGCGCCSV	CARLEGER	CGVYTPR	CGQGLRCY	PNPGSEL	PLRALVHGEGT	CEKH	GDA-EYSAS	PEQVAD	NG---	(109)			
IBP2_C (1)	-----	EVLFR	CPP	CTAERLAACS	PA-----	ARP	-----	P	CPELVRE	PGCGCCPV	CARLEDEAC	GVYTPR	CAAGLRCY	PDPGAE	PPQALVQGGT	CARP	PDTDEYGASTE	PPAD	NG---	(101)		
IBP2_H (1)	-----	EVLFR	CPP	CTPERLAAC	GPPPVA	PPAAVA	AVAGGARM	CAELVRE	PGCGCCSV	CARLEGEAC	GVYTPR	CGQGLRCY	PHPGSEL	PLQALVMGEGT	CEKR	RDA-EYGAS	PEQVAD	NG---	(114)			
IBP2_M (1)	-----	EVLFR	CPP	CTPEALAAC	GPPP---	-----	PDA	-----	P	CAELVRE	PGCGCCSV	CARQEGEAC	GVYIPR	CAQTLRCY	PNPGSEL	PLKALVTGAGT	CEKR	R---	VTTPQVAD	SD---	(97)	
IBP2_R (1)	-----	EVLFR	CPP	CTPERLAAC	GPPP---	-----	PDA	-----	P	CAELVRE	PGCGCCSV	CARQEGEAC	GVYIPR	CAQTLRCY	PNPGSEL	PLKALVTGAGT	CEKR	R---	VGATPQVAD	SE---	(97)	
IBP2_S (1)	-----	EVLFR	CPP	CTPESLAACK	PPP---	PGAAAG	PAGDARVP	C-ELVRE	PGCGCCSV	CARLEGER	CGVYTPR	CGQGLRCY	PNPGSEL	PLRALVHGEGT	CEKH	GDA-EYSAS	PEQVAD	NG---	(109)			
IBP3_B (1)	GAGTM	GAGPVVR	CEP	CDARAVAQC	CAPP---	-----	PPSP	-----	P	CAELVRD	AGCGCCLT	CALREGQP	CGVYTER	CGSGLRCQ	PPPGDPR	PLQALLDGRG	LCANA	S---AVGRLR	RPYLLP	SAS--	(107)	
IBP3_H (1)	GASSG	GLGPVVR	CEP	CDARALAQC	CAPP---	-----	PAV	-----	CAELVRE	PGCGCCLT	CALSEGQP	CGIYTER	CGSGLRCQ	PPSPDEAR	PLQALLDGRG	LCVNA	S---AVS	PLRAYLLP	APPAP	(107)	Ref.1,2,3	
IBP3_M (1)	-----	GGPVVR	CEP	CDARAVSQC	CAPP---	-----	PTAP	-----	A	CTELVRE	PGCGCCLT	CALREGD	ACGVYTER	CGTGLRCQ	PRPAEQY	PLRALLN	NGRGFCANA	S---AAGSL	STYLPS	QPAP-	(102)	
IBP3_P (1)	-----	TGPVVR	CEP	CDARALAQC	CAPP---	-----	PAAP	-----	P	CAELVRE	PGCGCCLT	CALREGQ	ACGVYTER	CGAGLRCQ	PPPGEPR	PLQALLDGRG	LCANA	S---AAGRL	RAYLLP	APPAP	(103)	
IBP3_R (1)	GAGAV	GAGPVVR	CEP	CDARALAQC	CAPP---	-----	PTAP	-----	A	CTELVRE	PGCGCCLT	CALREGD	ACGVYTER	CGTGLRCQ	PRPAEQY	PLKALLN	NGRGFCANA	S---AASNLS	SAYLPS	QPSP-	(108)	
IBP4_B (1)	-----	DEAHC	CPP	CSEEKLAR	CRPP---	-----	VG	-----	CEELVRE	PGCGCCAT	CALGKGM	CGVYTPR	CGSGLRCY	PPRGVEK	FLHTLVHGQ	GVCMEL	A---EIEAI	QESLQP	S----	(95)		
IBP4_H (1)	-----	DEAHC	CPP	CSEEKLAR	CRPP---	-----	VG	-----	CEELVRE	PGCGCCAT	CALGLGM	CGVYTPR	CGSGLRCY	PPRGVEK	FLHTLMHGQ	GVCMEL	A---EIEAI	QESLQP	S----	(95)		
IBP4_R (1)	-----	DEAHC	CPP	CSEEKLAR	CRPP---	-----	VG	-----	CEELVRE	PGCGCCAT	CALGLGM	CGVYTPR	CGSGMRCY	PPRGVEK	PLRTL	MHGQGVCTEL	S---EIEAI	Q	LQT	S----	(95)	ref.4
IBP4_S (1)	-----	DEAHC	CPP	CSEEKLAR	CRPP---	-----	VG	-----	CEELVRE	PGCGCCAT	CALGKGM	CGVYTPD	CGSGLRCH	PPRGVEK	FLHTLVHGQ	GVCMEL	A---EIEAI	QESLQP	S----	(95)		
IBP5_H (1)	-----	LGSFVH	CEP	CDEKALSM	CPPS---	-----	PLG	-----	C	ELVKE	PGCGCMT	CALAEGQS	CGVYTER	CAQGLRCL	PRQDEEK	PLHALLHGRG	VCLNE	K---SYRE	QVKI	-----	(92)	
IBP5_M (1)	-----	LGSFVH	CEP	CDEKALSM	CPPS---	-----	PLG	-----	C	ELVKE	PGCGCMT	CALAEGQS	CGVYTER	CAQGLRCL	PRQDEEK	PLHALLHGRG	VCLNE	K---SYGE	QTKI	-----	(92)	
IBP5_P (1)	-----	LGSFVH	CEP	CDEKALSM	CPPS---	-----	PLG	-----	C	ELVKD	PGCGCMT	CALAEGQS	CGVYTER	CAQGLRCL	PRQDEEK	PLHALLHGRG	VCLNE	K---SYRE	QAKI	-----	(92)	
IBP5_R (1)	-----	LGSFVH	CEP	CDEKALSM	CPPS---	-----	PLG	-----	C	ELVKE	PGCGCMT	CALAEGQS	CGVYTER	CAQGLRCL	PRQDEEK	PLHALLHGRG	VCLNE	K---SYGE	QTKI	-----	(92)	
IBP6_H (1)	-----	GGALAR	CPG	CGQGVQAG	CPGG---	-----	CVE	-----	E	EDGGS	PAEGCAE	AEAG	CLRREGQE	CGVYTPN	CAPGLQC	HPKDEEA	PLRALLLGRG	RCLPA	R----	APA	-----	(89)
IBP6_M (1)	-----	ALAGCP	G	CGPGMTG	CRGG---	-----	CVE	-----	E	EDAGS	PADGCTE	AGG	CLRREGQP	CGVYSPK	CAPGLQC	PRENEET	PLRALLIGQ	RQCRA	R----	GPS	-----	(87)
IBP6_R (1)	-----	ALAGCP	G	CGPGVQ	-----	-----	-----	-----	E	EDAGS	PADGCA	ETGG	CFRREGQP	CGVYIPK	CAPGLQC	PRENEET	PLRALLIGQ	RQCRA	R----	GPS	-----	(78)

References:

1. Firth & Baxter, 1995
2. Lalou *et al.*, 1997

3. Vorverk *et al.*, 1998
4. Chernausk *et al.*, 1995

Panel b

```

Alignment 126      140 141      155 156      170 171      185 186      200 201 215
IBP1_B (91) -----DTKDTTSP ENVSPESEITQE-- -QLLDNFHLMAE--- --SSED---LPILWN AISNYESLRALEISD :KK:K----(152) ref.5
IBP1_H (92) -----EAGSP E--SPESTEITEE-- -ELLDNFHLMAP--- --SEED---HSILWD AISTYDGSKALHVTN :KK:K----(148) ref.6
IBP1_M (98) -----HEEAKAAVAS EDELAESPMTTEE-- -QLLDSFHLMAP--- --SRED---QPILWN AISTYSSMRAREITD :KK:K----(161)

IBP2_B(110) -----EEHSEGGLV ENHVDGNVNLMSGGG GAGRKPLKSGMKELA VFREKVTE-QHRQMG KGGKHHGLGEE:PKKL RPPP----- (182) ref.5
IBP2_C(102) -----DDRSESI LA ENHVDSTGGMMSG-- ASSRKPLKTGMKEMP VMREKVNE-QQRQMG KVGKAHHNHEDSKKS RPP----- (171)
IBP2_H(115) -----DDHSEGGLV ENHVDSTMNMLGGGG SAGRKPLKSGMKELA VFREKVTE-QHRQMG KGGKHHGLGEE:PKKL RPPP----- (187) ref.7
IBP2_M (98) -----DDHSEGGLV ENHVDGTMNMLGGGG SAGRKPLKSGMKELA VFREKVNE-QHRQMG KGAK-HLSLEE:PKKL RPPP----- (168)
IBP2_R (98) -----DDHSEGGLV ENHVDGTMNMLGG-S SAGRKPPKSGMKELA VFREKVNE-QHRQMG KGAK-HLSLEE:PKKL RPPP----- (167) ref.8
IBP2_S(110) -----EEHSEGGQV ENHVDGNVNLMSGGG GAGRKPLKFRMKELA VFREKVTE-QHRQMG KGGKHHGLGEE:PKKL RPPP----- (181)

IBP3_B(108) GNGSESEEDHSMGST ENQAGPSTHRVPV-- -SKFHPHHTKMDVIK KGHAKDSQRYKVDYE SQSTDTONFSSSESKR ETEY----- (183)
IBP3_H(108) GNASESEEDRSAGSV ESPSVSTHRVSD-- -PKFHPHLSKIIIIK KGHAKDSQRYKVDYE SQSTDTONFSSSESKR ETEY----- (183) ref.1,9,10,2
IBP3_M(103) GNISESEEEHNAGSV ESQVVPSTHRVTD-- -SKFHPHLSKMDVIK KGHAKDSQRYKVDYE SQSTDTONFSSSESKR ETEY----- (178)
IBP3_P(104) GNGSESEEDRSVDSM ENQALPSTHRVPD-- -SKLHSVHTKMDVIK KGHAKDSQRYKVDYE SQSTDTONFSSSESKR ETEY----- (179)
IBP3_R(109) GNTTESEEDHNAGSV ESQVVPSTHRVTD-- -SKFHPHLSKMEVII KQARDSQRYKVDYE SQSTDTONFSSSESKR ETEY----- (184)

IBP4_B (96) -----DKDE-GDH PNN-----SFSF-- -CSAHDRKCLQKHLA KIRDRSTS-GGKMKV IGAPREEARPV---- (148) ref.11
IBP4_H (96) -----DKDE-SEH PNN-----SFPN-- -CSAHDRKCLQKHLA KIRDRSTS-GGKMKV VGTPREEPRPV---- (148) ref.12,13
IBP4_R (96) -----DKDE-SEH PNN-----SFPN-- -CSAHDRKCLQKHLA KVRDR-----SKMKV VGTPREEPRPV---- (144) ref.4
IBP4_S (96) -----DKDE-GDH PNN-----SFSF-- -CSAHDRKCLQKHLA KIRDRSTS-GGKMKV IGAPREEVPRV---- (148)

IBP5_H (93) -----ERDSRE-HEE PTTSEMAEETYSFKI FRPKHTRISELKAEA :KKDRRKK-ITQSKF VVGAENTAHP:ISA PEMRQESEQ(169) ref.14,5
IBP5_M (93) -----ERDSRE-HEE PTTSEMAEETYSFKV FRPKHTRISELKAEA :KKDRRKK-ITQSKF VVGAENTAHPRVI PA PEMRQESEQ(169)
IBP5_P (93) -----ERDSRE-HEE PTTSEMAEETYSFKI FRPKHTRISELKAEA :KKDRRKK-ITQSKF VVGAENTAHPRVI LA PEMRQESEQ(169)
IBP5_R (93) -----ERDSRE-HEE PTTSEMAEETYSFKV FRPKHTRISELKAEA :KKDRRKK-ITQSKF VVGAENTAHPRVI PA PEMRQESDQ(169)

IBP6_H (90) -----VAEENPKESKPGAG TARPDVNRDRDQQRN PGTSTTPSQPNSAGV QDT----- (136) ref. 15
IBP6_M (80) -----EETTKESKPGGG ASRSRDINHRDRQKN PRSAAPIRPN--PV QDSEM---- (132)
IBP6_R (79) -----EETTKESKPHGG ASRPRD---RDRQKN PRSAAPIRPS--PV QDGEM---- (120)

```

References:

- |                                    |                                  |
|------------------------------------|----------------------------------|
| 5. Hodgkinson <i>et al.</i> , 1994 | 13. Conover <i>et al.</i> , 1995 |
| 6. Jones <i>et al.</i> , 1993a     | 14. Zheng <i>et al.</i> , 1998   |
| 7. Ho & Baxter, 1997               | 15. Neumann <i>et al.</i> , 1998 |
| 8. Wang <i>et al.</i> , 1988       | 16. Jones <i>et al.</i> , 1993b  |
| 9. Hoeck & Mukku, 1994             | 17. Firth <i>et al.</i> , 1998   |
| 10. Fowlkes & Serra, 1996          | 18. Arai <i>et al.</i> , 1996b   |
| 11. Predicted in Swiss-Prot entry. | 19. Parker <i>et al.</i> , 1996  |
| 12. Parker <i>et al.</i> , 1995    |                                  |

Panel c

Alignment	216	230	231	245	246	260	261	275	276	290	291	305	306	320
IBP1_B(153)	--EPCQRELYKVLDR	LAREQQ--KAG--DK		LYKFFYLPNCNKGFY	HSKQCETSLEGE PGL	CWCVYPWSGKRILGS	VAV--RGD	PKCQQYFN	LQN-----	(238)	ref.16			
IBP1_H(149)	--EPCRIELYRVVES	LAKAQE--TSG--EE		ISKFFYLPNCNKGFY	HSRQCETSMDGEAGL	CWCVYPWNGKRIPGS	PEI--RGD	PNCQIYFN	VQN-----	(234)	ref.6			
IBP1_M(162)	--EPCQRELYKVLDR	LAAAQQ--KAG--DE		LYKFFYLPNCNKGFY	HSKQCETSLEGEAGL	CWCVYPWSGKKIPGS	LET--RGD	PNCQHYFN	VQN-----	(247)				
IBP2_B(183)	ARTPCQQEQLDQVLER	ISTMRLPDERGFLEH	LYSLHIPNCDKHGFLY	NLKQCKMSLNGERGE	CWCVNP-TGKLIQGA	PTI--RGD	PECHLFYN	EQ-QGARGVHTQRMQ	(284)	ref.17				
IBP2_C(172)	GRTPCQQEQLDQVLER	ISTMRLPDERGFLEH	LYSLHIPNCDKHGFLY	NLKQCKMSVNGQGE	CWCVDPIHGKVIQGA	PTI--RGD	PECHLFYT	AHEQEDRGAHALRSQ	(275)					
IBP2_H(188)	ARTPCQQEQLDQVLER	ISTMRLPDERGFLEH	LYSLHIPNCDKHGFLY	NLKQCKMSLNGQGE	CWCVNPNNTGKLIQGA	PTI--RGD	PECHLFYN	EQ-QEARGVHTQRMQ	(290)					
IBP2_M(169)	ARTPCQQEQLDQVLER	ISTMRLPDDRGFLEH	LYSLHIPNCDKHGFLY	NLKQCKMSLNGQGE	CWCVNPNNTGKPIQGA	PTI--RGD	PECHLFYN	EQ-QETGGAHAQSVQ	(271)					
IBP2_R(168)	ARTPCQQEQLDQVLER	ISTMRLPDDRGFLEH	LYSLHIPNCDKHGFLY	NLKQCKMSLNGQGE	CWCVNPNNTGKPIQGA	PTI--RGD	PECHLFYN	EQ-QENDGVHAQRVQ	(270)					
IBP2_S(182)	ARTPCQQEQLDQVLER	ISTMRLPDERGFLEH	LYSLHIPNCDKHGFLY	NLKQCKMSLNGQGE	CWCVNPNNTGKLIQGA	PTI--RGD	PECHLFYN	EQ-QGARGVHTQRMQ	(284)					
IBP3_B(184)	--GPCRREMEDTLNH	LKFLNMLS-----	PRGIHIPNCDKKGIFY	KKKQCRPSKGRKRF	CWCVDK-YGQPLPGF	DVKGKGDVHCYSMES	K-----	(264)	ref.5					
IBP3_H(184)	--GPCRREMEDTLNH	LKFLNVLS-----	PRGVHIPNCDKKGIFY	KKKQCRPSKGRKRF	CWCVDK-YGQPLPGY	TTKGKEDVHCYSMQS	K-----	(264)	ref.10,17					
IBP3_M(179)	--GPCRREMEDTLNH	LKFLNVLS-----	PRGVHIPNCDKKGIFY	KKKQCRPSKGRKRF	CWCVDK-YGQRLPGY	DTKGKDDVHCLSVQS	Q-----	(259)						
IBP3_P(180)	--GPCRREMEDTLNH	LKFLNMLS-----	PRGIHIPNCDKKGIFY	KKKQCRPSKGRKRF	CWCVDK-YGQPLPGF	DVKGKGDVHCYSMES	K-----	(260)						
IBP3_R(185)	--GPCRREMEDTLNH	LKFLNVLS-----	PRGVHIPNCDKKGIFY	KKKQCRPSKGRKRF	CWCVDK-YGQPLPGY	DTKGKDDVHCLSVQS	Q-----	(265)						
IBP4_B(149)	PQGSQSELHRALEH	LAASQS--RTH--ED	LYIIPNCDRNGNF	HPKQCHPALDGQRGK	CWCVDRKTGVKLPGG	LEP-KGELDCHQLAD	SFRE-----	(237)						
IBP4_H(149)	PQGSQSELHRALEH	LAASQS--RTH--ED	LYIIPNCDRNGNF	HPKQCHPALDGQRGK	CWCVDRKTGVKLPGG	LEP-KGELDCHQLAD	SFRE-----	(237)						
IBP4_R(145)	PQGSQSELHRALEH	LAASQS--RTH--ED	LFIIIPNCDRNGNF	HPKQCHPALDGQRGK	CWCVDRKTGVKLPGG	LEP-KGELDCHQLAD	SLQE-----	(233)						
IBP4_S(149)	PQGSQSELHRALEH	LAASQS--RTH--ED	LYIIPNCDRNGNF	HPKQCHPALDGQRGK	CWCVDRKTGVKLPGG	LEP-KGELDCHQLAD	SFRE-----	(237)						
IBP5_H(170)	--GPCRRHMEASLQE	LKASPRMV-----	PRAVYLPNCDRKGIFY	KRKQCKPSRGRKRF	CWCVDK-YGMKLPGM	EYVD-GDFQCHTFDS	SNVE-----	(252)	ref.14,18,19,5					
IBP5_M(170)	--GPCRRHMEASLQE	FKASPRMV-----	PRAVYLPNCDRKGIFY	KRKQCKPSRGRKRF	CWCVDK-YGMKLPGM	EYVD-GDFQCHAFDS	SNVE-----	(252)						
IBP5_P(170)	--GPCRRHMEASLQE	LKASPRMV-----	PRAVYLPNCDRKGIFY	KRKQCKPSRGRKRF	CWCVDK-YGMKLPGM	EYVD-GDFQCHSFD	SNVE-----	(252)						
IBP5_R(170)	--GPCRRHMEASLQE	FKASPRMV-----	PRAVYLPNCDRKGIFY	KRKQCKPSRGRKRF	CWCVDK-YGMKLPGM	EYVD-GDFQCHAFDS	SNVE-----	(252)						
IBP6_H(137)	EMGPCRRHLDVSLQQ	LQTEVYRG-----	AQTLVFNCDHRGFY	RRKQCRSSQGRRGP	CWCVDR-MGKSLPGS	PDGN-GSSSCPTGSS	G-----	(218)	ref.5					
IBP6_M(133)	--GPCRRHLDVSLQQ	LQTEVFRGG-----	ARGLYVFNCDLRGFY	RRKQCRSSQGNRRGP	CWCVDP-MGQPLPVS	PDGQ-GSTQCSARSS	G-----	(213)						
IBP6_R(121)	--GPCRRHLDVSLQQ	LQTEVFRGG-----	ANGLYVFNCDLRGFY	RRKQCRSSQGNRRGP	CWCVDP-MGQPLPVS	PDGQ-GSSQCSARSS	G-----	(201)						

Fig. 1.5 – Sequence alignment of IGFBP family members with a summary of IGFBP post-translational modifications. IGFBP sequences (IBP1-6) for bovine (B), chicken (C), human (H), mouse (M), pig (P), rat (R) and sheep (S) were collected from the Swiss-Prot database. The sequences were divided into N-terminal cysteine-rich (panel a), middle (panel b) and C-terminal cysteine-rich (panel c) regions according to their known or inferred gene structures (Landale *et al.*, 1995) and then aligned using the CLUSTAL-W internet server at the Baylor College of Medicine. Across the top of the figure is shown a common numbering system for all sequences in the alignment whereas the numbers in brackets at the beginning and end of each entry correspond to the numbering system of individual sequences, starting with the first residue of the mature protein. Highlighted features include conserved cysteine residues (C), protease sensitive sites (XX), phosphorylation sites (S), predicted glycosaminoglycan binding sites (SRGRKR), N-glycosylation sites (N), O-glycosylation sites (S/T), integrin binding site (RGD) and basic residues that are known to interact with heparin, the extracellular matrix, ALS or cell surfaces (RK/R).

Recently, it was shown that the N-terminal and C-terminal cysteine-rich domains of bIGFBP-2 and hIGFBP-6 form discrete entities with no inter-domain disulfide links (Forbes *et al.*, 1998; Neumann *et al.*, 1998). Furthermore, the connectivity of the disulfide bonds of the cysteine-rich C-terminal domain of bIGFBP-2 was elucidated to be Cys-186:Cys-220, Cys-231:Cys-242 and Cys-244:Cys-265 (Forbes *et al.*, 1998). The same disulfide bonding pattern was also observed in the cysteine-rich C-terminal domain of hIGFBP-1 (Dr. Anna Bilgren, Pharmacia and Upjohn, Stockholm, Sweden, personal communication) Peptide maps of the cysteine-rich N-terminal domains of hIGFBP-1 (Dr. Anna Bilgren, pers. comm.), bIGFBP-2 (Dr. Briony Forbes, University of Adelaide, Adelaide, Australia, personal communication), rIGFBP-3 (Hashimoto *et al.*, 1997) and hIGFBP-6 (Neumann *et al.*, 1998) have enabled the disulfide status of these regions to be partially defined. Thus, in rIGFBP-3, Cys-56 and Cys-69 have been shown to form a disulfide bond and likewise, Cys-63 and Cys-89 are linked by a disulfide bond (Hashimoto *et al.*, 1997). Similarly, in hIGFBP-1, Cys-46 and Cys-59 were linked, as were Cys-53 and Cys-79 (Bilgren, pers. com.). Although the disulfide bonds in the N-terminal cysteine-rich domain of hIGFBP-6 were not unambiguously defined, Cys-71, Cys-78, Cys-84 and Cys-104 (corresponding to Cys-56 and Cys-69, Cys-63 and Cys-89 of rIGFBP-3) were shown to participate in internal disulfide bonds to form a mini-domain (Neumann *et al.*, 1998).

All of the data that is currently available (as described above) holds consistent with the notion that all IGFBPs share a common arrangement of conserved disulfide bonds. Thus it follows that all IGFBPs possess a similar protein structure and as a consequence, a common mechanism of IGF binding. A prediction of the common disulfide-bonding pattern, based on the known disulfide linkages of bIGFBP-1, bIGFBP-2 and rIGFBP-3 is shown in Fig. 1.6

### 1.3.3 IGFBP Secondary Structure Prediction

Mathematical algorithms have been used to predict the secondary structural content of human IGFBP-4, and by comparison, the other IGFBP family members (Landale *et al.*, 1995). This approach predicted that the cysteine rich N-terminal domain was comprised predominantly of  $\beta$ -strands and  $\beta$ -turns. In contrast, the middle and C-terminal cysteine

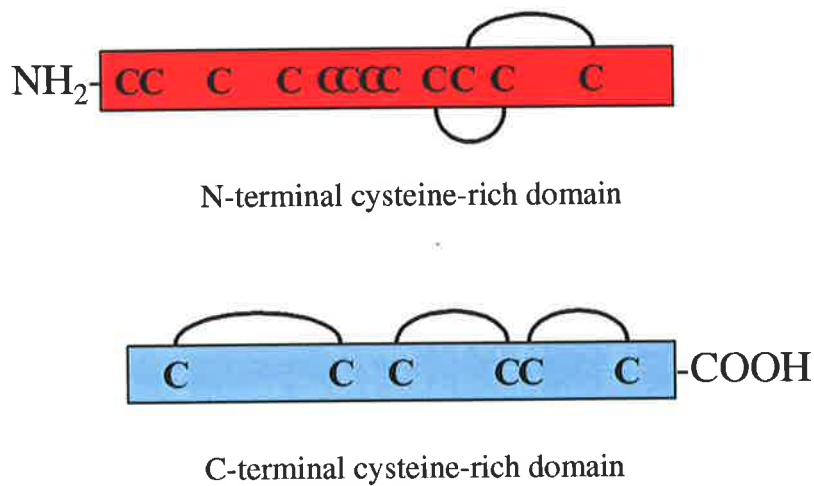


Fig. 1.6 - **Predicted partial disulfide bonding pattern for the IGFBP family.** The disulfide-bonding pattern shown is based on hIGFBP-1, bIGFBP-2 and rIGFBP-3 (N-terminus) and hIGFBP-1 and bIGFBP-2 (C-terminus) as discussed in Section 1.3.2. Only unambiguously defined linkages are shown.

rich domains were predicted to contain mostly helical secondary structural elements. The algorithm, PHD, used in this study, (Rost & Sander, 1993) was estimated to predict secondary structure with 70 % accuracy. Comparison of the predicted secondary structure of the N-terminal domain of hIGFBP-4 (Landale et al., 1995) with the NMR structure of mini-IGFBP-5 ( Kalus et al., 1998) shows that the prediction algorithm could accurately identify that this region contained  $\beta$ -turns and  $\beta$ -strands, but was unable to determine the location of these elements within the hIGFBP-4 sequence.

#### 1.4 IGFBP FUNCTION

**“It seems apparent that the post-translational modification of IGFbps by phosphorylation, glycosylation and proteolysis plays a crucial role in the control of IGF action at the end organ level” (Hintz, 1995)**

The IGFbps are multi-functional proteins; they bind IGFs with high affinity; they store IGFs in an inert form at tissue-specific locations; and finally, they release IGFs in a physiologically appropriate manner. Some aspects of IGFBP structure-function relationships have been studied in detail. These aspects include the analysis of structural elements that enable IGFbps not only to bind IGFs but to associate with specific cellular and extracellular sites. In addition, elements of the IGFBP structure that potentially

integrate the release of IGFs with cellular and physiological signals have also been investigated.

#### **1.4.1 Localisation Determinants Of IGFBPs**

IGFBPs transport IGFs to specific sites in the body by associating with tissue components. All of the IGFBPs have determinants that may interact with either the extracellular matrix of discrete tissues or with the surface of particular cells within the extracellular matrix. These localisation determinants include the integrin receptor binding motif which is present in the IGFBP-1 and IGFBP-2 sequences; the carbohydrate moieties of IGFBP-3, IGFBP-4, IGFBP-5 and IGFBP-6; and finally, the glycosaminoglycan-binding motifs that have been identified in all of the human IGFBPs except IGFBP-4 (reviewed by Rechler, 1993; Jones & Clemmons, 1995). The ALS binding site of IGFBP-3 may also be considered as a localisation determinant because the ternary complex of IGFBP-3, IGF and ALS is limited to the vasculature (reviewed by Baxter, 1994).

##### ***1.4.1.1 Integrin Interactions***

The amino acid sequences of IGFBP-1 and IGFBP-2 contain an Arg-Gly-Asp integrin binding motif that is also a feature of structural proteins of the extracellular matrix such as fibronectin, fibrinogen and vitronectin. The integrins are a family of cell surface receptors that are principally involved in the attachment of cells to the extracellular matrix (reviewed by Hynes, 1987). Both IGFBP-1 and IGFBP-2 are known to associate with cell surfaces (McCusker *et al.*, 1991). However, only IGFBP-1 has been conclusively shown to associate with cell surfaces via integrin interactions (Jones *et al.*, 1993b).

IGFBP-1 binds to Chinese hamster ovary (CHO) cell surfaces via the  $\alpha_5\beta_1$  integrin, also known as the fibronectin receptor (Jones *et al.*, 1993b). The critical residues involved in this interaction include Arg-221, Gly-222 and Asp-223 of IGFBP-1. Interestingly, cell surface integrin binding by IGFBP-1 not only led to the cell surface accumulation of IGFBP-1/IGF complexes, but also stimulated cellular migration (Jones *et al.*, 1993b). Mutagenic disruption of the integrin recognition site was achieved with Arg-221→Trp IGFBP-1. This IGFBP-1 mutant was unable to associate with CHO cells or to stimulate their migration (Jones *et al.*, 1993b).

##### ***1.4.1.2 Glycosylation***

The specificity of a range of glycosidases has indicated that IGFBP-3 and IGFBP-4 are N-glycosylated whereas IGFBP-5 and IGFBP-6 are O-glycosylated. However, IGFBP-3

and IGFBP-6 are the only IGFBPs with well characterised glycosylation sites. Mutagenic studies have confirmed that human IGFBP-3 is glycosylated at Asn-89, Asn-109 and Asn-172 as predicted by the N-linked glycosylation consensus motif Asn-X-Ser/Thr. Alanine substitution for either Asn-89, Asn-109 or Asn-172 reduced the molecular weight of IGFBP-3 by 4, 5 or 6 kDa respectively (Firth & Baxter, 1995). The triple Alanine mutant, Asn-89→Ala, Asn-109→Ala, Asn-172→Ala IGFBP-3 ran as a single band when analysed by SDS-PAGE, with an apparent molecular weight of 31.4 kDa in contrast to the 40-45 kDa doublet commonly observed for IGFBP-3 (Firth & Baxter, 1995). In contrast to IGFBP-3, the glycosylation sites of IGFBP-6 were identified directly by a combination of peptide mapping, N-terminal sequencing and mass spectrometry (Neumann *et al.*, 1998). The major O-glycosylation sites were thus shown to be Thr-126, Ser-144, Thr-145, Thr-146 and Ser-152 (Neumann *et al.*, 1998). Interestingly, the glycosylation sites of IGFBP-3 and IGFBP-6 as well as the putative glycosylation site of IGFBP-4 all occur in the connecting domain of the IGFBPs.

In general terms, the oligosaccharide moieties of glycoproteins are well known sites for cell surface or extracellular matrix interactions. In addition, glycosylation has also been proposed to retard the rate of clearance of glycoproteins from the circulation as well as afford protection against proteolysis (see review by Varki, 1993). Glycosylation bears no influence on the affinity of IGF interactions with IGFBP-3 (Conover, 1991; Firth & Baxter, 1995; Sommer *et al.*, 1991) or IGFBP-6 (Neumann *et al.*, 1998). It is therefore likely that glycosylation plays a role at least in the specific localisation, protease sensitivity or extending the circulating half-life of individual IGFBPs.

#### ***1.4.1.3 Glycosaminoglycan Interactions***

Glycosaminoglycans (GAGs) are major structural components of the extracellular matrix to which IGFBPs are known to bind. Some examples of common GAGs include hyaluronic acid, dermatan sulfate, heparan sulfate and heparin. All of the IGFBPs with the exception of IGFBP-4 contain heparin-binding consensus sequences (Cardin & Weintraub, 1989; Hodgkinson *et al.*, 1994) as summarised in Fig. 1.5. The heparin-binding motif Lys-Gly-Arg-Lys-Arg found in the C-terminal cysteine-rich domains of IGFBP-3 and IGFBP-5 has been shown to be critical for glycosaminoglycan binding (Booth *et al.*, 1995; Booth *et al.*, 1996; Firth *et al.*, 1998; Fowlkes & Serra, 1996). Synthetic peptides corresponding to the heparin binding motif of IGFBP-3 inhibited the ability of both IGFBP-3 and IGFBP-5 to associate with the extracellular matrix and endothelial cell surfaces (Booth *et al.*, 1995;

Parker *et al.*, 1996). Furthermore, the mutagenic disruption of this site in IGFBP-3 (Firth *et al.*, 1998) and IGFBP-5 (Arai *et al.*, 1996b) led to a reduction in heparin affinity and abolished cell surface binding. In contrast to IGFBP-3 and IGFBP-5, IGFBP-2 was only able to associate with the extracellular matrix when in a complex with IGF-I or IGF-II (Arai *et al.*, 1996a).

The heparin binding region appears to play a dual role in the function of IGFBP-3. Not only is this region important for glycosaminoglycan interactions, but it is also necessary for ALS interactions (Firth *et al.*, 1998; Hashimoto *et al.*, 1997). The mutagenic replacement of the heparin binding motif of IGFBP-3 (residues 228-232, as shown in Fig. 1.5) with acidic residues from the corresponding region of IGFBP-1 led to a 90 % reduction in the affinity of ALS and therefore dramatically impaired the formation of the 150 kDa ternary complex (Firth *et al.*, 1998). Furthermore, the co-incubation of IGFBP-3 with heparin was observed to inhibit the association of ALS with IGFBP-3 (Baxter, 1990).

#### **1.4.2 IGF-Release Mechanisms Of IGFBPs**

IGFBPs bind IGFs with an affinity that is typically equal to or an order of magnitude greater than the affinity between IGFs and the type-1 IGF-receptor (Jones & Clemmons, 1995). All evidence to date strongly suggests that IGFs interact with either IGFBPs or the type-1 IGF-receptor in an exclusive manner. It is therefore likely that IGFs must be released from the IGF-IGFBP complex before association with the type-1 IGF-receptor can be achieved (Baxter, 1990; Jones & Clemmons, 1995). The best characterised mechanism for the release of IGFs is by the limited proteolysis of IGFBPs. IGFBPs are cleaved at specific sites by a range of proteases including matrix metalloproteases (Fowlkes *et al.*, 1994), cathepsin D (Claussen *et al.*, 1997), prostate-specific antigen (Cohen *et al.*, 1992) and thrombin (Zheng *et al.*, 1998). Following limited proteolysis, IGFBPs exhibit a dramatically reduced affinity for IGFs.

Interestingly, some of the mechanisms that lead to the localisation of IGFBPs to extracellular matrix and cell surface sites also lead to a reduction in IGF-binding affinity. Thus glycosaminoglycan binding by IGFBPs is a reversible process that results in a reduction in IGF affinity (Arai *et al.*, 1994; Jones *et al.*, 1993c). Phosphorylation is another reversible process that can directly regulate IGFBP interactions. IGFBP phosphorylation can influence IGF activity both by modulating the affinity of IGF-IGFBP interactions and by altering the affinity of IGFBPs for cell surfaces (Coverley & Baxter, 1997).



#### **1.4.2.1 Proteolysis Of IGFBPs**

The degradation of IGFBPs by IGFBP-specific proteases is beginning to be recognised as a general paradigm for the post-translational control of IGFBP activity (reviewed by Rajah *et al.*, 1994; Fowlkes, 1997). Indeed, the tissue specific degradation of IGFBPs may be as important in determining the distribution of the IGFBPs as the tissue specific expression of IGFBPs (Davenport *et al.*, 1992). Each cleaved IGFBP exhibits a dramatically reduced affinity for IGFs, suggesting that IGFBP-proteolysis increases IGF bio-availability for type-1 IGF-receptor interactions. In addition, IGFBP-3 and IGFBP-5 fragments have also been shown to regulate cellular growth in their own right (Andress *et al.*, 1993; Lalou *et al.*, 1997; Zadeh & Binoux, 1997). Therefore, the physiological roles of IGFBP proteolysis are far from completely understood.

Proteolytic degradation has been described for IGFBP-1 (Huhtala *et al.*, 1986), IGFBP-2 (Cohick *et al.*, 1995; Gockerman & Clemmons, 1995; Ho & Baxter, 1997; Wang *et al.*, 1988), IGFBP-3 (Baxter & Skriver, 1993; Lassarre & Binoux, 1994), IGFBP-4 (Conover *et al.*, 1993; Durham *et al.*, 1995) and IGFBP-5 (Andress *et al.*, 1993; Nam *et al.*, 1994; Thrailkill *et al.*, 1995) but not IGFBP-6. In many studies, the IGFBP fragments have only been characterised by SDS-PAGE, an approach that crudely sizes the IGFBP fragments but does not identify the protease sensitive scissile bond(s) of the IGFBP. More recently, the purification and characterisation of IGFBP fragments by N-terminal sequence and mass spectrometric analysis has allowed the respective cleavage sites on the IGFBP molecule to be identified (Chernausek *et al.*, 1995; Conover *et al.*, 1995; Ho & Baxter, 1997; Lalou *et al.*, 1997; Wang *et al.*, 1988). The majority of protease sensitive sites in IGFBPs have been localised to the middle non-conserved domain as summarised in Fig. 1.5.

#### **1.4.2.2 Phosphorylation**

IGFBP-1, IGFBP-3 and IGFBP-5 are known to be serine-phosphorylated at multiple sites in their central domains (reviewed by Coverley & Baxter, 1997). The Phosphorylation state of IGFBP-1 constitutes an IGF-affinity switch, and there is preliminary evidence to suggest that IGFBP phosphorylation may decrease the affinity of IGFBP-3 interactions with ALS and cell surfaces (Coverley & Baxter, 1995). The functional significance of IGFBP-5 phosphorylation is yet to be determined.

Comparison of phosphorylated and non-phosphorylated IGFBP-1 revealed that there were significant alterations in both IGF affinity and biological activity between these

two IGFBP isoforms. Phosphorylated IGFBP-1 exhibited a 6-fold higher affinity for IGF-I compared with terminally dephosphorylated or bacterially expressed IGFBP-1 (Jones *et al.*, 1991). In addition to enhanced IGF-affinity, only phosphorylated IGFBP-1 was observed to inhibit IGF-activity in cell assays (Elgin *et al.*, 1987). In contrast, dephosphorylated IGFBP-1 possessed IGF-potentiating effects when pre-incubated with cultured cells (Busby *et al.*, 1988). This suggested that an inhibitory IGFBP could be converted into a potentiator of IGF activity through modifications that resulted in a modest reduction in IGF-affinity. Three serine residues of IGFBP-1, namely Ser-101 and Ser-119 in the middle domain and Ser-169 at the beginning of the C-terminal cysteine-rich domain, were labelled with  $^{32}\text{P}$  when CHO-K1 cells were grown in the presence of  $^{32}\text{P}$ -orthophosphoric acid (Jones *et al.*, 1993a). Mutagenic replacement of the major site of phosphorylation, Ser-101, with an alanine residue led to a 60 % reduction in  $^{32}\text{P}$  labeling and a 3-fold reduction in IGF-I affinity relative to wild-type IGFBP-1 (Jones *et al.*, 1993a).

Like IGFBP-1, the phosphorylation sites of IGFBP-3, Ser-111 and Ser-113, were also identified in the middle domain. The mutagenic replacement of Ser-111 and Ser-113 with alanine reduced the phosphorylation of IGFBP-3 by 80 % (Hoeck & Mukku, 1994) thus confirming that these residues were the major sites of IGFBP-3 phosphorylation. In contrast to IGFBP-1, the phosphorylation state of IGFBP-3 had no measurable impact on IGF affinity in competition binding assays (Hoeck & Mukku, 1994). However, preliminary evidence suggests that phosphorylated IGFBP-3 may bind with ALS and cell surfaces with greater affinity than does non-phosphorylated IGFBP-3 (Coverley & Baxter, 1997).

#### ***1.4.2.3 Integration of IGF Release With Cellular And Physiological Signals***

IGFBP proteolysis and de-phosphorylation both potentially integrate the release of IGFs with cellular and physiological signals. Protein phosphorylation/de-phosphorylation is a well described mechanism for the rapid and reversible regulation of protein activity (For example, the mediation of intracellular signaling by kinase cascades, reviewed by Shenolikar, 1988). Similarly, many biological systems such as complement activation, tissue remodeling and wound healing operate through proteolytic cascades. For example, the plasminogen system plays a central role in the regulated destruction of extracellular matrix during tissue remodeling (reviewed by Blasi *et al.*, 1987). Plasminogen activators (tissue-type and urokinase-type) are serine proteases that cleave the ubiquitous pro-enzyme plasminogen to its active form, plasmin. Plasmin is a non-specific serine protease that principally digests fibrin in blood clots, however, it also degrades plasma proteins and

proteins of the extracellular matrix (Blasi *et al.*, 1987; Mayer, 1990). In turn, plasmin can activate latent collagenases. As a result, up-regulation of plasminogen activators can bring about a major physiological event in tissue remodeling.

Several studies have identified links between the IGF and plasminogen systems. Urokinase-type plasminogen activator, tissue-type plasminogen activator and plasmin have all been shown to cleave IGFBPs (Campbell *et al.*, 1992; Koutsilieris *et al.*, 1993; Menouny *et al.*, 1997). In addition, IGFBP-5 has been observed to associate with plasminogen-activator inhibitor-I (Nam *et al.*, 1997), which is a regulatory protein that specifically inactivates urokinase-type plasminogen activator and tissue-type plasminogen activator. This highlights the possibility that proteolytic cascades may influence the activity of local IGF-system components.

### **1.4.3 IGFBP Structure And Function – Summary**

The characterisation of IGFBP structure-function relationships has been challenging in the absence of an IGFBP tertiary structure. However, the combination of motif searching and site-directed mutagenesis has provided insight into some of the mechanisms that allow IGFBPs to firstly deliver IGFs to specific locations and subsequently release IGFs for receptor activation. Post-translational modification appears to be a key mechanism for the regulation of IGFBP function. Furthermore, the most common sites of post-translational modification of IGFBPs whether it be glycosylation, phosphorylation or proteolytic cleavage occur in the middle non-conserved domain. Therefore, the middle regions of IGFBPs may be functionally relevant to the specific roles of each IGFBP family member.

Given the intensive study of IGFBP function over the past decade, it is surprising that so little is known about the IGF binding site of the IGFBPs. The next section of this review will summarise current evidence to suggest that the determinants for IGF binding occur in both the N- and C-terminal domains of IGFBPs.

## **1.5 STUDIES TO IDENTIFY THE IGF BINDING SITE OF IGFBPS**

The search for a minimal IGF binding domain has been a priority in IGFBP research. This has stemmed from observations that proteolysed fragments of IGFBPs often retain residual affinity for IGFs. Moreover, an IGFBP fragment which contained the complete and active IGF binding site would greatly facilitate structural studies and simplify efforts to identify IGF binding determinants. Mutagenesis has been used to generate IGFBP fragments either by progressive truncation from the N- or C- termini or by reproducing

naturally occurring fragments. In addition, random mutagenesis has also been used to investigate the N-terminal cysteine-rich domain of IGFBP-1 and its impact on IGF binding.

### **1.5.1 Naturally Occurring IGFBP Fragments.**

IGFBP fragments are present in biological fluids and tissues as a result of limited proteolysis (as discussed in Section 1.4.2.1). A number of IGFBP fragments have been purified and their IGF binding activity analysed by Western ligand blot or by solution binding assays. IGFBP fragments that have been shown to bind IGFs include C-terminally truncated IGFBP-1 (Huhtala *et al.*, 1986), IGFBP-3 (Sommer *et al.*, 1991; Lalou *et al.*, 1997), IGFBP-4 (Chernausk *et al.*, 1995) and IGFBP-5 (Andress *et al.*, 1993). In addition, there have been studies showing that N-terminally truncated IGFBP-2 (Ho & Baxter, 1997; Wang *et al.*, 1988) and IGFBP-3 (Sommer *et al.*, 1991) also possess residual IGF binding activity.

Notably, none of the N-terminal or C-terminal IGFBP fragments retain full IGF binding activity. This has several implications for possible IGF binding mechanisms. Firstly, critical IGF binding determinants may be located in sections of the IGFBP molecule that are absent. Thus, full IGF-binding affinity may only be possible in the presence of both N- and C-terminal domains. Secondly, the three dimensional arrangement of the IGF binding site of IGFBPs may be held in a strained conformation in the intact molecule. After cleavage, this constrained conformation may then collapse to distort the IGF binding site. Therefore, all of the determinants for IGF binding may be present in a given IGFBP fragment, but not correctly arranged for high affinity interactions to occur.

### **1.5.2 Deletion Studies**

Deletion studies have been the most popular strategy used to search for the IGF binding site of IGFBPs. Progressive deletion mutagenesis has been performed on the C-terminal cysteine rich domains of IGFBP-1 (Brinkman *et al.*, 1991b), IGFBP-2 (Forbes *et al.*, 1998) and IGFBP-3 (Hashimoto *et al.*, 1997; Firth *et al.*, 1998). N-terminal domains of IGFBP-3 (Vorverk *et al.*, 1998), IGFBP-4 (Qin *et al.*, 1998) and IGFBP-5 (Andress *et al.*, 1993) have also been produced by mutagenesis.

Early truncation studies of IGFBP-1 suggested that the removal of either 60 residues from the N-terminus (Brinkman *et al.*, 1991a) or 20 residues from the C-terminus (Brinkman *et al.*, 1991b) of IGFBPs would severely disrupt IGF binding. However in a more recent deletion study, up to 48 residues of the C-terminus of IGFBP-2 could be removed before a dramatic loss in IGF binding was observed (Forbes *et al.*, 1998). The key

difference between the two studies is that in the latter, the C-terminal disulfide bonding pattern was considered in the design of the deletion mutants. Whereas IGFBP-1 truncation mutants aggregated into disulfide linked multimers which suggested that gross structural disruption had occurred (Brinkman *et al.*, 1991b), aggregation was not observed in bIGFBP-2 truncation mutants where cysteine pairs were removed and unpaired cysteine altered to serine (Forbes *et al.*, 1998). Ultimately, the removal of a region of bIGFBP-2 that stretched from His-223 to Gln-284 (63 C-terminal residues) lead to a dramatic loss of IGF affinity. This bIGFBP-2 analog was incapable of binding  $^{125}\text{I}$ -IGF-II in Western ligand blots and exhibited an 80-fold reduction in IGF-affinity of the native molecule in solution binding assays.

Although deletion mutagenesis has identified mutants with greatly reduced affinity for IGFs, it is difficult to confidently correlate the loss of IGF binding to the loss of residues which are crucial for IGF binding, as opposed to residues which are important for the stability, solubility and folding of the truncated IGFBPs.

### 1.5.3 Random Mutagenesis

An attempt has been made to identify IGF binding determinants in the N-terminal cysteine rich region of IGFBP-1 by random mutagenesis (Brinkman *et al.*, 1991a). Eight IGFBP-1 analogs were generated with mutations that lay between residues Val-26 and Arg-55 and subsequently expressed in COS-1 cells. Culture medium samples that were conditioned by the transfected COS-1 cell populations were collected and subjected to Western ligand blot analysis with  $^{125}\text{I}$ -IGF-I. The only mutant that exhibited any reduction in apparent affinity for  $^{125}\text{I}$ -IGF-I was Cys-34→Tyr IGFBP-1. In addition to a reduction in IGF-affinity, Cys-34→Tyr IGFBP-1 also exhibited altered motility in the SDS-PAGE analysis and formed disulfide-linked multimers (Brinkman *et al.*, 1991a). These two observations suggest that the loss of  $^{125}\text{I}$ -IGF-I binding was due to gross structural changes in the IGFBP-1 structure. Moreover, it is likely that the disruption of native disulfide bond formation in the N-terminal cysteine rich region led to the observed loss of native IGFBP-1 structure. The results of this particular study were inconclusive for a number of reasons. Firstly, too few mutants were produced to systematically analyse the functional role of the targeted region. Secondly, the ligand blotting technique is insensitive to minor changes in IGF binding affinity and the mutants in this study were not purified or quantified to allow equivalent loading of each IGFBP-1 analog for SDS-PAGE analysis. It is therefore difficult to make direct comparisons of the IGF-binding abilities of the mutants produced in this

study. Finally, this study highlights the need to avoid mutation at structurally important residues. The loss of IGF binding affinity, when combined with gross structural distortion is not necessarily informative about the residues that comprise the IGF binding site of IGFBPs.

#### **1.5.4 Knowledge Of The IGFBP Binding Site Of IGFs**

The key residues of IGFs that are known to be important for IGFBP interactions (see Section 1.2.2.3) include Glu-3, Thr-4, Gln-15, Phe-16, Phe-49, Arg-50 and Ser-51 of IGF-I, and Glu-6, Phe-48, Arg-49 and Ser-50 of IGF-II. Assuming that these residues directly interact with IGFBPs, it is possible to speculate about which IGFBP residues could potentially form favorable contacts. It is possible that basic residues of IGFBPs form electrostatic linkages with Glu-3 and Glu-6 of IGF-I and IGF-II respectively. Clearly, in the absence of an IGFBP structure to assist in the identification of residues on the surface of IGFBPs, this predictive approach is of little benefit. However, as more structural information for the IGFBPs becomes available, knowledge of the IGFBP binding site of IGFs will become invaluable for the simulation of molecular docking between IGFBPs and IGFs and in the design of IGFBPs with altered IGF specificity.

In a recent study, a C-terminal fragment of IGFBP-2 was isolated from human milk and shown to be capable of associating with radio-labelled IGF-I and IGF-II (Ho & Baxter, 1997). However, Des(1-6)-IGF-II could not displace IGF-ligand from the C-terminal IGFBP-2 fragment. It was therefore proposed that the amino-terminal hexapeptide of IGF-II interacted with the C-terminal region of IGFBP-2 (Ho & Baxter, 1997).

#### **1.5.5 Studies To Identify The IGF Binding Site Of IGFBPs - Summary**

Truncation studies and the functional characterisation of IGFBP fragments have begun to provide a rough outline of the IGF binding mechanism. It would appear that both the N- and C-terminal cysteine rich domains are required for high-affinity IGF interactions. This is suggested by the fact that neither N- or C-terminal IGFBP fragments retain full IGF binding whether they be purified from natural sources or generated by mutagenic strategies. Furthermore, limited IGFBP cleavage results in a reduction in IGF affinity, and this may be a general mechanism for IGF release *in vivo*. Therefore, the conformation or spatial arrangement of the N- and C-terminal domains of IGFBPs may be altered after cleavage to result in disruption of the IGF binding site.

The next logical step in the elucidation of the IGF binding site of IGFBPs is in terms of the level of definition. IGF binding determinants need to be localised not simply to

IGFBP domains but to specific regions and residues within IGFBP domains. Whereas deletion mutagenesis is a powerful approach to identify minimal functional domains, it is not a practical approach for the detailed investigation of protein structure/function. Furthermore, as both the N- and C-terminal cysteine-rich domains appear to be involved in IGF interactions, future studies should consider the whole IGFBP molecule.

## **1.6 AIMS AND EXPERIMENTAL STRATEGY**

The lack of information regarding the IGF binding mechanism of IGFBPs constitutes a considerable gap in the understanding of IGFBP function. Furthermore, the growing number of IGFBP structure-function studies described to date have focussed on aspects of IGFBP biology such as heparin binding, integrin receptor binding, extracellular matrix binding, specific proteolysis or phosphorylation (as summarised in Section 1.3) rather than the systematic identification of an IGF-binding motif. Therefore, the purpose of the research presented in this thesis was to identify and characterise specific residues of IGFBP-2 that comprise the IGF binding site. From novel information regarding the IGF binding site of IGFBP-2, it was hoped that IGFBP-2 analogs with altered IGF affinity or specificity could be designed and produced.

As discussed above in Section 1.5, both the N- and C-terminal cysteine rich domains of IGFBPs are believed to participate in IGF-binding. Furthermore, there is a high degree of sequence homology throughout the IGFBP family in both the N- and C-terminal domains. Given that IGFBP molecules are typically over 210 amino acids in length (for example, bIGFBP-2 is 284 residues) and the N- and C-terminal regions account for approximately 2/3 of the IGFBP molecule, the detailed analysis of IGFBP structure-function relationships by alanine-scanning mutagenesis or random mutagenesis is not feasible. Thus, the initial research goal was to identify a small region of the IGFBP-2 molecule that was implicated in IGF binding. The strategy I chose involved the identification of tyrosine residues of bIGFBP-2 that were protected from iodination when IGFs were bound. A mutagenic strategy could then be used to characterise in detail the specific IGF-binding role of each amino acid side-chain that occurred within protected regions of the bIGFBP-2 sequence.

The tyrosine residues of IGFBP-2 provided the best target for chemical modification for five key reasons. Firstly, tyrosine residues are known to frequently occur at sites of protein-protein interactions, for example in antibody-antigen binding sites (Janin & Chothia, 1990; Mian *et al.*, 1991). Secondly, the tyrosine residues of IGFBP-2 are evenly

distributed throughout the primary sequence, thus maximising the possibility that one could occur in an IGF-binding region. Thirdly, of the six tyrosine residues of IGFBP-2, three are well conserved in other members of the IGFBP family. Fourthly, tyrosine residues can be selectively modified by chemical iodination and the iodine radio-isotope  $^{125}\text{I}$  can be detected with great sensitivity. Furthermore, tyrosine residues that are accessible for modification would be anticipated to be located on the surface of the IGFBP-2 molecule and thus potential sites for IGF interactions. Finally, tyrosine iodination is also a useful functional probe because the iodinated tyrosine side-chain has physico-chemical properties that are distinct from the original phenolic ring (Edelhoch, 1962; Cowgil, 1965). Therefore, valuable information about the IGFBP-2/IGF interaction could be gained through the assessment of both the availability of tyrosine residues for reaction as well as the functional impact of tyrosine modification.

Alanine-scanning mutagenesis was chosen as the method to characterise the regions of IGFBP-2 that were protected from iodination by IGFs. The alanine side-chain is chemically and physically “neutral” and therefore alanine substitution should minimise structural changes whilst removing potential sites for protein-protein interactions. The alanine-scanning approach has been used with great success to systematically map the residues of thrombomodulin that bind thrombin and subsequently lead to protein C activation (Nagashima *et al.*, 1993), the residues of growth hormone that confer affinity for the growth hormone receptor (Wells, 1996) and the residues of insulin that are critical for insulin receptor binding (Kristensen *et al.*, 1997) to name a few examples of its utility.

### **Specific aims of this thesis**

1. To identify, by differential chemical modification, the tyrosine residues of bIGFBP-2 which are located in the IGF-I and/or IGF-II binding site(s) of bIGFBP-2.
2. To design and produce analogs of bIGFBP-2 anticipated to show altered specificity or affinity for IGFs based on the information gathered in 1.
3. To characterise the resulting bIGFBP-2 analogs for structural integrity and alterations in IGF binding affinity and/or IGF specificity and thus draw conclusions about the possible roles of tyrosine residues in bIGFBP-2 for IGF binding.



**CHAPTER 2 - RECOMBINANT EXPRESSION OF IGFBP-2 IN  
MAMMALIAN CELL CULTURE**

## 2.1 Introduction

All of the studies presented in this thesis required active, highly purified bIGFBP-2 as starting material. Furthermore, a recombinant expression system was necessary so that ultimately the bIGFBP-2 molecule could be modified by mutagenesis. Initial attempts to express the bIGFBP-2 cDNA isolated by Upton *et al.*, 1990, used a bacterial system that had been established for the production of IGF-I (King *et al.*, 1992). In this system, bIGFBP-2 was expressed as a fusion protein C-terminal to the first 46 residues of porcine growth hormone in *E. coli* (Forbes *et al.*, 1994). The bIGFBP-2 fusion protein was highly expressed and accumulated within the bacteria as inclusion bodies (Forbes *et al.*, 1994). However, the recovery of active bIGFBP-2 relied on successfully refolding the denatured fusion protein and subsequently removing the fusion partner, two processes that presented significant technical difficulties (Polyak, 1994).

As some cultured eukaryotic cells naturally secrete high levels of IGFBPs, a eukaryotic expression system of IGFBP-2 was investigated. bIGFBP-2 was originally isolated from culture medium conditioned by the Madin Darby bovine kidney cell line MDBK (Szabo *et al.*, 1988), and so the monkey kidney cell line COS-1 was anticipated to provide similar cellular machinery for the correct processing and expression of recombinant bIGFBP-2. After reconstruction of the signal peptide for secretion, the bIGFBP-2 cDNA was inserted into the expression vector pXMT2 (Whyatt *et al.*, 1993) to yield the vector pGF8 (Forbes *et al.*, 1998), as illustrated in Fig. 2.1. Transient transfection of COS-1 cells with pGF8 led to the secretion of active bIGFBP-2 into the culture medium. A simple three step chromatographic protocol was then established to purify bIGFBP-2 from the cell culture supernatant (Forbes *et al.*, 1998).

This chapter describes the recombinant production of bIGFBP-2 using the procedures outlined above. Also described are the experiments that were undertaken to characterise the physical and functional integrity of recombinant bIGFBP-2. These experiments included N-terminal sequencing, mass spectrometry, Western ligand blot and solution IGF binding assays.

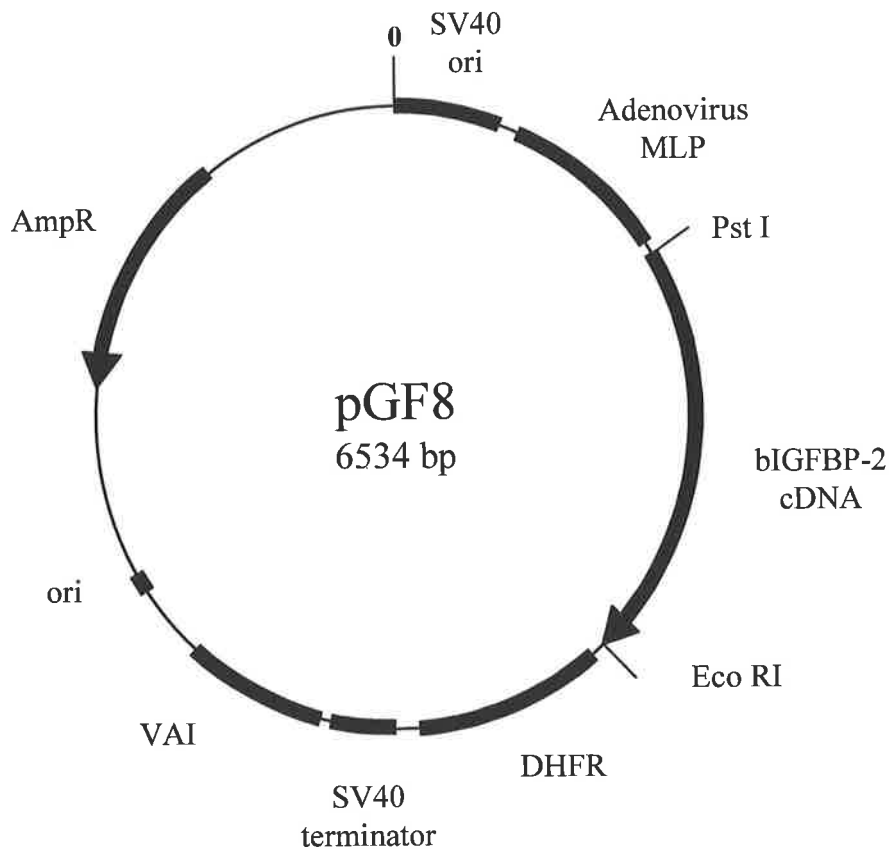


**FIG. 2.1 - Vector map of pGF8.**

The bIGFBP-2 expression vector pGF8 was constructed from the mammalian expression vector pXMT2 (Whyatt *et al.*, 1993). A colicin E1 origin of replication (ori) and the  $\beta$ -lactamase ampicillin resistance gene (AmpR) enabled pGF8 to be propagated in *E. coli*. Mammalian expression of the bIGFBP-2 cDNA was driven by the adenovirus major late promoter (MLP). The dihydrofolate reductase (DHFR) gene was present for selection, however this feature was not used in this study.

---

## 2.2 MATERIALS

### 2.2.1 Bacterial Cell Culture

The following media and solutions were prepared by Mrs. J. Brinkman (Central Services Unit, Dept. of Biochemistry, University of Adelaide). All solutions were sterilised by autoclave.

#### TE

10 mM Tris-HCl pH 8.0

10 mM EDTA

## **TEG**

25 mM Tris-HCl pH 8.0

10 mM EDTA

50 mM glucose

## **LB (Luria-Bertani medium)**

1 % (w/v) bactotryptone

0.5 % (w/v) bacto yeast extract

0.17 mM NaCl, pH 7.0

Bactotryptone and bacto yeast extract were purchased from DIFCO laboratories, MI, U.S.A. Ammonium persulphate, ampicillin, lithium chloride, lysozyme, proteinase K and Ribonuclease A (RNase A) were obtained from Sigma Chemical Co. MO, USA. Special grade phenol was purchased from Wako Pure Chemicals Industries Limited, Osaka, Japan. Chloroform and ammonium acetate were from BDH Chemicals Australia Pty Ltd, Kilsyth, Victoria, Australia. All other chemicals were analytical grade.

### **2.2.2 Mammalian Cell Culture**

Powdered Dulbecco's modified Eagle's media (DMEM), powdered serum-free DMEM, L-glutamine and trypsin were purchased from Gibco BRL, Glen Waverley, Victoria, Australia and fetal calf serum (FCS) was from Flow Laboratories, North Ryde, NSW, Australia. N-2-hydroxyethyl piperazine-N-2-ethane sulphonic acid (Hepes) was purchased from BDH Chemicals Australia, Kilsyth, Victoria, Australia.  $\beta$ -mercaptoethanol ( $\beta$ -ME) was purchased from Sigma Chemical Co. MO, USA. Insulin-transferrin sodium selenite media supplement (ITSS) was purchased from Boehringer Mannheim, Sydney, NSW, Australia. ITSS was resuspended as recommended by the manufacturers and stored as aliquots at  $-20^{\circ}\text{C}$ . Falcon plastic-ware (Becton Dickinson Labware, Franklin Lakes, N.J. USA) was used in all tissue culture experiments. Electroporation cuvettes were from Bio-Rad, North Ryde, NSW, Australia. GD1 $\mu\text{m}$  filters were purchased from Whatman Int. Ltd., Maidstone England. COS-1 cells (ATCC CRL 1650) were thawed from frozen stocks and routinely maintained in DMEM supplemented with 10 % (v/v) FCS at  $37^{\circ}\text{C}$  with 5 %  $\text{CO}_2$  by Mr. J. Wrin (Tissue Culture Facility, Biochemistry Dept., University of Adelaide). The following solutions were prepared and filter sterilised by Mrs. J. McLean (Tissue Culture Facility, Biochemistry Dept., University of Adelaide).

**HBS**

5 mM KCl  
1.2 mM MgSO<sub>4</sub>.7H<sub>2</sub>O  
137 mM NaCl  
20 mM Hepes pH 7.5.

**PBS**

20 mM sodium phosphate, pH 7.4.  
150 mM NaCl

**HEB**

HBS with 8 mM glucose.

**DMEM (1 litre)**

powdered DMEM concentrate  
1 mM L-glutamine  
40 mM NaHCO<sub>3</sub>  
20 mM Hepes, pH 7.5  
0.12 % (w/v) Gentamicin

**Serum-free DMEM**

powdered serum-free DMEM concentrate  
1 ml/l ITSS stock solution  
0.1 mM β-ME  
1 mM L-glutamine  
10 mM Hepes, pH 7.5  
0.12 % (w/v) Gentamicin

**2.2.3 Chromatography and Electrophoresis**

Sepharose CL-6B resin and Resource-S columns were from AMRAD Pharmacia Biotech, North Ryde, NSW, Australia. The Affi-Prep-10 affinity matrix, acrylamide and Bis-acrylamide were from Bio-Rad, North Ryde, NSW, Australia. Triton X-100 was from Boehringer Mannheim, Sydney, NSW, Australia. Activated charcoal, ammonium persulphate, goat anti-rabbit alkaline phosphatase-conjugate, 5-bromo-4-chloro-3-indolyl phosphate (BCIP), bromophenol blue, radio-immunoassay grade bovine serum albumin (BSA), Coomassie Brilliant Blue R250, nitroblue tetrazolium (NBT), polyoxethylenesorbitan monolaurate (Tween 20), protamine sulphate, sodium dodecyl sulphate (SDS) and TEMED were from Sigma Chemical Co., St Louis, MO, USA. Sequencing grade trifluoroacetic acid (TFA) was obtained from Perkin Elmer, Norwalk CT, USA. Acetonitrile was purchased from BDH Chemicals Australia Pty Ltd. Kilsyth, Victoria, Australia. Nitrocellulose filters for Western transfer were from Schleicher and Schuell, Dassel, Germany. Rabbit anti-serum raised against bIGFBP-2 was the kind gift of Dr B. Forbes, Biochemistry Dept., University of Adelaide, Adelaide, Australia.

## 2.3 METHODS

### 2.3.1 Large-Scale Plasmid Production

The plasmid pGF8 was propagated in the *E. coli* strain DH5 $\alpha$  (*supE44*,  $\Delta$ *lacU169*, *hsdR17*, *recA1*, *endA1*, *gyrA96*,  $\lambda^-$ , *relA1*, [ $\phi$ 80*lacZ* $\Delta$ M15]). A glycerol stock of DH5 $\alpha$  harboring pGF8 (10  $\mu$ l) was inoculated into 50 ml of LB that contained 100  $\mu$ g/ml ampicillin. Following overnight culture at 37°C with shaking, the cells were recovered by centrifugation at 2,000 x g for 5 min at 4°C. The cell pellet was suspended in 3 ml of cold lysis buffer (TEG) and the cell suspension treated with 30  $\mu$ l lysozyme (100 mg/ml) for 5 min on ice. Cell rupture was achieved by the addition of 6 ml freshly prepared 0.2 M NaOH containing 1 % (w/v) SDS whereupon the mixture was gently mixed by inversion and incubated on ice for 5 min. Chromosomal DNA was precipitated by the addition of 4.5 ml of 3 M sodium acetate, pH 5.2 followed by incubation for 15 min on ice with periodic gentle mixing. The cellular debris and chromosomal DNA were removed from the mixture by centrifugation at 10,000 x g for 10 min at 4°C. Plasmid DNA in the supernatant was precipitated by the addition of 8 ml isopropanol and left for 5 min at room temperature. After centrifugation at 10,000 x g (5 min at room temp), the supernatant was aspirated and the pellet dissolved in 1 ml H<sub>2</sub>O. To this was added 2.5 ml of 4 M LiCl and the mixture, which was left on ice for 15 min, then centrifuged at 10,000 x g for 5 min at room temp. Plasmid DNA was precipitated from the supernatant of the previous step by the addition of 6 ml ice cold ethanol followed by gentle mixing and incubation at -20°C for 30 min. Precipitated DNA was recovered as a pellet by centrifugation at 10,000 x g for 5 min at 4°C. The plasmid pellet was suspended in 400  $\mu$ l TE and residual RNA was digested by treatment with 2  $\mu$ l of Dnase-free RNase A (10 mg/ml) for 30 min at 45°C. After the solution was adjusted with 8  $\mu$ l of 10 % (w/v) SDS, contaminating protein was degraded by treatment with proteinase K (5  $\mu$ l of 10 mg/ml) for 15 min at 37°C.

The plasmid preparations were further purified by two rounds of phenol-chloroform extraction and one round of chloroform extraction. The phenol-chloroform extractions involved the addition to the aqueous plasmid preparation of 0.5 volume of special grade phenol (saturated with 0.1 M Tris-HCl pH 8.0) and 0.5 volume of chloroform. After vigorous mixing by vortex, the sample was centrifuged at 10,000 x g for 5 min and the aqueous phase recovered. The chloroform extraction was as described above but with 1 volume of chloroform instead of the phenol-chloroform mixture. The plasmid solution was then adjusted with 3 M sodium acetate to a final concentration of 0.3 M and

the DNA precipitated by the addition of 2.5 volumes of ice cold ethanol. After incubation at -20°C for 30 min, the DNA was recovered as a pellet by centrifugation at 10,000 x g for 10 min at 4°C. The pellet was washed with 1 ml ice-cold 70 % (v/v) ethanol, lyophilised under vacuum (Speed-Vac, Savant) and then dissolved in 100 µl of H<sub>2</sub>O.

Sepharose CL-6B spin columns were used as a final purification step to remove RNA fragments from the plasmid preparation. A mini-column was made by piercing the bottom of a 0.5 ml Eppendorf tube with a 21 gauge needle. A drop of acid-washed glass beads placed at the base of the Eppendorf tube then acted to retain the column bed of 500 µl of Sepharose CL-6B equilibrated with TE. The mini-column was placed inside an intact 1.5 ml Eppendorf tube to form the complete spin column. The spin column was centrifuged at approximately 350 x g for 3 min at room temperature, and the bottom 1.5 ml Eppendorf tube which contained the TE eluate was discarded. After replacing the bottom 1.5 ml Eppendorf tube, a plasmid sample (50 µl) was applied to the dry column bed and the column was centrifuged as described above. The eluate, which now contained the purified plasmid preparation was assessed for purity and yield by spectrophotometric means as described in Section 2.3.2.

### **2.3.2 Spectrophotometric Analysis of Plasmid DNA**

The concentration and purity of aqueous plasmid DNA was measured as described by Sambrook *et al.*, (1989). An aliquot of plasmid preparation was diluted by between 1/200 and 1/1000 in water and the A<sub>260</sub> nm and A<sub>280</sub> nm were measured using a Hewlett Packard 8451A DIODE Array Spectrophotometer. The concentration of plasmid DNA was estimated on the basis that a 1 mg/ml solution of DNA has a A<sub>260</sub> nm of 33. The preparation was considered to be suitably pure for transfection if A<sub>260</sub>/A<sub>280</sub> nm was between 1.6 and 1.7.

### **2.3.3 Transfection of COS-1 Cells**

For transfection studies, COS-1 cells were grown to 80-90 % confluency. The culture medium was aspirated and the cells washed with two consecutive 20 ml volumes of PBS. After the PBS was aspirated, the cells were covered with approximately 1 ml of 0.1 % trypsin (w/v) and incubated at room temperature for 5 min and then detached by light mechanical shock. The detached cells were recovered as a pellet by centrifugation at 1,000 x g for 5 min and the supernatant aspirated. The cells were then gently suspended in freshly prepared HEB by repeated withdrawal and dispensing through a Pasteur pipette. A 50 µl

aliquot of the cell suspension was removed, diluted 1/10 with Trypan blue and the viable cells were counted in a haemocytometer. The cells were recovered as a pellet a second time by centrifugation at 1,000 x g for 5 min. After the supernatant was aspirated, the cells were suspended in HEB as described above to a final density of  $1 \times 10^7$  viable cells/ml.

Transfection of pGF8 into the prepared COS-1 cells was achieved by electroporation. Briefly, 500  $\mu$ l of cell suspension, corresponding to  $5 \times 10^6$  cells was transferred to an electroporation cuvette along with 10  $\mu$ g of plasmid DNA, 50  $\mu$ l FCS and 50  $\mu$ l of 10 mg/ml solution of salmon sperm DNA. The cuvette contents were chilled at 4°C for 10 min, mixed gently and then electroporated at 0.27 V, 250  $\mu$ FD using a Gene Pulser (Bio-Rad). After electroporation, the cuvette contents were left at room temp for 10 min. The cells were then washed from the cuvette with approximately 1 ml of DMEM with 10 % (v/v) FCS and seeded into a fresh plastic flask that contained approximately 25 ml DMEM with 10 % (v/v) FCS. The contents of two electroporation cuvettes were used to seed each 150 cm<sup>2</sup> plastic tissue culture flask.

Transfected COS-1 cells were incubated overnight in DMEM with 10 % (v/v) FCS to allow recovery and reattachment to the flask substrate. However, as FCS is known to contain both IGFs and IGFBPs, the transfected cells were washed twice with PBS and thereafter maintained in serum-free DMEM over the course of the bIGFBP-2 production experiments. Serum-free DMEM which had been conditioned by the transfected cells over 24 hour periods was collected each day for 5 days and stored in siliconised bottles at -20°C.

### **2.3.4 Purification of bIGFBP-2 from Conditioned Medium**

#### **2.3.4.1 IGF-II Affinity Chromatography**

A 25 ml IGF-II affinity column (prepared as previously described; Forbes *et al.*, 1998) was equilibrated with 5 column volumes of PBS pH 6.5, 0.05 % (v/v) Tween-20, washed in 2 column volumes of 0.5 M acetic acid and then re-equilibrated with 5 column volumes of PBS pH 6.5, 0.05 % (v/v) Tween-20 at a flow rate of 1 ml/min. Conditioned medium was thawed, adjusted with neat Tween-20 to a final concentration of 0.05 % (v/v) and filtered through a GD1 $\mu$ m filter (Whatman). The filtered medium was loaded onto the IGF-II affinity column at a rate of 1 ml/min using a P-100 peristaltic pump (AMRAD Pharmacia Biotech, North Ryde, NSW, Australia). Unbound proteins were washed from the column with PBS, pH 6.5, 0.01 % (v/v) Tween 20, until baseline absorbance at 280 nm was reached. The bound IGFBPs were eluted in 0.5 M acetic acid. Eluted fractions that



contained protein according to the absorbance at 280 nm were pooled for further chromatography.

#### **2.3.4.2 Resource-S Cation Exchange Chromatography**

The protein pool from the IGF-II affinity column was further purified on a 1 ml Resource-S cation exchange column (AMRAD Pharmacia Biotech, North Ryde, NSW, Australia). The Resource-S column was washed with 10 column volumes of 1 M ammonium acetate pH 7.5 (buffer B) and then equilibrated with 10 column volumes of 0.5 M acetic. The IGF-II affinity-purified peak was then loaded onto the acid-equilibrated Resource-S column at 1 ml/min. After the load was applied, the column was washed with 5 column volumes of 50 mM ammonium acetate pH 6.0 (buffer A). The IGF-BPs were eluted using a linear gradient from 50 mM ammonium acetate pH 6.0 (buffer A) to 1 M ammonium acetate pH 7.5 (buffer B) over 20 min, at a flow rate of 1 ml/min. Protein peaks were detected by their absorbance at 280 nm and 1 ml fractions were collected across the gradient.

The affinity and cation exchange chromatographic steps were performed on an FPLC chromatography system (AMRAD Pharmacia Biotech, North Ryde, NSW, Australia).

#### **2.3.4.3 Reverse-phase High Performance Liquid Chromatography (HPLC)**

A final purification step for recombinant bIGFBP-2 involved semi-preparative reverse-phase HPLC on a Aquapore Prep-10 butyl column (7  $\mu\text{m}$  particle size, 300  $\text{\AA}$  pore size, dimensions of 10 mm x 100 mm; Brownlee Laboratories, Santa Clara, CA, USA). The pooled Resource-S fractions were acidified by the addition of neat TFA to a final concentration of 0.2 % and then applied at a rate of 2 ml/min to the Prep-10 column which had been equilibrated in 10 % (v/v) acetonitrile in 0.1 % (v/v) TFA. The proteins were eluted with a linear gradient of 25 to 50 % acetonitrile (v/v) in 0.1% (v/v) TFA over 100 min, at a flow rate of 2 ml/min. The bIGFBP-2 peak was collected and stored at  $-20^{\circ}\text{C}$ .

#### **2.3.4.4 Quantitation of bIGFBP-2**

Recombinant bIGFBP-2 was quantified by reverse-phase HPLC on an analytical column (Brownlee Aquapore BU300, 7  $\mu\text{m}$  particle size, 300  $\text{\AA}$  pore size and dimensions of 2.1 mm x 100 mm). An aliquot of bIGFBP-2 was injected onto the column and eluted with a linear gradient of 10 to 50 % acetonitrile (v/v) in 0.1% (v/v) TFA over 40 min, at a flow rate of 0.5 ml/min. The amount of bIGFBP-2 present was estimated by the integrated

peak area at  $A_{215}$  nm using the extinction coefficient  $\epsilon_0 = 1.03 \times 10^6 \mu\text{volt.s.}\mu\text{g}^{-1}$  (Forbes *et al.* 1998). bIGFBP-2 was subsequently dispensed as aliquots, lyophilised under vacuum (Speed-Vac, Savant) and stored dry at  $-20^\circ\text{C}$ .

All HPLC was performed with Waters 510 solvent pumps and a Waters 490 4-channel absorbance detector. The Waters Maxima software package was used for data collection and to control solvent gradients (Waters, Sydney, NSW, Australia).

### **2.3.5 SDS Polyacrylamide Gel Electrophoresis (SDS-PAGE)**

Samples of conditioned medium were concentrated approximately 4- to 10-fold in Centricon-10 micro-concentrators (Amicon, Denver, MA, USA) prior to SDS-PAGE. Proteins Samples for SDS-PAGE were diluted in 2 x non-reducing loading buffer (125 mM Tris, 4 % (w/v) SDS, 10 % (v/v) glycerol, 0.1 % (w/v) Bromophenol Blue, pH 6.8.) and then loaded onto discontinuous 12 % SDS-polyacrylamide gels, prepared as previously described (Laemmli, 1970). Gels of 1.5 mm thickness were used to analyse conditioned medium whereas pure protein samples were analysed on gels of 0.75 mm thickness. Electrophoresis was carried out at 35 mA per mini-gel over a period of approximately 60 min with 25 mM glycine, 25 mM Tris-HCl, 0.1 % (w/v) SDS as the running buffer. The protein samples were either stained with Coomassie blue (Section 2.3.5.1) or with silver (Section 2.3.5.2). SDS-7 molecular weight markers (Sigma Chemical Co., MO, USA.) were used for Coomassie and silver stained gels.

Proteins separated by SDS-PAGE were transferred to nitrocellulose filters (pore size  $0.45 \mu\text{m}$ ) using a semi-dry Western transfer NOVA Blot Apparatus (AMRAD Pharmacia Biotech, North Ryde, NSW, Australia) in freshly made transfer buffer (150 mM Glycine, 20 mM Tris-HCl pH 7.5, 20 % (v/v) methanol). Active IGFBPs were detected by ligand blot (Section 2.3.5.3) and bIGFBP-2 species were detected by immuno-blot (Section 2.3.5.4). Rainbow molecular weight markers (Amersham, North Ryde, NSW, Australia) were used for ligand blots and biotinylated molecular weight markers (Bio-Rad, North Ryde, NSW, Australia) were used for Western immuno-blots.

#### **2.3.5.1 Coomassie Blue Staining of SDS Polyacrylamide Gels**

On conclusion of electrophoresis, polyacrylamide gels were fixed in 50 % (v/v) methanol, 20 % (v/v) acetic acid for 20 min. Polyacrylamide gels were stained in a solution of 0.3 % (w/v) Coomassie blue R-250, 10 % (v/v) acetic acid for 60 min at  $45^\circ\text{C}$  and destained in 10 % (v/v) acetic acid, 5 % (v/v) methanol at  $45^\circ\text{C}$  for up to 2 hr. When

suitably destained, polyacrylamide gels were equilibrated with 35 % (v/v) methanol, 5 % (v/v) glycerol and then dried between two sheets of cellophane.

#### **2.3.5.2 Silver Staining of SDS Polyacrylamide Gels**

Polyacrylamide gels with bands that contained less than 200 ng of protein were stained by a method adapted from (Tunon & Johansson, 1984). Briefly, after electrophoresis mini-gels were fixed in 10 % (v/v) acetic acid, 40 % (v/v) methanol for 30 min and then rinsed in purified H<sub>2</sub>O for 5 min. Proteins were fixed with 12.5 % (v/v) glutaraldehyde followed by 2 x 10 min rinses in purified H<sub>2</sub>O. A 15 min rinse in 20 % (v/v) methanol preceded staining for 15 min in a freshly prepared solution containing 500 µl 20 % (w/v) AgNO<sub>3</sub>, 500 µl 25 % (v/v) ammonia and 2.5 ml 4 % (v/v) NaOH made up to 50 ml with 20 % (v/v) ethanol. Excess stain was rinsed from the mini-gels with 2 x 5 min rinses in 20 % (v/v) ethanol. The stain was developed typically over a period of 2 – 5 min in a freshly prepared solution that contained 50 µl formaldehyde and 12.5 µl 2.3 M citric acid made up to 50 ml with 20 % (v/v) ethanol. The developing process was halted by the addition of a solution of 1 % (v/v) glycerol and 10 % (v/v) acetic acid. As for Coomassie stained gels, silver stained gels were equilibrated with 35 % (v/v) methanol, 5 % (v/v) glycerol before being dried between two sheets of cellophane.

#### **2.3.5.3 <sup>125</sup>I-IGF-II Ligand Blot**

Western ligand blotting was by a method adapted from Hossenlopp *et al.*, 1986. The nitrocellulose strip that contained the rainbow molecular weight markers was firstly excised and stored. Proteins transferred to nitrocellulose filters were washed in PBS with 0.1 % (v/v) Triton X-100 for 10 min prior to being blocked in PBS that contained 1 % (w/v) BSA and 1 % (v/v) Tween-20 for 2 hrs (or overnight at 4°C). The filters were then incubated with <sup>125</sup>I-IGF-II (approximately 1 x 10<sup>6</sup> CPM diluted in 10 ml of PBS, 1 % (w/v) BSA, 1 % (v/v) Tween-20) for 4 hrs at room temp or overnight at 4°C. Unbound tracer was removed with 5 x 15 min washes with PBS, 0.1 % (v/v) Tween-20 at room temperature. Following this, the filters were air dried and the strip containing the molecular weight markers was replaced. The nitrocellulose filters were exposed in a Phosphor Storage Screen (Molecular Dynamics) for up to 24 hrs and visualised using a Phosphorimager and the ImageQuant Software (Molecular Dynamics).

#### **2.3.5.4 Western Immunoblot for bIGFBP-2**

Immunoblots were blocked in PBS with 1 % (w/v) BSA and 0.1 % (v/v) Tween-20 for 2 hrs at room temp (or overnight at 4°C). The filters were incubated in polyclonal rabbit anti-bIGFBP-2 antisera (diluted 1:3,000 in the same buffer) for at least 4 hrs at room temp (or overnight at 4°C). Excess primary antibody was removed by 3 x 10 min washes of PBS with 0.1 % (v/v) Tween-20. Next, the filters were bathed in goat anti-rabbit alkaline phosphatase-conjugate (diluted 1:10,000 in PBS, 0.1 % (v/v) Tween-20) for 2 hrs at room temperature. The filters were then washed once for 20 min in PBS with 0.1 % (v/v) Tween-20 followed by 2 x 20 min washes with 100 mM NaCl, 100 mM Tris-HCl pH 9.5, 5 mM MgCl<sub>2</sub>. The alkaline phosphatase mediated colour reaction was initiated by the addition of 10 ml of 100 mM NaCl, 100 mM Tris-HCl pH 9.5, 5 mM MgCl<sub>2</sub> containing NBT (75 µg/ml) and BCIP (75 µg/ml) as described by Bers & Garfin, 1985. When the colour had reached sufficient intensity, the reaction was stopped with TE.

#### **2.3.6 N-terminal Sequence Analysis**

Lyophilised protein samples of approximately 250 pmol were submitted for N-terminal sequencing. Edman degradation chemistry was carried out automatically on a Applied Biosystems (Foster City, CA, U.S.A) model 470A gas-phase Sequencer with a 900A Control/Data Analysis Module as previously described (Hunkapillar *et al.*, 1983). Sequencing was jointly performed by Ms. Denise Turner (Protein Sequencing Unit, Biochemistry Department, Adelaide University) and myself.

#### **2.3.7 Mass Spectrometry**

Molecular masses were determined by electrospray mass spectroscopy (ES-MS) on a VG Biotech Quattro mass spectrometer (VG Biotech Ltd, Altringham, Cheshire, UK). The analyses were performed by Dr. M. Sheil, Department of Chemistry, Wollongong University, Wollongong, NSW, Australia.

#### **2.3.8 Charcoal Binding Assay**

Charcoal binding assays were performed as previously described (Martin & Baxter, 1986; Szabo *et al.*, 1988).

##### **2.3.8.1 <sup>125</sup>I-IGF Titration**

Briefly, 66.7 nM bIGFBP-2 solution was prepared from lyophilised stock and serially diluted with CBA buffer (25 mM sodium phosphate adjusted to either pH 6.5 or pH

7.4, 0.25 % (w/v) BSA) in 9 steps to 0.083 nM. Reaction mixes for each bIGFBP-2 dilution, comprising 100 µl bIGFBP-2 dilution, 100 µl CBA buffer and 100 µl <sup>125</sup>I-IGF-I or <sup>125</sup>I-IGF-II tracer (equivalent to approximately 2,000 CPM) were prepared in triplicate. An additional three tubes were prepared with 100 µl of CBA buffer in lieu of a bIGFBP-2 treatment to measure non-specific binding of <sup>125</sup>I-IGF in the assay. The reaction mixes were equilibrated for 3 hrs at room temp (or overnight at 4°C). Unbound <sup>125</sup>I-IGF was adsorbed to activated charcoal by the addition of 500 µl ice cold CBA assay buffer containing a well-mixed suspension of 0.5 % (w/v) activated charcoal and 0.02 % (w/v) protamine sulfate. Following the addition of the charcoal suspension, the reactions were left on ice for 30 min. <sup>125</sup>I-IGF that was bound to charcoal was separated from soluble <sup>125</sup>I-IGF:IGFBP complexes by centrifugation at 13,000 g for 3 min. A 400 µl aliquot of each supernatant was sampled and measured for radioactivity in a multi-channel gamma counter (Bromma, LKB). Six tubes containing 100 µl of <sup>125</sup>I-IGF were counted to determine the total number of counts added to each reaction. The amount of <sup>125</sup>I-IGF tracer specifically bound by bIGFBP-2 as a percent of the total tracer added was calculated using the following equation:

$$\% \text{ }^{125}\text{I-IGF bound} = \frac{2(\text{CPM-NSB})}{\text{total}} \times 100$$

where CPM corresponds to the counts per minute determined for each supernatant and NSB corresponds to the non-specific binding of <sup>125</sup>I-IGF to components of the CBA buffer and assay tubes in the absence of bIGFBP-2.

The experimental data was fitted to a semi-log dose-response curve using the software Prism 2.01 (Graphpad Inc. San Diego, CA, USA).

#### **2.3.8.2 Competition Assays**

Competition assays were conducted in a modified form of the titration assay (Section 2.3.8.1). Firstly, the concentration of bIGFBP-2 was maintained at 0.1 nM in all reaction mixtures. Finally, the ability of increasing concentrations of unlabelled IGF and <sup>125</sup>I-IGF (2,000 CPM) to compete for IGFBP-2 binding was assayed. Thus unlabelled IGF was added to the reaction mixtures by serial dilution in 9 steps from 44.4 nM to 0.044 nM. The <sup>125</sup>I-IGF bound at each concentration of unlabelled IGF was calculated as a percentage of the maximal <sup>125</sup>I-IGF-II binding (ie: in the absence of unlabelled competitor).

## 2.4 RESULTS

### 2.4.1 Plasmid Purification

The bIGFBP-2 mammalian expression plasmid, pGF8 (Fig. 2.1) was designed with an *E. coli* origin of replication and the Amp<sup>R</sup> selectable marker to facilitate large-scale plasmid production in bacteria. Overnight cultures of *E. coli* harboring pGF8 were lysed and the plasmid fraction was purified (Section 2.3.1). One 50 ml bacterial culture yielded approximately 50 µg of highly purified plasmid as determined by spectrophotometric means (Section 2.3.2). Routinely, 4 x 50 ml cultures were processed as one batch. This provided sufficient plasmid DNA to transfect 1 x 10<sup>8</sup> COS-1 cells.

### 2.4.2 Transfection of COS-1 Cells

COS-1 cells were transfected with pGF8 by electroporation as outlined in Section 2.3.3. In a typical transfection experiment, 1 x 10<sup>8</sup> viable cells were recovered from 5 x 150 cm<sup>2</sup> tissue culture flasks with 85 % confluent COS-1 cells. After electroporation, 1 x 10<sup>8</sup> viable cells were sufficient to seed 9 x 150 cm<sup>2</sup> flasks. After an initial recovery period in DMEM with 10 % (v/v) FCS, the transfected cells were cultured in serum-free DMEM. Approximately 25 ml of conditioned medium were collected per flask per day. The transfected cells tended to lift off the flask substrate in the absence of serum (not shown) and thus cells were only cultured for 6 days after transfection. Over the 5 days that the cells were cultured in serum-free DMEM, approximately 1 litre of conditioned medium was accumulated and stored at -20°C.

The success of the transfection experiment was monitored by SDS-PAGE (Section 2.3.5). Aliquots of conditioned medium from each day of the experiment were concentrated approximately 10-fold, run on a 12 % polyacrylamide gel and then analysed by ligand blot with <sup>125</sup>I-IGF-II, as described in Section 2.3.5.3. Fig. 2.2b shows the ligand blot of serum-free conditioned medium (approximately 200 µl equivalents) collected on day 2 (lane 3), day 3 (lane 4), day 4 (lane 5) and day 6 (lane 6) of the transfection experiment. Lane 2 shows the IGFBP activity of the pooled conditioned medium (approximately 200 µl equivalent) after it was thawed and filtered in preparation for chromatography. A 3 µl sample of FCS (lane 1) was run as a positive control to show the electrophoretic motility of bIGFBP-2 and bIGFBP-3 (Upton *et al.*, 1990).

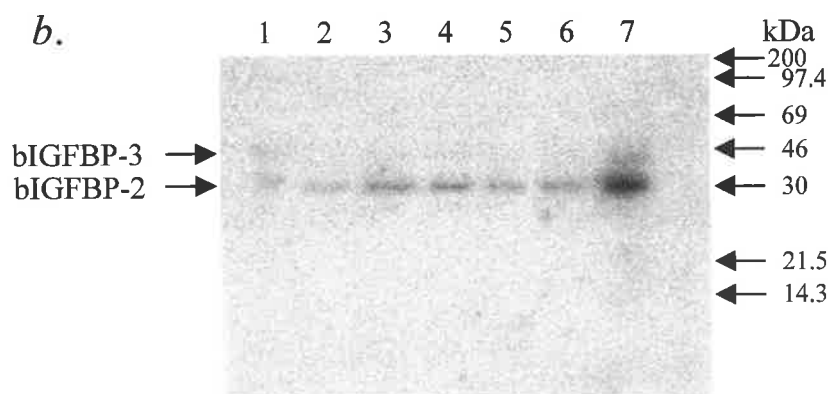
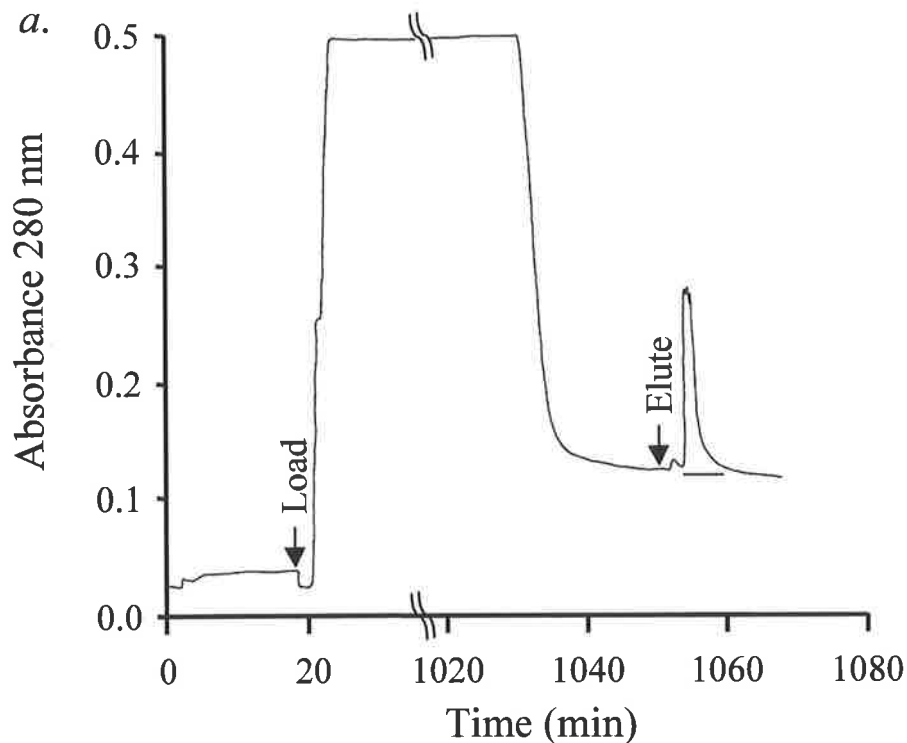


**Fig. 2.2 - Affinity purification of IGFBPs secreted into culture medium.**

(a.) IGFBPs were purified from conditioned medium using IGF-II affinity chromatography as described in Section 2.3.4.1. Eluted IGFBPs were collected as a single fraction as indicated by the bar. (b.) Shows the Western ligand blot of conditioned medium and chromatography fractions using  $^{125}\text{I}$ -IGF-II. Lanes 3 - 6 show the IGFBPs present in 200  $\mu\text{l}$  equivalents of conditioned medium collected on days 2, 3, 4, and 6 respectively. For comparison, an IGFBP-2 standard (3  $\mu\text{l}$  FCS) is shown in lane 1. The load for the IGF-II affinity column (200  $\mu\text{l}$  equivalent) is shown in lane 2 and the eluted IGFBP peak (20  $\mu\text{l}$ ) in lane 7. The electrophoretic motility of rainbow molecular weight markers is indicated on the left.

This chromatographic step yielded an approximate 40-fold concentration of IGFBP activity.

### 2.4.3 Purification of bIGFBP-2 From Conditioned Medium

A typical elution profile for the IGF-II affinity purification step (Section 2.3.4.1) is shown in Fig. 2.2a. The affinity column was loaded with 1.6 litres of conditioned medium

from pGF8 transfected COS-1 cells. After the column was loaded, non-specifically bound proteins were eluted by equilibrating the column in PBS, 0.05 % (v/v) Tween-20. Bound IGF-BPs were eluted from the affinity column with 0.5 M acetic acid and collected as a pooled fraction as indicated by the horizontal bar in Fig. 2.2a. The IGF-BP purification process was monitored by SDS-PAGE and ligand blot analysis (Fig. 2.2b). FCS (lane 1) has previously been shown to contain bIGFBP-2 (Upton *et al.*, 1990) and was therefore run as a positive control for bIGFBP-2. IGF-BP-2 species were clearly visible in a concentrated sample that corresponded to 200  $\mu$ l of the pooled conditioned medium (lane 2). A 20  $\mu$ l sample of the IGF-II affinity-purified peak (lane 7) showed that IGF-BP-2 and a second species with the apparent molecular weight of IGF-BP-3 were enriched by this chromatographic step.

The second step in the purification of recombinant bIGFBP-2 was cation exchange chromatography, as described in Section 2.3.4.2. The cation exchange elution profile (Fig. 2.3a) shows that the IGF-BPs present in the ex-affinity protein peak were resolved into a major peak (peak I) and a minor peak (peak II). SDS-PAGE analysis (Fig. 2.3b) showed that fractions from peak I (lanes 2 - 7) contained two species that migrated at approximately 30 kDa, according to molecular weight standards which are shown in lane 1. Western ligand analysis with  $^{125}$ I-IGF-II on a blot from a duplicate gel (Fig. 2.3c) showed that both of the 30 kDa doublet species possessed IGF binding affinity. Two minor bands of IGF-binding activity were also evident in fractions from peak I. One of these bands migrated above the 60 kDa marker and the other migrated below the 29 kDa marker (Fig. 2.3c). Previously, peak II was identified as simian (s) IGF-BP-3 (Forbes *et al.*, 1998) and was not further characterised in this study.

The final bIGFBP-2 purification step involved reversed-phase HPLC as described in Section 2.3.4.3. Peak I from the cation exchange step was further purified to yield peak A (retention time 44.43 min) and peak B (retention time 54.22 min) as shown in Fig. 2.4a. SDS-PAGE analysis of portions of peak A (Fig. 2.3b, lane 9, Fig. 2.3c, lane 9) and peak B (Fig. 2.3b, lane 10, Fig. 2.3c, lane 9) showed that both contained single protein species that ran at approximately 30 kDa, and that peak B possessed an apparent molecular weight that was slightly larger than peak A, based on electrophoretic motility. This suggests that the two protein species that are evident in lanes 3-4 of Fig. 2.3 could be resolved by reverse-phase HPLC.



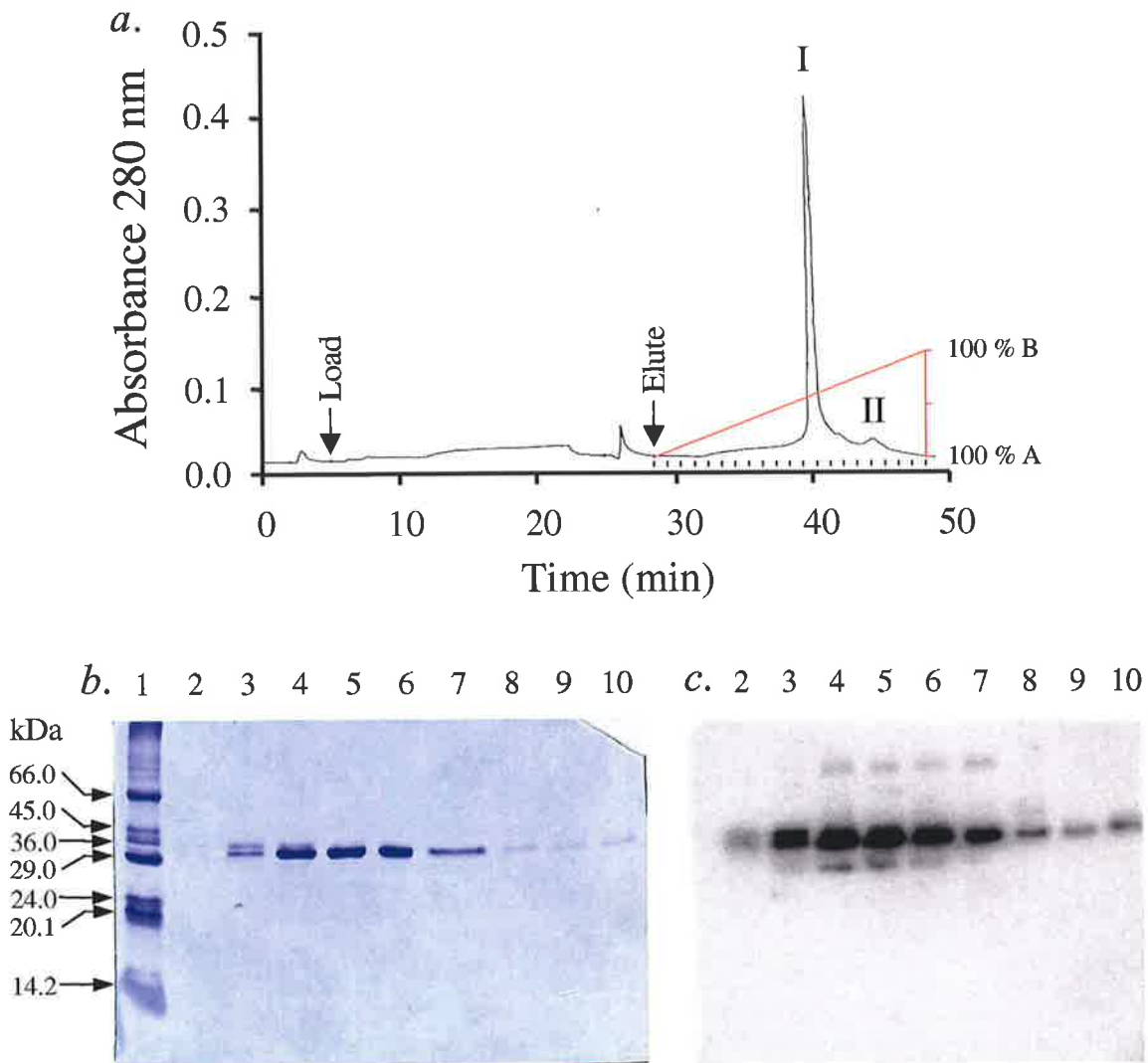


**Fig. 2.3 - Cation exchange chromatography of affinity purified IGFBPs.**

(a.) The IGFBP peak from the IGF-II affinity chromatography step (Fig. 2.2a) was further resolved into peak I and peak II by cation exchange chromatography as described in Section 2.3.4.2. Buffer A was 50 mM ammonium acetate pH 6.0 and buffer B was 1 M ammonium acetate pH 7.5 (b.) Shows Coomassie stained SDS-PAGE analysis (Section 2.3.5.1) of proteins recovered during the cation exchange chromatography step. Lanes 2 - 7 correspond to 20  $\mu$ l aliquots of fractions 9 - 14 across peak I respectively. A 20  $\mu$ l aliquot of the load for the cation exchange step is shown in lane 8. Lanes 9 and 10 show 5  $\mu$ l aliquots of peaks A and B, respectively from the reverse-phase HPLC chromatography of peak I (Section 2.3.4.3, Fig. 2.4). Molecular weight standards are shown in lane 1. (c.) A duplicate gel to b. was transferred to nitrocellulose and probed with  $^{125}$ I-IGF-II as described in Section 2.3.5.3.

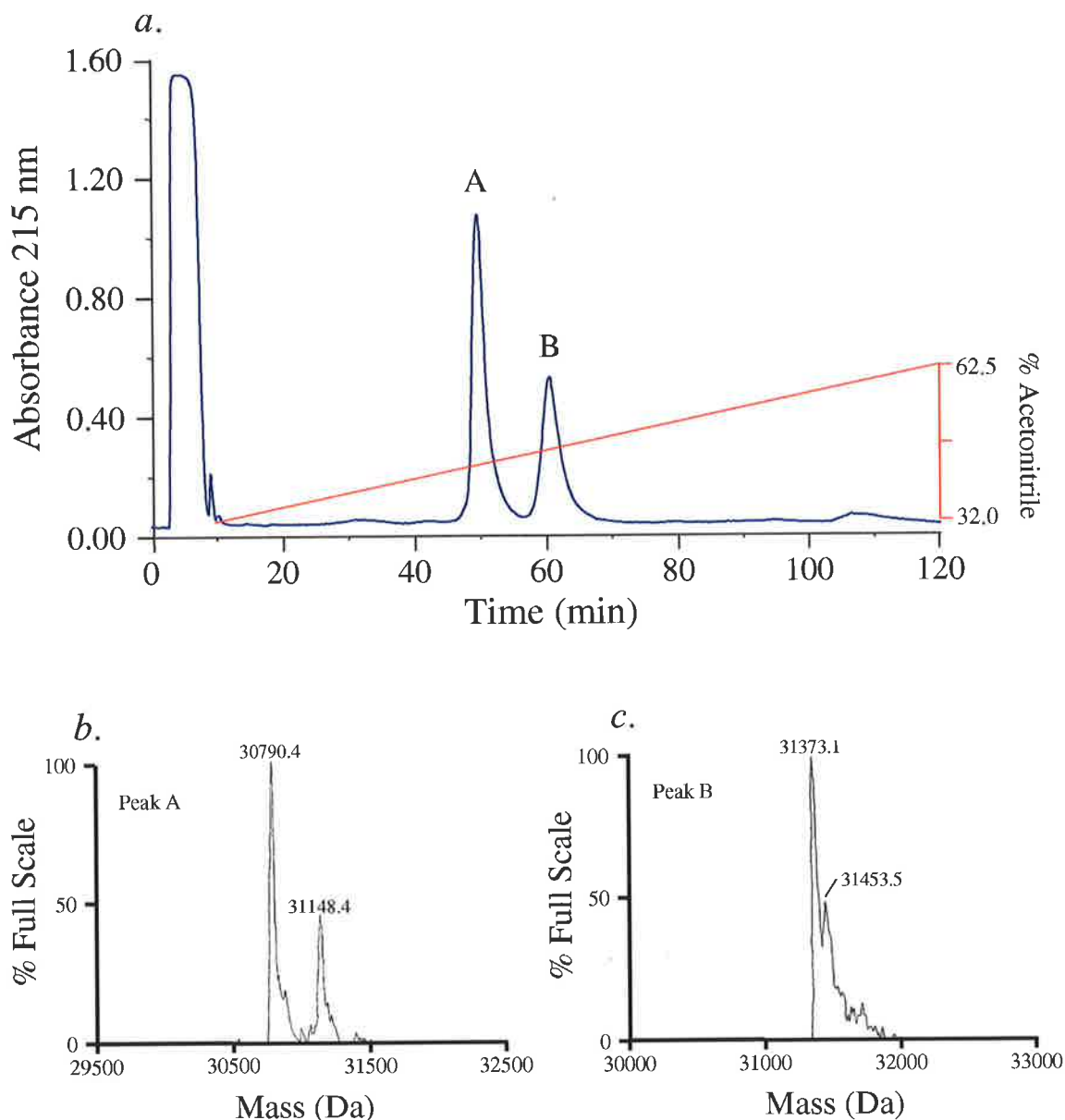


**Fig. 2.4 - Reverse-phase HPLC of peak I from the cation exchange step.**

(a) Peak I from the cation exchange chromatography step (Fig. 2.3a) was further resolved into peaks A and B by reversed phase HPLC as described in Section 2.3.4.3. (b) Electrospray mass spectrometry (Section 2.3.7) identified two species in peak A. The major species possessed a molecular weight of 30790.4 Da and the minor species was 31148.4 Da. (c) Two molecular weight species were also detected in peak B. The major species in peak B was 31373.1 Da.

Aliquots of peak A and peak B were analysed by Edman degradation (Section 2.3.6). Both peaks gave the same N-terminal sequence Glu-Val-Leu-Phe-Arg, which corresponded to the first 5 amino acids of IGF2BP-2. In peak A, however, there was a minor contaminating sequence (approximately 5 %) of Gly-Ala-Arg-Ala-Glu, which corresponded to the last four residues of the leader peptide and the first residue of mature bIG2BP-2 (Upton *et al.*, 1990; Bourner *et al.*, 1992). As a final measure of the success of

the bIGFBP-2 purification procedure, aliquots of peak A and peak B were submitted for mass spectrometric analysis as outlined in Section 2.3.7. Electrospray mass spectrometry of peak A (Fig. 2.4*b*) revealed a major species of  $30,790 \pm 4$  Da, corresponding with the predicted mass for bIGFBP-2 (30.797 kDa) and a minor species with an additional 357 mass units which corresponded to the mass Gly-Ala-Arg-Ala-bIGFBP-2. In contrast, peak B contained a major species (Fig. 2.4*c*) whose mass ( $31.376 \pm 0.004$  kDa) corresponded closely to the predicted mass of human IGFBP-2 (31.377 kDa) suggesting that this peak may contain endogenously produced sIGFBP-2. The minor species present in peak B possessed a molecular weight that was exactly 80 mass units larger than the major species. This peak may therefore represent a phosphorylated isoform of sIGFBP-2.

The final yield of purified bIGFBP-2 (peak A) as estimated by analytical reverse-phase HPLC (Section 2.3.4.4) was 980  $\mu$ g. Thus, the overall yield of bIGFBP-2 was approximately 0.6 mg/litre of conditioned medium. The final yield of the species predicted to be sIGFBP-2 was 560  $\mu$ g, using the bIGFBP-2 extinction coefficient. Both bIGFBP-2 species were dispensed as 70  $\mu$ g aliquots, dried under vacuum and stored at  $-20^{\circ}\text{C}$ .

#### **2.4.4 Titration IGF Binding Assay**

Fig. 2.5*a* shows the binding of  $^{125}\text{I}$ -IGF-II by increasing concentrations of bIGFBP-2 by the procedure described in Section 2.3.8.1. The data was fitted to a semi-log dose-response curve by non-linear regression using Prism (Graphpad, Inc. San Diego, CA, USA) with an  $R^2$  value of 0.966. The maximal specific binding of  $^{125}\text{I}$ -IGF-II by bIGFBP-2 was 43 % of the total tracer added. Non-specific binding of  $^{125}\text{I}$ -IGF-II in the assay was 15 % of the total IGF-tracer added. Half-maximal IGF-tracer binding was achieved by 0.1 nM bIGFBP-2.

#### **2.4.5 Competition IGF Binding Assay**

The affinity of recombinant bIGFBP-2 for  $^{125}\text{I}$ -IGF-II was assessed by competition binding assay (Section 2.3.8.2). Fig. 2.5*b* shows the competition of different ratios of unlabelled IGF-II and  $^{125}\text{I}$ -IGF-II for binding to purified recombinant bIGFBP-2. The half-maximal competition concentration of unlabelled IGF-II was  $0.18 \pm 0.07$  nM. The  $R^2$  value for the semi-log curve-fitting was 0.976.

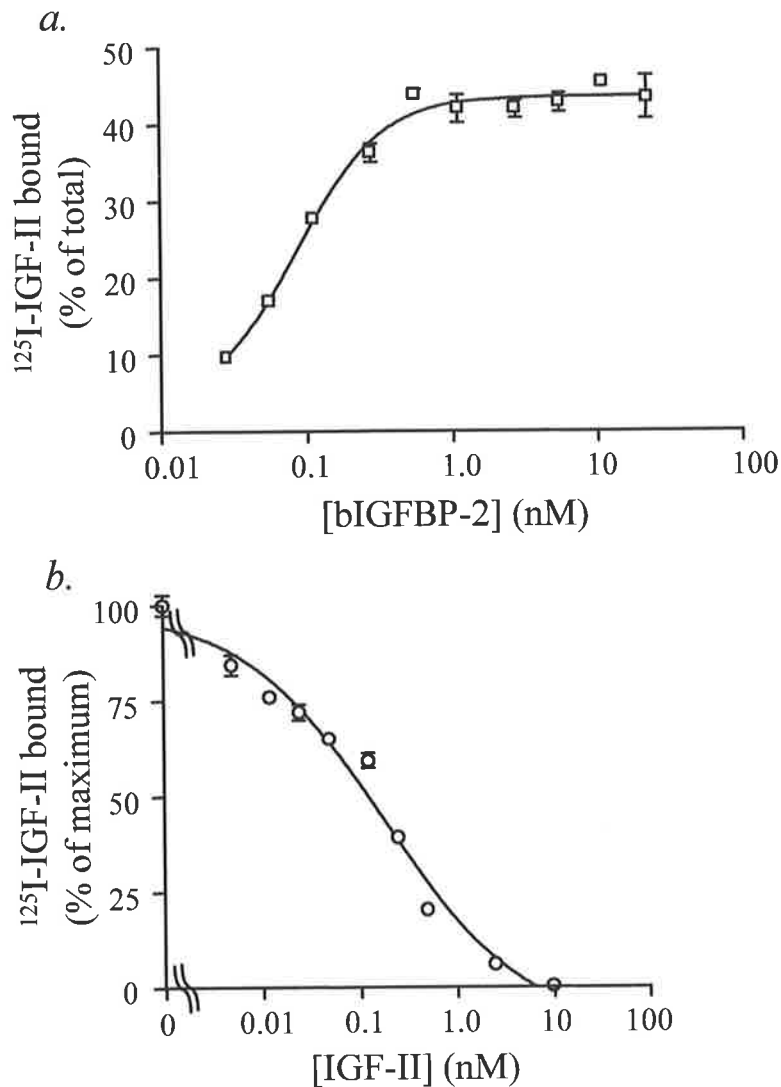


**Fig. 2.5 - Solution IGF binding assays with recombinant bIGFBP-2.**

(a) Shows the titration of free  $^{125}\text{I}$ -IGF-II by increasing concentrations of recombinant bIGFBP-2 (material dispensed from peak A, Fig. 2.4a) as described in Section 2.3.8.1. The maximal  $^{125}\text{I}$ -IGF-II binding attained by bIGFBP-2 was approximately 44 %. Half-maximal IGF-tracer binding was achieved by approximately 0.1 nM bIGFBP-2. (b) Shows the competition curve of IGF-II for  $^{125}\text{I}$ -IGF-II binding to bIGFBP-2 which was determined as described in Section 2.3.8.2. The apparent affinity of the interaction between IGF-II and bIGFBP-2 as estimated by the  $\text{EC}_{50}$  value was  $0.18 \pm 0.07$  nM.

## 2.5 Discussion

The studies presented in this thesis sought to investigate the molecular interactions between bIGFBP-2 and the IGFs. Moreover, the chemical iodination strategy that had been chosen to probe the bIGFBP-2/IGF complex required highly-purified and fully-active bIGFBP-2. It was also anticipated that mutant analogues of bIGFBP-2 might be required in

order to clarify findings from the chemical modification strategy. Early in my candidature, a eukaryotic bIGFBP-2 expression system was developed by Dr. Briony Forbes in the laboratory of Associate Professor John Wallace. I therefore chose to scale-up and routinely use this expression system to satisfy the short term need for active bIGFBP-2 material. In addition, the eukaryotic expression system also provided a mechanism for future modification of bIGFBP-2 by mutagenesis. This chapter describes the production of recombinant bIGFBP-2 and steps that were taken to assess the purity, yield and functional integrity of the bIGFBP-2 that was produced.

The expression of active bIGFBP-2 by pGF8 transfected COS-1 cells was confirmed by ligand blot analysis with  $^{125}\text{I}$ -IGF-II. In samples of conditioned medium, the most prominent band of  $^{125}\text{I}$ -IGF-II binding activity essentially co-migrated with the FCS bIGFBP-2 standard (Fig. 2.2*b*). However, the FCS bIGFBP-2 standard appeared to be compressed and slightly retarded on the gel compared with secreted recombinant bIGFBP-2. This was presumably due to the high concentration of serum proteins in the FCS sample. The intensity of the putative bIGFBP-2 band was not appreciably diminished in conditioned medium collected on the 6th day of the experiment, as shown in Fig. 2.2*b*. This indicated that the transfected COS-1 cells secreted bIGFBP-2 over the 6 day life of the culture. The reduced intensity of the bIGFBP-2 band from the pooled conditioned medium sample indicated that some bIGFBP-2 activity was lost during the storage and preparation of conditioned medium for chromatography. In contrast to COS-1 cells transfected with pGF8, non-transfected cells did not secrete sufficient levels of IGFBP-2 to be detected by ligand blot analysis with  $^{125}\text{I}$ -IGF-II (See Fig. 4.5, Chapter 4).

It has previously been shown that COS-1 cells transfected with pGF8 secreted recombinant bIGFBP-2 and to a lesser extent endogenous sIGFBP-3 into the culture medium (Forbes *et al.*, 1998). Therefore, the bIGFBP-2 purification scheme firstly involved IGF-II affinity chromatography to collect all of the IGFBPs from the conditioned medium. This was followed by a combination of cation exchange and reverse-phase chromatographic steps to resolve the various IGFBP species.

IGF-affinity chromatography successfully recovered IGFBP-2 and IGFBP-3 species from the pooled conditioned medium, as illustrated by Figs. 2.2*a,b*. Cation exchange chromatography (Fig. 2.3*a*) was then employed to resolve IGFBP-2 and IGFBP-3 species. SDS-PAGE analysis of fractions across the major protein species eluted from the cation exchange column (peak I), showed that two active forms of IGFBP-2 had been partially resolved (Figs. 2.3*b,c*). The presence of a minor protein band with affinity for  $^{125}\text{I}$ -

IGF-II and that ran above the 60 kDa molecular weight marker (Fig. 2.3c, lanes 3-6) suggested that IGFBP-2 may form dimeric complexes to a limited extent. Indeed, subsequent experiments showed that this band was immunoreactive to polyclonal anti-bIGFBP-2 antibodies and was absent when the electrophoresis was conducted under reducing conditions (data not shown). A minor  $^{125}\text{I}$ -IGF-II binding species of approximately 26 kDa was also evident in lanes 2-5 of Fig. 2.3c, suggesting that partial IGFBP-2 degradation may have taken place. However, the identity of this species was not determined.

Preparative reversed phase HPLC separated the two major IGFBP-2 species contained in peak I, to yield peaks A and B, as shown in Figs. 2.3b, 2.3c and 2.4. Aliquots of the A and B forms of IGFBP-2 (Fig. 2.4) were characterised by Edman degradation and electrospray mass spectrometry. Both IGFBP-2 forms possessed the same N-terminal sequence Glu-Val-Leu-Phe-Arg-, which is consistent with the N-terminus of mature IGFBP-2. In addition to mature IGFBP-2, peak A also contained the minor contaminating sequence (approximately 5 %) commencing Gly-Ala-Arg-Ala-Glu-, corresponding to the last 4 residues of the IGFBP-2 leader sequence and the first residue of mature IGFBP-2. This presumably arose from the incomplete processing of the leader peptide during bIGFBP-2 secretion from COS-1 cells. Indeed, Gly-Ala-Arg-Ala-bIGFBP-2 was predicted to be an alternative mature bIGFBP-2 form, using the SignalP internet server (<http://www.cbs.dtu.dk/services/SignalP>; Nielsen et al., 1997).

Electrospray mass spectrometry revealed that the A form of IGFBP-2 (Fig. 2.4b) had the same mass as the predicted mass of bIGFBP-2 and confirmed that the minor contaminant in peak A was GARA-bIGFBP-2. The mass of the B form of IGFBP-2 (Fig. 2.4c) closely corresponded to the predicted mass of hIGFBP-2. This suggested that the B form of IGFBP-2 was sIGFBP-2, the endogenous product of the COS-1 cells.

Throughout the purification process, ligand blot analysis confirmed that recombinant bIGFBP-2 retained its ability to bind IGFs (see Figs. 2.2b, 2.3c). However, a more rigorous method to assess the IGF binding ability of recombinant bIGFBP-2 was by charcoal binding assay. The concentration of unlabelled IGF-II required to displace 50 % of the  $^{125}\text{I}$ -IGF-II bound by bIGFBP-2 (the  $\text{EC}_{50}$ ) was 0.18 nM. This value is consistent with other published  $\text{EC}_{50}$  values for the interaction between bIGFBP-2 and  $^{125}\text{I}$ -IGF-II determined under similar assay conditions. Published  $\text{EC}_{50}$  values for this interaction range from 0.26 nM (Clemmons *et al.*, 1992) to 0.08 nM (Forbes *et al.*, 1998).

The procedures that have been described in this chapter were routinely used for the production of bIGFBP-2 during my Ph.D. studies. The yield of pure bIGFBP-2 in this particular example was approximately 0.6 mg/l of conditioned medium. In similar experiments (not shown), the overall yield of pure recombinant bIGFBP-2 typically ranged from 0.5 to 1 mg of purified protein per litre of conditioned medium.

In conclusion, bIGFBP-2 was transiently expressed in COS-1 cells and purified from conditioned medium. The purity of the bIGFBP-2 preparation was 95 % as determined by mass spectrometry and N-terminal sequence analysis. The only detectable contaminant in the preparation was an alternative form of bIGFBP-2 with an additional 4 amino acids at the N-terminus. Several rounds of bIGFBP-2 expression and purification generated milligram amounts of bIGFBP-2 that was fully active when analysed by Western ligand blot and charcoal binding assay. The bIGFBP-2 material was therefore considered to be highly suitable for the chemical iodination studies described in Chapter 3. Interestingly, sIGFBP-2 and sIGFBP-3 were by-products of the bIGFBP-2 production process.

However, as recombinant bIGFBP-2 could be fully purified from the contaminating sIGFBP-2, this expression system was considered to be suitable for the production of bIGFBP-2 mutants as discussed in Chapter 4.

**CHAPTER 3 - CHEMICAL IODINATION OF IGFBP-2 AS A  
FUNCTIONAL AND STRUCTURAL PROBE**





## **3.1 INTRODUCTION**

### **3.1.1 Background**

Central to the biological function of the IGFbps is their ability to form a high-affinity complex with IGF-I and IGF-II. Yet the determinants of IGF-affinity are currently the least characterised aspects of IGFbp structure-function in the literature (as discussed in Sections 1.4 and 1.5 of Chapter 1). Therefore, the aim of this study was to identify a region of bIGFBP-2 that participated in IGF-binding.

To date, deletion mutagenesis has been the most popular strategy used to localise the IGF binding regions of IGFbps (see Section 1.5, Chapter 1). In general terms, deletion mutagenesis can readily identify a functionally irrelevant region of an IGFbp. The removal of such a region does not affect IGF interactions and this technique can readily identify a minimal binding domain. However, it is more difficult to interpret the underlying cause should the IGFbp truncation lead to a loss of IGF affinity. A reduction in IGF affinity may be due to the loss of essential binding site residues, but equally, it may be due to the general loss of native protein structure. In addition, the probability of structural disruption would be expected to increase as residues that are normally buried in the protein structure become more exposed in IGFbps that are truncated inappropriately, for example, within a domain. The lack of IGFbp structural information further complicates the situation as the actual number and arrangement of IGFbp domains have only been inferred by sequence alignments and these predictions may be inaccurate.

In this study, the molecular interactions between bIGFBP-2 and IGFs have been probed by chemical iodination. The chemical iodination strategy (differential iodination for short) sought to highlight differences in the reactivity of tyrosine residues when bIGFBP-2 was iodinated in the presence and the absence of IGF-ligand. Tyrosine residues that were available for modification in bIGFBP-2 but were protected in the bIGFBP-2/IGF complex could thus be implicated in the IGF-binding site of bIGFBP-2. The key advantage of the chemical modification approach over truncation mutagenesis was that the entire bIGFBP-2 molecule could be investigated in its active state. This would avoid the possibility of gross structural disruption that is inherent in the truncation approach.

### **3.1.2 Iodination and Studies of the Insulin and IGF Systems**

Tyrosine radio-iodination has been extensively used for the production of insulin and IGF radio-labelled tracers. However, the utility of iodination as a probe of protein

function was highlighted when specific iodinated isomers of insulin exhibited reduced affinity for the insulin-receptor (Gliemann *et al.* 1979). Similarly, Schäffer *et al.*, 1993 showed that specific iodinated isomers of IGF-I bound to the type 1 IGF-receptor with reduced affinity. These observations suggested that Tyr-A19 of insulin and Tyr-60 of IGF-I were critical for insulin-receptor and type-1 IGF-receptor interactions respectively. Furthermore, these predictions were confirmed by mutagenesis. Thus Tyr-A19→Leu insulin (Kitagawa *et al.*, 1984) and Tyr-60→Leu IGF-I (Bayne *et al.*, 1990) both showed severely compromised interactions with their respective receptors.

Differential iodination has been previously used to investigate structure-function relationships of the IGF molecule. Accordingly, differential iodination revealed that all three tyrosine residues of IGF-I (Tyr-24, Tyr-31 and Tyr-60) were protected from modification by the type-1 IGF-receptor (Maly & Lüthi, 1988). In contrast, only Tyr-60 of IGF-I and Tyr-59 of IGF-II were protected from iodination by bIGFBP-2 (Moss *et al.*, 1991). Thus differential iodination suggested that the type-1 IGF-receptor and IGFBP-2 binding faces of IGFs overlapped.

### 3.1.3 The Iodination Reaction

Hypiodous acid (HOI), generated by the oxidation of iodide salts with chloramine-T, reacts with the non-ionised phenolic group of the tyrosine side chain (Dunford & Ralston, 1983). As a result, the phenolic ring becomes substituted with iodine atoms at the meta- and ortho- positions to produce 3-iodo-tyrosine and then 3,5-di-iodo-tyrosine respectively. Although HOI will also iodinate the imidazole ring of histidine residues, iodination at tyrosyl residues predominates at neutral or weakly acidic pH (Means & Feeney, 1971; Tsomides & Eisen, 1993).

The physical properties of the tyrosyl side-chain are substantially altered by iodination. Firstly, iodine atoms are similar in size to a methyl group and so iodination changes the shape and increases the volume of the derivatised phenolic ring. Secondly, iodine atoms are highly electronegative and therefore, iodination markedly alters the pKa of the tyrosyl para-hydroxyl group. In studies of free amino acids in solution, the apparent pKa of the phenolic hydroxyl of tyrosine residues is typically 10.1. In contrast, mono- and di-iodination reduce the pKa of the para-hydroxyl group to 8.2 and 6.4 respectively (Edelhoch, 1962). Thirdly, iodination modifies the spectral properties of tyrosyl residues. Thus the absorption maximum of the tyrosine side-chain (275 nm) is shifted to longer wavelengths by progressive incorporation of iodine (Edelhoch, 1962). Significantly,

tyrosine-specific fluorescence (absorbance 275 nm, emission 305 nm) is abolished by iodination (Cowgill, 1965). Finally, iodination increases the hydrophobicity of the tyrosyl side-chain (Tsomides & Eisen, 1993). This was particularly evident by progressive increases in the retention time of mono- and di-iodinated 8-residue peptides separated by reverse-phase HPLC (Tsomides & Eisen, 1993). In the work presented in this Chapter, the different properties of the iodo-tyrosyl and tyrosyl side-chains were exploited to characterise the tyrosine labelling pattern of different iodo-bIGFBP-2 preparations.

### **3.1.4 Overview of the Experimental Strategy**

The first task of this study was to characterise the stoichiometry of iodine incorporation into bIGFBP-2 when iodinated in the presence and absence of IGF-II over a range of iodination conditions. This would directly show whether the presence of IGF-ligand protected bIGFBP-2 against iodination. Thereafter, the respective IGF affinities of differentially iodinated bIGFBP-2 species were investigated to determine whether any of the tyrosine residues of bIGFBP-2 were important for IGF-interactions.

The final task in this study was to characterise the exact sites of iodine incorporation in the differentially iodinated bIGFBP-2 species. The primary structure of bIGFBP-2 contains six tyrosine residues which are distributed within regions of the bIGFBP-2 sequence that have been predicted to be functionally important (See Section 1.5). Tyr-60, Tyr-71 and Tyr-98 are located in cysteine-rich N-terminal region, whereas Tyr-213, Tyr-226 and Tyr-269 are located in the C-terminal cysteine-rich region of bIGFBP-2. Each tyrosine residue could theoretically be isolated in a discrete peptide after trypsin digestion. The tyrosine-containing peptides could subsequently be separated by reverse-phase HPLC, and non-modified tyrosine-containing peptides could be identified by their characteristic tyrosine-specific fluorescence. Importantly, <sup>125</sup>I-iodinated tyrosine residues could be detected by <sup>125</sup>I-associated  $\gamma$ -radiation. Therefore, the tyrosine labelling patterns of differentially iodinated bIGFBP-2 species could be directly compared by tryptic mapping.

## **3.2 MATERIALS**

bIGFBP-2 was recombinantly produced in the COS-1 (ATCC CRL 1650) monkey kidney cell line and purified from conditioned media as described in Chapter 2. Receptor grade IGF-I and IGF-II were the kind gift of GroPep Pty. Ltd., (Adelaide, Australia). Radio-labelled <sup>125</sup>I-IGF-I and <sup>125</sup>I-IGF-II peptides were kindly provided by Spencer Knowles (CRC for Tissue Growth and Repair, Adelaide, Australia). Modified, sequencing

grade trypsin was purchased from Boehringer Mannheim, (North Ryde, N.S.W., Australia). HPLC columns were purchased from Brownlee Laboratories, (Santa Clara, CA) and Pharmacia Pty. Ltd., (Sydney, Australia). Carrier-free Na<sup>125</sup>I was purchased from Amersham International (Sydney, Australia). Pre-siliconised tubes (Sorenson BioScience, Inc., Salt Lake City, Utah) were used for reaction vessels and for the collection of fractions during chromatography. All HPLC was carried out using Waters 510 solvent pumps, a Waters 490 4-channel absorbance detector and a Perkin Elmer LS4 fluorescence spectrometer in series. The Waters Maxima software package was used to control solvent gradients and for data collection. HPLC-grade acetonitrile was purchased from Merck (Kilsyth, Vic., Australia) and TFA from Sigma-Aldridge (Castle Hill, N.S.W., Australia). All other reagents were analytical grade.

### **3.3 METHODS**

#### **3.3.1 Titration of Reactive bIGFBP-2 Tyrosine Residues**

Using 0.1 nmole of bIGFBP-2 per reaction, a series of iodinations were performed by a modified form of the chloramine-T method (Van Obberghen-Schilling & Pouyssegur, 1983). The amount of NaI (specific radioactivity 50 nCi / nmole) was maintained at 4 nmole per reaction which was the equivalent of a 40-fold molar excess of NaI over bIGFBP-2. The amount of chloramine-T was varied between 0.5 and 5 nmole per reaction, the purpose being to generate a range of concentrations of the reactive HOI species.

Two stock solutions, one containing bIGFBP-2 and the other containing both bIGFBP-2 and IGF-II were prepared. Thus, two 0.8 nmole samples of lyophilised bIGFBP-2 were dissolved in 350 µl of iodination buffer (250 mM sodium phosphate, pH 6.5, 0.05 % (v/v) Tween-20) in separate vials. To one bIGFBP-2 stock solution was added 40 µl of 10 mM acetic acid and to the other was added 3.2 nmole of IGF-II in 40 µl of 10 mM acetic acid resulting in a 5-fold molar excess of IGF-II over bIGFBP-2. The vials were left at room temperature for 120 min to allow the complex between bIGFBP-2 and IGF-II to form. Then 36 nmole of NaI was added to each reaction mixture in 10 µl of 5 mM NaOH. After mixing, both of the reaction mixtures were divided into 8 x 50 µl (0.1 nmole) aliquots of bIGFBP-2. Iodination was initiated by the addition of 5 µl of the appropriate chloramine-T solution (prepared in a 10-fold serial dilution in 8 steps from 1.0 mM to 0.10 mM with water) followed by an incubation at room temperature for 45 sec. Each reaction

This was achieved by calculating the theoretical extinction coefficients of IGF-II and bIGFBP-2 (Buck *et al.*, 1989 *Anal. Biochem.* **182**, 295-299) and then calibrating the HPLC detector with IGF-II standards of known concentration kindly supplied by GroPep Pty. Ltd.

was quenched by the addition of 20 nmole of sodium metabisulphite in 10  $\mu$ l of water. The 16 reaction mixtures were stored at -20°C prior to HPLC gel-filtration at acid pH.

### 3.3.2 HPLC Gel-Filtration at Acid pH

Reaction products were thawed and acidified by the addition of 50  $\mu$ l of 2 M acetic acid to dissociate the IGF/bIGFBP-2 complex. Iodinated bIGFBP-2 was separated from free iodide and iodinated IGF (when present) by gel-filtration on a TSK G3000SW Ultragel HPLC column (7.5 mm x 600 mm) equilibrated with a solution containing 150 mM NaCl, 10 mM HCl and 0.05% (v/v) Tween-20. The column was eluted at a flow rate of 0.5 ml/min and 1 ml fractions were collected for  $\gamma$ -counting. Protein was detected by absorbance at 215 nm and tyrosine fluorescence (excitation 275 nm, emission 305 nm). The amount of bIGFBP-2 recovered from the column was estimated by the integrated area of the 215 nm absorbance peak using the molar extinction coefficient  $\epsilon_0 = 1.03 \times 10^6$   $\mu$ volt.sec. $\mu$ g<sup>-1</sup> (Forbes *et al.*, 1998) and standardised with accurately quantified IGF-II standards (GroPep Pty. Ltd.). The amount of iodine incorporated was estimated by the radioactivity associated with the bIGFBP-2 peak, adjusting for the known <sup>125</sup>I specific activity. The elution times of bIGFBP-2, IGF-II and radioactive iodide were established by independent injection of the respective components.

### 3.3.3 Iodinations of bIGFBP-2 for IGF Binding Assays

bIGFBP-2 was modified as described in Section 3.3.1 in this Chapter, except that the radioactive iodine isotope <sup>125</sup>I was omitted from the reaction. Again, bIGFBP-2 was iodinated alone as well as in a complex with both IGF-I and IGF-II. The molar ratio of bIGFBP-2:NaI:chloramine-T was maintained at 1:40:30. The iodinated bIGFBP-2 species were then purified by HPLC gel-filtration as described above (Section 3.3.2) and the incorporation of iodine was confirmed by the loss of tyrosine-specific fluorescence during the chromatography. The relative affinities of the respective iodinated bIGFBP-2 species for both <sup>125</sup>I-labelled IGF-I and IGF-II were determined by charcoal binding assay, as described in Section 2.3.8, Chapter 2.

### 3.3.4 Iodinations of bIGFBP-2 for Peptide Mapping

bIGFBP-2 (3.9 nmole) was dissolved in 255  $\mu$ l of iodination buffer and divided into three equal 1.3 nmole aliquots. Either IGF-I or IGF-II (5 nmole in 40  $\mu$ l of 10 mM acetic acid) was added to one aliquot, whilst 40  $\mu$ l of 10 mM acetic acid was added to the other

two bIGFBP-2 solutions. The reaction mixtures were incubated at room temperature for 120 min to allow the complex between IGF and bIGFBP-2 to form. Then 52 nmole of NaI (specific radioactivity 2 nCi / nmole) was added to each of the three bIGFBP-2 solutions. Sodium metabisulphite, 200 nmole in 10  $\mu$ l of water, was added to one of the bIGFBP-2 solutions to prevent iodination in this tube. Following the addition of 40 nmole of chloramine-T in 10  $\mu$ l of water (corresponding to a bIGFBP-2:NaI:chloramine-T molar ratio of 1:40:30) to each tube, the iodination reactions proceeded as described above. The iodinations of bIGFBP-2 alone and bIGFBP-2 in complex with IGF-I or IGF-II were then stopped by the addition of 200 nmole of sodium metabisulphite in 10  $\mu$ l of water. All of the reaction mixtures were acidified by the addition of 100  $\mu$ l of 4 M acetic acid and the bIGFBP-2 species were then purified by HPLC gel-filtration as described above and the bIGFBP-2 peaks were dried under vacuum (Speed-Vac, Savant).

### 3.3.5 Tryptic Mapping of bIGFBP-2

Iodinated and non-iodinated bIGFBP-2 species were subjected to tryptic peptide mapping as follows. Each of the lyophilised bIGFBP-2 species was denatured and reduced in 1 ml of S-carboxymethylation buffer (8 M urea, 0.6 M guanidine.HCl, 20 mM dithioerythritol (DTE), 50 mM Tris.HCl, pH 8.5) and the cysteine thiols were blocked by reaction with 69  $\mu$ moles of iodoacetic acid (IAA) in 200  $\mu$ l of 1 M Tris.HCl, pH 8.5. The reaction was allowed to proceed in the dark at room temperature for 15 min and subsequently, the S-carboxymethylated bIGFBP-2 species was purified on a C4 reverse-phase HPLC cartridge (Brownlee Aquapore BU300 C4, 7  $\mu$ m particle size, 300 Å pore size and dimensions of 2.1 mm x 100 mm). The protein was eluted over a linear gradient of 10 to 50 % acetonitrile (v/v) in 0.1 % (v/v) TFA over 20 min, at a flow rate of 0.5 ml / min. The bIGFBP-2 peak was collected and concentrated to approximately 20  $\mu$ l by solvent evaporation under vacuum (Savant Speed-Vac), then diluted to 1 ml with digestion buffer (250 mM Tris.HCl pH 8.5, 20 mM CaCl<sub>2</sub>). Digestion was initiated by the addition of 2  $\mu$ g of trypsin in 2  $\mu$ l of 10 mM acetic acid and the mixture was incubated at 37° C for 12 h after which a further 2  $\mu$ g trypsin was added and the digestion continued for an additional 12 h. This corresponded to a final enzyme to substrate ratio of 1:10 (w/w) and a total reaction time of 24 h. Due to the high enzyme to substrate ratio and extended reaction times, the self-digestion products of trypsin were also determined in a control incubation of trypsin in digestion buffer alone, under the same conditions. The digestions were stopped by the addition of 10  $\mu$ l of TFA. The digested bIGFBP-2 peptides were

separated by C4 reverse-phase HPLC (using the same cartridge as described above) at 40°C with a linear gradient of acetonitrile from 0 to 50 % (v/v) in 0.1 % (v/v) TFA over 50 min at 0.5 ml / min. The absorbance of the peptide backbone bonds were monitored at 215 nm, aromatic residues at 275 nm and tryptophan at 295 nm. Unmodified tyrosyl peptides were detected by their specific fluorescence (excitation 275 nm, emission 305 nm) whilst iodinated tyrosyl peptides were detected at 295 nm and by detection of  $\gamma$ -radiation as tyrosine iodination abolished tyrosine fluorescence (Cowgill, 1965). Eluate was collected in 0.25 min fractions starting with the first fluorescent peak.

Peptides which contained tyrosyl peptides were subjected to N-terminal sequencing. Edman degradation was carried out automatically on an Applied Biosystems model 470A gas-phase Sequencer with a 900A Control/Data Analysis Module. Mono-iodo-tyrosine and Di-iodo-tyrosine were identified in the sequencer chromatograms (Tsomides & Eisen, 1993) and were confirmed by their radioactivity. The separate tryptic peptides which encompass the six tyrosine residues of bIGFBP-2 (Tyr-60, Tyr-71, Tyr-98, Tyr-213, Tyr-226 and Tyr-269) will be referred to subsequently as the peptides P1, P2, P3, P4, P5 and P6 respectively and the iodinated derivatives will be referred to as Px\* (mono-iodotyrosyl derivative) and Px\*\* (di-iodotyrosyl derivative) where (x) refers to the peptides 1-6.

The positions of P1, P2, P3, P4, P5, P6 and the iodinated derivatives of these peptides in the elution profile of the tryptic map were established by N-terminal sequencing. The identities of tyrosine containing peptides were confirmed by electrospray mass spectroscopy (ES-MS) on a Perkin Elmer Sci-ex triple quadrupole mass spectrometer by Mr. Yoji Hayasaka at Australian Research Council Mass Spectrometry Unit, Urrbrae, Adelaide.

### **3.4 RESULTS**

In this study, differential iodination was used to investigate the interaction between bIGFBP-2 and IGF-I or IGF-II at the molecular level. As the 6 tyrosine residues of bIGFBP-2 are distributed within both the N- and C-terminal cysteine-rich domains, the pattern of tyrosine iodination could be used to identify the region(s) of bIGFBP-2 to which the IGFs bound. Firstly, the tyrosine residues of bIGFBP-2 that were available for iodination in the presence and absence of IGF-ligand were titrated with increasing concentrations of HOI. Maximal loss of tyrosine-fluorescence in the bIGFBP-2 molecule was chosen as a suitable end-point for the iodination reaction. Thereafter, the biological activity of differentially iodinated bIGFBP-2 species were compared. Fig. 3.1 shows the



basic strategy that was used to identify specific tyrosine residues of bIGFBP-2 which are protected from chemical iodination when IGFs are bound.

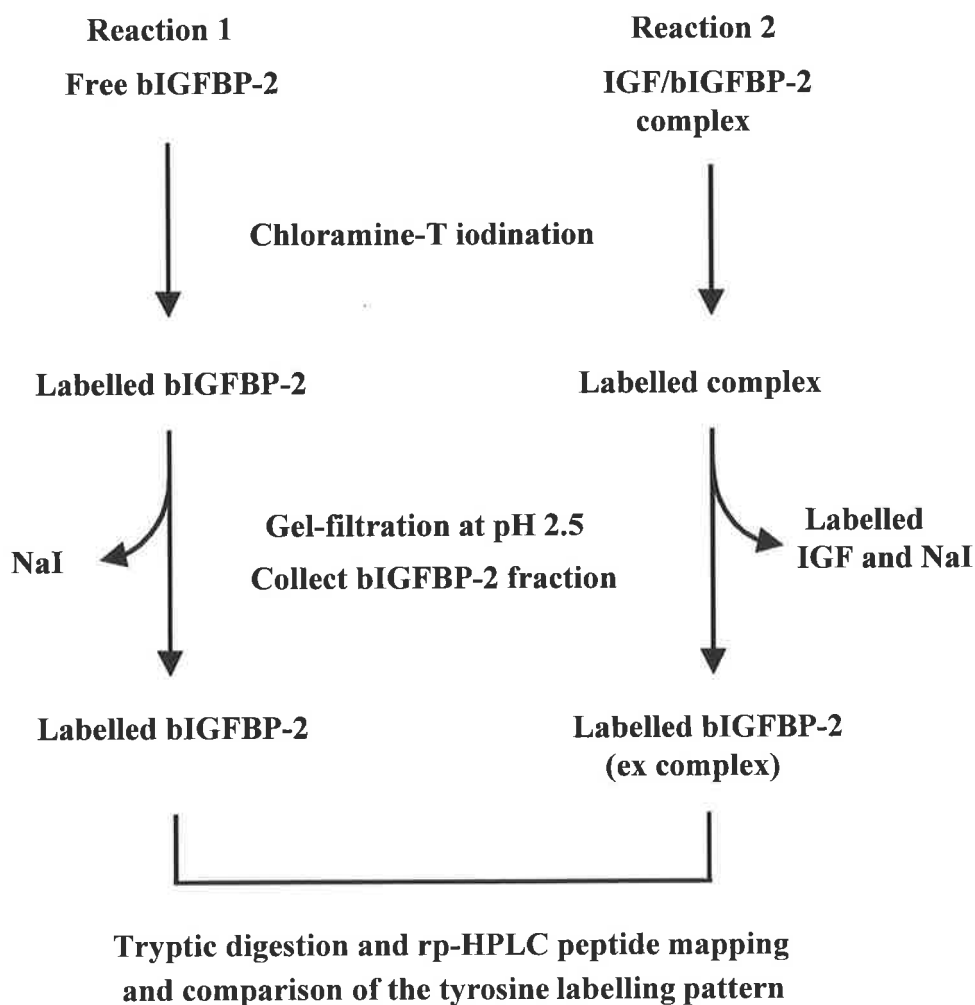
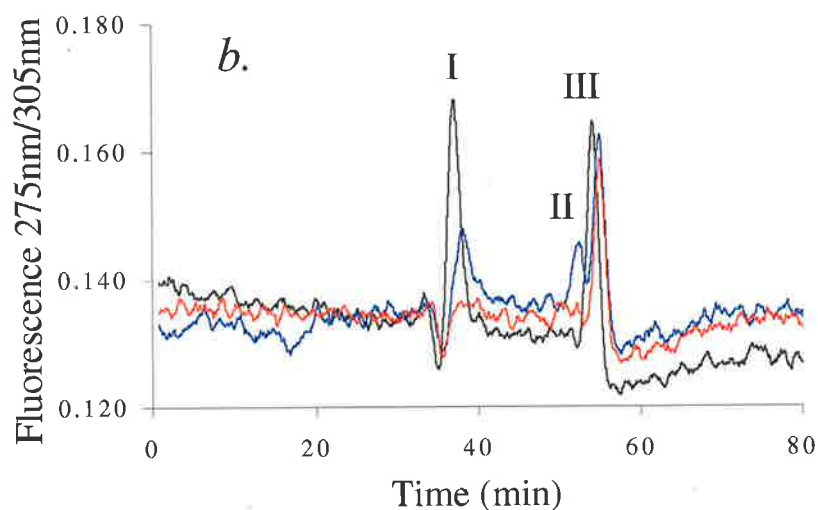
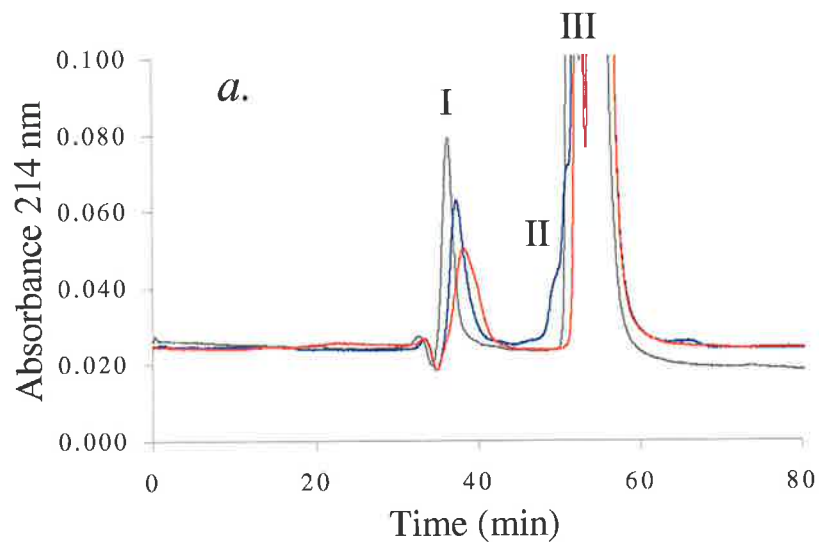


Fig. 3.1 - The differential iodination strategy used to locate an IGF-binding region of bIGFBP-2

### 3.4.1 Titration of Reactive bIGFBP-2 Tyrosine Residues

bIGFBP-2 was iodinated over a range of reaction conditions that differed in the concentration of the reactive HOI species. The strength of HOI was controlled by altering the chloramine-T/NaI molar ratio (Section 3.3.1). Separation of iodinated bIGFBP-2 species from the reaction salts and IGF-ligand (when present) was achieved by HPLC gel filtration chromatography at acid pH, as described in Section 3.3.2. The chromatography eluate was monitored at 215 nm with an online absorbance detector to quantify protein species (Fig. 3.2a). From the peak area at 215 nm, the amount of bIGFBP-2 was calculated

as described in Section 2.3.4.4. In addition, an on-line fluorescence detector provided an estimate of the fraction of tyrosine residues that had not been iodinated (Fig. 3.2*b*). This was possible as iodination abolished tyrosine-specific fluorescence (Cowgill, 1965). The peak area of tyrosine-fluorescence, after correction for the amount of bIGFBP-2 recovered, was expressed as a percentage of the unmodified bIGFBP-2 molecule. As trace amounts of  $\text{Na}^{125}\text{I}$  were included in the reaction mixtures, iodine incorporation into bIGFBP-2 could be quantified by the  $^{125}\text{I}$ -associated  $\gamma$ -radiation in chromatography fractions as shown in Fig. 3.2*c*. Accordingly, the molar incorporation of iodine into bIGFBP-2 for each reaction condition was calculated. Tab. 3.1 and Fig. 3.3 summarise the molar incorporation of iodine into differentially iodinated bIGFBP-2 species and the corresponding tyrosine-specific fluorescence loss.



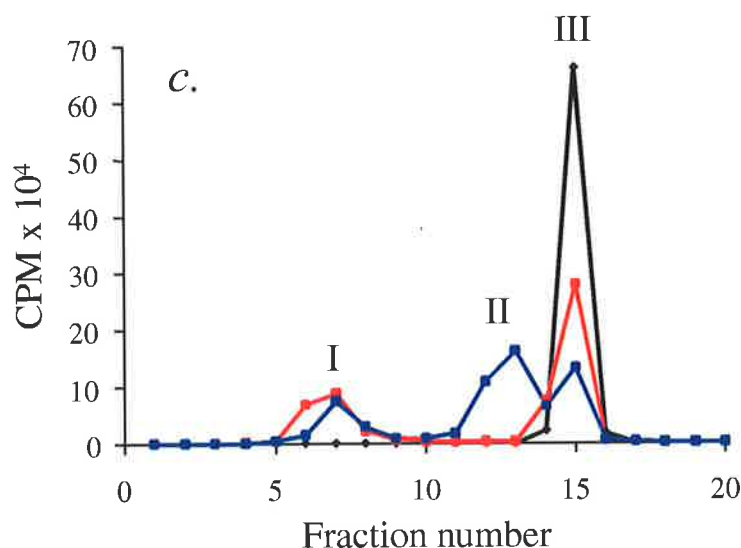


Fig. 3.2 – Analysis of iodinated bIGFBP-2 species by HPLC gel-filtration chromatography. A range of iodination conditions that differed in the concentration of the reactive HOI species were screened to optimise the iodination reaction. Shown are overlaid chromatograms of non-iodinated bIGFBP-2 and differentially iodinated bIGFBP-2 that was modified under the conditions indicated as arrows in Fig. 3.3. (a.) Shows the absorbance at 215 nm, (b.) shows the tyrosine-specific fluorescence and (c.) shows the <sup>125</sup>I-associated  $\gamma$ -radiation of chromatography fractions that were collected during the chromatography (see Sections 3.3.1 and 3.3.2). The samples shown are non-iodinated bIGFBP-2 (—) and bIGFBP-2 that was iodinated in the presence (—) and absence (—) of IGF-ligand with a chloramine-T/NaI molar ratio of 0.75. Peak I corresponds to bIGFBP-2, peak II corresponds to IGF-II and peak III corresponds to the reaction salts.

Increasing molar incorporation of iodine into 0.1 nmole aliquots of bIGFBP-2 was observed when the chloramine-T/NaI molar ratio was increased from 0.125 to 1.25 (Fig. 3.3a). This figure also shows that when bIGFBP-2 was iodinated in a complex with IGF-II, the molar incorporation of iodine into bIGFBP-2 was substantially reduced. A steady increase in iodine incorporation was observed for both differentially iodinated bIGFBP-2 species as the molar ratio of chloramine-T/NaI in the reaction was increased from 0.125 to 0.75. However, when the chloramine-T/NaI molar ratio was increased beyond 0.75, the subsequent increase in iodine incorporation into both protected and free bIGFBP-2 was less, on a molar basis. For IGF-protected bIGFBP-2 this change in the reactivity of the bIGFBP-2 tyrosine residue population was observed to occur when approximately 4 moles of iodine had been incorporated per bIGFBP-2 molecule compared with approximately 7 moles of iodine for bIGFBP-2 alone. These results suggests that the number of reactive tyrosine residues of bIGFBP-2 was reduced when IGF-II was bound.

Table 3.1 - A summary of the molar fluorescence and molar iodine incorporation of iodo-bIGFBP-2 species

bIGFBP-2 was iodinated in the absence (*a*) or presence of IGF-II-ligand (*b*) and the concentration of the reactive HOI species was altered by variation of the molar ratio of chloramine-T/NaI. The iodo-bIGFBP-2 species were separated from reaction salts and IGF-ligand, if present, by HPLC gel-filtration chromatography (Section 3.3.2). The absorbance at 215 nm and tyrosine-specific fluorescence (275 nm/305 nm) were both monitored on-line during the chromatography and fractions of the eluate were collected for the measurement of <sup>125</sup>I-associated  $\gamma$ -radiation. The amount of bIGFBP-2 recovered was estimated from the area of the peak at 215 nm as described in Section 2.3.4.4. The molar fluorescence was the peak area of tyrosine-specific fluorescence divided by the amount of bIGFBP-2 recovered, with the molar fluorescence of the unmodified bIGFBP-2 molecule expressed as 100 %. Direct measurement indicated that 1 nmole of iodine corresponded to 317095 CPM after dilution of carrier free Na<sup>125</sup>I. Accordingly, the molar incorporation of iodine into bIGFBP-2 was the amount of iodine recovered in the bIGFBP-2 peak divided by the amount of bIGFBP-2 recovered.

<i>a</i>						
[chloramine-T]/ [NaI]	bIGFBP-2 recovered (nmole)	Molar fluorescence 275 nm/305 nm (x 10 <sup>6</sup> )	Residual molar Fluorescence (% of unmodified)	bIGFBP-2 associated radioactivity (CPM)	Iodine incorporated into bIGFBP-2 (nmole)	Molar Incorporation of iodine into bIGFBP-2
0	0.10	33.9	100	928	0.00	0
0.125	0.09	20.2	59.6	30812	0.10	1.11
0.250	0.09	13.7	40.4	69748	0.22	2.44
0.375	0.09	7.1	20.9	118437	0.37	4.11
0.500	0.09	4.7	13.9	164466	0.52	5.78
0.625	-	-	-	-	-	-
0.750	0.08	3.9	11.5	183783	0.58	7.25
1.000	0.08	3.6	10.6	197143	0.67	8.38
1.250	0.06	3.5	10.3	183549	0.58	9.65
<i>b</i>						
[chloramine-T]/ [NaI]	bIGFBP-2 recovered (nmole)	Molar fluorescence 275nm/305nm (x 10 <sup>6</sup> )	Residual molar Fluorescence (% of unmodified)	bIGFBP-2 associated radioactivity (CPM)	Iodine incorporated into bIGFBP-2 (nmole)	Molar Incorporation of iodine into bIGFBP-2
0	0.10	33.9	100	928	0.00	0
0.125	0.10	29.4	86.7	5868	0.02	0.2
0.250	0.10	26.5	78.2	36286	0.11	1.1
0.375	0.10	23.4	69.0	60214	0.19	1.9
0.500	0.08	20.0	59.0	92395	0.29	3.6
0.625	0.09	20.1	59.3	101853	0.32	3.6
0.750	0.09	15.9	46.9	126706	0.40	4.4
1.000	0.08	18.4	54.3	131625	0.42	5.3
1.250	0.07	17.1	50.4	128946	0.41	5.9

The tyrosine fluorescence of the intact bIGFBP-2 molecule was a useful measure of the degree of iodination of the tyrosine residues. Hence, the chloramine-T dependent increase in bIGFBP-2 iodination was accompanied by a corresponding drop in tyrosine-specific fluorescence (Fig. 3.3*b*). As the ratio of chloramine-T/NaI per reaction was increased between 0.125 and 0.5, there was a rapid loss of bIGFBP-2 associated fluorescence. However, when the ratio of chloramine-T/NaI was increased beyond 0.5, the differentially iodinated bIGFBP-2 species sustained little further loss in tyrosine-fluorescence. Fig. 3.3*b* shows that the tyrosine-fluorescence ultimately dropped to approximately 10 % of the unmodified molecule when bIGFBP-2 was iodinated alone. In contrast, bIGFBP-2 which had been iodinated whilst protected by IGF-II still retained 50 % of the fluorescence of the unmodified molecule. Both sets of data outlined above, which are representative examples of 4 independent experiments, suggest that normally reactive tyrosine residues of bIGFBP-2 were protected from iodination when IGF-II was bound. The titration of tyrosine residues with increasing levels of HOI was used to determine suitable reaction conditions for the terminal mono-iodination of differentially iodinated bIGFBP-2 species. Iodination of 0.1 nmole of bIGFBP-2 in reaction conditions that contained 4 nmole of NaI and greater than 3 nmole of chloramine-T resulted in an increased molar incorporation of iodide (Fig. 3.3*a*), but no further loss of tyrosine-specific fluorescence (Fig. 3.3*b*). Evidently, the observed increments of iodine incorporation were due to di-iodination of tyrosyl residues that had previously been mono-iodinated and therefore, limiting tyrosine-fluorescence loss indicated that all of the available tyrosine residues of bIGFBP-2 had been terminally mono-iodinated. Accordingly, the reaction conditions that are indicated by the arrows in Fig. 3.3 (ie: a 1:40:30 molar ration of bIGFBP-2, NaI and chloramine-T respectively) were used for all subsequent iodination studies.

#### **3.4.2 Determination of the Biological Activity of Iodinated Forms of bIGFBP-2**

The abilities of non-radioactive iodinated bIGFBP-2 species to bind radio-labelled IGF-I or IGF-II were compared. Fig. 3.4 shows the binding of radio-labelled IGF-I (*a.*) and IGF-II (*b.*) respectively by increasing amounts of iodinated bIGFBP-2 species. All of the iodinated bIGFBP-2 species were observed to bind the same maximal percentage of radio-labelled IGF-I or IGF-II tracer as unmodified bIGFBP-2. However, the

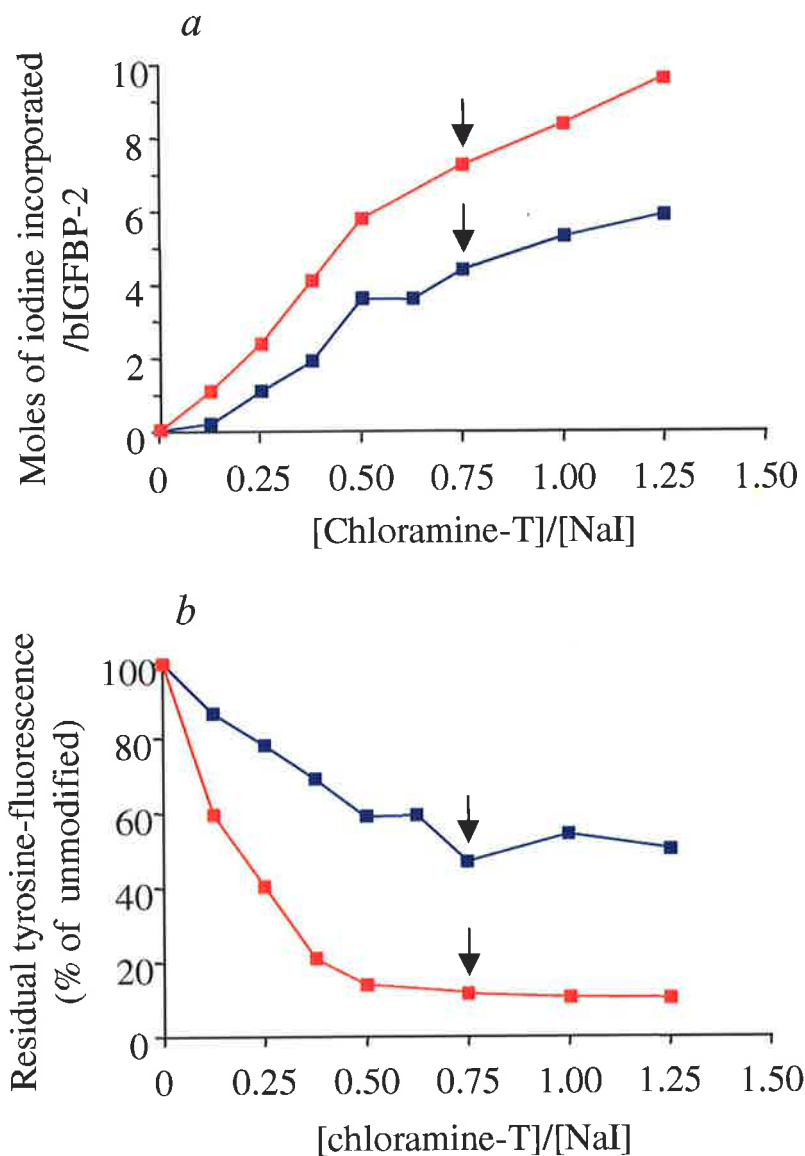
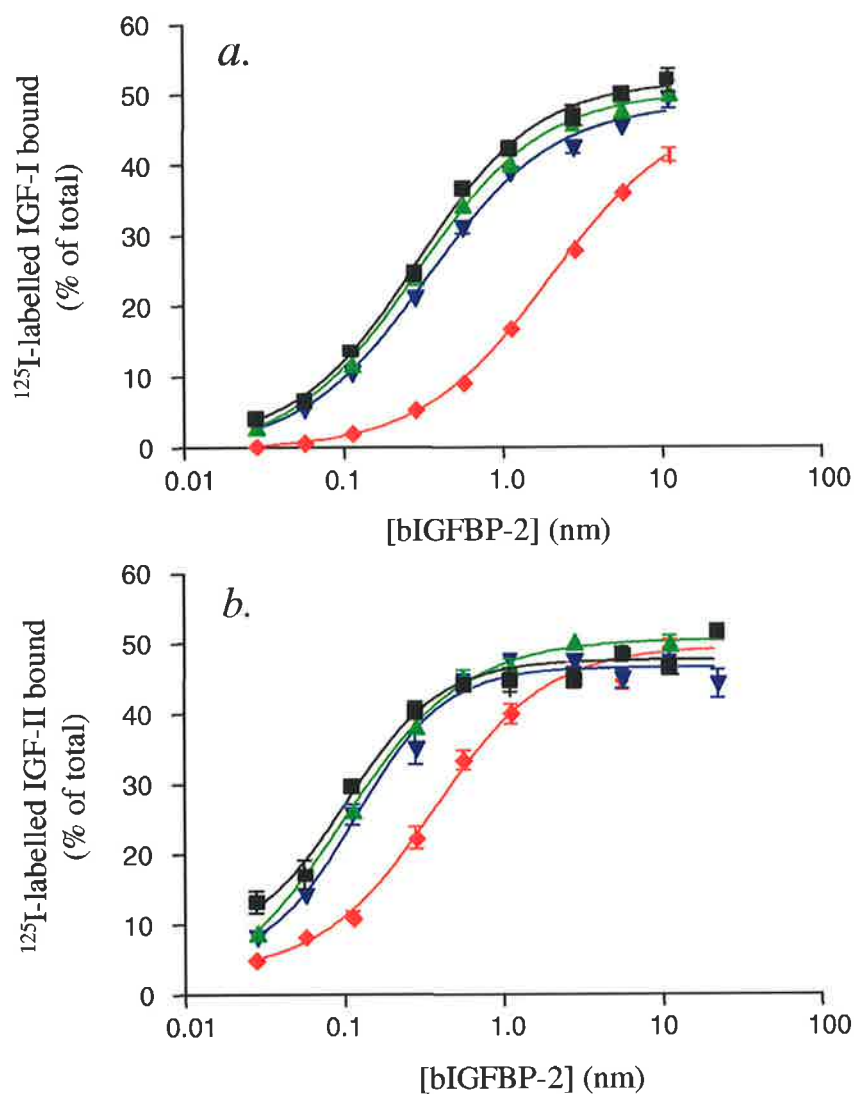


Fig. 3.3 - **The molar incorporation of iodine into bIGFBP-2 and resultant loss of tyrosine-fluorescence.** bIGFBP-2 was iodinated alone ( ■ ) or in a complex with IGF-II ( ■ ) under reaction conditions where the concentration of the reactive HOI species was varied by the amount of chloramine-T. Each point represents an independent reaction performed in the same experiment. (a.), The molar incorporation of iodine into bIGFBP-2 as calculated by the absorbance peak area of bIGFBP-2 at 215nm and the radiation of incorporated  $^{125}\text{I}$ . (b.), The residual bIGFBP-2 tyrosine-fluorescence (excitation 275 nm, emission 305 nm). Arrows indicate limiting tyrosine fluorescence loss which is indicative of terminal bIGFBP-2 mono-iodination. These results are representative of four similar experiments.

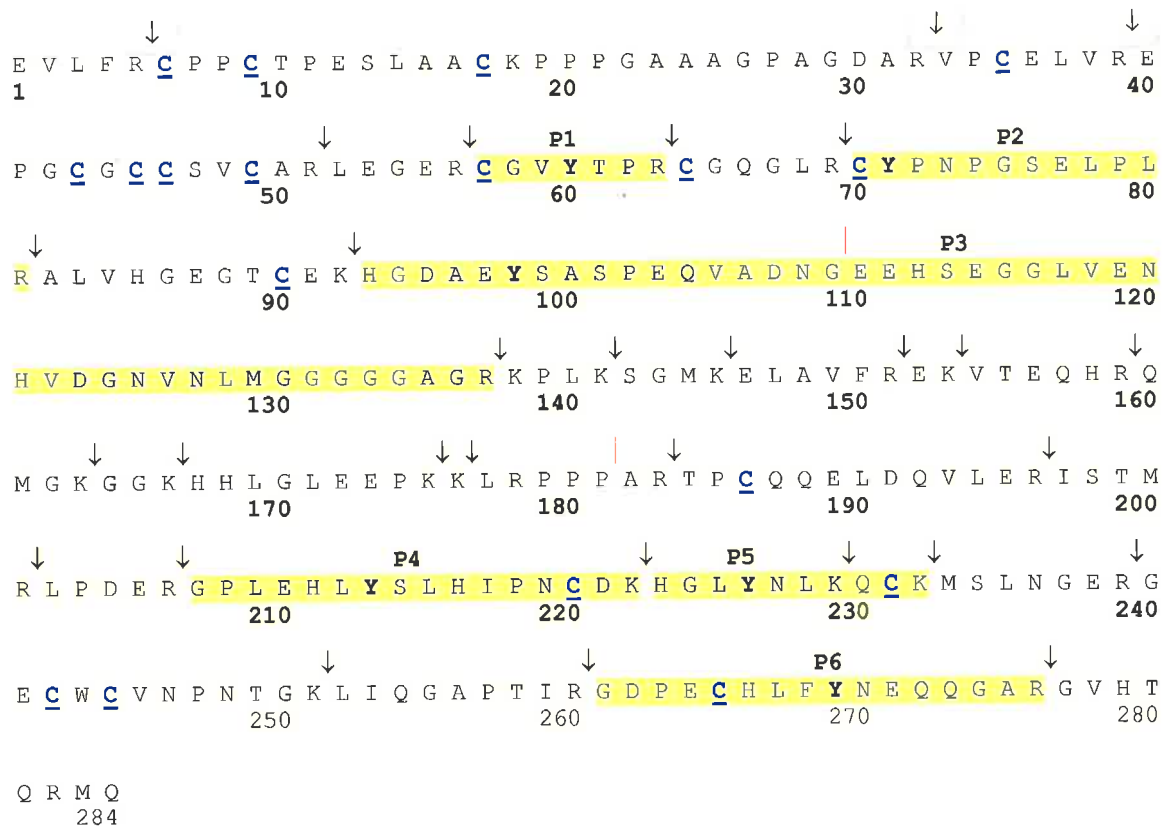


**Fig. 3.4 - The IGF binding assays of iodinated and non-iodinated bIGFBP-2 species.** Increasing amounts of unmodified bIGFBP-2 (■); IGF-I protected iodinated bIGFBP-2 (▲); IGF-II protected iodinated bIGFBP-2 (▼) and unprotected iodinated bIGFBP-2 (◆) were incubated with either radio-labelled IGF-I (15,000 CPM) (a) or radiolabelled IGF-II (6000 CPM) (b). The unbound IGF was separated from the bIGFBP-2 bound (see section 2.3.8), and then the bound IGF was quantitated by counting the radioactivity and expressed as a percent of total.

concentration of iodinated bIGFBP-2 peptide required to bind half of the maximal percentage of IGF tracer was increased from 0.29 nM to 1.98 nM for IGF-I and 0.1 nM to 0.36 nM for IGF-II, if bIGFBP-2 was not iodinated in a complex with either IGF-I or IGF-II. In contrast, bIGFBP-2 iodinated whilst in a complex with either IGF-I or IGF-II, showed half-maximal binding that was essentially the same as unmodified bIGFBP-2.

### 3.4.3 Identification of IGF/IGFBP Binding Site

Complete tryptic digestion of bIGFBP-2 would theoretically generate 32 fragments ranging in size from single amino acids up to a peptide of 45 residues (Fig. 3.5).



### Partial digestion products identified

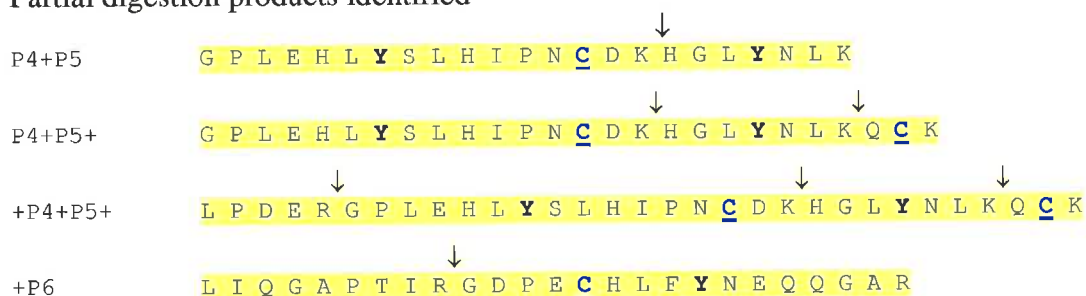


Fig. 3.5 – **Tryptic peptides of bIGFBP-2.** The amino acid sequence of bIGFBP-2 is in the single letter code. Trypsin-sensitive peptide bonds are indicated (↓) and tyrosine containing tryptic peptides of bIGFBP-2 are highlighted in yellow and labelled P1 to P6 with respect to their order in the sequence. The tyrosine residues are shown in bold and the IGFBP cysteine residues are shown in blue and underlined. The putative domain junctions of bIGFBP-2 as predicted by the common IGFBP family gene structure (Landale *et al.*, 1995) are also shown (|). Partial trypsin digestion products from the C-terminal region of bIGFBP-2 are also highlighted underneath the main sequence.

Despite known problems of self-degradation, trypsin was chosen as the proteolytic mapping enzyme because in theory it should liberate each tyrosine residue in a discrete peptide fragment. Following tryptic digestion, the peptides of bIGFBP-2 were separated by reverse-phase HPLC (Fig. 3.6). Auto-digestion of trypsin (Fig. 3.6d) generated a background of 3 fluorescent peaks. Digestion of unmodified bIGFBP-2 (Fig. 3.6a) resulted in the generation of 9 tyrosine containing peptides in addition to those derived from trypsin



as detected by fluorescence. The pattern of digestion shown in Fig. 3.6 is representative of the many experiments performed (data not shown). N-terminal sequence analysis and ES-MS identified the fluorescent tryptic peptides of bIGFBP-2 to be (in order of elution) P1, P6, P2 and P3, +P6, P4+P5+, P4+P5, +P4+P5, where (+) indicates an intact trypsin sensitive bond, as defined in Fig. 3.5. The tyrosyl peptides P4, P5 and P6 were all identified as partial digestion fragments whilst the peptides P2 and P3 were not resolved by this chromatography. The mass of the peptide which was identified as P3 by N-terminal sequencing was between 15 and 16 mass units greater than the predicted mass. One possible explanation for this observation is the previously documented oxidation of methionine by chloramine-T (Baker *et al.*, 1990; Mistry *et al.*, 1991). The ES-MS and N-terminal sequencing results are summarised in Tab.3.2a.

The loss of tyrosine fluorescence due to iodination can clearly be seen when the tryptic map of unmodified bIGFBP-2 shown in Fig. 3.6a is compared with the tryptic fluorescence maps of bIGFBP-2 iodinated either alone (Fig. 3.6b) or in a complex with IGF-II (Fig. 3.6c). In Tab. 3.2b, the differences in the residual fluorescence tryptic map of bIGFBP-2 which was iodinated in a complex with IGF-II or alone are summarised. An additional fluorescent peak (A) was present in the iodinated bIGFBP-2 maps but not the unmodified bIGFBP-2 map. This peak was most probably an artifact of the iodination reaction as both N-terminal sequence and ES-MS analysis showed conclusively that this peak was not a peptide. The order of tyrosine reactivity when calculated in terms of the residual tyrosine fluorescence (Tab. 3.2b) changed from P6>P1>P2&P3>P4+P5 when bIGFBP-2 was modified alone to P2&P3>P6>P4+P5>P1 when bIGFBP-2 was modified in a complex with IGF-II. However, the major difference in the iodination pattern of both free bIGFBP-2 and IGF-II associated bIGFBP-2 was the large residual fluorescence of the peptide P1 in the map of IGF-II associated bIGFBP-2 (Fig. 3.6c). When quantified, the residual fluorescence of this peptide was 94 % of the fluorescence yielded by the same peptide isolated from unmodified bIGFBP-2 (Fig. 3.6a) and was 5.7-fold more intense than for the same peptide from bIGFBP-2 which had been iodinated free of IGF-II (Fig. 3.6b). The amount of unmodified P6 peptide was very low in all of the iodinated bIGFBP-2 tryptic maps which indicated that this residue was freely available for iodination, although complex formation with IGF-II afforded a 2.5-fold protection against modification at this site (Fig. 3.6c) in comparison to bIGFBP-2 modified alone (Fig. 3.6b). The unmodified tyrosyl peptides P2 and P3, were 2.8 times more abundant in the peptide map of bIGFBP-2

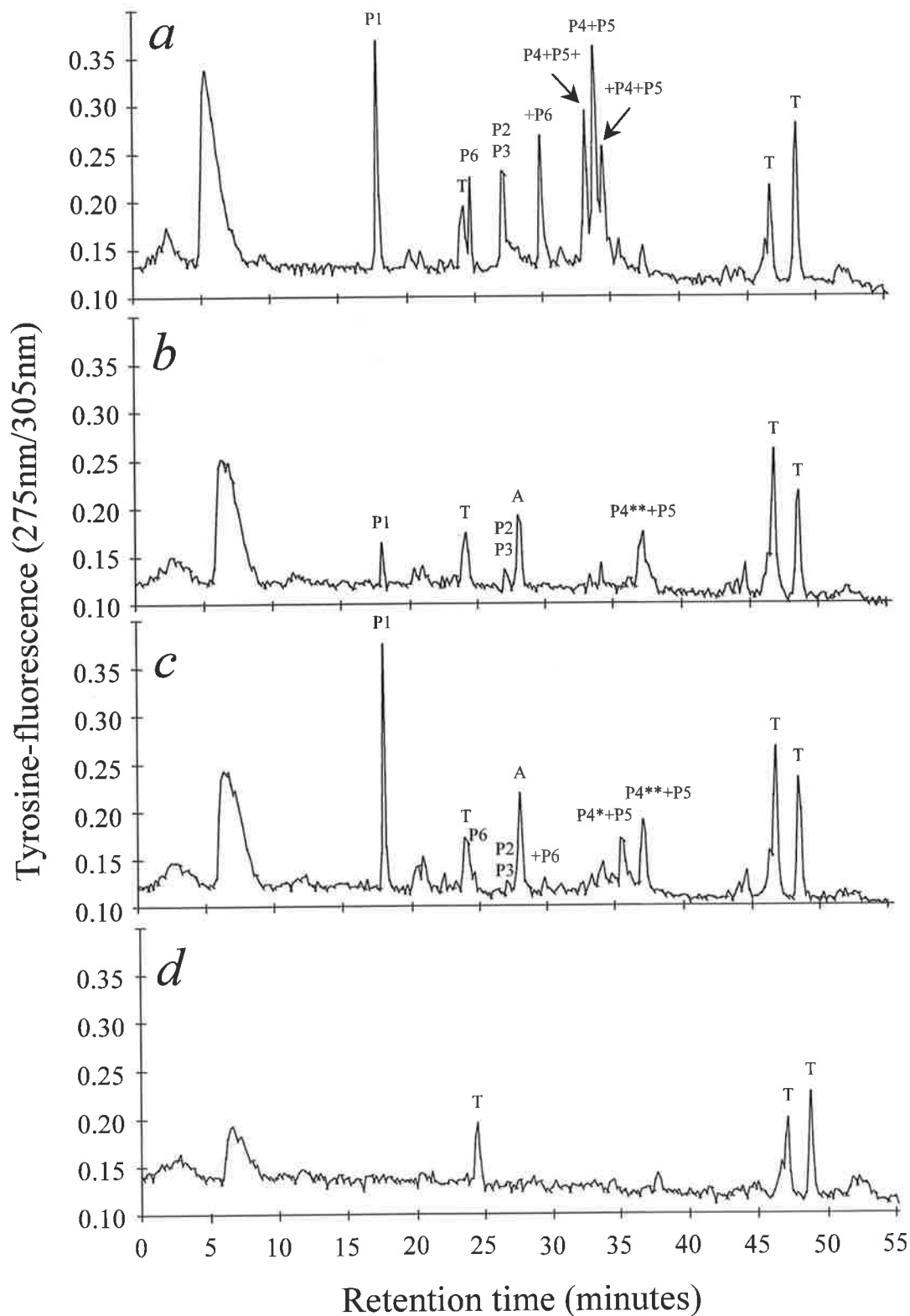


Fig. 3.6 - The tyrosine fluorescence of reverse-phase HPLC-resolved tryptic bIGFBP-2 fragments and trypsin. Shown are the tyrosine-specific fluorescence chromatograms of unmodified bIGFBP-2 (*a*), bIGFBP-2 iodinated free (*b*), and associated with IGF-II (*c*). The fluorescent auto-digestion products of trypsin are shown in (*d*). The retention pattern of tyrosyl peptides of bIGFBP-2, as identified by N-terminal sequencing and mass spectroscopy, is shown in chromatograms *a*, *b* and *c*. The peptides P4, P5 and P6 were all identified as partial digestion products and intact trypsin-sensitive peptide bonds are

indicated by (+). Peptides labelled with (T) corresponded to peptides from auto-digestion of trypsin and the peak labelled (A) was a non-peptide artifact of the iodination reaction. a complex with IGF-II.

modified alone (Fig. 3.6*b*) than bIGFBP-2 iodinated with IGF-II bound (Fig. 3.6*c*). The additive residual fluorescence of partially digested peptides which contained P4 and P5 were similar (Fig. 3.6, *b* and *c*) regardless of IGF association prior to the iodination reaction. The fluorescence associated with P4+P5 peptides was significant, accounting for 36 % of the total remaining fluorescence of the unmodified tyrosyl peptides.

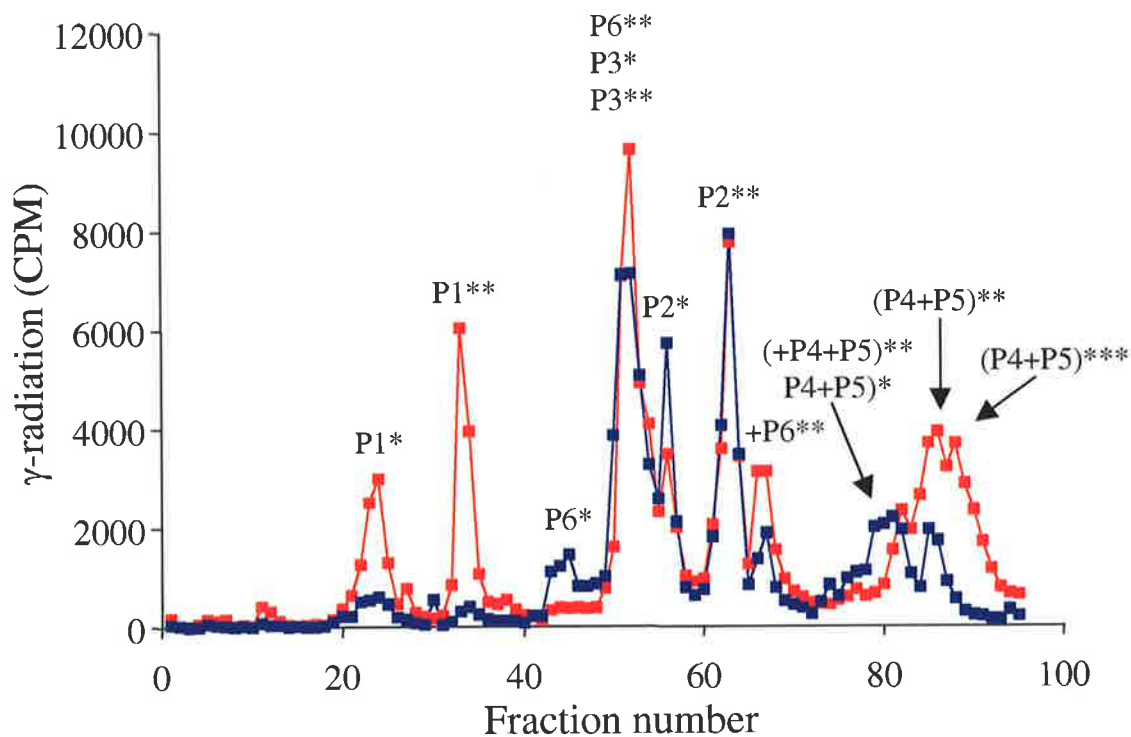


Fig. 3.7 - **Identification of iodinated tyrosyl peptides of bIGFBP-2.** Shown are the overlaid radioactivity chromatograms of bIGFBP-2 iodinated free (-■-), and associated with IGF-II (-■-). The peptides were separated by rp-HPLC as described in Section 3.3.5. Peaks which were shown by N-terminal sequencing and mass spectroscopy to correspond to modified tyrosyl peptides of bIGFBP-2 are shown. \* and \*\* indicate that one and two iodine atoms respectively have been incorporated into the tyrosyl peptide. P4, P5 and P6 were all identified as partial digestion products and intact trypsin sensitive peptide bonds are indicated by a (+).

The tryptic peptides of bIGFBP-2 which had incorporated iodine were also directly identified by their  $^{125}\text{I}$  radioactivity. Fig. 3.7 shows an overlay of the tryptic map fractions of bIGFBP-2 iodinated free and bIGFBP-2 iodinated as a complex with IGF-II which contain  $^{125}\text{I}$  radioactivity. Fractions which contained iodinated peptides were characterised by both N-terminal sequencing and ES-MS as summarised in Tab. 3.3*a*. Tyrosine

containing peptides were the only peptides of bIGFBP-2 which were found to incorporate iodine under our reaction conditions. As shown in Fig. 3.7, the order of elution of iodinated tyrosyl peptides of bIGFBP-2 was determined to be P1\*, P1\*\*, P6\*, P6\*\* & P3\* & P3\*\*, P2\*, P2\*\*, +P6\*\*, (+P4+P5)\*\* & (P4+P5)\*, (P4+P5)\*\* and (P4+P5)\*\*\*, where brackets indicate that the locations of the iodine atoms in these peptides were not characterised. The incorporation of iodine was observed to increase the hydrophobicity of tyrosine containing peptides as can be seen in the longer retention times of modified peptides (Tab. 3.2a). The exceptions to this were the mono-iodotyrosyl (\*) and di-iodotyrosyl (\*\*) derivatives of P3, which did not exhibit significantly increased retention times, presumably due to the larger size of this tyrosyl peptide (45 residues). Edman degradation of the iodinated derivatives of P4+P5 peptides indicated that the tyrosine residue in P4 (Tyr-213) and not P5 (Tyr-226) was a major site of iodine incorporation into bIGFBP-2.

It is immediately evident on comparison of panels *a.* and *b.* in Fig. 3.6 that the peptide P1 was shielded from iodination when IGF-II was bound. Quantification of the iodinated peptides helped to decipher the impact of IGF-association on the modification of other bIGFBP-2 tyrosyl peptides. The extent of iodine incorporation at each tyrosine residue could be calculated as a fraction of the total radioactivity incorporated into bIGFBP-2 thereby allowing the relative reactivity of each tyrosine residue to be compared, as summarised in Tab. 3.3b. These data also show that the association of IGF-II with bIGFBP-2 did not significantly reduce the incorporation of iodine into the peptides P2, P3 or P6. In fact, there was a slight increase in the modification of the peptides P2, P3 and P6 when IGF was associated with bIGFBP-2. The fluorescence data described above also showed an increase in the degree of modification of the peptides P2 and P3 when bIGFBP-2 was iodinated in a complex with IGF. A slight protection against modification in either P4 or P5 was observed when bIGFBP-2 was iodinated in a complex with IGF-II. The peptide P1 accounted for 15 % of the total iodine incorporation when bIGFBP-2 was iodinated alone. In contrast, the labeling of this peptide was reduced by a factor of 4.3 to only 3.5 % of the total iodine incorporation when bIGFBP-2 was iodinated in a complex with IGF. This result is in strong agreement with the fluorescence data reported above.

Presented in Fig. 3.7 is the profile of  $^{125}\text{I}$  radioactivity in tryptic peptides of bIGFBP-2 iodinated whilst in a complex with IGF-II. Essentially the same modification pattern was observed when the protective ligand was IGF-I or IGF-II, as shown in Fig. 3.8. The major difference between the peptide maps shown in Fig. 3.7 and Fig. 3.8 is that the

tryptic cleavage in the C-terminal region of bIGFBP-2 was more successful in the maps shown in Fig. 3.8.

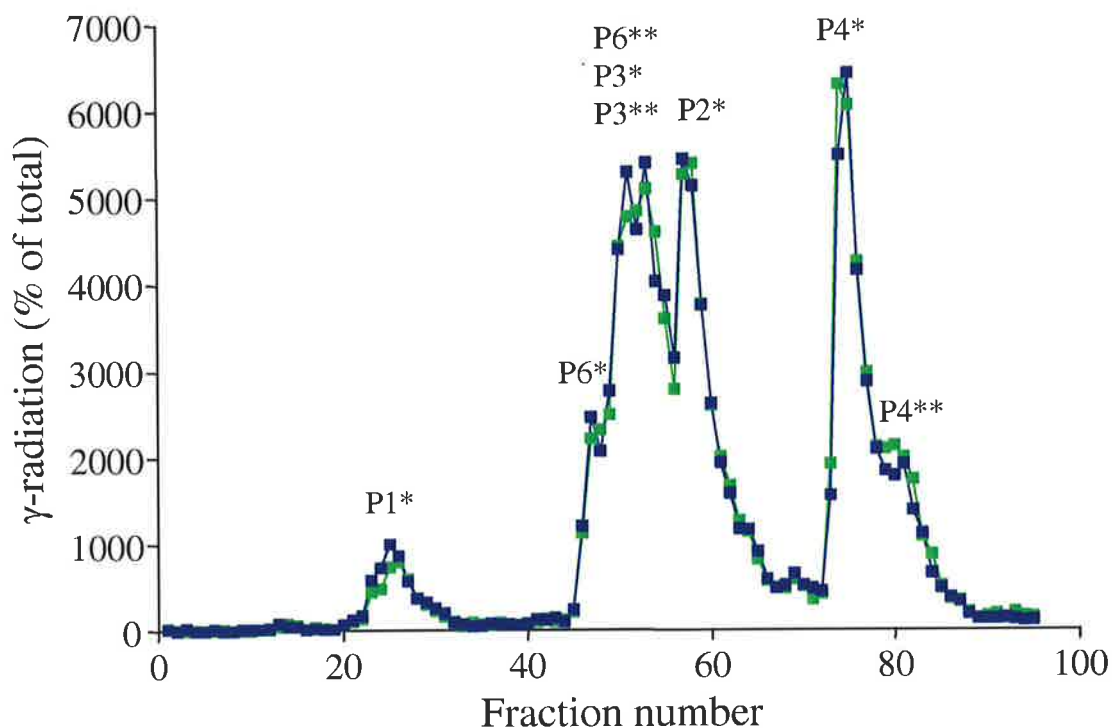


Fig. 3.8 - Comparison the iodination pattern of bIGFBP-2 iodinated in the presence of IGF-I and IGF-II. Shown are the overlaid radioactivity chromatograms of bIGFBP-2 iodinated in a complex with IGF-I (—■—) or IGF-II (—■—). Peaks which were shown by N-terminal sequencing and mass spectroscopy to correspond to modified tyrosyl peptides of bIGFBP-2 are shown. \* and \*\* indicate that one and two iodine atoms respectively have been incorporated into the tyrosyl peptide.

### 3.5 DISCUSSION

Iodination is a very sensitive chemical modification technique which, under mildly acidic conditions, specifically labels tyrosine residues (Means & Feeney, 1971). In this study, chemical iodination has been used as a structural and functional probe to investigate the interaction between bIGFBP-2 and its ligands IGF-I and IGF-II. Assessment of the alteration in IGF-binding activity after the bIGFBP-2 molecule had been iodinated provided insight into the functional significance of the tyrosine residues of bIGFBP-2 for IGF-interactions. In contrast, characterisation of the tyrosine modification pattern of bIGFBP-2 identified the tyrosine side-chains that were surface accessible in the bIGFBP-2 structure. Moreover, the differential iodination of bIGFBP-2, in the presence and absence

Table 3.2 - A summary of bIGFBP-2 tryptic peptides identified by tyrosine-specific fluorescence

*a*, bIGFBP-2 tryptic peptides which contained tyrosyl residues were detected by their tyrosine-specific fluorescence (excitation 275 nm, emission 305 nm) following reverse-phase HPLC. Tyrosyl peptides (P1-P6 according to their position in the bIGFBP-2 primary structure) were characterised by Edman degradation and ES-MS. The peptides P2 and P3 were not resolved. Tyrosine-containing partial digestion products in the C-terminal half of bIGFBP-2 were identified, the uncleaved trypsin sensitive bonds are shown (+). A period (.) indicates that a peptide was sequenced to the C-terminus. *b*, the residual fluorescence of each tyrosyl peptide after iodination represents the fraction of non-iodinated tyrosine in the maps of bIGFBP-2 iodinated in a complex with IGF-II, or free. Therefore, the fold protection which IGF-II afforded to each tyrosyl residue of bIGFBP-2 is the ratio of the residual tyrosine-fluorescence of peptides from bIGFBP-2 iodinated with IGF-II bound over the residual tyrosine-fluorescence of peptides from bIGFBP-2 iodinated free.

*a*

Peptide Identity	Retention time (min)	Partial N-terminal sequence	Predicted Mass <sup>1</sup>	Identified Mass
P1	17.84	CGVYTPR.	854	853
P6	24.64	GDPECHLFYNEQQGAR.	1922	1922
P2	27.09	CYPNPGSELPLR.	1404	1404
P3	27.09	HGDAEYSASPEQVADNGEEHA	4476	4491 <sup>2</sup>
+P6	29.88	LIQGAPT	2872	2873
P4+P5+	33.33	GPLEHLYS	3139	3139
P4+P5	33.95	GPLEHLYS	2719	2721
+P4+P5+	34.57	not done	3750	3349

*b*

Iodinated bIGFBP-2 species	iodine incorporation (% of total)			
	P1	P2	P6 and P3	P4+P5
IGF-protected	94	8	36	14
Free	17	23	35	6
Fold protection	5.7	0.3	1.0	2.5

1. The predicted mass takes into account the extra 58 mass units of the S-carboxymethyl group and an extra 126 mass units per iodine atom.
2. The mass of P3 was 16 mass units larger than the mass based on the amino acid composition (see Section 3.4.3)

Table 3.3 - A summary of bIGFBP-2 tryptic peptides identified by <sup>125</sup>I radioactivity

*a*, Iodinated tryptic peptides of bIGFBP-2 were separated by reverse-phase HPLC and then identified by their <sup>125</sup>I radioactivity. Tyrosyl peptides (designated P1-P6 according to their position in the bIGFBP-2 primary structure) were then characterised by Edman degradation and ES-MS. Peptides that had incorporated one or two atoms of iodine are indicated by \* and \*\*, respectively, whereas (+) indicates the presence of an intact trypsin sensitive bond. A period at the end of a peptide indicates that it was sequenced to the C-terminus. *b*, the radioactivity of each peptide is expressed as a percentage of the total radioactivity recovered in the peptide map. The radioactivity of related peptides (*e.g.* P1\* and P1\*\*) or peptides that were not resolved (*e.g.* P3\*\* and P6\*\*) are considered together. The fold-protection is the ratio of the percent iodine incorporation into given tyrosyl peptides of bIGFBP-2, when iodinated free divided by when iodinated with IGF-II bound.

<i>a</i>				
Peptide Identity	Retention time (min)	Partial N-terminal sequence	Predicted Mass <sup>1</sup>	Identified Mass
P1*	21.79	CGVYTPR.	979	979
P1**	24.00	CGVYTPR.	1104	1105
P6*	26.91	GDPECHLFYNEQQGAR.	2048	2048
P6**	28.57	GDPECHLFYNEQQGAR.	2173	2174
P3*	28.57	HGDAEYSASPEQVADNGEEHA	4602	-
P3**	28.57	HGDAEYSASPEQVADNGEEHA	4728	4746 <sup>3</sup>
P2*	29.68	CYPNPGSELPLR.	1530	1529
P2**	31.36	CYPNPGSELPLR.	1654	1655
+P6** <sup>2</sup>	32.36	LIQGAPT	3124	3124
P4**+P5+	35.82	not done	3389	3389
P4*+P5	35.82	GPLEHLYS	2846	2846
P4**+P5	37.04	GPLEHLYS	2972	2972
P4**+P5*	37.60	not done	3098	3098

<i>b</i>				
Iodinated bIGFBP-2 species	iodine incorporation (% of total)			
	P1	P2	P6 and P3	P4+P5
IGF-protected	3.5	29.8	39.2	19.5
Free	15.2	19.8	29.0	25.6
Fold protection	4.3	0.7	0.7	1.3

1. The predicted mass takes into account the extra 58 mass units of the S-carboxymethyl group and an extra 126 mass units per iodine atom.
2. The iodinated peptides P6\*\*, P3\* and P3\*\* were not resolved by the tryptic map chromatography.
3. The mass of P3 was 16 mass units larger than the mass based on the amino acid composition (see Section 3.4.3)

of IGF-ligand could directly implicate tyrosine residues of bIGFBP-2 that participated in interactions with the IGFs.

As briefly mentioned in Section 3.1.2, the chemical iodination approach has previously been used with great success to identify the tyrosine residues of both insulin and IGF-I that are functionally important for association with the insulin-receptor (Gliemann *et al.* 1979) and type-1 IGF-receptor (Schäffer *et al.*, 1993), respectively. In addition, the differential iodination approach has been used to reveal which IGF-tyrosine residues are protected from iodination by the type-1 IGF-receptor and bIGFBP-2 (Maly & Lüthi, 1988; Moss *et al.*, 1991). However, the chemical iodination approach had yet to be used to investigate IGFBP structure-function relationships.

The primary structure of bIGFBP-2 contains six tyrosine residues. Tyr-60, Tyr-71 and Tyr-98 are located in the cysteine-rich N-terminal region and the three remaining tyrosine residues, Tyr-213, Tyr-226 and Tyr-269 lie in the cysteine-rich C-terminal region of the molecule (Bourner *et al.*, 1992; Upton *et al.*, 1990). Notably, there is evidence to suggest that both the N- and C-terminal regions of IGFBPs contain elements of the IGF-binding site (see Section 1.5, Chapter 1).

In this study, the differential iodination of bIGFBP-2 showed that the presence of IGF-I or IGF-II bound to bIGFBP-2 directly prevented the modification of a population of tyrosine residues (Fig. 3.3). However, it could be argued that the additional tyrosine residues of IGF-II which are present in the “complex” iodination reaction compete with bIGFBP-2 for the reactive HOI species and therefore non-specifically reduce bIGFBP-2 modification. Yet, a range of reaction conditions were identified where the concentration of HOI was sufficiently high to mono-label all of the available tyrosine residues of bIGFBP-2, irrespective of the presence of IGF-II. This was evident when further incorporation of iodine into bIGFBP-2 did not result in a further loss of the tyrosine fluorescence associated with this molecule (Fig. 3.3*b*). Whereas bIGFBP-2 had lost 90 % of tyrosine fluorescence before a stable fluorescence minimum was reached, IGF-II associated bIGFBP-2 had only lost a maximum of 50 % of its original tyrosine-specific fluorescence. Therefore, the reduced iodination of bIGFBP-2 in the presence of IGF-ligand cannot be due to titration of HOI by the tyrosyl residues of IGF alone.

Tryptic mapping established that all of the tyrosine residues of bIGFBP-2 with the exception of Tyr-226 were readily iodinated. This was apparent as both mono- and di-iodo-tyrosyl derivatives of the tyrosine containing peptides P1, P2, P3, P4 and P6 were



identified. This suggests that Tyr-60, Tyr-71, Tyr-98, Tyr-213 and Tyr-269 are solvent accessible and are all thus potential sites for interaction with IGF-I or IGF-II.

Indeed, complex formation with IGF-II changed the availability of tyrosine residues for iodination, predominantly in the N-terminal region of bIGFBP-2. The major difference in the iodination patterns of IGF-protected and free bIGFBP-2 was iodination at Tyr-60, which was reduced by a factor of 5 when bIGFBP-2 was iodinated in a complex with IGF-II (See Fig. 3.6 and Fig. 3.7). In contrast, Tyr-71 was more reactive when IGF-II was bound to bIGFBP-2 compared with bIGFBP-2 iodinated free. Furthermore, the trends in tyrosine reactivity described above were consistent when the iodination reactions were repeated at chloramine-T/NaI molar ratios of 0.125, 0.375 and 1.25 (data not shown).

There are two likely explanations for IGF-II mediated protection of bIGFBP-2 at Tyr-60. Firstly, Tyr-60 may lie in the binding interface between bIGFBP-2 and IGF-II. Alternatively, Tyr-60 may become less accessible for iodination following a conformational rearrangement of the bIGFBP-2 tertiary structure on IGF-II binding. In contrast, the increased availability of Tyr-71 for iodination when IGF-II was bound may be due a change in the conformation of bIGFBP-2 which rendered Tyr-71 more accessible to HOI.

When the binding ability of non-iodinated bIGFBP-2 was compared with differentially iodinated bIGFBP-2 species, it was evident that iodination did not reduce the binding ability of bIGFBP-2 if this modification was carried out whilst IGF was bound (Fig. 3.4). This suggests that the residues of bIGFBP-2 that were available for iodination when IGF was bound are not involved in the binding interaction between IGF and bIGFBP-2. Therefore, it is likely that Tyr-71, Tyr-98, Tyr-213 Tyr-226 and Tyr-269 all occur in regions of the IGFBP structure that do not interact with IGF in an exclusive manner. In contrast, bIGFBP-2 that was iodinated in the absence of IGF-ligand sustained an 8-fold reduction in apparent affinity for IGF-I and a 4-fold reduction in apparent affinity for IGF-II as a result of this modification (Fig. 3.4, *a* and *b*). Therefore, not only was Tyr-60 rendered less accessible for iodination by IGF-association, but iodination at Tyr-60 also resulted in the loss of apparent affinity for both IGF-I and IGF-II.

The tyrosine labeling pattern of bIGFBP-2 was the same regardless of whether IGF-I or IGF-II was used as the protective ligand (Fig. 3.8). Yet when bIGFBP-2 was iodinated alone, the loss in binding affinity for IGF-I was 2-fold more severe than that observed for IGF-II. This result was of interest considering the difference in relative affinity of bIGFBP-2 for IGF-II over IGF-I, which has been reported to be 4-fold (Clemmons *et al.*, 1992) and

as high as 20-fold (Forbes *et al.*, 1988; Szabo *et al.*, 1988). Therefore, Tyr-60 may influence the binding of IGF-I more strongly than IGF-II. These results are consistent with the notion that bIGFBP-2 possesses distinct but overlapping binding sites for IGF-I and IGF-II. Thus Tyr-60 may be one of a number of common sites of interaction between bIGFBP-2 and both IGF structures. However, bIGFBP-2 and IGF-II may possess additional contacts that are absent in the bIGFBP-2/IGF-I interaction.

Tyr-60 is located in the cysteine rich N-terminal region of bIGFBP-2, a region in which all IGFBP family members exhibit strong sequence homology (Landale *et al.*, 1995). Alignment of the known amino acid sequences of the IGFBP family shows that there is high degree of homology in the vicinity of Tyr-60, which is consistent with conserved structure or function. Furthermore, tyrosine residues are found at the position equivalent to Tyr-60 of bIGFBP-2 in all family members with the sole exceptions being the IGFBP-1 family members, where an alanine occurs at this position (Landale *et al.*, 1995). As an alanine residue exists at this site in IGFBP-1, it is not likely that Tyr-60 is an exclusive determinant of IGF-binding. Furthermore, when the Ala residue of IGFBP-1 corresponding to Tyr-60 was mutated to Thr, there was no gross loss of IGF-affinity that could be detected by ligand-blotting (Brinkman *et al.*, 1991a). Therefore, other highly conserved residues adjacent to Tyr-60 such as Val-59 and Thr-61 may also be important for the interaction between IGFBPs and IGFs.

The strong sequence conservation in both the cysteine rich N- and C- terminal regions of IGFBPs, and the isolation of IGF binding fragments of IGFBPs which account for little more than either the N- or C-terminal regions has lead to the prediction that there are at least two independent domains in the IGFBP tertiary structure. Furthermore, it has been predicted that both the N- and C-terminal domains cooperatively bind IGF, as discussed in Section 1.5 of Chapter 1. Previous studies have been carried out to identify the minimal binding domain of IGFBP-1. These studies include deletion analysis of the N-terminus (Brinkman *et al.*, 1991a) and C-terminus (Brinkman *et al.*, 1991b), as well as random mutagenesis within the N-terminal and C-terminal regions of this molecule (Brinkman *et al.*, 1991a; Brinkman *et al.*, 1991b). The mutation of Cys to Tyr at position 38 in the N-terminal region of IGFBP-1 resulted in the loss of IGF-binding ability (Brinkman *et al.*, 1991a). However, this mutant was also observed to aggregate, presumably through non-native disulfide formation as a result of an unpaired cysteine residue in the structure. Therefore, it is likely that the loss of IGF binding was due largely to the disruption of the IGFBP-1 structure. Similarly, deletion mutants of IGFBP-1 with

abolished IGF binding activity may have resulted from a similar disruption of structure through the loss of native disulfide-bonds in the putative N- and C-terminal domains (Brinkman *et al.*, 1991a; Brinkman *et al.*, 1991b).

In conclusion, this study has shown for the first time that Tyr-60 is an important residue for the association of bIGFBP-2 with IGF-I and IGF-II. To minimise the structural disruption which may be introduced by the random substitution of amino acids, the binding interaction between bIGFBP-2 and IGF-I or IGF-II was probed by differential iodination. Complex formation with IGF-I or IGF-II specifically protected Tyr-60 of bIGFBP-2 from iodination. Furthermore, iodination of bIGFBP-2 at Tyr-60 and not Tyr-71, Tyr-213 or Tyr-269 lead to an 8-and 4-fold reduction in affinity for IGF-I and IGF-II respectively. These results are further proof to suggest that major determinants of IGF binding reside in the putative N-terminal domain of IGFBPs.

**CHAPTER 4 - ALANINE SCREENING MUTAGENESIS  
ESTABLISHES TYR-60 OF IGFBP-2 AS A  
DETERMINANT OF IGF BINDING**

## 4.1 INTRODUCTION

Differential iodination of bIGFBP-2 showed that Tyr-60 was protected from modification when bIGFBP-2 was iodinated in a complex with either IGF-I or IGF-II (Chapter 3; *Hobba et al.*, 1996). Furthermore, bIGFBP-2 sustained a reduction in binding affinity for its IGF ligands when Tyr-60 was iodinated. In combination, these two observations suggested that Tyr-60 was located in the IGF-binding site of bIGFBP-2. However, other residues in the bIGFBP-2 structure that occur in close proximity to Tyr-60 could also conceivably play a role in IGF binding that is disrupted when Tyr-60 is iodinated. In the absence of IGFBP structural information, the only residues that can be predicted to occur in close proximity to Tyr-60 are Val-59, Thr-61, Pro-62 and Arg-63. Moreover, these latter residues are highly conserved across the whole IGFBP family, except for the described IGFBP-1 sequences where an alanyl rather than tyrosyl residue occurs at the position corresponding to Tyr-60 in bIGFBP-2, as shown in Fig. 4.1. Therefore, to determine which residues in the Tyr-60 region of bIGFBP-2 do influence IGF binding, alanine-scanning mutagenesis was performed across residues 59 to 63 inclusive. Tyr-60 was also substituted with Phe to distinguish between the hydrogen bonding properties and the hydrophobic and aromatic properties of the tyrosyl side-chain with respect to IGF binding.

The mutagenic approach depended critically on an accurate and precise measurement of the binding affinities of the IGFBP-2 analogs for IGF-ligand. Therefore, traditional approaches such as Western ligand blot and solution-phase IGF-binding assays were augmented with biosensor studies. The kinetics of the interaction between bIGFBP-2 analogs and immobilised IGF-I-ligand were studied with the BIAcore instrument. The flow-cell of this instrument contains an optical interface between the fluid sample and the plasmon resonance detection assembly. The sample side of the optical interface is derivatised with a gold film and a dextran layer within which the IGF molecules could be covalently immobilised. As bIGFBP-2 solutions were applied through the flow cell, binding interactions could be detected by changes in surface plasmon resonance (resonance units, RU), which corresponded directly with the mass of bIGFBP-2 bound to the dextran layer. The association rates were measured by modelling the rate of RU change in terms of bIGFBP-2 concentration. The dissociation rate was simply the rate of RU decay as the bIGFBP-2 molecules were released from the immobilised IGF-surface.

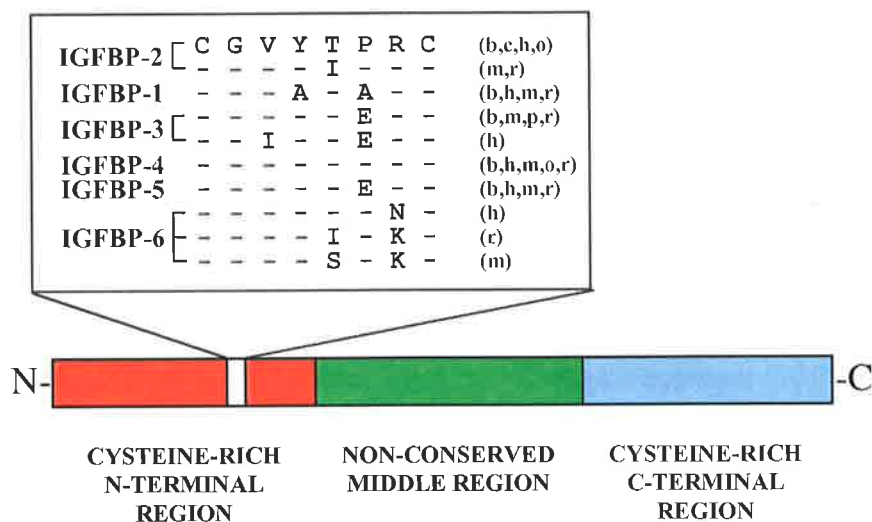


Fig. 4.1. Sequence homology of the IGFBP family across the "Tyr-60 region". The Tyr-60 region lies in the N-terminal cysteine-rich region of the IGFBP family sequences and is found between the 9th and 10th cysteine residues from the N-terminus (corresponding to Cys-57 and Cys-64 of bIGFBP-2 respectively). The sequences shown are a summary of 27 aligned IGFBPs using the single letter amino acid code, representing a range of species including bovine (b), chicken (c), human (h), murine (m), ovine (o), porcine (p), and rat (r). All of the observed sequence variation in this region is shown. The square open brackets ([]) indicate species variation within an IGFBP type and complete sequence identity with the bIGFBP-2 sequence is denoted by a dash (-). Percent identity relative to bIGFBP-2, at each amino acid position is as follows: Cys-57 (100), Gly-58 (100), Val-59 (96), Tyr-60 (85), Thr-61 (93), Pro-62 (56), Arg-63 (82), Cys-64 (100).

## 4.2 MATERIALS

### 4.2.1 General Chemicals and Materials

Recombinant bIGFBP-2 was transiently expressed in the COS-1 (ATCC:CRL 1650) monkey kidney cell line and purified from medium conditioned by the transfected cells as described in Chapter 2. Receptor grade IGF-I and IGF-II were the kind gift of GroPep Pty. Ltd., (Adelaide, Australia). Radio labelled  $^{125}\text{I}$ -IGF-I and  $^{125}\text{I}$ -IGF-II peptides were prepared to a specific activity of approximately 0.08 mCi/mole as previously described (Francis *et al.*, 1988). Carrier-free  $\text{Na}^{125}\text{I}$  was purchased from Amersham International (Sydney, Australia). BIAcore reagents and supplies including CM5 sensor chips, HEPES buffered saline (HBS), amine coupling reagents, *N*-ethyl-*N'*-[(dimethylamino)propyl]carbodiimide (EDC), *N*-hydroxysuccinimide (NHS) and ethanolamine were kindly provided by Pharmacia & Upjohn AB, Metabolic Diseases Research, Stockholm, Sweden or purchased from AMRAD Biotech, Melbourne, Australia.

#### 4.2.2 Molecular Biology Reagents

Restriction enzymes were purchased from Pharmacia Biotech, Sydney, NSW, Australia and New England Biolabs (Beverly, MA, USA). Calf intestinal phosphatase (CIP) and T4 polynucleotide kinase (PNK) were purchased from Boehringer Mannheim Australia, Sydney, NSW, Australia. The Muta-Gene™ phagemid *in vitro* mutagenesis kit (version 2) was from Bio-Rad, North Ryde, Sydney, NSW, Australia. Adenosine 5'-triphosphate ribonucleoside (ATP), ampicillin, chloramphenicol, dithiothreitol (DTT), kanamycin and spermidine (N-[3-aminopropyl]-1,4-butanediamine) were from Sigma Chemical Co., St Louis, MO, U.S.A. The BRESA-CLEAN DNA purification kit, radionucleosides [ $\alpha$ -<sup>32</sup>P]dATP (3,000 Ci/mmol), [ $\gamma$ -<sup>32</sup>P]dATP (3,000 Ci/mmol) and mutagenic oligonucleotides were purchased from Bresatec Ltd., Adelaide, SA, Australia. The *fmoI*™ PCR DNA sequencing kit was purchased from Promega Corporation, Sydney, NSW, Australia.

#### 4.2.3 Bacterial Strains

DH5 $\alpha$  *supE44*,  $\Delta$ *lacU169*, *hsdR17*, *recA1*, *endA1*, *gyrA96*,  $\lambda^-$ , *relA1*, [ $\phi$ 80*lacZ* $\Delta$ M15]  
CJ236 *dut*<sup>-</sup>, *ung*<sup>-</sup>, *thi*<sup>-</sup>, *relA1*; pCJ105 (Cm<sup>r</sup>)

#### 4.2.4 Bacterial Culture Media and Solutions

<b>LB (Luria-Bertani medium)</b>	<b>10 X TE</b>
1 % (w/v) bactotryptone	0.1 M Tris pH 7.5
0.5 % (w/v) bacto-yeast extract	1 mM EDTA
0.17 M NaCl pH 7.0	
	<b>10 X PNK buffer</b>
<b>LB + agar plates</b>	1.0 M Tris pH 9.0
LB + 1.5 % (w/v) bacto-agar	0.1 M MgCl <sub>2</sub>
<b>LB + agarose plates</b>	0.05 M DTT
LB + 0.7 % (w/v) agarose	0.04 M rATP
<b>20 X TBE</b>	<b>TES</b>
1 M Tris pH 8.3	25 mM Tris pH 8.0
0.02 M EDTA	10 mM EDTA
0.8 M boric acid	15 % (w/v) sucrose

### **5 X sequencing buffer**

250 mM Tris-HCl pH 9.0

10 mM MgCl<sub>2</sub>

### **10 X SPNK buffer**

0.5 M Tris pH 7.5

0.1 M MgCl<sub>2</sub>

50 mM DTT

1.0 mM spermidine

### **10 X Ligase buffer**

0.5 M Tris pH 7.5

0.1 M MgCl<sub>2</sub>

10 mM DTT

10 mM rATP

40 % (w/v) PEG 6000

### **10 X CIP buffer**

0.5 M Tris pH 7.5

0.1 M MgCl<sub>2</sub>

### **10 X Annealing buffer**

20 mM Tris-HCl pH 7.4

2 mM MgCl<sub>2</sub>

50 mM NaCl

### **10 X Synthesis buffer**

0.4 mM each dNTP

0.75 mM ATP

17.5 mM Tris-HCl pH 7.4

3.75 mM MgCl<sub>2</sub>

1.5 mM DTT

### **Sequencing stop solution**

10 mM NaOH

95 % (v/v) formamide

0.05 % (w/v) bromophenol blue

0.05 % (w/v) xylene cyanol

## **4.2.5 Cell Culture Media**

Cell culture media and solutions were as described in Section 2.2.2.

## **4.2.6 Chromatography and Electrophoresis**

Chromatography materials were as described in Section 2.2.3

## **4.3 METHODS**

### **4.3.1 Mutagenesis of the Tyr-60 Region of bIGFBP-2 – Overview**

Site directed mutagenesis was performed by the Kunkel method (Kunkel, 1985, Kunkel *et al.*, 1987) with the Muta-Gene phagemid *in vitro* mutagenesis kit (Bio-Rad, North Ryde, Sydney, NSW, Australia). Briefly, a fragment of the bIGFBP-2 cDNA (Upton *et al.*, 1990) which included the Tyr-60 region was subcloned into the phagemid vector pBKS<sup>-</sup> (Section 4.3.2). Single-stranded template DNA that contained random substitutions



of uracil for thymine bases was then synthesised in the *dut ung E. coli* strain CJ236 following super-infection with the helper phage M13K07 (Section 4.3.3). Mutagenic oligonucleotides, (Fig. 4.2) that coded for the bIGFBP-2 point mutations Val-59→Ala, Tyr-60→Ala, Tyr-60→Phe, Thr-61→Ala, Pro-62→Ala and Arg-63→Ala were annealed to the single-stranded template DNA and thereby used to prime the *in vitro* synthesis of complementary DNA (Section 4.3.4). The resultant double-stranded plasmid constructs were transformed into DH5- $\alpha$  *E. coli* where the parental DNA strand was selected against on the basis of its uracil content (Section 4.3.4). For screening purposes, the mutagenic oligonucleotides also disrupted the 5'-GTAC-3' *RsaI* endonuclease site between the codons GTG and TAC of Val-59 and Tyr-60 respectively, as shown in Fig. 4.2. Therefore, mutant clones were identified by diagnostic *RsaI* digestion followed by PCR DNA sequencing (Gyllensten, 1989) using the *fmoI*<sup>TM</sup> kit from Promega Corporation, Sydney, NSW, Australia (Section 4.3.5.1). *PstI/SmaI* bIGFBP-2 fragments with the desired point mutations were excised from pGDH-1 and re-cloned into the mammalian expression vector pGF8 and their sequences confirmed by the DyeDeoxy<sup>TM</sup> terminator sequencing procedure (Section 4.3.5.2).

```

bIGFBP-2      - 5' -GAGAGCGGTGCGGCGTGTACACCCCCCGCTGCGGTCAGGGGCTG-3'
Val-59→Ala   - 5' -GAGAGCGGTGCGGCGCTTACACCCCCGCTGC-3'
Tyr-60→Ala   - 5' -GAGCGGTGCGGCGTGCTACCCCCCGCTGCGGT-3'
Tyr-60→Phe   - 5' -GAGCGGTGCGGCGTTTCACCCCCCGCTGCGGT-3'
Thr-61→Ala   - 5' -AGAGCGGTGCGGCGTCTACGCTCCCCGCTGCGGTCAG-3'
Pro-62→Ala   - 5' -AGAGCGGTGCGGCGTGTATACAGCTCGCTGCGGTCAGGGG-3'
Arg-63→Ala   - 5' -AGAGCGGTGCGGCGTCTACACCCCCGCTTGCGGTCAGGGGCTG-3'

```

Fig. 4.2. A summary of the mutagenic oligonucleotides used to produce the bIGFBP-2 mutants. Specific bases that have been altered in the synthetic oligonucleotides to yield point mutations or to facilitate clone selection are shown in bold and highlighted. The *RsaI* site used for clone selection is underlined in the wild-type bIGFBP-2 sequence.

## 4.3.2 Construction of the Mutagenic Plasmid pGDH-1

### 4.3.2.1 Preparation of Vector and Insert DNA

pBKS(-) and the bIGFBP-2 expression vector pGF8 were digested in separate tubes with 2 U of *SmaI* for 120 min and then 2 U of *PstI* for 120 min under the appropriate salt and temperature conditions recommended by each enzyme manufacturer. The digested



vector and the 344 bp *Pst*I-*Sma*I fragment of the BIGFBP-2 cDNA were both purified using the BRESA-CLEAN™ kit, according to the supplied method. Briefly, after separation by electrophoresis on an agarose TBE gel, DNA was visualised by ethidium bromide staining and excised under long wave ultra violet (UV) light. The gel slice was then solubilised with ½-volume of TBE-MELT™ and 4½-volumes of NaI solution (BRESA-SALT™) followed by a 10 min incubation at 55°C. BRESA-BIND™ glassmilk solution (5 µl) was added and the DNA was allowed to bind at room temperature for 5 min with regular mixing. The glassmilk beads were subsequently pelleted by centrifugation for 15 sec at 10,000 x g and washed three times with BRESA-WASH™ solution, with gentle resuspension and centrifugation between washes, as described above. DNA was eluted from the glass beads with 20 µl of water by heating the slurry to 55°C for 5 min. The glass beads were pelleted at 10,000 x g for 1 min, and the DNA supernatant immediately removed and transferred to a fresh tube. DNA recovery was monitored by electrophoresis on an agarose mini-gel.

The *Pst*I/*Sma*I digested plasmid was dephosphorylated with 1 U of calf intestinal phosphatase (CIP) in 1 X CIP buffer at 37°C for 15 min to prevent recircularisation of singly cut plasmid species. The dephosphorylated plasmid DNA was recovered from the CIP reaction mixture with BRESA-CLEAN™ essentially as described above, however, TBE-MELT™ was omitted from the initial step and only 3-volumes of NaI was added to the DNA-solution.

#### **4.3.2.2 Ligation of DNA**

To produce pGDH-1 *Pst*I/*Sma*I digested, dephosphorylated pBKS(-) and the 344 bp BIGFBP-2 fragment were mixed in a ratio of approximately 1 : 3 and ligated in 1 X Ligase buffer with 1 U of T4 DNA ligase overnight at 14°C. For negative and positive controls of the ligation, reaction mixtures were prepared with vector alone and *Eco*RI cut SPP1 DNA markers, respectively. DNA was transformed into the *E. coli* strain DH5α, (Section 4.3.2.3), and transformants with DNA inserts were identified by the color of colonies when plated onto LB agar supplemented with IPTG (120 µg/ml) and X-Gal (40 µg/ml). Wild-type colonies were blue due to α-complementation of the β-galactosidase (*lacZ*) gene by pBKS(-) (Sambrook et al., 1989). In contrast, successful insertion of DNA disrupted the plasmid encoded portion of the *lacZ* gene thus resulting in the loss of functional β-galactosidase activity and a white colony.

#### **4.3.2.3 Transformation of *E. coli***

With aseptic technique, the relevant glycerol stock of *E. coli* (DH5 $\alpha$  or CJ236) was streaked onto LB agar plates and grown overnight at 37°C. A single colony was then inoculated into 5 ml LB and grown overnight at 37°C with shaking. Overnight cultures were subcultured into fresh LB at 1/100 dilution, and grown to an optical density of between 0.4 and 0.6 absorbance units at 600 nm. Cells were recovered as a pellet by centrifugation at 3,000 x g for 5 min at 4°C. The cell pellet was gently resuspended in 1/20<sup>th</sup> the original volume of the culture with 50 mM CaCl<sub>2</sub>, 20 mM MgCl<sub>2</sub>. The cell suspension was left on ice for at least 1 hr or overnight at 4°C to become competent. Competent cells were stored at 4°C and were considered suitable for transformation for up to 7 days.

To achieve transformation, plasmid DNA was incubated with 200  $\mu$ l of competent cells on ice for 30 min then heat shocked by incubation for 2 min at 42°C and 1 min on ice. An equal volume of LB was added and the cells were incubated at 37°C for 10 min before being spread onto warm antibiotic supplemented LB agar plates. Transformations that contained cut vector alone and wild-type vector provided negative and positive controls respectively for the transformation step.

#### **4.3.2.4 Small-Scale Preparation of Plasmid DNA by the Alkaline Lysis Method**

Cells from a single colony were used to inoculate 2 ml LB with 50  $\mu$ g/ml ampicillin and grown overnight at 37°C with shaking. Overnight culture (1.5 ml) was transferred to 1.5 ml tubes and the cells pelleted at 2,000 x g for 5 min. The supernatant was aspirated and pellets resuspended in 100  $\mu$ l TES solution. Freshly made solutions of 0.2 M NaOH, 1% (w/v) SDS (200  $\mu$ l) and 3 M sodium acetate, pH 4.6 (135  $\mu$ l) were added to each tube and the suspensions were gently mixed by inversion. Genomic DNA was precipitated on ice for 5 min and pelleted by centrifugation for 15 min at 4°C and 8,000 x g. The supernatant was taken and digested with Dnase-free Rnase A (25  $\mu$ g/ml) at 37°C for 30 min then phenol/chloroform extracted (Section 2.3.1). After extraction, the aqueous phase was recovered and precipitated with two volumes of ethanol at room temperature for 30 min. Precipitated DNA was pelleted by centrifugation, 8,000 x g, 4°C, for 15 min, washed with 70 % (v/v) ethanol and resuspended in 50  $\mu$ l of 0.1 mM EDTA, pH 8.0. DNA quantity and purity was estimated by agarose mini-gel electrophoresis.

### 4.3.3 Synthesis of Single-Stranded Template DNA

CJ236 cells harboring pGDH-1 were streaked onto LB agar supplemented with chloramphenicol (30 µg/ml) and ampicillin (100 µg/ml) and grown overnight at 37°C. A single colony was then inoculated into 2 ml of LB containing 15 µg/ml chloramphenicol and 100 µg/ml ampicillin. Following overnight culture at 37°C with shaking, the cells were subcultured at a dilution of 1/400 into fresh LB supplemented with chloramphenicol and ampicillin as described above and incubated at 37°C with shaking for 5 hr. The cells were then subcultured at a dilution of 1/20 into LB and inoculated with approximately  $5 \times 10^8$  p.f.u. of the helper phage strain M13K07 (Bio-Rad, North Ryde, NSW, Australia). The phage-infected cells were cultured at 37°C for 60 min with shaking and then adjusted with kanamycin to a final concentration of 14 µg/ml prior to overnight culture at 37°C with shaking.

Following overnight culture, cells were separated from the phagemid containing supernatant by centrifugation at 13,200 x g for 15 min at 4°C. To 1 ml of the phagemid supernatant was added 2 µl of Rnase A (10 mg/ml). After incubation at room temperature for 30 min, 300 µl of 20 % (w/v) PEG-6000/2.5 M NaCl was added and the phagemid particles were precipitated on ice for 30 min. The phagemid particles were recovered as a pellet by centrifugation at 13,200 x g for 15 min at 4°C. The supernatant was carefully drained and the pellet was resuspended in 200 µl of 1 x TE followed by phenol/chloroform extraction (Section 2.3.1). After phenol/chloroform extraction, the phagemid DNA was precipitated by the addition of 18 µl of 3 M sodium acetate, pH 5.2 and 500 µl of ice cold Rnase-free ethanol and left at -20°C for 30 min. The supernatant was drained and the DNA pellet was rinsed with ice-cold 70 % (v/v) ethanol. The pellet was suspended in 20 µl of TE and stored at -20°C.

### 4.3.4 The *In Vitro* Mutagenesis Reaction

In separate tubes, the mutagenic DNA oligomers (200 pmol) were each heat denatured, then cooled immediately on ice. The 5' ends of the oligomers were phosphorylated with 3 U T4 polynucleotide kinase in 1 X PNK buffer (final volume 30 µl) at 37°C for 45 min. Kinase activity was inactivated at 65°C for 15 min.

The phosphorylated mutagenic oligonucleotides (approximately 9 pmol of each) were annealed with uracil-containing single-stranded pGDH-1 (approximately 200 ng) in 1 x Annealing buffer (final volume of 10 µl) in separate tubes. The reactions were heated to

65°C for 2 min and allowed to cool at a rate of 1°C per min over 30 min before incubation on ice. The reactions were adjusted with 1 µl 10 X Synthesis buffer, 3 U of T4 DNA ligase and 0.5 U of T7 DNA polymerase. The reactions were incubated on ice for 5 min, then 5 min at room temperature and finally for 30 min at 37°C to allow T4 DNA polymerase extension. The DNA synthesis and ligation reactions were stopped by the addition of 90 µl of TE.

Synthesis of the complementary DNA strand was assessed by agarose gel electrophoresis. Successful production of circular double-stranded DNA was evident by a species that migrated with an larger apparent molecular weight than the single-stranded template DNA. Competent DH5-α cells were transformed (Section 4.3.2.3) with 20 µl of each mutagenesis reaction mixture and subsequently plated onto LB agar plates that contained 100 µg/ml ampicillin. In theory, replication of duplex pGDH-1 in DH5α cells resulted in the digestion of the uracil containing parental strand and thereby provided positive selection for the mutagenic DNA strand.

### 4.3.5 DNA Sequencing

#### 4.3.5.1 PCR DNA Sequencing With End-Labelled Primers

In separate tubes, 100 ng each of the pBKS sequencing primers - universal sequencing primer (USP) 5'-GTTTTCCCAGTCACGAC-3' and reverse sequencing primer (RSP) 5'-CACACAGGAAACAGCTATGACCATG-3' were end-labelled with { $\gamma$ -<sup>32</sup>P}ATP (3,000 Ci/mmol) with 5 U of polynucleotide kinase in 1 x SPNK buffer (final volume 10 µl). The labelling reaction proceeded for 30 min at 37°C whereupon the kinase activity was inactivated at 90°C for 2 min. The labelled primers were stored at -20°C prior to their use in the sequencing reaction.

Sequencing reactions were performed according to the instructions of the *fmol*<sup>TM</sup> DNA cycle sequencing kit (Promega Corporation, Sydney, NSW, Australia). The sequencing reactions were assembled with radiolabelled primer (1.5 µl), approximately 1 µg of template DNA, 5 µl of 5 x Sequencing buffer and 5 U of sequencing grade Taq DNA polymerase made up to a final volume of 17 µl with sterile water. After gentle mixing by pipette, 4 µl of the sequencing reaction was added to four separate tubes that contained 2 µl each of d/ddGTP, d/ddATP, d/ddTTP and d/ddCTP mixtures. The reactions were sealed with one drop of mineral oil and then placed in a thermal cycler (Perkin-Elmer Cetus DNA Thermal Cycler, Norwalk, Connecticut, USA) preheated to 95°C. The PCR cycling profile

was as follows: initial denaturation was at 95°C for 2 min; thereafter followed 30 cycles, each with a 95°C denaturation step for 30 sec, a 55°C annealing step for 30 sec, and a 70°C extension step for 1 min. When the cycling profile was completed, the reactions were stopped by the addition of 4 µl sequencing stop solution to each tube.

Sequencing reactions were denatured at 70°C for 2 min and 3 µl of each loaded directly onto a 0.3 mm, 7 M Urea, 1 x TBE, 6 % polyacrylamide gel (w/v, 25 : 1, acrylamide : bis-acrylamide) and run at 40 Watts constant power (approximately 20 mA, 1500 V) for the appropriate migration distance. Gel plates were separated and the gel fixed by soaking for 20 min with 20 % (v/v) ethanol, 10 % (v/v) acetic acid. The fixed gel was then transferred to Whatman 3 MM paper and dried under vacuum at 65°C for 60 min. Dried gels were exposed to x-ray film at room temperature overnight.

#### ***4.3.5.2 Dye Terminator DNA Sequencing***

Reactions were carried out according to the instructions supplied with the PRISM Dye Terminator Cycle Sequencing Ready Reaction Kit (Applied Biosystems, Sydney, NSW, Australia). Sequencing reactions were assembled with 8 µl of the supplied sequencing reagent mix, to which was added 3.2 pmole of the sequencing primer 5'-CTCGCCGTTGTCTGCAACCTGCTCCGGG-3' and approximately 1 µg of template DNA, and the mixture made up to a final volume of 20 µl with sterile water. Sequencing reactions were performed with the following PCR cycling profile: 25 cycles were performed, each with a 96°C denaturation step for 30 sec, a 50°C annealing step for 15 sec, and a 60°C extension step for 4 min. When the cycling profile was completed, the reaction products were purified by ethanol precipitation as follows. To a 1.5 ml tube was added 2 µl of 3 M sodium acetate pH 4.6, 50 µl of 95 % (v/v) ethanol and the entire 20 µl sequencing reaction. The contents were mixed by vortex and incubated on ice for 10 min. The precipitated DNA was recovered as a pellet by centrifugation at 13,000 x g for 15 min at 4°C. The supernatant was aspirated and the pellet washed with 275 µl of ice cold 75 % (v/v) ethanol. After the supernatant was aspirated, the pellet was dried under vacuum by speedvac (Speed-Vac, Savant).

Completed sequencing reactions were submitted to the DNA sequencing facility at the Institute of Medical and Veterinary Science for analysis on an ABI 373 DNA sequencer (Applied Biosystems, Sydney, NSW, Australia).

#### **4.3.6 Production of bIGFBP-2 Analogs**

bIGFBP-2 mutants were transiently expressed in COS-1 cells and purified from conditioned medium following the procedures that are described in detail in Chapter 2.

#### **4.3.7 Analysis of the Mutant bIGFBP-2 Analogs**

##### ***4.3.7.1 SDS-PAGE and Western-Ligand Blot***

Conditioned medium samples collected during the mammalian expression of bIGFBP-2 analogs were concentrated in Centricon-10 micro-concentrators and analysed by SDS-PAGE as described in Section 2.3.5. Protein samples, equivalent to 200  $\mu$ l of conditioned medium from the mammalian expression of bIGFBP-2, Val-59 $\rightarrow$ Ala bIGFBP-2, Tyr-60 $\rightarrow$ Ala bIGFBP-2, Tyr-60 $\rightarrow$ Phe bIGFBP-2, Thr-61 $\rightarrow$ Ala bIGFBP-2, Pro-62 $\rightarrow$ Ala bIGFBP-2, Arg-63 $\rightarrow$ Ala bIGFBP-2 and non-transfected COS-1 cells were separated on a 12 % acrylamide gel under non-reducing conditions, transferred to nitrocellulose and then probed with anti-bIGFBP-2 polyclonal antibodies. Western immunoblot of the nitrocellulose filter was performed as described in Section 2.3.5.4.

Purified bIGFBP-2 samples (200 ng/lane) were electrophoresed on discontinuous 12 % SDS-polyacrylamide gels under non-reducing conditions as described in Section 2.3.5. The samples were either stained with silver (Section 2.3.5.2) and quantified by densitometry (Molecular Dynamics), or transferred onto nitrocellulose filters for Western ligand blotting (Section 2.3.5.3). The level of  $^{125}$ I-IGF-II binding to the bIGFBP-2 samples on the filter was visualised and quantified on a PhosphorImager (Molecular Dynamics).

##### ***4.3.7.2 Mass Spectrometry***

Lyophilised samples of approximately 10  $\mu$ g of each bIGFBP-2 mutant were submitted for electrospray mass spectrometry. The analysis was carried out on a Perkin Elmer SCI-EX API-300 triple quadrupole mass spectrometer at the Australian Research Council electrospray mass spectrometry unit, Adelaide.

##### ***4.3.7.3 Amino Acid Analysis***

Peptide concentrations were accurately quantified by both reverse-phase HPLC as described in Section 2.3.4.4 and by amino acid analysis on an AminoQuant II/M High Sensitivity Instrument from Hewlett Packard, Waldbronn, Germany (Godel *et al.*, 1992), using the orthophthalaldehyde 9-fluorenylmethyl chloroformate (OPA-FMOC) two-stage

derivatization procedure. The amino acid analyses were performed by Kristina Zachrisson, Pharmacia & Upjohn, Stockholm.

#### **4.3.7.4 Circular Dichroism**

CD spectra were recorded using a Jasco J 720 spectropolarimeter equipped with a PTC-348W1 Peltier Type Temperature Controller set to 20°C. bIGFBP-2 samples were adjusted to a final concentration of 0.25 mg/ml with 10 mM sodium phosphate, 60 mM NaCl, pH 7.4 and placed in a quartz cuvette with a path length of 1 mm. Spectra were recorded from 250 nm to 190 nm with a step resolution of 0.2 nm and a scanning speed of 20 nm/min. The response time was set to 1 sec and the bandwidth was 0.5 nm. Each spectrum is the average of 5 accumulated scans.

#### **4.3.7.5 Isoelectric Focussing**

bIGFBP-2 samples (0.5 mg/ml in 10 mM HCl, 5 µg/lane) were applied to a pH 3-10 CleanGel IEF polyacrylamide gel (Pharmacia Biotech, Uppsala, Sweden) and subsequently focussed for 90 min at 10°C. The separated isoforms were visualised by Coomassie Brilliant Blue R-250 staining as described in Section 2.3.5.1. Isoelectric focussing was performed by Elin Arvesson, Pharmacia & Upjohn, Stockholm.

#### **4.3.7.6 Soluble IGFBP Assay**

The relative IGF binding affinities of the bIGFBP-2 mutants were determined at equilibrium by charcoal binding assay, essentially as described in Section 2.3.8.1, with the following modifications. The assay buffer pH was 7.4 and the IGFBP/IGF-tracer incubation period was 24 hrs at room temperature. Each bIGFBP-2 concentration was assayed in triplicate and the total analysis was performed twice. In assays containing <sup>125</sup>I-IGF-I, approximately 7,000 cpm/tube were used and the non-specific binding was 6 % of the total radioactivity added. Similarly, 10,000 cpm/tube of <sup>125</sup>I-IGF-II were used with a non-specific binding of 8 % of the total radioactivity added. The experimental data were fitted to a semi-log dose-response model with variable slope using GraphPad Prism (GraphPad Inc., San Diego, USA).

#### **4.3.7.7 BIAcore**

All BIAcore analyses was carried out with IGF as the immobilised ligand. Covalent attachment of either IGF-I or IGF-II to the CM5 biosensor chip was achieved by the amine coupling method (Johnsson *et al.*, 1991). Briefly, the carboxymethyl dextran matrix of the



CM5 biosensor chip was activated by the injection of 35  $\mu$ l of a 1:1 mixture of 0.2 M N-ethyl-N'-[(dimethylamino)propyl]carbodiimide (EDC) and 0.05M N-hydroxysuccinimide (NHS) at 5  $\mu$ l/min. IGF (12.5  $\mu$ g/ml in 50 mM sodium acetate pH 4.7) was injected onto the activated CM5 surface at 5  $\mu$ l/min with HBS (10 mM HEPES, 150 mM NaCl, 3.4 mM EDTA, pH 7.4) as the running buffer. Residual binding sites were quenched with ethanolamine. The multi-channel capability of the BIAcore 2000 was used to generate channels with either IGF-I or IGF-II surfaces (prepared to final resonance values of approximately 60 to 120 RU above the resonance value of the activated, but non-derivatised chip) as well as a reference surface to which no IGF was bound. In a kinetic study, bIGFBP-2 and bIGFBP-2 mutants (5 nM to 100 nM in HBS, n=6 per bIGFBP-2 species) were injected for 5 min at a flow rate of 40  $\mu$ l/min with HBS as the running buffer. The dissociation phase, initiated by switching from the stream of the bIGFBP-2 sample to HBS, was carried out over a period of 10 min. The IGF surfaces were regenerated by a 90 sec injection of 0.1 M HCl.

Due to the large number of bIGFBP-2 samples and the extended length of the experiment, samples were injected in random order and the experiment was carried out twice on two different chips rather than with duplicate samples on a single chip. The apparent analyte association and dissociation rates were derived by fitting the experimental data to either a one-site (IGF-I) or two-site (IGF-II) association model and a two-site dissociation model with the BIAevaluation software (version 2.1) supplied with the instrument.

## **4.4 RESULTS**

### **4.4.1 *In Vitro* Mutagenesis**

The mutagenic plasmid pGDH-1 was constructed by the insertion of a 344 bp fragment of the bIGFBP-2 cDNA, which included the Tyr-60 region, into the phagemid vector pBKS(-) via *Pst*I/*Sma*I cloning sites. Successful construction of pGDH-1 was confirmed by diagnostic restriction digestion with the cloning restriction endonucleases, *Pst*I and *Sma*I. Subsequent agarose gel electrophoresis of the digestion products indicated the exclusive presence of insert DNA and linearised vector of the correct sizes, according to the motility of DNA standards (data not shown).

Six mutagenic oligonucleotides were designed to introduce point mutations in the Tyr-60 region of bIGFBP-2, as summarised in Fig. 4.2. Mutagenesis was then carried out

using the Kunkel method (Kunkel, 1985; Kunkel *et al.*, 1987) to provide selective pressure against the template DNA strand, on the basis of its uracil content. Using the mutagenic oligonucleotides as primers and single-stranded pGDH-1 as template, six individual *in vitro* DNA synthesis reactions were performed (Section 4.3.4). Agarose gel electrophoresis (Fig. 4.3) was then used to verify that the single-stranded template DNA had been successfully converted to duplex DNA during the mutagenesis reaction. In Fig. 4.3, lane 1 contained *Eco*R1 cut SPP1 DNA markers, lanes 2 and 9 contained products of the mutagenesis reaction in the absence of mutagenic primer and lanes 3-8 contained the products of the mutagenesis reactions carried out in the presence of mutagenic oligonucleotides that coded for the point mutations Val-59→Ala, Tyr-60→Ala, Tyr-60→Phe, Thr-61→Ala, Pro-62→Ala and Arg-63→Ala, respectively.

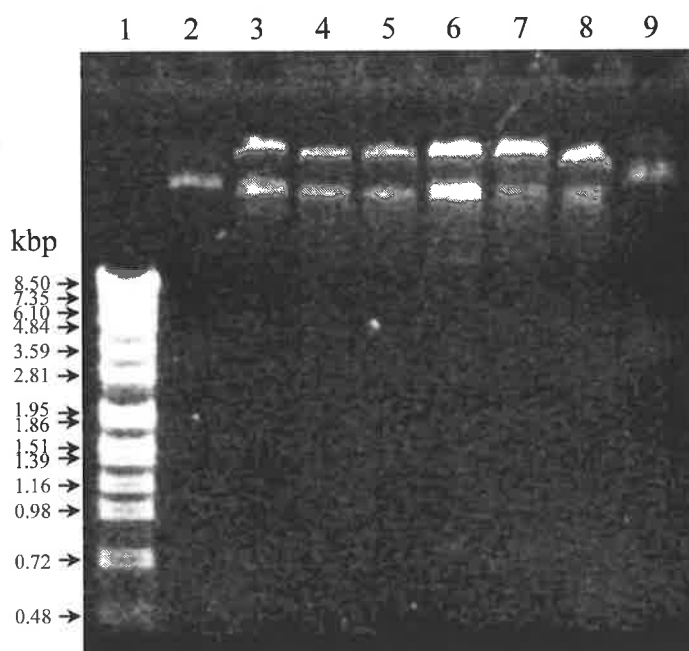


**Fig. 4.3. Agarose gel electrophoretic analysis of the products of *in vitro* mutagenesis reactions.** In separate tubes, six mutant oligonucleotides were annealed to templates of single-stranded pGDH-1. Complementary strands were synthesised and the ends ligated to produce duplex covalently closed plasmid species. Lane 1 shows *Eco*RI/SPP-1 DNA molecular weight markers with their masses indicated on the left. Lanes 2 and 9 contain single-stranded pGDH template DNA. Lanes 3-8 contain the products of the *in vitro* mutagenesis reactions with oligonucleotides coding for the bIGFBP-2 point mutations Val-59→Ala, Tyr-60→Ala, Thr-61→Ala, Pro-62→Ala and Arg-63→Ala respectively. This figure shows that the single-stranded template DNA is converted to less mobile duplex DNA species during the course of the *in vitro* mutagenesis reaction.

Fig. 4.3 shows that all of the mutagenic primers were capable of annealing to pGDH-1 template and were able to prime DNA synthesis. This is evident by the presence of DNA species in lanes 3-8 that migrated more slowly than the single-stranded template DNA present in lanes 2 and 9.

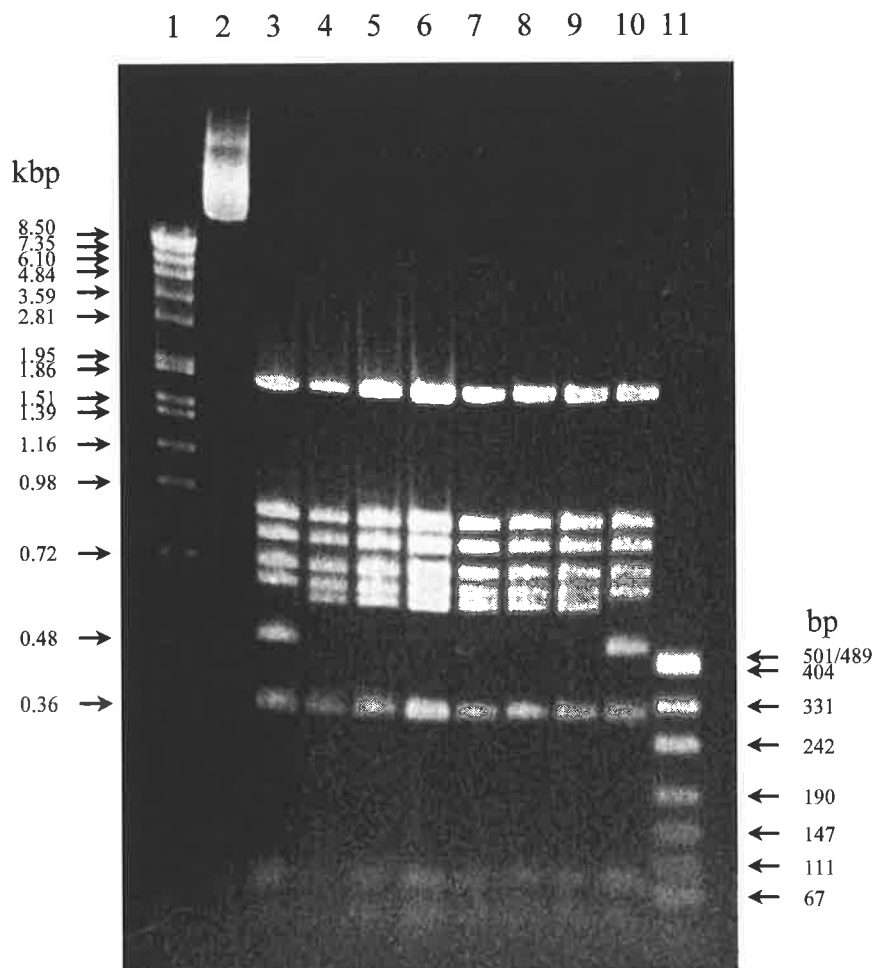


**Fig. 4.4. Diagnostic *RsaI* digestions of bIGFBP-2 mutant constructs in the expression vector pGF8.** Lane 1 shows *EcoRI*/SPP-1 molecular weight markers with their sizes indicated on the left. Lane 11 shows *HpaI*/pUC molecular weight markers with sizes as defined on the right. Lane 2 contains undigested pGF8 whereas lanes 3 and 10 contain pGF8 that was digested with *RsaI*. Lanes 4-9 contain the *RsaI* digestion products of the expression vectors pBP2-59A, pBP2-60A, pBP2-60F, pBP2-61A, pBP2-62A and pBP2-263A respectively. The mutant oligonucleotides were designed to eliminate an *RsaI* site located in the Tyr-60 region of bIGFBP-2. The mutant clones all lack a 0.48 kbp DNA fragment that is present in the *RsaI* digestion products of pGF8.

The mutagenesis reaction products were transformed into *E. coli* DH5 $\alpha$  and transformants that harbored pGDH-1 were selected on the basis of their resistance to ampicillin (Section 4.3.4). As the mutagenic oligonucleotides (Fig. 4.2) were designed to

eliminate the *RsaI* endonuclease site between codons GTG and TAC of Val-59 and Tyr-60 respectively, diagnostic digestion with *RsaI* was used to screen for positive clones. Thus, plasmid preparations (Section 4.3.2.4) were generated from single colonies selected from each of the six transformation plates and then subjected to *RsaI* digestion. Approximately 100 colonies in total were screened in this way before representative positive clones were identified for each of the six mutagenesis reactions (data not shown). The exclusive presence of the desired point mutations in each positive clone (corresponding to Val-59→Ala, Tyr-60→Ala, Tyr-60→Phe, Thr-61→Ala, Pro-62→Ala and Arg-63→Ala in the bIGFBP-2 primary structure) was confirmed by PCR DNA sequencing as described in Section 4.3.5.1 (data not shown). Subsequently, the mutagenised bIGFBP-2 inserts were excised with *PstI/SmaI* and re-cloned into the expression vector pGF8 to produce pBP2-59A, pBP2-60A, pBP2-60F, pBP2-61A, pBP2-62A and pBP2-63A respectively. The presence of the correct sequence in pBP2-59A, pBP2-60A, pBP2-60F, pBP2-61A, pBP2-62A and pBP2-63A was reconfirmed by diagnostic *RsaI* digestion (Fig. 4.4) and Dye Terminator PCR sequencing (Section 4.3.5.2, data not shown).

#### 4.4.2 Expression and Purification of bIGFBP-2 Analogs

The bIGFBP-2 analogs encoded on the plasmid constructs pBP2-59A, pBP2-60A, pBP2-60F, pBP2-61A, pBP2-62A and pBP2-63A were transiently expressed in COS-1 cells using the procedures described in Chapter 2. The presence of each bIGFBP-2 analog in medium conditioned by transfected COS-1 cells was confirmed by SDS-PAGE analysis (Section 2.3.5). Shown in Fig. 4.5 are the protein species in transfected COS-1 conditioned media that were immuno-reactive to bIGFBP-2 polyclonal anti-sera. Fig. 4.5, lane 9 shows that conditioned medium from COS-1 cells that were electroporated in the absence of pGF8 or bIGFBP-2 mutant construct did not contain detectable levels of bIGFBP-2. In contrast transient transfection of COS-1 cells with pGF8 (lane 10), pBP2-59A (lane 3), pBP2-60A (lane 4), pBP2-60F (lane 5), pBP2-61A (lane 6), pBP2-62A (lane 7) and pBP2-63A (lane 8) resulted in the expression of protein species that were immuno-reactive to bIGFBP-2 anti-sera and co-migrated with a purified bIGFBP-2 standard (Lane 2). Little or no bIGFBP-2 protein breakdown was detected during the secretion of bIGFBP-2, Val-59→Ala, Tyr-60→Ala, Tyr-60→Phe, Pro-62→Ala bIGFBP-2 or Arg-63→Ala bIGFBP-2 as there were no lower molecular weight bIGFBP-2 species present in lanes 10,3,4,5,7 and 8 of Fig. 4.5 respectively. However, lower molecular weight bIGFBP-2 species were detected in conditioned medium from the expression of mutant construct pBP2-61A (Fig

4.5, lane 6) indicating that this Thr-61→Ala bIGFBP-2 was more protease sensitive than bIGFBP-2.

The bIGFBP-2 analogs were purified from conditioned medium using the procedures that are described in detail in Section 2.3.4. All of the bIGFBP-2 analogs

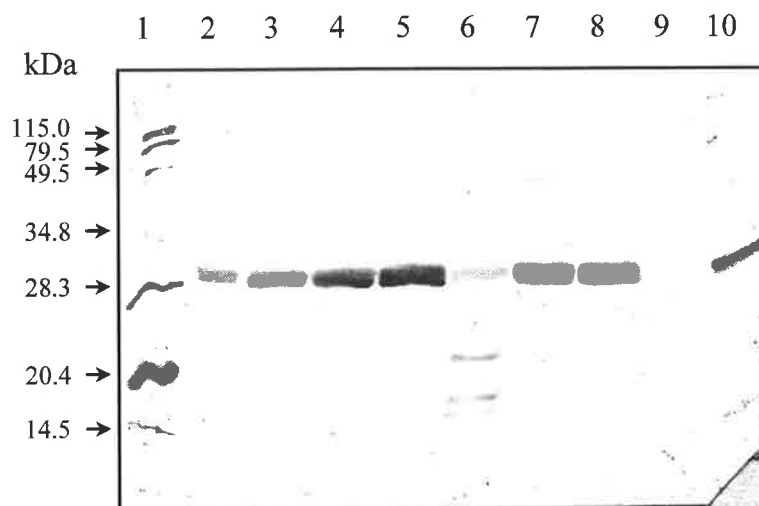


**Fig. 4.5. SDS-PAGE and Western antibody blot analysis of bIGFBP-2 and bIGFBP-2 mutant analogs in conditioned medium.** 200 ng of purified bIGFBP-2 (lane 2) and 200  $\mu$ l equivalents of conditioned medium from the mammalian expression (Section 4.3.6) of Val-59→Ala bIGFBP-2 (lane 3), Tyr-60→Ala bIGFBP-2 (lane 4), Tyr-60→Phe bIGFBP-2 (lane 5), Thr-61→Ala bIGFBP-2 (lane 6), Pro-62→Ala bIGFBP-2 (lane 7), Arg-63→Ala bIGFBP-2 (lane 8), and wild-type bIGFBP-2 (lane 10) were separated on a 12 % polyacrylamide gel under non-reducing conditions, transferred to nitrocellulose and then probed with anti-bIGFBP-2 polyclonal antibodies (Section 2.3.5.4). Conditioned medium (200  $\mu$ l equivalent) collected from non-transfected COS-1 cells is shown in lane 9. Biotinylated molecular weight markers are shown in lane 1 and their molecular weights are indicated on the left.

exhibited essentially the same elution profiles as bIGFBP-2 (See section 2.4.3) during the IGF-II affinity, cation exchange and reverse-phase HPLC chromatographic steps (data not shown). The concentration of each bIGFBP-2 analog in the respective pooled peak recovered from the reverse-phase HPLC step was quantified by reverse-phase HPLC (Section 2.3.4.4) and in addition, by amino acid analysis (Section 4.3.7.3). The analogs were dispensed as 5  $\mu$ g, 20  $\mu$ g and 50  $\mu$ g aliquots and then lyophilised for storage at -20°C.

#### 4.4.3 Protein Characterisation

Transient expression of bIGFBP-2 analogs in transfected COS-1 cells yielded approximately 400  $\mu$ g of each purified protein from 0.5 l of conditioned medium. All of the bIGFBP-2 mutants migrated as single bands of the same size as wild-type bIGFBP-2 when

run on non-reducing SDS-PAGE (Fig. 4.6a). A minor band corresponding to bIGFBP-2 dimer was also evident in the SDS-PAGE analysis (Figs. 4.6a,b). When analysed by electrospray mass spectrometry (ES-MS), the observed mass of each mutant with the exception of Tyr-60→Ala corresponded with the sequence-predicted mass to within 3 mass

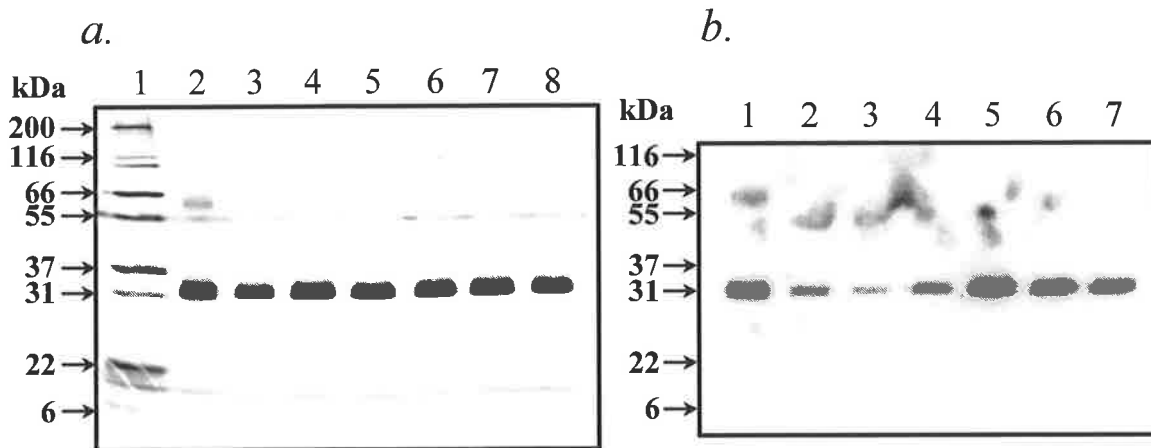


**Fig. 4.6. SDS-PAGE analysis of bIGFBP-2 and the bIGFBP-2 mutant analogs.** (a.) 200 ng of purified bIGFBP-2 (lane 2), Val-59→Ala bIGFBP-2 (lane 3), Tyr-60→Ala bIGFBP-2 (lane 4), Tyr-60→Phe bIGFBP-2 (lane 5), Thr-61→Ala bIGFBP-2 (lane 6), Pro-62→Ala bIGFBP-2 (lane 7) and Arg-63→Ala bIGFBP-2 (lane 8) were separated on a 12% polyacrylamide gel under non-reducing conditions, and the gel was silver stained. Molecular weight markers are shown in lane 1 and their molecular weights are indicated on the left. (b.) The  $^{125}\text{I}$ -IGF-II ligand blot of a duplicate gel to (a.), with 200 ng of purified bIGFBP-2 (lane 1), Val-59→Ala bIGFBP-2 (lane 2), Tyr-60→Ala bIGFBP-2 (lane 3), Tyr-60→Phe bIGFBP-2 (lane 4), Thr-61→Ala bIGFBP-2 (lane 5), Pro-62→Ala bIGFBP-2 (lane 6) and Arg-63→Ala bIGFBP-2 (lane 7).

units. Tyr-60→Ala bIGFBP-2 possessed a mass that was 18 mass units greater than expected, possibly due to methionine oxidation. ES-MS also indicated that in each of the bIGFBP-2 and bIGFBP-2 mutant samples there was a small but consistent contamination (approximately 5 %) with a species that was 355 mass units greater than the predicted mass. When the N-terminal sequence of the minor contaminant of wild-type bIGFBP-2 was determined, the larger species was identified as an incompletely processed form of bIGFBP-2. The N-terminus of the contaminant was Gly-Ala-Arg-Ala, corresponding to the last four residues of the leader peptide prior to the normal cleavage site (Bourner *et al.*, 1992) of pro-bIGFBP-2.

#### 4.4.4 Circular Dichroism

The secondary structure compositions of the bIGFBP-2 mutants were compared with wild-type bIGFBP-2 using CD spectroscopy. An overlay of the far UV spectra of Val-59→Ala, Tyr-60→Ala, Tyr-60→Phe, Thr-61→Ala, Pro-62→Ala, Arg-63→Ala bIGFBP-2 and wild-type bIGFBP-2 (Fig. 4.7) shows that the spectra of all engineered bIGFBP-2 analogs with the exception of Pro-62→Ala were essentially the same as wild-type bIGFBP-2. In contrast with the other 5 bIGFBP-2 analogs, the CD spectra of Pro-62→Ala was reduced in amplitude by approximately 20 % with respect to the CD spectra of wild-type bIGFBP-2.

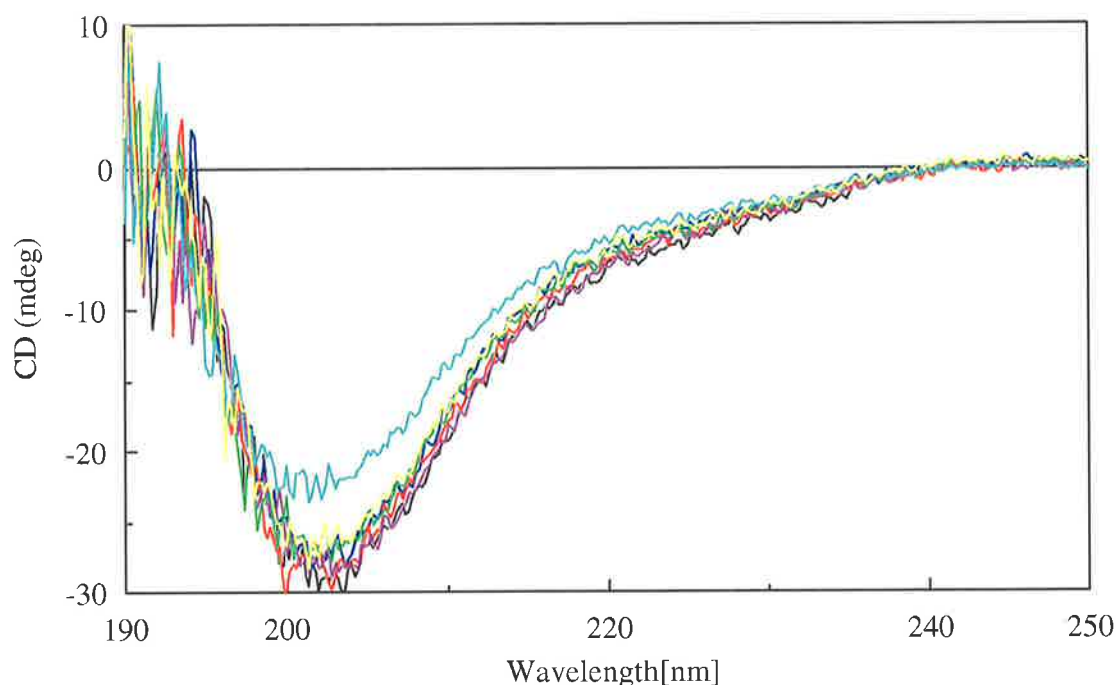


Fig 4.7. **Far-UV CD spectra of bIGFBP-2 and bIGFBP-2 mutants from 190 nm to 250 nm.** The CD spectra of 0.25 mg/ ml solutions of purified bIGFBP-2 ( — ), Val-59→Ala bIGFBP-2 ( — ), Tyr-60→Ala bIGFBP-2 ( — ), Tyr-60→Phe bIGFBP-2 ( — ), Thr-61→Ala bIGFBP-2 ( — ), Pro-62→Ala bIGFBP-2 ( — ) and Arg-63→Ala bIGFBP-2 ( — ) were analysed as described in Section 4.3.7.4.

---

#### 4.4.5 Isoelectric Focussing Electrophoresis

The purity of each bIGFBP-2 analog preparation was investigated by isoelectric focussing electrophoresis. Fig. 4.8 shows the protein isoforms that were present in purified aliquots of bIGFBP-2 (lane 2), Val-59→Ala bIGFBP-2 (lane 3), Tyr-60→Ala bIGFBP-2 (lane 4), Tyr-60→Phe bIGFBP-2 (lane 5), Thr-61→Ala bIGFBP-2 (lane 6), Pro-62→Ala

bIGFBP-2 (lane 7), Arg-63→Ala bIGFBP-2 (lane 8). bIGFBP-2 (Fig. 4.8, lane 2) was resolved into two species, the major of which focussed to an isoelectric point of approximately pH 7.6, according to protein standards of known pI (lanes 1 and 9). A minor band that focussed to an isoelectric point of approximately pH 8.0 was also present in the bIGFBP-2 preparation. The fact that the minor contaminant was more basic suggests that the species corresponds to Gly-Ala-Arg-Ala-bIGFBP-2 which possesses an additional arginine residue compared with bIGFBP-2. The bIGFBP-2 analogs Val-59→Ala bIGFBP-2 (lane 3), Tyr-60→Ala bIGFBP-2 (lane 4), Tyr-60→Phe bIGFBP-2 (lane 5), Thr-61→Ala bIGFBP-2 (lane 6), Pro-62→Ala bIGFBP-2 (lane 7) all possessed major and minor

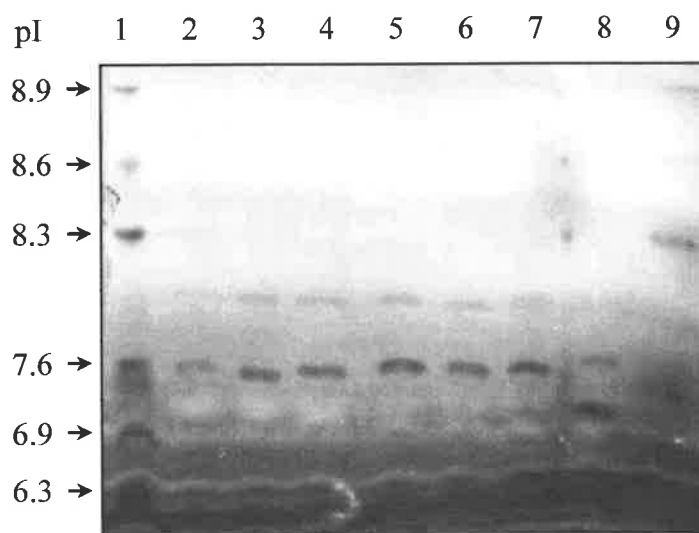


**Fig. 4.8. Isoelectric focussing of bIGFBP-2 and bIGFBP-2 mutants.** 5  $\mu$ g purified aliquots of bIGFBP-2 (lane 2), Val-59→Ala bIGFBP-2 (lane 3), Tyr-60→Ala bIGFBP-2 (lane 4), Tyr-60→Phe bIGFBP-2 (lane 5), Thr-61→Ala bIGFBP-2 (lane 6), Pro-62→Ala bIGFBP-2 (lane 7) and Arg-63→Ala bIGFBP-2 (lane 8) were separated by isoelectric focussing as described in Section 4.4.4. The gel was stained with Coomassie Brilliant Blue R-250. Protein standards are shown in lanes 1 and 9, and their pI values are indicated on the left.

Isoforms with pI values of approximately pH 7.6 and pH 8.0 as observed for bIGFBP-2. In contrast, the Arg-63→Ala bIGFBP-2 preparation contained a major isoform that focussed at approximately pH 7.0 and a minor isoform that focussed at approximately pH 7.7. The more acidic characteristics of the Arg-63→Ala bIGFBP-2 species is consistent with the substitution of the positively charged arginine side-chain with a neutral alanine side-chain.



#### 4.4.6 Western Ligand Blots

The  $^{125}\text{I}$ -IGF-II binding by the bIGFBP-2 mutants was analysed by Western ligand blot (Fig. 4.6*b*). Val-59→Ala, Tyr-60→Ala and Tyr-60→Phe bIGFBP-2 (Fig. 4.6*b*, lanes 2,3 and 4) showed reduced  $^{125}\text{I}$ -IGF-II binding compared with wild type bIGFBP-2 (Fig. 4.6*b*, lane 1). An estimate of the relative binding of each bIGFBP-2 mutant was provided by direct comparison of the band intensities from the ligand blot and the silver stained gel (Fig 4.6*a*). After the bound  $^{125}\text{I}$ -IGF-II radioactivity corresponding to each bIGFBP-2 species was quantified by PhosphorImager analysis (Fig. 4.6*b*) and corrected for the amount of peptide present on the silver stained gel (Fig. 4.6*a*), it was estimated that Val-59→Ala, Tyr-60→Ala and Tyr-60→Phe bIGFBP-2 retained approximately 40 %, 9 % and 15 % of the  $^{125}\text{I}$ -IGF-II bound by bIGFBP-2 respectively. In contrast, Thr-61→Ala, Pro-62→Ala and Arg-63→Ala bIGFBP-2 (Fig. 4.6*b*, lanes 5,6,7) all bound  $^{125}\text{I}$ -IGF-II to a similar extent to bIGFBP-2 (Fig. 4.6*b*, lane 1).

#### 4.4.7 Solution IGF Binding Assay

The IGF binding abilities of the bIGFBP-2 mutants were characterised in solution binding assays (Fig. 4.9, Table 4.1). Alanine substitution for Val-59, Thr-61, Pro-62 and Arg-63 of bIGFBP-2 did not significantly alter the half-maximal binding concentration ( $\text{EC}_{50}$ ) of bIGFBP-2 for either  $^{125}\text{I}$ -IGF-I (Fig. 4.9*a*) or  $^{125}\text{I}$ -IGF-II (Fig. 4.9*b*). In contrast both Ala and Phe substitution for Tyr-60 of bIGFBP-2 resulted in a significant increase in the  $\text{EC}_{50}$  for both  $^{125}\text{I}$ -IGF-I (Tyr-60→Ala = 3.4-fold, Tyr-60→Phe = 4.7-fold) and  $^{125}\text{I}$ -IGF-II (Tyr-60→Ala = 2.2-fold, Tyr-60→Phe = 3.3-fold). The maximal  $^{125}\text{I}$ -IGF binding of the bIGFBP-2 mutants were similar to wild-type bIGFBP-2 with 60 % of added IGF-tracer for  $^{125}\text{I}$ -IGF-I and 47 % of added IGF-tracer for  $^{125}\text{I}$ -IGF-II. An exception was  $^{125}\text{I}$ -IGF-II tracer binding to Tyr-60→Phe bIGFBP-2, where the maximal binding was 37 %, a reduction by 1/5 with respect to wild-type bIGFBP-2 (Table 4.1).

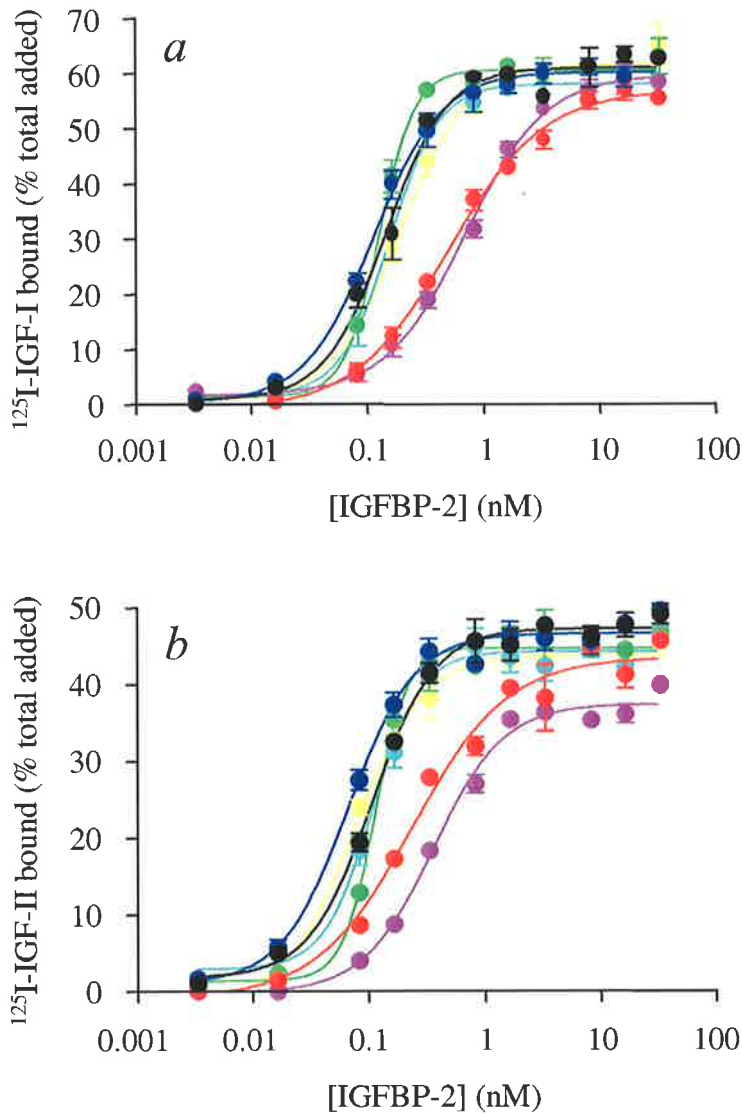


Fig. 4.9. **Solution phase IGF binding assays of bIGFBP-2 and IGFBP-2 mutants.** Increasing amounts of purified, recombinant bIGFBP-2 (●); Val-59→Ala bIGFBP-2 (●); Tyr-60→Ala bIGFBP-2 (●); Tyr-60→Phe bIGFBP-2 (●); Thr-61→Ala bIGFBP-2 (●); Pro-62→Ala bIGFBP-2 (●) and Arg-63→Ala bIGFBP-2 (●) were incubated with (a)  $^{125}\text{I}$ -IGF-I (7,000 cpm/tube) or (b)  $^{125}\text{I}$ -IGF-II (10,000 cpm/tube). The unbound IGF was separated from the bound (as described in experimental procedures) and the bound IGF was quantified by measuring the  $^{125}\text{I}$ -radioactivity. The data presented is the mean of triplicate determinations and error bars indicate the standard deviation where greater than the symbols.

Table 4.1 - Summary of IGF binding parameters derived from solution binding assays

<sup>125</sup> I-IGF-I	Max. bound (%) <sup>a</sup>	relative maximal binding	EC <sub>50</sub> (nM) <sup>b</sup>	relative EC <sub>50</sub>
bIGFBP-2	61	1.0	0.15	1.0
Val-59→Ala	60	1.0	0.12	0.8
Tyr-60→Ala	57	0.9	0.51	3.4
Tyr-60→Phe	60	1.0	0.70	4.7
Thr-60→Ala	61	1.0	0.13	0.9
Pro-62→Ala	58	0.9	0.16	1.1
Arg-63→Ala	62	1.0	0.19	1.3

<sup>125</sup> I-IGF-II	Max. bound (%) <sup>a</sup>	relative maximal binding	EC <sub>50</sub> (nM) <sup>b</sup>	relative EC <sub>50</sub>
bIGFBP-2	47	1.0	0.11	1.0
Val-59→Ala	47	1.0	0.07	0.6
Tyr-60→Ala	44	0.9	0.24	2.2
Tyr-60→Phe	37	0.8	0.36	3.3
Thr-61→Ala	45	1.0	0.11	1.0
Pro-62→Ala	44	0.9	0.11	1.0
Arg-63→Ala	44	0.9	0.08	0.7

<sup>a</sup> the maximum level of <sup>125</sup>I-IGF binding attained in the assay, expressed as a percentage of total <sup>125</sup>I-IGF added.

<sup>b</sup> the concentration of bIGFBP-2 peptide required to bind 50 % of the maximum <sup>125</sup>I-IGF binding level attained in the assay. R<sup>2</sup> values for the dose/response curve fits were equal to, or were greater than 0.95.

#### 4.4.8 BIAcore Analysis

Kinetic analyses of the association and dissociation of bIGFBP-2 and the bIGFBP-2 mutants with immobilised IGF-I and IGF-II were carried out in the BIAcore. Fig. 4.10 shows a representative subset of the sensorgram data (for qualitative comparison) that were used to generate the kinetic constants summarised in Table 4.2. The interactions between all of the bIGFBP-2 peptides and both IGF-I and IGF-II were difficult to resolve to a single binding site model. In the case of IGF-I interactions, a single apparent association constant and two apparent dissociation constants produced the best fit of the sensorgram data. In contrast, two apparent association and two apparent dissociation constants were necessary

for modeling bIGFBP-2 interactions on the IGF-II biosensor surface. The absolute values of the apparent kinetic constants for the IGFBP/IGF interactions ( $k_{on}$ ,  $k_{off}$  and  $K_D$  - Table 4.2) varied by up to 25 % of the mean value between the two biosensor chips used in this study. However, the ranking of the bIGFBP-2 mutants relative to bIGFBP-2 (ie: the fold-differences in  $k_{on}$ ,  $k_{off}$  and  $K_D$  - Table 4.2), were the same on both biosensor chips used in this study.

Mutagenesis in the Tyr-60 region of bIGFBP-2 produced a range of effects on the association rates, dissociation rates and hence the overall affinity for IGFs that were clearly evident in the BIAcore experiments. On the IGF-I biosensor surface (Fig. 4.10a, Table 4.2) Val-59→Ala, Tyr-60→Ala and Thr-61→Ala bIGFBP-2 exhibited association rates ( $k_{on}$ ) that were 5.5, 5.0 and 2.2-fold more rapid than wild-type bIGFBP-2 respectively. In contrast, the association rates ( $k_{on}$ ) of Pro-62→Ala and Arg-63→Ala bIGFBP-2 were slightly less than bIGFBP-2. The slowest association rate ( $k_{on}$ ) was observed for Tyr-60→Phe bIGFBP-2 which bound 3.0-fold more slowly than bIGFBP-2. While two dissociation components ( $k_{off1}$  and  $k_{off2}$ ) were necessary to model the behavior of bIGFBP-2 and the bIGFBP-2 mutants on IGF-I biosensor surfaces, the rapid dissociation component ( $k_{off1}$ ), which accounted for approximately 10 % of the total interaction, was essentially the same for all of the bIGFBP-2 peptides. In contrast, the slow dissociation component ( $k_{off2}$ ) was affected by mutagenesis in the Tyr-60 region. Therefore, the slow dissociation component ( $k_{off2}$ ), which represented the major proportion of the dissociating population, was considered the more relevant component in this analysis. Three bIGFBP-2 mutants, Thr-61→Ala, Pro-62→Ala and Arg-63→Ala bIGFBP-2 exhibited apparent dissociation rates ( $k_{off2}$ ) that were similar to bIGFBP-2 (Fig. 4.10a, Table 4.2). The apparent dissociation rate ( $k_{off2}$ ) of Tyr-60→Phe bIGFBP-2 was 2.6-fold more rapid than bIGFBP-2. Large increases in the apparent rate of dissociation ( $k_{off2}$ ) were observed for Val-59→Ala and Tyr-60→Ala bIGFBP-2 which were released from the IGF-I biosensor surface 9.4 and 18.4 times more rapidly than bIGFBP-2. (Fig. 4.10a, Table 4.2). The apparent affinity of bIGFBP-2 and the Tyr-60 region bIGFBP-2 mutants for the IGF-I surface, expressed as the dissociation rate constant ( $K_D$ ) were derived from the apparent association rate ( $k_{on}$ ) and the slow dissociation rate ( $k_{off2}$ ) according to the relationship:  $K_D = k_{off2}/k_{on}$ . The only bIGFBP-2 mutants that exhibited apparent  $K_D$  values that were significantly higher than bIGFBP-2 (0.5 nM) were Tyr-60→Ala bIGFBP-2 (2.0 nM) and Tyr-60→Phe bIGFBP-2 (4.2 nM) corresponding to a 4.0-fold and 8.4-fold drop in apparent affinity respectively.

The interactions of bIGFBP-2 and the Tyr-60 region bIGFBP-2 mutants with the IGF-II biosensor surface are shown in Fig. 4.10*b*. Two association components were derived from the sensorgram data and the relative contribution of each to the total binding

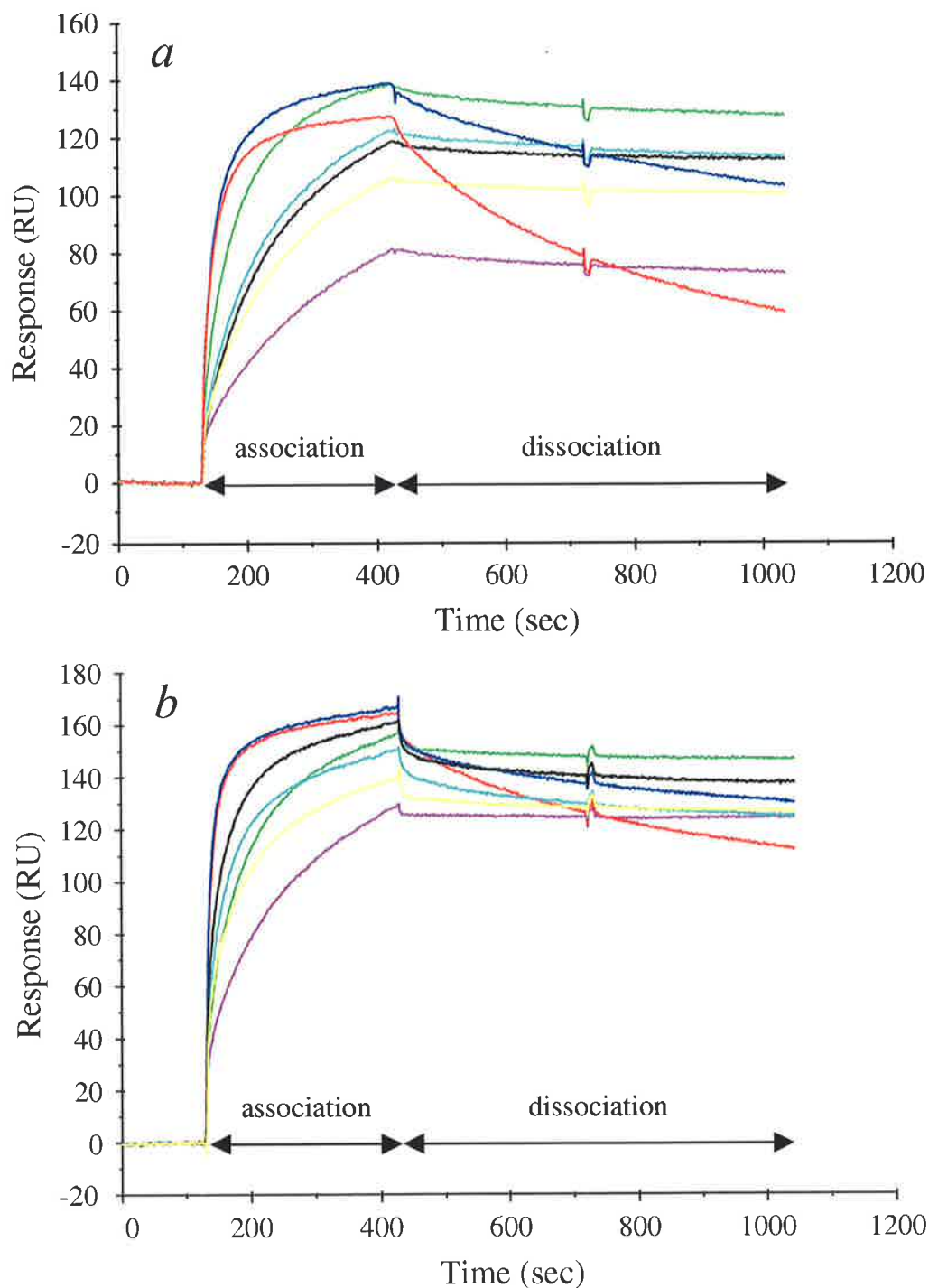


Fig 4.10. **BIAcore analysis of bIGFBP-2 and bIGFBP-2 analogs.** Shown are representative sensorgrams for the interactions of bIGFBP-2 ( — ), Val-59→Ala bIGFBP-2 ( — ), Tyr-60→Ala bIGFBP-2 ( — ), Tyr-60→Phe bIGFBP-2 ( — ), Thr-61→Ala bIGFBP-2 ( — ), Pro-62→Ala bIGFBP-2 ( — ) and Arg-63→Ala bIGFBP-2 ( — ) with (a) IGF-I biosensor surfaces (60 - 120 RU) and (b) IGF-II biosensor surfaces (60 - 120 RU) as described in Section 4.3.7.6.

Table 4.2. - Summary of kinetic parameters derived from the interaction of bIGFBP-2 species on IGF biosensor surfaces

IGF-I (60 RU)	$k_{on} \times 10^5$ (1/Ms)	relative $k_{on}$	$k_{off1} \times 10^{-3}$ (1/s)	$k_{off2} \times 10^{-5}$ (1/s)	relative $k_{off2}$	$K_D^a$ (nM)	relative $K_D$
<b>bIGFBP-2</b>	0.6 <sup>b</sup>	1.0 <sup>c</sup>	7.8	3.2	1.0	0.5	1.0
<b>Val-59→Ala</b>	3.3	5.5	6.6	30.0	9.4	0.9	1.8
<b>Tyr-60→Ala</b>	3.0	5.0	5.0	59.0	18.4	2.0	4.0
<b>Tyr-60→Phe</b>	0.2	0.3	6.0	8.4	2.6	4.2	8.4
<b>Thr-61→Ala</b>	1.3	2.2	8.6	4.5	1.4	0.4	0.8
<b>Pro-62→Ala</b>	0.5	0.8	8.6	2.1	0.7	0.4	0.8
<b>Arg-63→Ala</b>	0.4	0.7	18.0	3.4	1.1	0.9	1.8

IGF-II (66 RU)	$k_{on1} \times 10^5$ (1/Ms)	$k_{on2} \times 10^5$ (1/Ms)	weighting factor	$k_{on(app)}$ $\times 10^5$ (1/Ms)	relative $k_{on(app)}$	$k_{off1} \times 10^{-3}$ (1/s)	$k_{off2} \times 10^{-5}$ (1/s)	relative $k_{off2}$	$K_D^d$ (nM)	relative $K_D$
<b>bIGFBP-2</b>	1.1	22.6	0.95	2.2	1.0	7.6	5.0	1.0	0.2	1.0
<b>Val-59→Ala</b>	1.4	9.2	0.70	3.7	1.7	6.3	11.5	2.3	0.3	1.5
<b>Tyr-60→Ala</b>	1.7	10.1	0.70	4.2	1.9	7.9	30.9	6.2	0.7	3.5
<b>Tyr-60→Phe</b>	0.4	-	1.00	0.4	0.2	-	3.2	0.6	0.8	4.0
<b>Thr-61→Ala</b>	1.1	-	1.00	1.1	0.5	12.6	3.3	0.7	0.3	1.5
<b>Pro-62→Ala</b>	0.8	30.3	0.95	2.3	1.1	7.9	1.0	0.2	0.04	0.2
<b>Arg-63→Ala</b>	0.7	21.1	0.95	1.7	0.8	7.0	3.6	0.7	0.2	1.0

<sup>a</sup> IGF-I biosensor data:  $K_D = k_{off2}/k_{on}$ .

<sup>b</sup> Chi<sup>2</sup> values for sensorgram curve fits were equal to 1.0, or were less. R<sup>2</sup> values generated during the linear regression derivation of binding constants were equal to 0.95, or were greater. Inter-chip variation was 25% of the value or less for the apparent kinetic constant values  $k_{on}$ ,  $k_{off}$  and  $K_D$ .

<sup>c</sup> The ranking of the bIGFBP-2 mutants relative to bIGFBP-2 with respect to  $k_{on}$ ,  $k_{off}$  and  $K_D$  was the same on both biosensor chips. The interchip variation in the fold-differences of kinetic constants was 12% of the mean value or less.

<sup>d</sup> IGF-II biosensor data:  $K_D = k_{off2}/k_{on(app)}$ .

The BIA simulation program generates a sensorgram based on user-provided kinetic parameters. In the case of multiple-phase kinetics, the proportions of each phase can be manually varied within the program. Thus, an approximate value for the proportion of each on-rate (and each off rate) could be determined by comparing the ideal sensorgram generated by the BIA simulation program with the experimental data when a two-phase model best fitted the experimental data.

profile was estimated using the BIASimulation program. Between the bIGFBP-2 mutants, the rapid binding component played a varying role in the interaction. Therefore, for each bIGFBP-2 mutant, the two association constants were weighted to yield a single apparent association constant  $k_{on(app)}$ . In the case of Val-59→Ala and Tyr-60→Ala bIGFBP-2, the rapid association component accounted for approximately 30 % of the total association interaction with the IGF-II surface. It was estimated that for bIGFBP-2, Pro-62→Ala and Arg-63→Ala bIGFBP-2 only 5 % of the total IGF-II association interaction was due to the rapid association phase. In the case of Tyr-60→Phe and Thr-61→Ala bIGFBP-2, a single association component adequately modeled the association interaction to yield a single association constant  $k_{on(app)}$ . The trends of the apparent association rates, dissociation rates and overall affinities of bIGFBP-2 mutants on the IGF-II surface were similar to those observed for the mutants on the IGF-I surface, yet the magnitudes of the changes were generally less marked. Thus Val-59→Ala and Tyr-60→Ala bIGFBP-2 bound 1.7-fold and 1.9-fold more rapidly ( $k_{on(app)}$ ) to the IGF-II surface than did bIGFBP-2. (Fig. 4.10b, Table 4.2). Pro-62→Ala and Arg-63→Ala bIGFBP-2 bound with similar apparent association rates  $k_{on(app)}$  to bIGFBP-2. The bIGFBP-2 mutants that exhibited reduced apparent association rates  $k_{on(app)}$  were Thr-61→Ala and Tyr-60→Phe bIGFBP-2. The most significant reduction in apparent affinity was observed for Tyr-60→Phe bIGFBP-2, which bound 5.0-fold more slowly to the IGF-II surface than bIGFBP-2.

As was observed for the IGF-I surface, the dissociation of bIGFBP-2 and the bIGFBP-2 mutants from the IGF-II surface occurred in two phases to generate two dissociation constants ( $k_{off1}$  and  $k_{off2}$ ). Again, the rapid dissociation component  $k_{off1}$  was essentially the same for all of the bIGFBP-2 peptides and accounted for approximately 10 % of the total dissociation phase of the IGF/IGFBP interaction. Tyr-60→Phe, Thr-61→Ala and Arg-63→Ala bIGFBP-2 all exhibited dissociation rates ( $k_{off2}$ ) that were similar to the dissociation rate of bIGFBP-2. Pro-62→Ala bIGFBP-2 was released 5.0-fold more slowly from the IGF-II surface than bIGFBP-2. On the other hand, Val-59→Ala and Tyr-60→Ala bIGFBP-2 were released 2.3-fold and 6.2-fold more rapidly than bIGFBP-2 respectively. In terms of their overall apparent dissociation constants ( $K_D$ ), calculated by the relationship:  $K_D = k_{off2}/k_{on(app)}$ , Val-59→Ala (0.3 nM), Thr-61→Ala (0.3 nM) and Arg-63→Ala bIGFBP-2 (0.2 nM) were similar to bIGFBP-2 (0.2 nM) on the IGF-II surface. With an apparent  $K_D$  of 0.04 nM, Pro-62→Ala bIGFBP-2 bound to the IGF-II surface with a greater affinity than bIGFBP-2. In contrast, Tyr-60→Ala and Tyr-60→Phe bIGFBP-2 bound to the



IGF-II surface with  $K_D$  values of 0.7 nM and 0.8 nM respectively which corresponded to 3.5-fold and 4.0-fold lower affinities for IGF-II than bIGFBP-2 respectively.

#### 4.5 DISCUSSION

In this study, the Tyr-60 region of bIGFBP-2 has been investigated by mutagenesis to confirm and extend the findings from the chemical iodination study (Chapter 3; Hobba *et al.*, 1996). In the chemical iodination study, Tyr-60 was implicated in the IGF-binding site of bIGFBP-2 as this residue was protected from iodination in the bIGFBP-2/IGF complex and iodo-Tyr-60-bIGFBP-2 exhibited reduced apparent affinity for both IGF-I and IGF-II. The high degree of sequence homology in the Tyr-60 region of the whole IGFBP family (Fig. 4.1) suggested that other residues in this vicinity might also play a role in IGF binding. To investigate this possibility, Val-59→Ala, Tyr-60→Ala, Tyr-60→Phe, Thr-61→Ala, Pro-62→Ala and Arg-63→Ala bIGFBP-2 were recombinantly expressed, purified and characterised for changes in IGF affinity. The only bIGFBP-2 mutants that were observed to exhibit significantly reduced affinity for IGF-I and IGF-II using a variety of complementary analyses were Tyr-60→Ala and Tyr-60→Phe bIGFBP-2. With the exception of Pro-62→Ala bIGFBP-2, all of the Tyr-60 region bIGFBP-2 mutants produced essentially the same CD spectra (Fig. 4.7) and all ran as single bands at the same molecular weight as bIGFBP-2 in SDS-PAGE analysis (Fig. 4.5 and Fig. 4.6). Therefore, any changes in the IGF binding characteristics of Val-59→Ala, Tyr-60→Ala, Tyr-60→Phe, Thr-61→Ala and Arg-63→Ala bIGFBP-2 were considered to be due to the loss of side chain interactions at the mutagenic site in question and not to gross changes in protein structure.

There was good agreement between the three functional analyses that were used to investigate the IGF binding abilities of the bIGFBP-2 mutants. Western ligand blot (Fig. 4.6), solution binding assays (Fig. 4.9, Table 4.1) and the BIAcore analyses (Fig. 4.10, Table 4.2) all indicated that both Ala and Phe substitution for Tyr-60 resulted in a bIGFBP-2 molecule with reduced affinity for IGFs. However, some differences were noted. For example, Val-59→Ala bIGFBP-2 bound  $^{125}\text{I}$ -IGF-II at a visibly reduced level compared with bIGFBP-2 in the Western ligand blot (Fig. 4.6), yet bound  $^{125}\text{I}$ -IGFs as well as bIGFBP-2 in the solution binding assay (Fig. 4.9, Table 4.1). Similarly, the decrease in  $^{125}\text{I}$ -IGF-II binding of Tyr-60→Ala bIGFBP-2 was far more apparent in the Western ligand blot (Fig. 4.6) than in the solution binding assay (Fig. 4.9, Table 4.1).

Direct measurement of the association and dissociation kinetics of the IGFBP-2/IGF interaction in the BIAcore experiments could explain the observed

differences between the Western ligand blot and the solution binding assay results. Whereas Val-59→Ala and Tyr-60→Ala bIGFBP-2 dissociated 2.3-fold and 6.2-fold more rapidly from the IGF-II biosensor surface than bIGFBP-2 respectively, both also associated with this surface approximately 2-fold more rapidly than bIGFBP-2. Under the equilibrium conditions of the solution binding assay, the increased dissociation rates of Val-59→Ala and Tyr-60→Ala bIGFBP-2 were offset by the increases in the association rate. However, in the Western ligand blot, non-specifically bound <sup>125</sup>I-IGF-II was washed from the filter by buffer replacement, and so after washing commenced, the possibility of IGF and IGFBP-2 regaining a binding equilibrium was prevented. Therefore, it is evident that the Western ligand blot ranked the bIGFBP-2 mutants with respect to their relative dissociation rates, whereas the solution binding assay ranked the bIGFBP-2 mutants according to their overall affinities.

Insight into the reduced IGF binding affinity of Tyr-60→Ala and Tyr-60→Phe bIGFBP-2 was provided by BIAcore analysis. Substitution of Tyr-60 of bIGFBP-2 with Ala and Phe produced very different changes in the kinetics of IGF interactions. Tyr-60→Ala bIGFBP-2 associated with and dissociated from IGF biosensor surfaces more rapidly than bIGFBP-2. In contrast, Tyr-60→Phe bIGFBP-2 exhibited a reduced rate of association with, and an increased rate of dissociation from IGF biosensor surfaces compared with bIGFBP-2. Interestingly, Tyr-60→Ala and Val-59→Ala bIGFBP-2 exhibited very similar kinetics on the IGF-I and IGF-II biosensor surfaces. The altered association and dissociation kinetics of Val-59→Ala bIGFBP-2 with immobilised IGF suggests that this mutation produced subtle changes to the structure of the IGF binding site of bIGFBP-2, without significantly altering the free energy ( $\Delta G$ ) of IGF-binding. In contrast, Tyr-60→Ala bIGFBP-2 exhibited a net reduction in the  $\Delta G$  of IGF binding, which was manifested by a large increase in the dissociation rate of Tyr-60→Ala bIGFBP-2 from IGF surfaces. Therefore, the shape and volume of the side-chains of Val-59 and Tyr-60 may help to define the IGF binding site of bIGFBP-2. However, the aromatic function and the hydrogen bonding potential of Tyr-60 are clearly the most significant contributors to the stability of the bIGFBP-2/IGF complex. The replacement of Tyr-60 with Phe was anticipated to be the most subtle mutation, with the aromatic side-chain packing maintained and the loss of the tyrosyl hydroxyl group the only change. Surprisingly, Tyr-60→Phe bIGFBP-2 exhibited the lowest affinities for IGFs, thus providing further evidence to suggest that Tyr-60 participates in hydrogen bond(s) that stabilise IGF-binding interactions.

The apparent affinity constants that were calculated with the derived association and dissociation constants of bIGFBP-2 and the IGF-I and IGF-II surfaces (0.5 nM for IGF-I and 0.2 nM for IGF-II) correspond very well with published constants generated by competition solution binding assays (Clemmons *et al.*, 1992; Bach *et al.*, 1993). Yet, the interactions of bIGFBP-2 and the bIGFBP-2 mutants with immobilised IGFs deviated from pseudo-first-order kinetics in the BIAcore (Fig. 4.10). In circulation, IGFBPs bind IGFs with a 1:1 stoichiometry (reviewed by Baxter, 1994), and therefore a single site kinetic model should provide a valid approximation of the IGFBP/IGF interaction. Multiple-phase kinetics for single site interactions can be due to artifacts of the BIAcore assay conditions (Edwards *et al.*, 1995; Bowles *et al.*, 1997). In this study, steps have been taken to address some of the common artifactual causes of multiple-phase kinetics. Thus, very low density IGF biosensor surfaces (60 -120 RU) and moderate flow rates (40  $\mu$ l/min) have been deliberately used to minimise mass transfer limitations and the steric masking of binding sites. Amine coupling was used to immobilise IGFs in this study and this strategy can lead to a mixed population of ligand on the biosensor surface with a range of different affinities for the analyte (Bowles *et al.*, 1997). However, the same non-pseudo-first-order kinetic behavior was observed when immobilised hIGFBP-3 was analysed with free IGF (Heding *et al.*, 1996). It is therefore possible that the multiple association and dissociation phases present in IGF/IGFBP sensorgrams reflect a physical characteristic of the protein interaction, such as multiple step binding. It is interesting to note that Scatchard analysis of competitive solution binding assays have also shown that IGFBPs may exhibit both low and high affinity binding sites for IGFs under some conditions (McCusker *et al.*, 1991, Roghani *et al.*, 1991).

Overall, the effects of mutagenesis in the Tyr-60 region of bIGFBP-2 were more severe for interactions with IGF-I than IGF-II. For example, Tyr-60 $\rightarrow$ Phe bIGFBP-2 bound to the IGF-I biosensor surface with a 8.4-fold lower affinity than bIGFBP-2, whereas it bound to the IGF-II biosensor surface with a 4.0-fold lower affinity than bIGFBP-2. This corresponds well with earlier findings that iodo-bIGFBP-2 exhibited an 8-fold reduction in apparent affinity for IGF-I compared to a 4-fold reduction in apparent affinity to IGF-II (Chapter 3; Hobba *et al.*, 1996). The high degree of structural similarity between IGF-I and IGF-II (Torres *et al.*, 1995) suggests that both IGF molecules interact with IGFBPs through similar side-chain contacts. Mutagenic support for this idea can be seen in the similar reduction in IGFBP affinity of Glu-3 $\rightarrow$ Arg IGF-I (Bagley *et al.*, 1989) and its structural homologue Glu-6 $\rightarrow$ Arg IGF-II (Francis *et al.*, 1993). The disproportionate sensitivity of

the Tyr-60 bIGFBP-2 mutants towards IGF-I binding, in addition to the natural preference of bIGFBP-2 for IGF-II, (Jones and Clemmons, 1995) suggests that the bIGFBP-2/IGF-II complex contains additional points of molecular interaction that are absent in the bIGFBP-2/IGF-I complex. Indeed, in a recent truncation study (Forbes *et al.*, 1998), mutagenic removal of 62 amino acid residues from the C-terminus of bIGFBP-2 resulted in a dramatic loss of IGF binding. More importantly, this bIGFBP-2 mutant had lost all binding preference for IGF-II over IGF-I. It was thus concluded that the C-terminal cysteine-rich domain of bIGFBP-2 contains determinants of IGF-II binding specificity.

The ability of Tyr-60 to form a hydrogen bond that is important for IGF binding is evident by the reduced affinity of both Tyr-60→Ala and Tyr-60→Phe bIGFBP-2 for IGF-I and IGF-II. Moreover, the presence of an aromatic function at position 60 of bIGFBP-2 reduces the rate of formation of bIGFBP-2/IGF complex but also enhances the stabilization of the complex. This study raises the question as to whether the hydrogen bond acceptor of Tyr-60 is within the bIGFBP-2 molecule or within the IGF molecule. It appears likely that Tyr-60 is located in the IGF binding interface of bIGFBP-2 and that modification or mutagenic replacement of Tyr-60 directly disrupts contacts between IGF and bIGFBP-2. Alternatively, it is possible that Tyr-60 modification and mutagenic replacement indirectly affects IGF binding for example, by preventing a change in conformation that is necessary for high affinity IGF binding. However the simplest interpretation of the earlier observation that iodination of Tyr-60 can be blocked by the formation of an bIGFBP-2/IGF complex supports a direct interaction between Tyr-60 of bIGFBP-2 and IGF. Clearly, distinction between these two models must await biophysical characterisation of the bIGFBP-2/IGF complex, for example by the HSQC-NMR approach recently described by Craik & Wilce, 1997.

In this approach, chemical shifts in the heteronuclear single quantum correlation (HSQC) NMR spectra can be observed to alter due to changes in the electronic environment of specific side-chains. For example, when side-chains in the binding interface between two proteins change from an exposed to a buried state upon complex formation.

## **CHAPTER 5 – GENERAL DISCUSSION AND CONCLUDING REMARKS**

The broad objective of the studies presented in this thesis was to identify amino-acid residues which comprise the IGF binding site of bIGFBP-2. In the absence of an IGFBP structure, this objective was addressed using a two-tiered approach. Firstly, a region that was implicated in IGF-interactions was identified using a chemical modification strategy. Thereafter, alanine-scanning mutagenesis was employed to investigate the functional significance of each residue in that putative IGF-binding region.

## **5.1 SUMMARY OF FINDINGS**

A recombinant expression system was routinely used to produce bIGFBP-2 for structural and functional analyses (Chapter 2). This expression system provided reference bIGFBP-2 material which possessed binding affinities for IGF-I and IGF-II that were consistent with published values. Moreover, the bIGFBP-2 expression system enabled bIGFBP-2 mutant analogs to be generated.

Initially, the IGF-binding site of bIGFBP-2 was probed by chemical iodination (Chapter 3). Of the five bIGFBP-2 tyrosine residues that were readily available for chemical iodination (Tyr-60, Tyr-71, Tyr-98, Tyr-213 and Tyr-269) only Tyr-60 was significantly protected from modification when IGF-ligand was present. The simplest explanation for the observed change in Tyr-60 reactivity is that Tyr-60 is located in the binding interface between the bIGFBP-2 and IGF molecules. Alternatively, IGF-association with bIGFBP-2 may alter the conformation of the Tyr-60 side-chain to render it less accessible for modification.

The possibility that Tyr-60 was functionally significant for molecular interactions between bIGFBP-2 and IGFs was confirmed with chemically modified and mutant bIGFBP-2 analogs. Tyrosine-iodination did not alter the ability of bIGFBP-2 to bind IGF-ligand if bIGFBP-2 was iodinated in a complex with IGF (Chapter 3). It therefore follows that the sites that were available for iodination in the bIGFBP-2/IGF complex (Tyr-71, Tyr-98, Tyr-213 and Tyr-269) do not interact with the IGF molecule. In contrast, an 8-fold reduction in apparent affinity for IGF-I and a 4-fold reduction in apparent affinity for IGF-II was sustained by bIGFBP-2 when iodinated in the absence of protective IGF-ligand. Furthermore, mutant bIGFBP-2 analogs Val-59→Ala, Tyr-60→Ala and Tyr-60→Phe bIGFBP-2 showed reduced capacity to bind <sup>125</sup>I-labelled IGF-II in Western-ligand blots (Chapter 4). Analysis of these bIGFBP-2 analogs in solution binding assays and on IGF-biosensor chips revealed an interesting story. Val-59→Ala and wild-type bIGFBP-2 exhibited essentially the same equilibrium affinities for IGF-I and IGF-II in solution

binding assays. However, BIAcore analysis indicated that Val-59→Ala bIGFBP-2 associated with and dissociated from IGF-I–biosensor surfaces 5.5-fold and 9.4-fold more rapidly than bIGFBP-2 respectively. In contrast, both Tyr-60→Ala and Tyr-60→Phe bIGFBP-2 exhibited reduced equilibrium affinities for IGF-I and IGF-II in solution binding assays, but surprisingly, for different kinetic reasons. Tyr-60→Ala bIGFBP-2, like Val-59→Ala bIGFBP-2 associated more rapidly with and dissociated more rapidly from IGF-biosensor surfaces. However, unlike Val-59→Ala bIGFBP-2, the increase in dissociation rate of Tyr-60→Ala bIGFBP-2 (18.4-fold for IGF-I surfaces) far outweighed any increase in association rate (5.0-fold for IGF-I surfaces) to yield a substantial reduction in equilibrium affinity. In contrast, Tyr-60→Phe bIGFBP-2 exhibited a 3-fold reduced rate of association with, and a 2.6-fold increased rate of dissociation from IGF-I surfaces and thereby yielding an 8.4-fold net reduction in equilibrium affinity.

Taken together, IGF-mediated protection at Tyr-60 and the loss of IGF-affinity due to iodination or amino-acid substitution at Tyr-60 strongly suggests that Tyr-60 of bIGFBP-2 participates in IGF-interactions. The non-native kinetics of Val-59→Ala bIGFBP-2 binding to IGF-surfaces suggests that this mutation produced subtle changes in the IGF-binding site.

## **5.2 POSSIBLE IGF BINDING ROLES FOR TYR-60 AND VAL-59**

To understand how the chemical iodination or mutagenic replacement of Tyr-60 destabilised the complex between bIGFBP-2 and IGF, it is necessary to consider the general properties of protein-protein interactions and how these properties were potentially altered by the modification of bIGFBP-2. The physical forces and stabilising interactions that result in a folded protein molecule are no different to the forces and interactions that stabilise a protein complex (Abler, 1989; Janin & Chothia, 1990; Jones & Thornton, 1996; Wells, 1996). Thus, the cumulative contributions of numerous hydrophobic interactions, hydrogen bonds and electrostatic contacts enable the complementary surfaces to remain bound in a high-affinity complex.

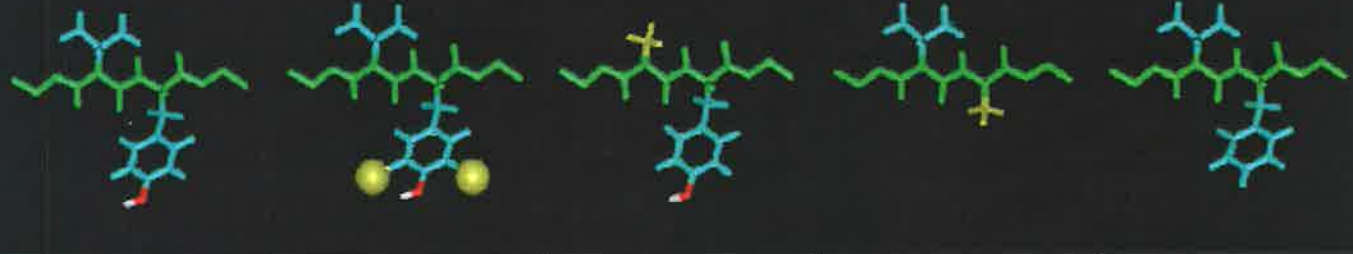
Some general characteristics of protein-protein interactions are highlighted by studies of the growth hormone receptor complex (reviewed by Wells, 1996). The interface between growth hormone (hGH) and the growth hormone receptor (hGHbp) in the crystal structure of the growth hormone receptor complex involved 31 residue side-chains from the ligand and 33 from the receptor. Alanine-scanning mutagenesis of the entire set of contact residues in each binding partner and kinetic studies showed that the most critical

side chain interactions for high affinity complex formation were well intercalated hydrophobic contacts provided by Trp-104 and Trp-169 of hGHbp and the aliphatic portions of Asp-171, Lys-172 and Thr-175 of hGH (Wells, 1996). Furthermore, alanine substitution for these essential residues generally increased rates of hGH dissociation from hGHbp, whereas the rates of association remained largely unchanged (Wells, 1996). Therefore, it was concluded that the purpose of these essential side-chain contacts was to maintain the complex rather than facilitate complex formation. It has previously been argued that diffusion effects dominate the rate of association of protein complexes and that these effects are largely independent of the side-chain composition of the protein-protein interface (Northrup and Erickson 1992, in Wells, 1996). Mutations of hGH which did produce subtle changes in its association rate with hGHbp were correlated to alterations in the electrostatics of the binding site, for example the substitution of acidic or basic binding-site residues with alanine (Wells 1996). Therefore, it is possible that attractive electrostatic forces may prevent the immediate diffusion of the binding partners and allow productive collisions to occur more rapidly.

A reduction in the stability of the complex between modified bIGFBP-2 analogs and IGF in comparison to the wild-type complex may be due to the loss of stabilising interactions or equally, to the introduction of energetically unfavourable interactions at the protein-protein interface. Fig. 5.1 summarises the modifications that were made to the bIGFBP-2 molecule during the course of the studies described in Chapters 3 and 4. In addition, this figure highlights the physico-chemical alteration that each modification achieved relative to the original side-chain and the effect that each modification potentially evoked in terms of the affinity for IGF-I.

Tyrosine iodination is known to alter the physico-chemical properties of the phenolic side-chain. Not only is the bulk of the phenolic ring increased, but the pKa of the *p*-OH group is also substantially reduced. Therefore tyrosine iodination at essential residues can alter the biological or structural properties of an iodinated protein. For example, it has been shown previously that iodination at Tyr-59 disrupts the interaction between iodo-ubiquitin and ubiquitin-conjugating enzyme E2(25K) for steric reasons (Pickart *et al.*, 1992). Similarly, iodination at Tyr-60 of bIGFBP-2 may sterically interfere with the association of IGF. In contrast, recombinant iodo-Tyr-63 hirudin exhibited a greater affinity for thrombin than recombinant hirudin. It was concluded that iodination reduced the pKa of Tyr-63 to yield an ionised iodo-phenolic ring, and this modification





bIGFBP-2 Val-59-Tyr-60	Iodo-Tyr-60 bIGFBP-2	Val-59→Ala bIGFBP-2	Tyr-60 → Ala bIGFBP-2	Tyr-60 → Phe bIGFBP-2
<b>Predicted Physical Change</b>	↓ <i>p</i> -OH pKa, Tyr-60 no longer an H-bond donor ↑ steric interference	↓ side-chain volume  ↓ steric interference and altered packing	aromatic bulk and <i>p</i> -OH lost  ↓ steric interference and altered packing	aromatic bulk kept and <i>p</i> -OH lost  ↑ hydrophobicity  same packing
<b>Observed Impact on IGF-I Binding</b>	↑ $k_D$ (8-fold)	↑ $k_{on}$ and $k_{off}$ no change in $k_D$	↑ $k_{on}$ and $k_{off}$ ↑ $k_D$ (4-fold)	↓ $k_{on}$ and ↑ $k_{off}$ ↑ $k_D$ (8-fold)
<b>Possible IGF Binding Role(s) of w/t Side-chain</b>	1. <i>p</i> -OH H-bond stabilises complex 2. aromatic contacts stabilise complex	1. hinders IGF binding, but also stabilises complex	1. hinders IGF binding, but also stabilises complex 2. <i>p</i> -OH H-bond stabilises complex	1. <i>p</i> -OH H-bond facilitates IGF binding and stabilises complex

Fig. 5.1. - Summary of modifications to bIGFBP-2 and the resultant changes in affinity for IGF-I

more closely mimicked the negatively charged sulfate-ester of Tyr-63 which occurs in native hirudin isolated from the leach (Winant *et al.*, 1991). A reduction in the IGF-affinity of iodo-Tyr-60 bIGFBP-2 may therefore result from ionisation of the *p*-OH group. If indeed iodo-Tyr-60 is ionised, the negative charge could introduce energetically unfavourable electrostatic repulsion in the IGF binding site or result in a buried charge. In addition, ionisation of iodo-Tyr-60 may be deleterious to IGF interactions by reducing the ability of this residue to participate in side-chain hydrogen bonds compared with non-modified Tyr-60.

The mutagenic replacement of Val-59 with alanine shortened the side chain length by one methylene group and reduced the side-chain volume by essentially two methyl groups. Therefore the observed changes in the IGF-binding kinetics of Val-59→Ala bIGFBP-2 may be due to altered packing of hydrophobic side-chains at the interface between IGF and Val-59→Ala bIGFBP-2. The enhanced dissociation rate of Val-59→Ala bIGFBP-2 from IGF-surfaces may be due to the loss of hydrophobic contacts or the introduction of an energetically unfavourable cavity in the interface. An explanation for the increased rate of association of Val-59→Ala bIGFBP-2 with IGF is more difficult to provide. It is possible that Val-59 of bIGFBP-2 sterically hinders IGF association but contributes to the stability of the complex once IGF is bound.

Of the two mutagenic substitutions that were investigated at Tyr-60, the most conservative was Tyr-60→Phe, yet this mutation resulted in the most severe defect in the equilibrium affinity of bIGFBP-2 for IGF. Both tyrosine and phenylalanine possess a common aromatic ring structure, however, phenylalanine lacks the *p*-OH group of tyrosine. As a result, the phenylalanine side-chain is more hydrophobic and is unable to act as a hydrogen-bonds donor. The reduced IGF-affinity of Tyr-60→Phe bIGFBP-2 therefore indicates that the hydrogen-bonding capacity of Tyr-60 is important for IGF-interactions. Tyr-60→Phe bIGFBP-2 associated 3-fold more slowly with IGF-I surfaces than bIGFBP-2 and was released 2.6-fold more rapidly than bIGFBP-2. The *p*-OH group of Tyr-60 must therefore participate in hydrogen bonds that both initiate and stabilise the IGF-bIGFBP-2 complex.

In contrast to the conservative substitution of phenylalanine for Tyr-60, alanine substitution for Tyr-60 was more radical as both the polar *p*-OH and the aromatic functional groups were replaced with a methyl side-chain. The 18.4-fold increased dissociation rate of Tyr-60→Ala bIGFBP-2 from IGF-I surfaces, compared with bIGFBP-2, was the most dramatic kinetic change observed during this work. Favourable side-chain

contacts that were possibly lost with the Tyr-60→Ala substitution include hydrophobic contacts, aromatic interactions between the delocalised  $\pi$ -electrons of Tyr-60 and aromatic side-chains of IGF, and hydrogen bonding through the *p*-OH group. In terms of possible aromatic-aromatic interactions, Tyr-60 of bIGFBP-2 could possibly interact with Phe-49 and/or Tyr-59 of IGF-I and Phe-48 and/or Tyr-60 of IGF-II. Tyr-59 of IGF-I and Tyr-60 of IGF-II are both protected from iodination in a complex with IGFBP-2 (Moss *et al.*, 1990). In addition, Phe-49 of IGF-I and Phe-48 of IGF-II are both known to be important for IGFBP interactions (Cascieri *et al.*, 1989a,b; Bach *et al.*, 1990). Interestingly, Tyr-60→Ala bIGFBP-2, like Val-59→Ala bIGFBP-2 showed a 5-fold enhancement in the association rate with IGF-I surfaces, compared with bIGFBP-2. Again, the enhanced association rates of Val-59→Ala and Tyr-60→Ala may be due to reduced steric hindrance of IGF-association from the smaller alanine side-chain.

In conclusion, the shape and the volume of the side-chains of Val-59 and Tyr-60 may help to define the IGF binding site of bIGFBP-2. Ala substitution for either Val-59 or Tyr-60 substantially altered both the rate of association and the rate of dissociation with IGF-I and IGF-II biosensor surfaces. More importantly, mutations that lead to the loss of the *p*-OH of Tyr-60 led to a reduction in the apparent affinity of bIGFBP-2 for IGF-ligand. It is therefore apparent that hydrogen-bond contacts between Tyr-60 and residues of the IGF moiety facilitate the association of IGF with bIGFBP-2 as well as stabilise the IGF/bIGFBP-2 complex.

### **5.3 IMPLICATIONS OF FINDINGS**

During the preparation of this thesis, the molecular structure of an IGF-binding fragment of hIGFBP-5 was published (Kalus *et al.*, 1998). This constituted the first example of an IGFBP structure in the literature. Importantly, the contact residues between mini-IGFBP-5 and IGF-II were identified using NMR techniques. This section will discuss the research findings of Chapter 4 in light of the new mini-IGFBP-5 structure.

Mini-IGFBP-5 was originally identified as a product of hIGFBP-5 proteolytic digestion that retained affinity for IGF-ligands (Kalus *et al.*, 1998). Mini-IGFBP-5 comprises residues 40-92 in the N-terminal cysteine-rich domain of hIGFBP-5 and a similar minimal IGF-binding fragment has also been identified for rIGFBP-3 (residues 52 to 92; Hashimoto *et al.*, 1997). Furthermore, this region exhibits an identical cysteine arrangement in all IGFBP primary structures and a common pattern of disulfide-linkages has been demonstrated for hIGFBP-1 (A. Bilgren, pers. com.), bIGFBP-2 (B. Forbes, pers.

com.), rIGFBP-3 (Hashimoto *et al.*, 1997), hIGFBP-5 (Kalus *et al.*, 1998) and hIGFBP-6 (Neumann *et al.*, 1997) (see Section 1.3.2 of Chapter 1). Thus, it is likely that the mini-IGFBP-5 structure is representative of the other IGFBP family members. Fig. 5.2 highlights the strong sequence homology between the mini-IGFBP-5 and bIGFBP-2 primary structures. Importantly, the Tyr-60 region of bIGFBP-2 (residues 59-63) is identical to the mini-IGFBP-5 sequence (residues 49-53) in 4 of the 5 positions. It is highly likely that the homologous regions of mini-IGFBP-5 and bIGFBP-2 adopt the same structure.

Mini-BIGFBP-5 forms a rigid and globular structure that is stabilised by two buried disulfide-bonds and a three stranded  $\beta$ -sheet. Titration of  $^{15}\text{N}$ -labelled mini-bIGFBP-5 with IGF-II and analysis of the HSQC spectra showed that IGF-binding produced large chemical shifts in the spectra of Val-49, Tyr-50, Pro-62 and Lys-68 to His-75 inclusive. Kalus *et al.*, (1998) thus concluded that these residues comprised the primary IGF-II binding site in the N-terminal cysteine-rich domain of hIGFBP-5. Significantly, Val-59 and Tyr-60 of bIGFBP-2 were identified as potential determinants of the IGF-binding in this thesis by a combination of chemical iodination and mutagenesis strategies (Chapters 3 and 4, respectively) and the corresponding residues Val-49 and Tyr-50 of hIGFBP-5 have now also been identified as IGF-binding determinants using biophysical techniques. It is therefore reasonable to predict that the equivalent residues to Val-59 and Tyr-60 of bIGFBP-2 play equivalent IGF-binding roles throughout the IGFBP family, except the IGFBP-1 members which possess an alanine residue at the position corresponding to Tyr-60 of bIGFBP-2.



**Fig. 5.2 – Sequence alignment of mini-IGFBP-5 and the equivalent region of bIGFBP-2.** Shown are the residues involved in  $\beta$ -turns (t) and  $\beta$ -sheets (b) in the structure. Residues in the two sequences that are conserved are highlighted in yellow. Residues of mini-IGFBP-5 that have been shown by NMR to be involved in IGF-interactions are underlined.

Fig. 5.3 shows the molecular structure of mini-IGFBP-5 (PDB code 1boe), oriented so that the IGF-II binding site identified by NMR forms a frontward facing plane across the top of the structure. In Fig. 5.3a, residues of the Tyr-60 region of bIGFBP-2 are illustrated in the mini-IGFBP-5 structure as space-filling CPK models. Side-chains coloured yellow

correspond to bIGFBP-2 residues implicated in the IGF-binding site by the studies of this thesis. In contrast, residues coloured cyan correspond to the residues of the Tyr-60 region of bIGFBP-2 that could be substituted with alanine with little impact in IGF-interactions (Chapter 4; Hobba *et al.*, 1998). Fig. 5.3*b* highlights all of the side-chain atoms of mini-IGFBP-5 that are implicated in IGF-II interactions by NMR (Kalus *et al.*, 1998). Coloured yellow (Val-49 and Tyr-50) are the homologous side chains identified in this thesis and by NMR. Coloured in red (Pro-62, Lys-68, Pro-69, Leu-70, His-71, Ala-72, Leu-73, Leu-74 and His-74) are the remaining IGF-binding site residues identified by NMR. Comparison of Fig. 5.3*a* and *b* shows that the side-chain atoms of Val-49 and Tyr-50 project into the plane of the IGF-binding site and that the *p*-OH group of Tyr-60 is directed toward the centre of the binding interface. In contrast to Val-49 and Tyr-50, the side-chain atoms of Thr-51, Glu-52 and Arg-53 (which correspond to Thr-61, Pro-62 and Arg-63 of bIGBP-2 respectively), project down and away from the plane of the IGF-binding site. Therefore, assuming that mini-IGFBP-5 and the equivalent domain of bIGFBP-2 adopt the same structure, Fig. 5*a* provides a structural explanation for why mutations at Val-59 and Tyr-60 altered the ability of bIGFBP-2 to interact with IGFs, yet mutations at Thr-61, Pro-62 and Arg-63 did not.

#### **5.4 FUTURE DIRECTIONS**

Future studies will begin to address how the newly identified IGF-binding determinants of IGFBPs interact with the well characterised IGFBP binding site of IGFs. The work presented in this thesis could thus be extended by identifying residues of IGF-I and IGF-II that interact with Tyr-60 of bIGFBP-2. This could be achieved by observing chemical shifts in the heteronuclear single quantum correlation (HSQC) NMR spectra of <sup>15</sup>N-IGF when titrated with either bIGFBP-2 or Tyr-60→Ala or Tyr-60→Phe bIGFBP-2. Large chemical shifts in the HSQC spectra of <sup>15</sup>N-IGF complexed with bIGFBP-2 compared with the HSQC spectra of <sup>15</sup>N-IGF would identify which residues in the IGF-structure change their electronic environment as a result of complex formation. This would implicate residues of IGF that comprise the bIGFBP-2-binding site and thus provide evidence complementary to our current understanding of IGF structure/function relationships. Indeed this type of study has recently been performed to identify residues of IGF-I that interact with hIGFBP-1 (Jansson *et al.*, 1998). More importantly, the HSQC spectra of the <sup>15</sup>N-IGF complexed with Tyr-60→Ala bIGFBP-2 would not include chemical shift contributions from the IGF residues that normally form contacts with

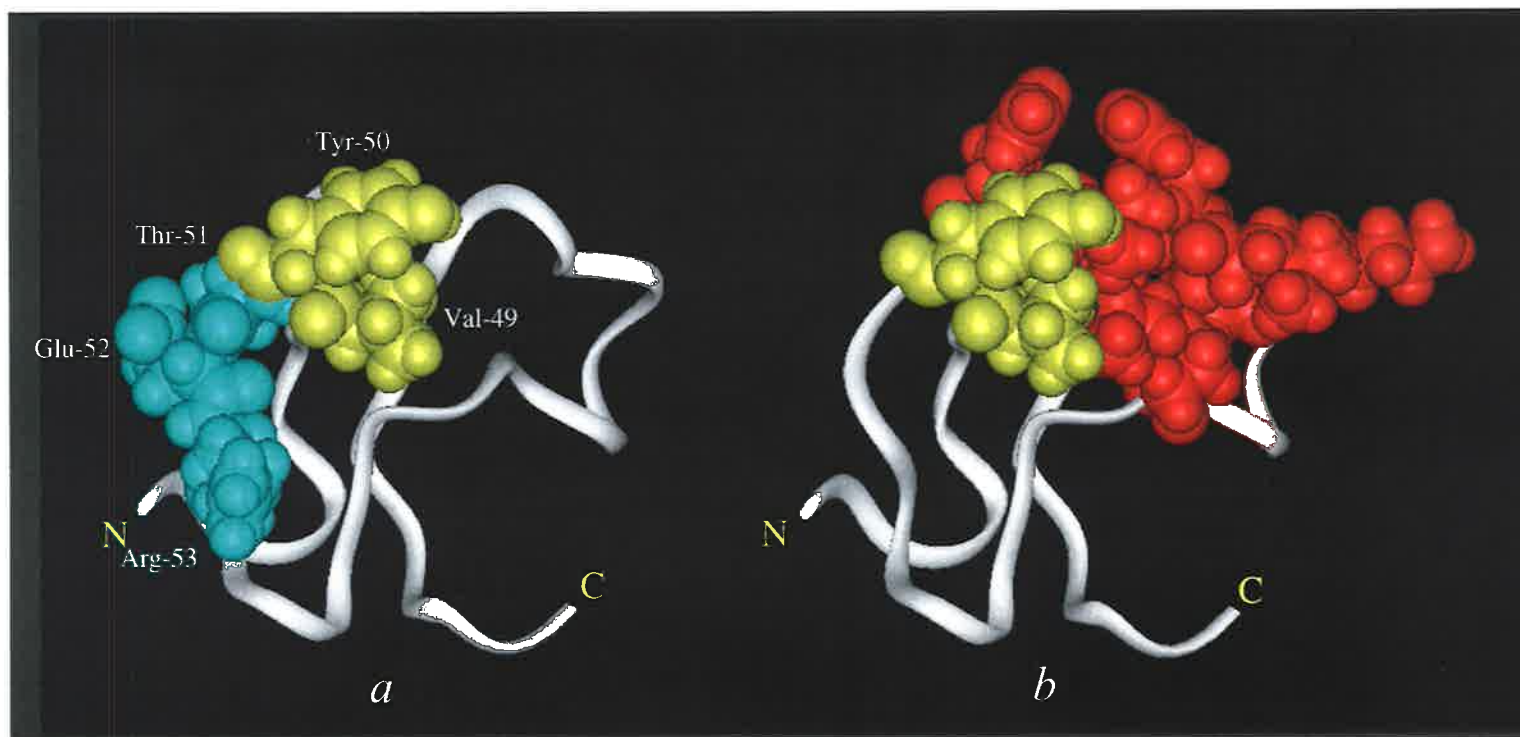


Fig. 5.3 - The location of “Tyr-60 region” residues of bIGFBP-2 in the molecular structure of mini-IGFBP-5. Panel *a* shows the molecular structure of mini-IGFBP-5 (Kalus *et al.*, 1998) with homologous residues to Val-59, Tyr-60, Thr-61, Pro-62 and Arg-63 of bIGFBP-2 rendered as space-filling CPK models. Together, the iodination study (Chapter 3) and the alanine-scanning mutagenesis study (Chapter 4) identified Val-59 and Tyr-60 of bIGFBP-2 as potential determinants of the IGF-binding site. Homologous residues in mini-IGFBP-5 (Val-49 and Tyr-50) are highlighted in yellow. Homologous residues to those which did not significantly influence IGF-interactions (Thr-61, Pro-62 and Arg-63 of bIGFBP-2) are depicted in cyan. Panel *b* shows the residues of mini-IGFBP-5 whose NMR spectra were chemically shifted as a result of complex formation with IGF-II (Kalus *et al.*, 1998). Residues thus implicated in IGF-binding and homologous to residues identified in this thesis are shown in yellow (Val-49 and Tyr-50). Additional IGF-binding site residues of mini-IGFBP-5 (Pro-62, Lys-68, Pro-69, Leu-70, His-71, Ala-72, Leu-73, Leu-74 and His-75) are shown in red. The atomic coordinates of mini-IGFBP-5, were from the Brookhaven Protein Structure Data Bank (Bernstein *et al.*, 1977) and were displayed using Insight II (BIOSYM Technologies).

Tyr-60. Therefore the identity of Tyr-60 binding-partners would be evident by the conspicuous absence of their chemical shifts in the HSQC spectra.

Chemical shift changes are indicative of alterations in the electronic environment of specific side chains and as such provide a good picture of residues that may interact in a protein-protein interface. However, an X-filtered NOESY experiment would provide a more direct approach to identify residues of IGF that interact with Tyr-60 of bIGFBP-2. The X-filtered NOESY approach (as described in Mulhern *et al.*, 1997) could be used to identify magnetisation transfer from unlabelled bIGFBP-2 samples to  $^{15}\text{N}^{13}\text{C}$ -IGF. Comparison of the NOESY spectra produced by a complex between IGF and bIGFBP-2 and the spectra produced by a complex between IGF and Tyr-60→Phe bIGFBP-2 would indicate which residues of IGF interact with Tyr-60 of bIGFBP-2.

Two of the mutant analogs of bIGFBP-2 produced in this research exhibited reduced affinity for IGF-I and IGF-II when measured by *in vitro* assays. Interestingly, Tyr-60→Phe bIGFBP-2 was predominantly compromised in its ability to associate with IGF, whereas Tyr60\_Ala bIGFBP-2 was greatly compromised in its ability to maintain the IGF/bIGFBP-2 complex. It is unclear which of these mutant analogs would be the least effective inhibitor of IGF-activity in a cellular assays. Future experiments should therefore contrast the abilities of bIGFBP-2, Tyr60\_Ala bIGFBP-2 and Tyr-60→Phe bIGFBP-2 to inhibit the stimulation of cellular growth by IGF.

The IGFBPs are multifunctional proteins. Their respective biological roles extend beyond influencing IGF half-life in circulation or transporting IGFs to target tissues. It is abundantly clear from the intensive study of IGFBP structure and function that IGFBPs also directly modulate IGF activity (See chapter 1). Therefore, IGFBPs must bind IGFs with sufficiently high affinity for latent complexes to endure, yet these complexes must be highly labile under certain physiological conditions that call for the release of IGF. It is therefore likely that the mechanism(s) that underlie IGFBP-IGF interactions are complicated. Perhaps the underlying complexity of IGF-IGFBP interactions is implicit in the fact that both the N- and C-terminal regions of IGFBPs are necessary for high affinity interactions with IGFs. Therefore, a full understanding of the IGF-binding mechanism of IGFBPs will rely on research in two main areas. Firstly, there will need to be further identification of IGF-binding determinants in other regions of IGFBPs such as the C-terminal cysteine rich domain. Finally, the molecular dynamics that allow multiple domains of IGFBPs to cooperatively interact with IGFs will need to be studied.

The involvement of IGFs in pathological states such as cancer and the therapeutic potential of IGFs in the treatment of growth deficiency and diabetes has led to an increased interest in how the activities of IGFs are regulated. Future studies that define the nature of the IGF/IGFBP interaction at the molecular level will enable the design of IGFBPs with altered IGF affinity or specificity. Such novel IGFBP analogs would be invaluable tools for further defining the IGF system and may facilitate the control of IGF activity in disease states.



## REFERENCES

- Abler T. (1989) Mutational effects on protein stability. *Ann. Rev. Biochem.* **58**: 765-7798.
- Allander S.V., Bajalica S., Larsson C., Luthman H., Powell D.R., Stern I., Weber G., Zazzi H., Ehrenborg E. (1993) Structure and chromosomal localization of human insulin-like growth factor-binding protein genes. *Growth Regul.* **3**: 3-5.
- Andress D.L., Loop S.M., Zapf J., Kiefer M.C. (1993) Carboxy-truncated insulin-like growth factor binding protein-5 stimulates mitogenesis in osteoblast-like cells. *Biochem. Biophys. Res. Com.* **195**: 25-30.
- Arai T., Busby W., Jr., Clemmons D.R. (1996a) Binding of insulin-like growth factor (IGF) I or II to IGF-binding protein-2 enables it to bind to heparin and extracellular matrix. *Endocrinology* **137**: 4571-4575.
- Arai T., Clarke J., Parker A., Busby W., Jr., Nam T., Clemmons D.R. (1996b) Substitution of specific amino acids in insulin-like growth factor (IGF) binding protein 5 alters heparin binding and its change in affinity for IGF-I in response to heparin. *J. Biol. Chem.* **271**: 6090-6106.
- Arai T., Parker A., Busby W., Jr., Clemmons D.R. (1994) Heparin, Heparan Sulfate, and Dermatan Sulfate Regulate Formation of the Insulin-like Growth Factor-I and Insulin-like Growth Factor-binding protein Complexes. *J. Biol. Chem.* **269**: 20388-20393.
- Bach L.A., Hsieh S., Sakano K.I., Fujiwara H., Perdue J.F., Rechler M.M. (1993) Binding of mutants of human insulin-like growth factor II to insulin-like growth factor binding proteins 1-6. *J. Biol. Chem.* **268**: 9246-9254.
- Bagley C.J., May B.L., Szabo L., McNamara P.J., Ross M., Francis G.L., Ballard F.J., Wallace J.C. (1989) A key functional role for the insulin-like growth factor 1 amino-terminal pentapeptide. *Biochem. J.* **259**: 665-672.

- Bairoch A. (1991) PROSITE: a dictionary of sites and patterns in proteins. *Nucleic Acids Res.* **25**: 2241-2245.
- Baker J., Liu J.P., Robertson E.J., Efstratiadis A. (1993) Role of insulin-like growth factors in embryonic and postnatal growth. *Cell* **75**: 73-82.
- Baker M.S., Green S.P., Goss N., Katrantzis M., Doe W.F. (1990) Plasminogen activator inhibitor 2 (PAI-2) is not inactivated by exposure to oxidants which can be released from activated neutrophils. *Biochem. Biophys. Res. Commun.* **166**: 993-1000.
- Ballard F.J., Francis G.L., Ross M., Bagley C.J., May B., Wallace J.C. (1987) Natural and synthetic forms of insulin-like growth factor 1 (IGF-1) and the potent derivative, destriptide IGF-1: Biological activities and receptor binding. *Biochem. Biophys. Res. Com.* **149**: 398-404.
- Baxter R.C. (1990) Glycosaminoglycans inhibits formation of the 140-kDa insulin-like growth factor-binding protein complex. *Biochem. J.* **271**: 773-778.
- Baxter R.C. (1994) Insulin-Like Growth Factor Binding Proteins in the Human Circulation: A Review. *Horm. Res.* **42**: 140-144.
- Baxter R.C., Skriver L. (1993) Altered ligand specificity of proteolysed insulin-like growth factor binding protein-3. *Biochem. Biophys. Res. Com.* **196**: 1267-1273.
- Bayne M.L., Applebaum J., Chicchi G.G., Hayes N.S., Green B.G., Cascieri M.A. (1988) Structural analogs of human insulin-like growth factor I with reduced affinity for serum binding proteins and the type 2 insulin-like growth factor receptor. *J. Biol. Chem.* **263**: 6233-6239.
- Bayne M.L., Applebaum J., Chicchi G.G., Miller R.E., Cascieri M.A. (1990) The roles of tyrosines 24, 31, and 60 in the high affinity binding of insulin-like growth factor-I to the type 1 insulin-like growth factor receptor. *J. Biol. Chem.* **265**: 15648-15652.

- Bernstein F.C., Koetzle T.F., Williams G.J.B., Meyer E.F., Brice M.D., Rodgers J.R., Kennard O., Shimanouchi T. Tasui M. (1977) The Protein Data Bank: a computer-based archival file for macromolecular structures. *J. Mol. Biol.* **112**: 535-542
- Bers G., Garfin D. (1985) Protein and nucleic acid blotting and immunobiochemical detection. *Biotechniques* **3**: 275-289.
- Blasi F., Vassalli J.D., Danø K. (1987) Urokinase-type plasminogen activator: proenzyme, receptor, and inhibitors. *J. Cell. Biol.* **104**: 801-804.
- Blundell T.L., Bedarkar S., Rinderknecht E., R.E. H. (1978) Insulin-like growth factor: a model for tertiary structure accounting for immunoreactivity and receptor binding. *Proc. Natl. Acad. Sci. USA* **75**: 180-184.
- Blundell T.L., Humbel R.E. (1980) Hormone families: pancreatic hormones and homologous growth factors. *Nature* **287**: 781-787.
- Booth B.A., Boes M., Andress D.L., Dake B.L., Kiefer M.C., Maack C., Linhardt R.J., Bar K., Caldwell E.E.O., Weiler J., Bar R.S. (1995) IGFBP-3 and IGFBP-5 association with endothelial cells: Role of C-terminal heparin binding domain. *Growth Regul.* **5**: 1-17.
- Booth B.A., Boes M., Dake B.L., Linhardt R.J., Caldwell E.E.O., Weiler J.M., Bar R.S. (1996) Structure-Function Relationships In the Heparin-Binding C-Terminal Region Of Insulin-Like Growth Factor Binding Protein-3. *Growth Regul.* **6**: 206-213.
- Bourner M.J., Busby W.H.J., Siegel N.R., Krivi G.G., McCusker R.H., Clemmons D.R. (1992) Cloning and sequence determination of bovine insulin-like growth factor binding protein-2 (IGFBP-2): Comparison of its structural and functional properties with IGFBP-1. *J. Cell. Biochem.* **48**: 215-226.

- Bowles M.R., Hall D.R., Pond S.M., Winzor D.J. (1997) Studies of protein interactions by biosensor technology: an alternative approach to the analysis of sensorgrams deviating from pseudo-first-order kinetic behavior. *Anal. Biochem.* **244**: 133-143.
- Brinkman A., Kortleve D.J., Schuller A.G.P., Zwarthoff E.C., Drop S.L.S. (1991a) Site-directed mutagenesis of the N-terminal region of IGF binding protein 1; analysis of IGF binding capability. *Febs Lett.* **291**: 264-268.
- Brinkman A., Kortleve D.J., Zwarthoff E.C., Drop S.L.S. (1991b) Mutations in the carboxyl-terminal part of insulin-like growth factor (IGF)-binding protein-1 result in dimer formation and loss of IGF binding capacity. *Mol. Endocrinol.* **5**: 987-994.
- Busby W.H., Jr., Klapper D.G., Clemmons D.R. (1988) Purification of a 31,000-dalton insulin-like growth factor binding protein from human amniotic fluid. Isolation of two forms with different biologic actions. *J. Biol. Chem.* **263**: 14203-14210.
- Campbell P.G., Novak J.F., Yanosick T.B., McMaster J.H. (1992) Involvement of the plasmin system in dissociation of the insulin-like growth factor-binding protein complex. *Endocrinology* **130**: 1401-1412.
- Carr J.M., Owens J.A., Grant P.A., Walton P.E., Owens P.C., Wallace J.C. (1995) Circulating insulin-like growth factors (IGFs), IGF-binding proteins (IGFBPs) and tissue mRNA levels of IGFBP-2 and IGFBP-4 in the ovine fetus. *J. Endocrinol.* **145**: 545-557.
- Cardin A.D., Weintraub H.J. (1989) Molecular modeling of protein-glycosaminoglycan interactions. *Arteriosclerosis* **9**: 21-32.
- Cascieri M.A., Chicchi G.G., Applebaum J., Hayes N.S., Green B.G., Bayne M.L. (1988) Mutants of human insulin-like growth factor I with reduced affinity for the type 1 insulin-like growth factor receptor. *Biochemistry* **27**: 3229-3233.

- Cascieri M.A., Chicchi G.G., Applebaum J., Green B.G., Hayes N.S., Bayne M.L. (1989a) Structural analogs of human insulin-like growth factor (IGF) I with altered affinity for type 2 IGF receptors. *J. Biol. Chem.* **264**: 2199-2202.
- Cascieri M.A., Hayes N.S., Bayne M.L. (1989b) Characterization of the increased biological potency in BALB/C 3T3 cells of two analogs of human insulin-like growth factor I which have reduced affinity for the 28 K cell-derived binding protein. *J. Cell. Physiol.* **139**: 181-188.
- Chernausek S.D., Smith C.E., Duffin K.L., Busby W.H., Wright G., Clemmons D.R. (1995) Proteolytic cleavage of insulin-like growth factor binding protein 4 (IGFBP-4): Localization of cleavage site to non-homologous region of native (IGFBP-4). *J. Biol. Chem.* **270**: 11377-11382.
- Cianfarani S., Rossi P. (1997) Neuroblastoma and Insulin-Like Growth Factor System - New Insights and Clinical Perspectives. *Eur. J. Pediatr.* **156**: 256-261.
- Claussen M., Kubler B., Wendland M., Neifer K., Schmidt B., Zapf J., Braulke T. (1997) Proteolysis Of Insulin-Like Growth Factors (IGF) and IGF Binding Proteins By Cathepsin D. *Endocrinology* **138**: 3797-3803.
- Clemmons D.R., Dehoff M.L., Busby W.H., Bayne M.L., Cascieri M.A. (1992) Competition for binding to insulin-like growth factor (IGF) binding protein-2,3,4, and 5 by the IGFs and IGF analogs. *Endocrinology* **131**: 890-895.
- Cohen P., Graves H.C.B., Peehl D.M., Kamarei M., Giudice L.C., Rosenfeld R.G. (1992) Prostate-specific antigen (PSA) is an insulin-like growth factor binding protein-3 protease found in seminal plasma. *J. Clin. Endocrinol. Metab.* **75**: 1046-1053.
- Cohick W.S., Gockerman A., Clemmons D.R. (1995) Regulation of insulin-like growth factor (IGF) binding protein-2 synthesis and degradation by platelet-derived growth factor and the IGFs is enhanced by serum deprivation in vascular smooth muscle cells. *J. Cell. Physiol.* **164**: 187-196.

- Conover C.A. (1991) Glycosylation of insulin-like growth factor binding protein-3 (IGFBP-3) is not required for potentiation of IGF-I action: evidence for processing of cell-bound IGFBP-3. *Endocrinology* **129**: 3259-3268.
- Conover C.A., Durham S.K., Zapf J., Masiarz F.R., Kiefer M.C. (1995) Cleavage analysis of insulin-like growth factor (IGF)-dependent IGF-binding protein-4 proteolysis and expression of protease-resistant IGF-binding protein-4 mutants. *J. Biol. Chem.* **270**: 4395-4400.
- Conover C.A., Kiefer M.C., Zapf J. (1993) Posttranslational regulation of insulin-like growth factor binding protein-4 in normal and transformed human fibroblasts: Insulin-like growth factor dependence and biological studies. *J. Clin. Invest.* **91**: 1129-1137.
- Conover C.A., Ronk M., Lombana F., Powell D.R. (1990) Structural and biological characterization of bovine insulin-like growth factor binding protein 3. *Endocrinology* **127**: 2795-2803.
- Cooke R.M., Harvey T.S., Campbell I.D. (1991) Solution structure of human insulin-like growth factor 1: a nuclear magnetic resonance and restrained molecular dynamics study. *Biochemistry* **30**: 5484-5491.
- Coverley J.A., Baxter R.C. (1995) Regulation of insulin-like growth factor (IGF) binding protein-3 phosphorylation by IGF-I. *Endocrinology* **136**: 5778-5781.
- Coverley J.A., Baxter R.C. (1997) Phosphorylation Of Insulin-Like Growth Factor Binding Proteins. *Mol. Cell. Endocrinol.* **128**: 1-5.
- Cowgill R.W. (1965) Fluorescence and Protein Structure. IV. Iodinated Tyrosyl Residues. *Biochim. Biophys. Acta* **94**: 74-80.
- Craik D.J., Wilce J.A. (1997) Studies of protein-ligand interactions by NMR. *Methods Mol. Biol.* **60**: 195-232.

- Davenport M.L., Pucilowska J., Clemmons D.R., Lundblad R., Spencer J.A., Underwood L.E. (1992) Tissue-specific expression of insulin-like growth factor binding protein-3 protease activity during rat pregnancy. *Endocrinology* **130**: 2505-2512.
- Dunford H.B., Ralston I.M. (1983) On the mechanism of iodination of tyrosine. *Biochem. Biophys. Res. Commun.* **116**: 639-643.
- Durham S.K., Riggs B.L., Harris S.A., Conover C.A. (1995) Alterations in insulin-like growth factor (IGF)-dependent IGF-binding protein-4 proteolysis in transformed osteoblastic cells. *Endocrinology* **136**: 1374-1380.
- Edelhoch H. (1962) The Properties of Thyroglobulin. VIII. The Iodination of Thyroglobulin. *J. Biol. Chem.* **237**: 2778-2787.
- Edwards P.R., Gill A., Pollard Knight D.V., Hoare M., Buckle P.E., Lowe P.A., Leatherbarrow R.J. (1995) Kinetics of protein-protein interactions at the surface of an optical biosensor. *Anal. Biochem.* **231**: 210-217.
- Elgin R.G., Busby W.H., Jr., Clemmons D.R. (1987) An insulin-like growth factor (IGF) binding protein enhances the biologic response to IGF-I. *Proc. Natl. Acad. Sci. USA* **84**: 3254-3258.
- Feld S., Hirschberg R. (1996) Growth hormone, the insulin-like growth factor system, and the kidney. *Endocr. Rev.* **17**: 423-480.
- Firth S.M. (1998) Methods to detect and analyse modified insulin-like growth factor binding proteins. In Takano K, Hizuka N, Takahashi S (eds): *Molecular Mechanisms to Regulate the Activities of Insulin-like Growth Factors*. Amsterdam: Elsevier Science B.V, pp 79-87.
- Firth S.M., Baxter R.C. (1995) The role of glycosylation in the action of IGFBP-3. *Prog. Growth Factor Res.* **6**: 223-229.

- Firth S.M., Ganeshprasad U., Baxter R.C. (1998) Structural determinants of ligand and cell surface binding of insulin-like growth factor-binding protein-3. *J. Biol. Chem.* **273**: 2631-2638.
- Florini J.R., Ewton D.Z., Coolican S.A. (1996) Growth hormone and the insulin-like growth factor system in myogenesis. *Endocr. Rev.* **17**: 481-517.
- Flyvbjerg A., Mogensen O., Mogensen B., Nielsen O.S. (1997) Elevated serum insulin-like growth factor-binding protein 2 (IGFBP-2) and decreased IGFBP-3 in epithelial ovarian cancer - correlation with cancer antigen 125 and tumor-associated trypsin inhibitor. *J. Clin. Endocrinol. Metab.* **82**: 2308-2313.
- Forbes B.E., Aplin S.E., Upton Z. (1994) Expression and partial purification of recombinant bovine IGFBP-2. *Growth Regul.* **4** **supp.1**: 131.
- Forbes B., Szabo L., Baxter R.C., Ballard F.J., Wallace J.C. (1988) Classification of the insulin-like growth factor binding proteins into three distinct categories according to their binding specificities. *Biochem. Biophys. Res. Com.* **157**: 196-202.
- Forbes B.E., Turner D., Hodge S.J., McNeil K., Forsberg G., Wallace J.C. (1998) Localization of an insulin-like growth factor (IGF) binding site of bovine IGF binding protein-2 using disulfide mapping and deletion mutation analysis of the C-terminal domain. *J. Biol. Chem.* **273**: 4647-4652.
- Fowlkes J.L. (1997) Insulin-like growth factor proteolysis - an emerging paradigm in insulin-like growth factor physiology [Review]. *Trends Endocrinol. Metab.* **8**: 299-306.
- Fowlkes J.L., Serra D.M. (1996) Characterization of glycosaminoglycan-binding domains present in insulin-like growth factor-binding protein-3. *J. Biol. Chem.* **271**: 14676-14679.



- Fowlkes J.L., Suzuki K., Nagase H., Thrailkill K.M. (1994) Proteolysis of insulin-like growth factor binding protein-3 during rat pregnancy: a role for matrix metalloproteinases. *Endocrinology* **135**: 2810-2813.
- Francis G.L., Upton F.M., Ballard F.J., McNeil K.A., Wallace J.C. (1988) Insulin-like growth factors 1 and 2 in bovine colostrum: Sequences and biological activities compared with those of a potent truncated form. *Biochem. J.* **251**: 95-104.
- Francis G.L., Aplin S.E., Milner S.J., McNeil K.A., Ballard F.J., Wallace J.C. (1993) Insulin-like growth factor (IGF)-II binding to IGF-binding proteins and IGF receptors is modified by deletion of the N-terminal hexapeptide or substitution of arginine for glutamate-6 in IGF-II. *Biochem. J.* **293**: 713-719.
- Francis G.L., Ross M., Ballard F.J., Milner S.J., Senn C., McNeil K.A., Wallace J.C., King R., Wells J.R.E. (1992) Novel recombinant fusion protein analogues of insulin-like growth factor (IGF)-I indicate the relative importance of IGF-binding protein and receptor binding for enhanced biological potency. *J. Mol. Endocrinol.* **8**: 213-223.
- Froesch E.R., Hussain M.Y., Donath M.Y., Zapf J.L. (1998) Diabetes and the Heart: Physiological and Therapeutic Aspects of IGF-I. In Takano K, Hizuka N, Takahashi S (eds): Molecular Mechanisms to Regulate the Activities of Insulin-like Growth Factors. Amsterdam: Elsevier Science B.V, pp 11-22.
- Gammeltoft S. (1984) Insulin receptors: binding kinetics and structure-function relationship of insulin. *Physiol. Rev.* **64**: 1321-1378.
- Gliemann J., Sonne O., Linde S., Hansen B. (1979) Biological potency and binding affinity of monoiodoinsulin with iodine on tyrosine A14 or tyrosine A19. *Biochem. Biophys. Res Commun.* **87**: 1183-1190.
- Gockerman A., Clemmons D.R. (1995) Porcine aortic smooth muscle cells secrete a serine protease for insulin-like growth factor binding protein-2. *Circ. Res.* **76**: 514-521.
- Godel G., Seitz P., Verhoef M. (1992) Automated amino acid analysis using combined

OPA and FMOC-CL precolumn derivatization. *LC-GC Int.* **5**: 44-49.

Gyllensten U.B. (1989) PCR and DNA sequencing. *Biotechniques* **7**: 700-708.

Hashimoto R., Ono M., Fujiwara H., Higashihashi N., Yoshida M., Enjoh Kimura T., Sakano K. (1997) Binding sites and binding properties of binary and ternary complexes of insulin-like growth factor-II (IGF-II), IGF-binding protein-3, and acid-labile subunit. *J. Biol. Chem.* **272**: 27936-27942.

Heding A., Gill R., Ogawa Y., De Meyts P., Shymko R.M. (1996) Biosensor measurement of the binding of insulin-like growth factors I and II their analogues to the insulin-like growth factor-binding protein-3. *J. Biol. Chem.* **271**: 13948-13952.

Hintz R.L. (1995) The annals of IGF binding proteins: into the next millennium. *Prog. Growth Factor Res.* **6**: 79-89.

Ho P.J., Baxter R.C. (1997) Characterization of truncated insulin-like growth factor-binding protein-2 in human milk. *Endocrinology* **138**: 3811-3818.

Hobba G.D., Forbes B.E., Parkinson E.J., Francis G.L., Wallace J.C. (1996) The insulin-like growth factor (IGF) binding site of bovine insulin-like growth factor binding protein-2 (bIGFBP-2) probed by iodination. *J. Biol. Chem.* **271**: 30529-30536.

Hobba G.D., Lothgren A., Holmberg E., Forbes B.E., Francis G.L., Wallace J.C. (1998) Alanine screening mutagenesis establishes tyrosine 60 of bovine insulin-like growth factor binding protein-2 as a determinant of insulin-like growth factor binding. *J. Biol. Chem.* **273**: 19691-19698.

Hober S., Forsberg G., Palm G., Hartmanis M., Nilsson B. (1992) Disulfide exchange folding of insulin-like growth factor I. *Biochemistry* **31**: 1749-1756.

Hodgkinson S.C., Napier J.R., Spencer G.S., Bass J.J. (1994) Glycosaminoglycan binding characteristics of the insulin-like growth factor-binding proteins. *J. Mol. Endocrinol.* **13**: 105-112.

- Hoeck W.G., Mukku V.R. (1994) Identification of the major sites of phosphorylation in IGF binding protein-3. *J. Cell. Biochem.* **56**: 262-273.
- Hossenlopp P., Seurin D., Segovia Quinson B., Hardouin S., Binoux M. (1986) Analysis of serum insulin-like growth factor binding proteins using western blotting: use of the method for titration of the binding proteins and competitive binding studies. *Anal. Biochem.* **154**: 138-143.
- Huhtala M.L., Koistinen R., Palomaki P., Partanen P., Bohn H., Seppala M. (1986) Biologically active domain in somatomedin-binding protein. *Biochem. Biophys. Res. Commun.* **141**: 263-270.
- Humbel R.E. (1990) Insulin-like growth factors I and II. *Eur. J. Biochem.* **190**: 445-462.
- Hunkapillar M.W., Hewick R.M., Dreyer W.J., Hood L.E. (1983) High sensitivity sequencing with a gas phase sequenator. *Methods Enzymol.* **91**: 399-413.
- Hynes R.O. (1987) Integrins: a family of cell surface receptors. *Cell* **48**: 549-554.
- Izzo J.L., Roncone A., Izzo M.J., Bale W.F. (1964) Relationship between degree of iodination of insulin and its biological, electrophoretic, and immunological properties. *J. Biol. Chem.* **239**: 3749-3754.
- Janin J., Chothia C. (1990) The structure of protein-protein recognition sites. *J. Biol. Chem.* **265**: 16027-16030.
- Jansson M., Andersson G., Uhlen M., Nilsson B., Kordel J. (1998) The Insulin-like growth factor (IGF)binding protein 1 binding epitope on IGF-I probed by heteronuclear NMR spectroscopy and mutational analysis. *J. Biol. Chem.* **273**: 24701-24707.
- Jones J.I., Busby W.H., Jr., Wright G., Clemmons D.R. (1993a) Human IGFBP-1 is phosphorylated on 3 serine residues: effects of site-directed mutagenesis of the major phosphoserine. *Growth. Regul.* **3**: 37-40.

- Jones J.I., Clemmons D.R. (1995) Insulin-like growth factors and their binding proteins: biological actions. *Endocr. Rev.* **16**: 3-34.
- Jones J.I., D'Ercole A.J., Camacho Hubner C., Clemmons D.R. (1991) Phosphorylation of insulin-like growth factor (IGF)-binding protein 1 in cell culture and in vivo: Effects on affinity for IGF-I. *Proc. Natl. Acad. Sci. USA* **88**: 7481-7485.
- Jones J.I., Gockerman A., Busby W.H., Jr., Wright G., Clemmons D.R. (1993b) Insulin-like growth factor binding protein 1 stimulates cell migration and binds to the alpha-5-beta-1 integrin by means of its Arg-Gly-Asp sequence. *Proc. Natl. Acad. Sci. USA* **90**: 10553-10557.
- Jones J.I., Gockerman A., Busby W.H.J., Camacho Hubner C., Clemmons D.R. (1993c) Extracellular matrix contains insulin-like growth factor binding protein-5: Potentiation of the effects of IGF-I. *J. Cell Biol.* **121**: 679-687.
- Jones S., Thornton J.M. (1996) Principles of protein-protein interactions. *Proc. Natl. Acad. Sci. USA* **93**: 13-20.
- Johnsson U., Löfås S., Lindqvist G. (1991) Immobilisation of proteins to a carboxymethylated dextran-modified gold surface for biospecific interaction analysis in surface plasmon resonance sensors. *Anal. Biochem.* **198**: 268-277.
- Kalus W., Zweckstetter M., Renner C., Sanchez Y., Georgescu J., Grol M., Demuth D., Schumacher R., Dony C., Lang K., Holak T.A. (1998) Structure of the IGF-binding domain of the insulin-like growth factor binding protein-5 (IGFBP-5): implications for IGF and IGF-receptor interactions. *EMBO J.* **17**: 6558-6572.
- Karam J.H. (1987) Pancreatic Hormones and Antidiabetic Drugs. In Katzung BG (ed): Basic and Clinical Pharmacology. Norwalk, Connecticut: Appleton and Lange, pp 484-496.

- Katsoyannis P.G., Zalut C., Harris A., Meyer R.J. (1971) Analogs of insulin. I. Synthesis of destriptide B28-B30 bovine insulin and destriptide B28-B30 porcine (human) insulin. *Biochemistry* **10**: 3884-3889.
- Kikuchi K., Larner J., Freer R.J., Day A.R., Morris H., Dell A. (1980) Studies on the biological activity of degraded insulins and insulin fragments. *J. Biol. Chem.* **255**: 9281-9288.
- King R., Wells J.R.E., Krieg P., Snoswell M., Brazier J., Bagley C.J., Wallace J.C., Ballard F.J., Ross M., Francis G.L. (1992) Production and characterization of recombinant insulin-like growth factor-I (IGF-I) and potent analogues of IGF-I with Gly or Arg substituted for Glu-3, following their expression in *Escherichia coli* as fusion proteins. *J. Mol. Endocrinol.* **8**: 29-42.
- Kitagawa K., Ogawa H., Burke G.T., Chanley J.D., Katsoyannis P.G., Kitagawa K., Ogawa H., Burke G.T., Chanley J.D., Katsoyannis P.G. (1984) Interaction between the A2 and A19 amino acid residues is of critical importance for high biological activity in insulin: [19-leucine-A]-insulin: critical role of the A2 amino acid residue in the biological activity of insulin: [2-glycine-A]- and [2-alanine-A]-insulins. *Biochemistry* **23**: 4444-4448.
- Kobayashi M., Ohgaku S., Iwasaki M., Maegawa H., Shigeta Y., Inouye K. (1982) Characterization of [LeuB-24]- and [LeuB25]-insulin analogues. Receptor binding and biological activity. *Biochem. J.* **206**: 597-603.
- Koutsilieris M., Frenette G., Lazure C., Lehoux J.G., Govindan M.V., Polychronakos C. (1993) Urokinase-type plasminogen activator: A paracrine factor regulating the bioavailability of IGFs in PA-III cell-induced osteoblastic metastases. *Anticancer Res.* **13**: 481-486.
- Kristensen C., Kjeldsen T., Wiberg F.C., Schäffer L., Hach M., Havelund S., Bass J., Steiner D.F., Andersen A.S. (1997) Alanine scanning mutagenesis of insulin. *J. Biol. Chem.* **272**: 12978-12983.

- Kunkel T.A. (1985) Rapid and efficient site-specific mutagenesis without phenotypic selection. *Proc. Natl. Acad. Sci. U.S.A* **82**: 488-492.
- Kunkel T.A., Roberts J.D., Zakour R.A. (1987) Rapid and efficient site-specific mutagenesis without phenotypic selection. *Methods Enzymol.* **154**: 367-382.
- Lalou C., Sawamura S., Segovia B., Ogawa Y., Binoux M. (1997) Proteolytic Fragments Of Insulin-Like Growth Factor Binding Protein-3 - N-Terminal Sequences and Relationships Between Structure and Biological Activity. *C. R. Acad. Sci. III* **320**: 621-628.
- Laemmli U.K. (1970) Cleavage of structural proteins during the assembly of the head of bacteriophage T4. *Nature* **227**: 680-685.
- Landale E.C., Strong D.D., Mohan S., Baylink D.J. (1995) Sequence Comparison and Predicted Structure For the Four Exon-Encoded Regions Of Human Insulin-Like Growth Factor Binding Protein 4. *Growth Factors* **12**: 245-250.
- Lassarre C., Binoux M. (1994) Insulin-like growth factor binding protein-3 is functionally altered in pregnancy plasma. *Endocrinology* **134**: 1254-1262.
- Lee P.D., Conover C.A., Powell D.R. (1993) Regulation and function of insulin-like growth factor-binding protein-1. *Proc. Soc. Exp. Biol. Med.* **204**: 4-29.
- LeRoith D. (1996) Insulin-like growth factor receptors and binding proteins. *Baillieres Clin. Endocrinol. Metab.* **10**: 49-73.
- Lewitt M.S., Baxter R.C. (1991) Insulin-like growth factor-binding protein-1: a role in glucose counterregulation? *Mol. Cell. Endocrinol.* **79**: C147-152.
- Logan A., Hill D.J. (1992) Bioavailability: is this a key event in regulating the actions of peptide growth factors? *J. Endocrinol.* **134**: 157-161.

- Maly P., Lüthi C. (1988) The binding sites of insulin-like growth factor I (IGF I) to type I IGF receptor and to a monoclonal antibody: Mapping by chemical modification of tyrosine residues. *J. Biol. Chem.* **263**: 7068-7072.
- Manes S., Kremer L., Albar J.P., Mark C., Llopis R., Martineza C. (1997) Functional Epitope Mapping Of Insulin-Like Growth Factor I (IGF-I) By Anti-IGF-I Monoclonal Antibodies. *Endocrinology* **138**: 905-915.
- Martin J.L., Baxter R.C. (1986) Insulin-like growth factor binding protein from human plasma; Purification and characterisation. *J. Biol. Chem.* **261**: 8754-8760.
- Mayer M. (1990) Biochemical and biological aspects of the plasminogen activation system. *Clin. Biochem.* **23**: 197-211.
- McCusker R.H., Busby W.H., Dehoff M.H., Camacho Hubner C., Clemmons D.R. (1991) Insulin-like growth factor (IGF) binding to cell monolayers is directly modulated by the addition of IGF-binding proteins. *Endocrinology* **129**: 939-949.
- Means G.E., Feeney R.E. (1971) Chemical Modification of Proteins, p181. San Francisco: Holden-Day, Inc.
- Menouny M., Binoux M., Babajko S. (1997) Role Of Insulin-Like Growth Factor Binding Protein-2 and Its Limited Proteolysis In Neuroblastoma Cell Proliferation - Modulation By Transforming Growth Factor-Beta and Retinoic Acid. *Endocrinology* **138**: 683-690.
- Mian I.S., Bradwell A.R., Olson A.J. (1991) Structure, function and properties of antibody binding sites. *J. Mol. Biol.* **217**: 133-151.
- Milner S.J., Francis G.L., Wallace J.C., Magee B.A., Ballard F.J. (1995) Mutations in the B-domain of insulin-like growth factor-I influence the oxidative folding to yield products with modified biological properties. *Biochem. J.* **308**: 865-871.

- Mistry R., Snashall P.D., Totty N., Guz A., Tetley T.D. (1991) Isolation and characterization of sheep alpha 1-proteinase inhibitor. *Biochem. J.* **273**: 685-90.
- Moss J.A., Francis G.L., Ross M., Wallace J.C., Ballard F.J. (1991) Insulin-like growth factor (IGF)-I and IGF-II binding to an IGF binding protein: An investigation using chemical modification of tyrosine residues as a structural probe for the sites of interactions. *J. Biol. Chem.* **266**: 909-914.
- Mulhern T.D, Shaw G.L., Morton C.J., Day A.J., Campbell I.D. (1997) The SH2 domain from the tyrosine kinase FYN in complex with a phosphotyrosyl peptide reveals insights into domain stability and binding specificity. *Structure* **5**: 1313-1323.
- Nagashima M., Lundh E., Leonard J.C., Morser J., Parkinson J.F. (1993) Alanine-scanning mutagenesis of the epidermal growth factor-like domains of human thrombomodulin identifies critical residues for its cofactor activity. *J. Biol. Chem.* **268**: 2888-2892.
- Nam T.J., Busby W., Jr., Clemmons D.R. (1997) Insulin-like growth factor binding protein-5 binds to plasminogen activator inhibitor-I. *Endocrinology* **138**: 2972-2978.
- Nam T.J., Busby W.H., Jr., Clemmons D.R. (1994) Human fibroblasts secrete a serine protease that cleaves insulin-like growth factor-binding protein-5. *Endocrinology* **135**: 1385-1391.
- Neumann G.M., Marinaro J.A., Bach L.A. (1998) Identification of O-glycosylation sites and partial characterization of carbohydrate structure and disulfide linkages of human insulin-like growth factor binding protein 6. *Biochemistry* **37**: 6572-6585.
- Nissley P., Lopaczynski W. (1991) Insulin-like growth factor receptors. *Growth Factors* **5**: 29-43.
- Nielsen H., Engelbrecht J., Brunak, S., Von Heijne, G. (1997) Identification of prokaryotic and eukaryotic signal peptides and prediction of their cleavage sites. *Protein Engineering* **10**: 1-6.



- Oh Y., Mueller H.L., Lee D.Y., Fielder P.J., Rosenfeld R.G. (1993) Characterization of the affinities of insulin-like growth factor (IGF)-binding protein 1-4 for IGF-I, IGF-II, IGF-I/insulin hybrid, and IGF-I analogs. *Endocrinology* **132**: 1337-1344.
- Ohlsson C., Bengtsson B.A., Isaksson O.G., Andreassen T.T., Słotweg M.C. (1998) Growth hormone and bone. *Endocr. Rev.* **19**: 55-79.
- Parker A., Gockerman A., Busby W.H., Clemmons D.R. (1995) Properties of an insulin-like growth factor-binding protein-4 protease that is secreted by smooth muscle cells. *Endocrinology* **136**: 2470-2476.
- Parker A., Clarke J.B., Busby W.H., Jr., Clemmons D.R. (1996) Identification of the extracellular matrix binding sites for insulin-like growth factor-binding protein 5. *J. Biol. Chem.* **271**: 13523-13529.
- Pickart C.M., Haldeman M.T., Kaspersek E.M., Chen Z. (1992) Iodination of tyrosine 59 of ubiquitin selectively blocks ubiquitin's acceptor activity in diubiquitin synthesis catalyzed by E2(25K). *J. Biol. Chem.* **267**: 14418-14423.
- Pintar J.E., Schuller A., Cerro J.A., Czick M., Grewal A., Green B. (1995) Genetic ablation of IGFBP-2 suggests functional redundancy in the IGFBP family. *Prog. Growth Factor Res.* **6**: 437-445.
- Polyak, S. (1994) Improving the folding and site-specific proteolysis characteristics of fusion proteins. Honours thesis, Biochemistry Dept., University of Adelaide, Adelaide, Australia.
- Powell D.R., Lee P.D., Suwanichkul A. (1993) Multihormonal regulation of IGFBP-1 promoter activity. *Adv. Exp. Med. Biol.* **343**: 205-214.
- Qin X., Strong D.D., Baylink D.J., Mohan S. (1998) Structure-function analysis of the human insulin-like growth factor binding protein-4. *J. Biol. Chem.* **273**: 23509-23516.

- Rajah R., Katz L., Nunn S., Solberg P., Beers T., Chohen P. (1994) Insulin-like growth factor binding protein (IGFBP) proteases: functional regulators of cell growth. *Prog. Growth Factor Res.* **6**: 273-284.
- Rajaram S., Baylink D.J., Mohan S. (1997) Insulin-like Growth Factor-Binding Proteins in Serum and Other Biological Fluids: Regulation and Functions. *Endocrine Rev.* **18**: 801-831.
- Rechler M.M. (1993) Insulin-like growth factor binding proteins. *Vitam. Horm.* **47**: 1-114.
- Reeve J.G., Kriby L.B., Brinkman A., Hughes S.A., Schwander J., Bleehen N.M. (1992) Insulin-like growth-factor-binding protein gene expression and protein production by human tumor cell lines. *Int. J. Cancer* **51**: 818-821.
- Rinderknecht E., Humbel R.E. (1978a) The amino acid sequence of human Insulin-like growth factor I and its structural homology with pro-insulin. *J. Biol. Chem.* **253**: 2769-2776.
- Rinderknecht E., Humbel R.E. (1978b) Primary structure of insulin-like growth factor II. *FEBS Lett.* **89**: 283-286.
- Roghani M., Lassarre C., Zapf J., Pova G., Binoux M. (1991) Two insulin-like growth factor (IGF)-binding proteins are responsible for the selective affinity for IGF-II of cerebrospinal fluid binding proteins. *J. Clin. Endocrinol. Metab.* **73**: 658-666.
- Rost B., Sander C. (1993) Improved prediction of protein secondary structure by use of sequence profiles and neural networks. *Proc. Natl. Acad. Sci. USA* **90**: 7558-7562.
- Sakano K., Enjoh T., Numata F., Fujiwara H., Marumoto Y., Higashihashi N., Sato Y., Perdue J.F., Fujita Yamaguchi Y. (1991) The design, expression, and characterization of human insulin-like growth factor II (IGF-II) mutants specific for either the IGF-II/cation-independent mannose 6-phosphate receptor or IGF-I receptor. *J. Biol. Chem.* **266**: 20626-20635.

- Sambrook J., Fritsch E.F., Maniatis T. (1989) *Molecular Cloning, a laboratory manual*. New York: Cold Spring Harbour Press.
- Sato A., Nishimura S., Ohkubo T., Kyogoku Y., Koyama S., Kobayashi M., Yasuda T., Kobayashi Y. (1993) Three-dimensional structure of human insulin-like growth factor-I (IGF-I) determined by proton NMR and distance geometry. *Int. J. Pept. Prot. Res.* **41**: 433-440.
- Schäffer L., Larsen U.D., Linde S., Hejnaes K.R., Skriver L. (1993) Characterization of the three 125I-iodination isomers of human insulin-like growth factor I (IGF1). *Biochim. Biophys. Acta* **1203**: 205-209.
- Shenolikar S. (1988) Protein phosphorylation: hormones, drugs, and bioregulation. *FASEB J.* **2**: 2753-2764.
- Shimasaki S., Ling N. (1991) Identification and molecular characterization of insulin-like growth factor binding proteins (IGFBP-1, -2, -3, -4, -5 and -6). *Prog. Growth Factor Res.* **3**: 243-66.
- Sohar I., Sleat D., Liu C.G., Ludwig T., Lobel P. (1998) Mouse Mutants Lacking the Cation-Independent Mannose 6-Phosphate Insulin-Like Growth Factor II Receptor Are Impaired In Lysosomal Enzyme Transport - Comparison Of Cation-Independent and Cation-Dependent Mannose 6-Phosphate Receptor-Deficient Mice. *Biochem. J.* **330**: 903-908.
- Sommer A., Maack C.A., Spratt S.K., Mascarenhas D., Tresse T.J., Rhodes E.T., Lee R., Roumas M., Tatsuno G.P., Flynn J.A., Gerber N., Taylor J., Cudny H., Nanney L., Hunt T.K., Spencer E.M. (1991) Molecular genetics and actions of recombinant insulin-like growth factor binding protein-3. In Spencer EM (ed): *Modern Concepts of Insulin-Like Growth Factors*. Elsevier Science Publishing Co., Inc., pp 715-728.
- Spencer E.M., Chan K. (1995) A 3-dimensional model for the insulin-like growth factor binding proteins (IGFBPs); supporting evidence using the structural determinants of the IGF binding site on IGFBP-3. *Prog. Growth Factor Res.* **6**: 209-214.

- Stryer L. (1988) *Biochemistry* (3<sup>rd</sup> ed.), p23. New York: W.H. Freeman and Co.
- Szabo L., Mottershead D.G., Ballard F.J., Wallace J.C. (1988) The bovine insulin-like growth factor (IGF) binding protein purified from conditioned medium requires the amino-terminal tripeptide in IGF-1 for binding. *Biochem. Biophys. Res. Com.* **151**: 207-214.
- Terasawa H., Kohda D., Hatanaka H., Nagata K., Higashihashi N., Fujiwara H., Sakano K., Inagaki F. (1994) Solution structure of human insulin-like growth factor II; recognition sites for receptors and binding proteins. *EMBO J.* **13**: 5590-5597.
- Thraillkill K.M., Quarles L.D., Nagase H., Suzuki K., Serra D.M., Fowlkes J.L. (1995) Characterization of insulin-like growth factor-binding protein 5-degrading proteases produced throughout murine osteoblast differentiation. *Endocrinology* **136**: 3527-3533.
- Torres A.M., Forbes B.E., Aplin S.E., Wallace J.C., Francis G.L., Norton R.S. (1995) Solution structure of human insulin-like growth factor II: Relationship to receptor and binding protein interactions. *J. Mol. Biol.* **248**: 385-401.
- Tressel T.J., Tatsuno G.P., Spratt K., Sommer A. (1991) Purification and characterization of human recombinant insulin-like growth factor binding protein 3 expressed in Chinese hamster ovary cells. *Biochem. Biophys. Res. Com.* **178**: 625-633.
- Tsomides T.J., Eisen H.N. (1993) Stoichiometric labeling of peptides by iodination on tyrosyl or histidyl residues. *Anal. Biochem.* **210**: 129-135.
- Tunon P., Johansson K.E. (1984) A sensitive method for staining proteins in polyacrylamide gels. *J. Biochem. Biophys. Methods* **9**: 171-179.
- Upton F.Z., Szabo L., Wallace J.C., Ballard F.J. (1990) Characterization and cloning of a bovine insulin-like growth factor-binding protein. *J. Mol. Endocrinol.* **5**: 77-84.

- Varki A. (1993) Biological roles of oligosaccharides: all of the theories are correct. *Glycobiology* **3**: 97-130.
- Van Obberghen Schilling E., Pouyssegur J. (1983) Mitogen-potentiating action and binding characteristics of insulin and insulin-like growth factors in Chinese hamster fibroblasts. *Exp. Cell. Res.* **147**: 369-378.
- Vorwerk P., Yamanaka Y., Spagnoli A., Oh Y., Rosenfeld R.G. (1998) Insulin and IGF binding by IGFBP-3 fragments derived from proteolysis, baculovirus expression and normal human urine. *J. Clin. Endocrinol. Metab.* **83**: 1392-1395.
- Wang J.F., Hampton B., Mehlman T., Burgess W.H., Rechler M.M. (1988) Isolation of a biologically active fragment from the carboxyl-terminus of the fetal rat binding protein for insulin-like growth factors. *Biochem. Biophys. Res. Com.* **157**: 718-726.
- Wells J.A. (1996) Binding in the growth hormone receptor complex. *Proc. Natl. Acad. Sci. USA* **93**: 1-6.
- Whyatt L.M., Duwel A., Smith A.G., Rathjen P.D. (1993) The responsiveness of embryonic stem cells to alpha and beta interferons provides the basis of an inducible expression system for analysis of developmental control genes. *Mol. Cell. Biol.* **13**: 7971-7976.
- Winant R.C., Lazar J.B., Johnson P.H. (1991) Chemical modifications and amino acid substitutions in recombinant hirudin that increase hirudin-thrombin affinity. *Biochemistry* **30**: 1271-1277.
- Wood T.L. (1995) Gene-targeting and transgenic approaches to IGF and IGF binding protein function. *Am. J. Physiol.* **269**: E613-622.
- Wood T.L., Streck R.D., Pintar J.E. (1992) Expression of the IGFBP-2 gene in post-implantation rat embryos. *Development* **114**: 59-66.

Zadeh S.M., Binoux M. (1997) The 16-kDa proteolytic fragment of insulin-like growth factor (IGF) binding protein-3 inhibits the mitogenic action of fibroblast growth factor on mouse fibroblasts with a targeted disruption of the type 1 IGF receptor gene. *Endocrinology* **138**: 3069-3072.

Zapf J. (1995) Physiological role of the insulin-like growth factor binding proteins. *Eur. J. Endocrinol.* **132**: 645-654.

Zheng B., Clarke J.B., Busby W.H., Duan C., Clemmons D.R. (1998) Insulin-like growth factor-binding protein-5 is cleaved by physiological concentrations of thrombin. *Endocrinology* **139**: 1708-1714.

Hobba, G.D., Forbes, B.E., Parkinson, E.J., Francis, G.L. & Wallace, J.C. (1996) The insulin-like growth factor (IGF) binding site of bovine insulin-like growth factor binding protein-2 (bIGFBP-2) probed by iodination.

*The Journal of Biological Chemistry*, v. 271(48), pp. 30529-30536

NOTE:

This publication is included on pages 161-168 in the print copy of the thesis held in the University of Adelaide Library.

It is also available online to authorised users at:

<http://doi.org/10.1074/jbc.271.48.30529>

Hobba, G.D., Lothgren, A., Holmberg, E., Forbes, E.J., Francis, G.L. & Wallace, J.C. (1998) Alanine screening mutagenesis establishes tyrosine 60 of bovine insulin-like growth factor binding protein-2 as a determinant of insulin-like growth factor binding.  
*The Journal of Biological Chemistry*, v. 273(31), pp. 19691-19698

NOTE:

This publication is included on pages 169-176 in the print copy of the thesis held in the University of Adelaide Library.

It is also available online to authorised users at:

<http://doi.org/10.1074/jbc.273.31.19691>